Crustal Structure and Mesozoic Tectonic Evolution of Conjugate Volcanic Passive Margins of the South-Central and South Atlantic Oceans

A Dissertation Presented to

the Faculty of the Department of Earth and Atmospheric Sciences

University of Houston

_____

in Partial Fulfillment

of the Requirements for the Degree

Doctor of Philosophy

_____

By

Kyle R. Reuber

May 2017

Crustal Structure and Mesozoic Tectonic Evolution of Conjugate Volcanic Passive Margins of the South-Central and South Atlantic Oceans

---

Kyle R. Reuber

APPROVED:

Dr. Paul Mann, Chairman

Dr. Dale Bird

Dr. William Sager

Dr. Michael Murphy

Dr. Jim Pindell

Dean, College of Natural Sciences and Mathematics

Dedication

For my wife, Erin, and my daughters, Emma, Allison, and Sophie.

Acknowledgements

I would like to thank, my dissertation supervisor, Dr. Paul Mann for his enthusiasm, guidance, and patience over these past five years. I would also like to extend my sincere gratitude to Dr. Brian W. Horn of Ion Geophysical without whose encouragement, support and access to geophysical data were all critical for the completion of this study. I am also deeply indebted to Drs. Jim Pindell and Dale Bird for their mentoring and enthusiasm to share their vast knowledge with me on the topic of this study. Special thanks go to the University of Houston PhD committee members - Drs. William Sager and Mike Murphy - for their many contributions to my study and their careful reading of the text.

I am deeply grateful to the following friends and colleagues at the University of Houston and ION Geophysical that have shared their ideas and provided constant encouragement and companionship over the past five years: Alex Dale, Bryan Ott, Patrick Loureiro, Naila Dowla, Gulce Dinc, Joe Paul, Dr. Rod Graham, Al Danforth, Andy Bliss, and Doug Allinson.

I am also endlessly grateful for my family (both near and far); who have always supported me through all my endeavors.

Crustal Structure and Mesozoic Tectonic Evolution of Conjugate Volcanic Passive Margins of the South-Central and South Atlantic Oceans

---

An Abstract of a Dissertation Presented to

the Faculty of the Department of Earth and Atmospheric Sciences

University of Houston

In Partial Fulfillment

of the Requirements for the Degree

Doctor of Philosophy

By

Kyle R. Reuber

May 2017

Abstract

Volcanic passive margins (VPM) initiate with the eruption of flood basalts in continental rift settings that overlie an active mantle plume. Magmatism on conjugate VPM's increases in volume and intensity during continued lithospheric stretching and includes the generation of igneous belts ranging from 10-200+ km in width and to 8-24 km-thick. Conjugate volcanic passive margin belts include seaward-dipping reflectors (SDR's) whose dips range from 0 to 20°. I use 33,000 line km of 40-km-record 2D seismic reflection data to identify a VPM beneath the Demerara Rise, offshore Suriname and to investigate VPM's along the conjugate margins of the South America (Brazil and Uruguay) and West Africa (Namibia).

My 5500 km of 2D seismic data from the Demerara Rise - previously characterized as a continental plateau – reveals a basement composed of >22-km-thick, 250-km-long, steeply-dipping (>20°) packages of SDR's related to Jurassic rifting of North America and South America. 2D gravity modeling and VPM analogs are used to support its proposed magmatic origin.

I investigated the crustal structure of conjugate VPMs in Uruguay/Southern Brazil and Namibia using 27,500 km of 2D seismic data. An asymmetrical distribution of SDRs is proposed as a consequence of increased plate velocities relative to a fixed mantle position. The faster plate – South America - contains 30% less volume of SDR's (201,700 km^3) compared to the slower plate – Africa (296,400 km^3). I identify rifting along crustal weaknesses inherited from Paleozoic orogenic belts trending either parallel or perpendicular

to the Cretaceous rift margin. I calculate crustal stretching factors (Δ_c) for: 1) rift-orthogonal orogenic belts (Δ_c=4.3-5); 2) suture zones and rift-parallel orogenic belts (Δ_c=2.5-3.5). Obliquely-oriented belts show evidence of moderate thinning with intermediate thinning factors. The relationship between crustal and trend of crustal fabric is supported by my compilation of thinning factors from other rift zones worldwide.

CONTENTS

CHAPTER ONE:

INTRODUCTION TO THE DISSERTATION

CHAPTER TWO:

DEMERARA RISE, OFFSHORE SURINAME: MAGMA-RICH SEGMENT OF THE CENTRAL ATLANTIC OCEAN, AND CONJUGATE TO THE BAHAMAS HOT SPOT

CHAPTER THREE:

HOTSPOT ORIGIN FOR ASYMMETRY OF CONJUGATE, VOLCANIC MARGINS OF THE SOUTH ATLANTIC OCEAN AS IMAGED ON DEEPLY-PENETRATING SEISMIC REFLECTION IMAGES

CHAPTER FOUR:

CONTROL OF PALEOZOIC OROGENIC TRENDS ON ALONG-STRIKE VARIATIONS OF CRETACEOUS, CONTINENTAL STRETCHING AND FORMATION OF SOUTH ATLANTIC VOLCANIC PASSIVE MARGINS

CHAPTER ONE:

INTRODUCTION TO THE DISSERTATION

1.1 History and development of this dissertation

In the fall of 2011, I chose to leave a 12-year-long career in the construction and contracting industry and enrolled in the master's degree program in Geology at the Department of Earth and Atmospheric Sciences at the University of Houston (UH). I had earned a B.S. degree in Geology from Wright State University in 1999, but had opted to enter the burgeoning construction and contracting industry following graduation. In 2011 had decided my career path would be more fulfilling in geosciences and that a MS degree with a thesis study would help facilitate the goal of facilitating a job in the Houston-based oil exploration where my wife was also employed.

My original plan in graduate school in the fall of 2011 was to earn a Master's degree in the standard time of two years and seek a job in the Houston oil industry upon graduation in August of 2013. By the end of the spring semester of 2012, I realized that that the questions that I was interested in studying in the Central and South Atlantic Oceans needed to be addressed in a more systematic and detailed study than allowed by a two-year MS program. It was that point and with the support of Dr. Mann, my wife, and three children, I made the decision to change from the MS program to the PhD program of the UH Department of Earth and Atmospheric Sciences.

Dr. Mann encouraged grad students like myself to regularly present their research at UH seminar seminars and at conferences as a way to communicate their main results, receive critical feedback from a larger peer group, and gain self-confidence. Through the course of this five-year study I have given 8 seminars at UH, 4 seminars at ION Geophysical (my employer since 2013) and 7 seminars at national and international meetings. In addition, my presentations included my involvement in the AAPG Imperial Barrel Award class at UH taught by Drs. Mann and John Castagna in the spring semester of 2013. The five-person UH team - for which I was elected team captain – placed third out of a field of nine universities of the AAPG Gulf Coast Section based on our analysis of the subsurface data from the Cooper basin, Australia.

I was also selected with 14 other grad students to compete in the poster competition of the 2012 AAPG ACE conference held in Pittsburgh, Pennsylvania, and I placed third in a student poster competition at the September, 2016 meeting of the Houston Geological Society-Africa conference held in Houston. I also received a third place poster award for the advanced PhD category at the May, 2016 student poster competition at the annual Student Research Day of the Department of Earth and Atmospheric Sciences.

Spectrum Geo Inc., one of the sponsors and seismic data providers of the Caribbean Basin Tectonic and Hydrocarbon (CBTH) hired me as a summer intern in 2012 where my main task was interpreting seismic data from the Brazilian Equatorial Atlantic. This experience exposed me to the area of seismic

interpretation. This summer internship experience led me to investigate other rifted margins of South America and to ask more questions and seek larger geophysical data sets regarding the evolution of Atlantic rifted margins.

I returned to UH in the fall of 2012 and began to expand my learning beyond the classroom by reading about topics of interest for my studies in peer-reviewed journals as summarized in this dissertation. In areas of my interest, I searched for areas of consensus, areas of controversy, and how the controversial areas were sometimes the result of different groups using different data types to investigate the controversial issue.

I was hired as an intern for the summer of 2013 at ION GXT, which is well-known for regional, tectonic scale seismic data and an emerging interpretation team. The first week at ION GXT reaffirmed my purpose and focus to study rifted-passive margins. I was intrigued with tectonic-scale processes at rifted margins and wanted to pursue that aspect as the focus of my dissertation. At ION, I was provided access to the highest-quality crustal-scale global seismic data and began to explore more areas of South America and the South Atlantic. The majority of my full-time work at ION GXT included work from the South Atlantic and occasionally the conjugate margins of West Africa, so there was a strong overlap between my job and my dissertation study.

Shortly after my arrival at ION GXT, the raw data from offshore Suriname were being processed. Brian Horn, Jim Pindell, and my colleagues at ION GXT

were intrigued, as was I, on the possibility that the Demerara Rise, offshore Suriname, was a volcanic passive margin based on the new data. These new ION data from this margin provided an opportunity to contribute new ideas about the Demerara Rise and function as Chapter 2 for my dissertation. I was offered a full time position at ION GXT in the fall of 2013 with the understanding that I would be able to juggle the new job, the UH courses, and dissertation research, and my family life.

As most of my ION work continued to focus on the South Atlantic, I began to notice certain similarities and differences between South Atlantic conjugate margins. Many “water-cooler” type conversations with an ION colleague, Joe Paul, made the asymmetrical nature between the west African margin and the South American margin evident. My supervisor, Brian Horn, agreed that such a comparative study could be added to my ION workload and be contributed to my project as Chapters 3 and 4 of this dissertation.

The subject of volcanic passive margins (VPM) offers many remaining processes to be explained using high-quality geophysical data. This dissertation attempts to explain several of these processes of VPMs of Suriname, Uruguay, Southern Brazil, and Namibia.

1.2 Outline and organization of this dissertation on volcanic margins of the south-Central and South Atlantic

This dissertation contains three chapters on the geological and geophysical study using 33,000 km of 2D seismic data from the volcanic margins of the

Demerara Rise (offshore Suriname) in the south-Central Atlantic and the conjugate margins of the South Atlantic. The main scientific themes for all three chapters include: 1) defining the geographical limits of the crustal domains (oceanic, SDRs/igneous, continental) and establishing criteria for their interpretation based mainly on interpretation of deeply-penetrating seismic reflection data; 2) recognizing internal features and transitions between the domains; and 3) reconstructing the tectonic evolution of the margins both in map view and in cross sectional view.

Chapters 2, 3, and 4 were written in the format of journal papers. Chapter 2 on the Demerara Rise was submitted to the SEG journal Interpetation in November, 2014, and published in February, 2016. The coauthors of the paper were Dr. Brian W. Horn and Dr. James Pindell and the reviewers of the manuscript included Douglas Paton (University of Leeds) and Rod Graham. I plan to submit Chapter 3, which was coauthored by Dr. Paul Mann and Dr. James Pindell, to the journal *Geochemistry, Geophysics, Geosystems* in May, 2017, and Chapter 4, which was coauthored by Dr. Paul Mann, to the journal Tectonophysics in May, 2017.

1.2.1 Chapter 2 summary

The Demerara Rise of offshore Suriname was previously thought by Greenroyd et al. (2008) and Basile et al. (2013) to be a broad (110,000 km^2) plateau of continental origin that marked the intersection of the Central and Equatorial domains of the Atlantic Ocean (Fig 1.1). These previous studies

utilized short-record (8-second TWT) seismic profiles to base interpretations of the younger, Cenozoic intervals of the Demerara Rise (Gouyet, 1988; Greenroyd et al., 2008; 2009; Basile et al., 2013). In 2013, 40-km-deep record seismic profiles were acquired by ION that imaged a much more complex Mesozoic tectonic evolution for the Demerara Rise than had been previously known (Fig 1.1).

Chapter 2 uses 5,500 km of deep-penetrating data over the Demerara Rise to support the hypothesis that a magma-rich VPM formed during the initial Jurassic phase of opening of the Central Atlantic by separation of the North American and combined Africa-South American plates (Fig 1.1). The Demerara Rise is underlain by up to 24 km-thick SDRs/ igneous crust that is overlain by Jurassic and younger passive margin sediments related to the Central Atlantic rift and passive margin phase. The VPM interpretation I propose for the Demerara Rise in Chapter 2 raises the question of whether its conjugate margins in Guinea Bissau, Florida, and the Bahamas are also VPM's (Fig 1.1).

The VPM's of the South Atlantic have been previously studied using limited refraction data, shallow-record 2D reflection data, and sparse, deep-record seismic data (Abreu et al., 1997; Gladczenko et al., 1997; Jackson et al., 2000; Mohriak et al., 2002; Franke et al., 2010; Blaich et al., 2011; Blaich et al., 2013; Becker et al., 2014; Koopman et al., 2014; Stica et al., 2014) (Fig 1.1). Margin-parallel zones of seaward-dipping reflectors (SDRs) have been mapped using the shallow-penetrating seismic data. More deeply-penetrating seismic data has constrained the limits of this igneous belt of the VPM related to the second

phase of Barremian (131 Ma) South Atlantic opening related to the separation of Africa and South America (White and McKenzie, 1989; O'Connor and Duncan, 1990; Gladczenko et al., 1997; Jackson et al., 2000; Blaich et al., 2011; Becker et al., 2014; Koopman et al., 2014).

1.2.2 Chapter 3 Summary

Chapter 3 of this dissertation focuses on using this same type of deeply-penetrating seismic data to map the conjugate distribution of the SDR complexes at the margins between Uruguay/southern Brazil and Namibia in the South Atlantic Ocean (Fig 1.1). Using 27,550 km of 40-km-deep 2D seismic data, I mapped the crustal limits of the SDR complexes/igneous crust on both conjugate margins. Mapping and quantitative analysis efforts led to my recognition of the asymmetrical distribution of SDRs (South American margin: 201,700 km^3; Namibian margin: 296,400 km^3). I identified the wider and thicker emplacement of SDR's on the trailing plate of Africa within the tectonic context of northwest-directed absolute plate motion and rapid initial continental break-up during the Barremian-Aptian (131-126 Ma) opening of the South Atlantic Ocean.

1.2.3 Chapter 4 Summary

Chapter 4 uses the same 27,550 km of 2D seismic data from the South Atlantic used in Chapter 2 to map the conjugate zones of stretched continental crust on the margins of Uruguay/southern Brazil and Namibia (Fig 1.1). Chapter 4 integrates previously studied onshore orogenic belts and suture zones of the South Atlantic. Results of my interpretation and mapping confirms that rifting in

the South Atlantic occurred along pre-existing zones of weakness controlled by north-south-trending, rift-parallel orogenic fold belts and by intersections between north-south-trending rift-parallel and east-west-trending rift-orthogonal, Paleozoic orogenic belts. The amount of crustal stretching as measured by thickness of un-thinned continental crust/thickness of thinned continental crust ranges from stretching factor values of 2.5 to 3.5 at rift-parallel margin segments and 4 to 5 at rift-orthogonal oriented foldbelts. These stretching factors fall within published calculated values that I compiled from other VPM's and non-VPMs.

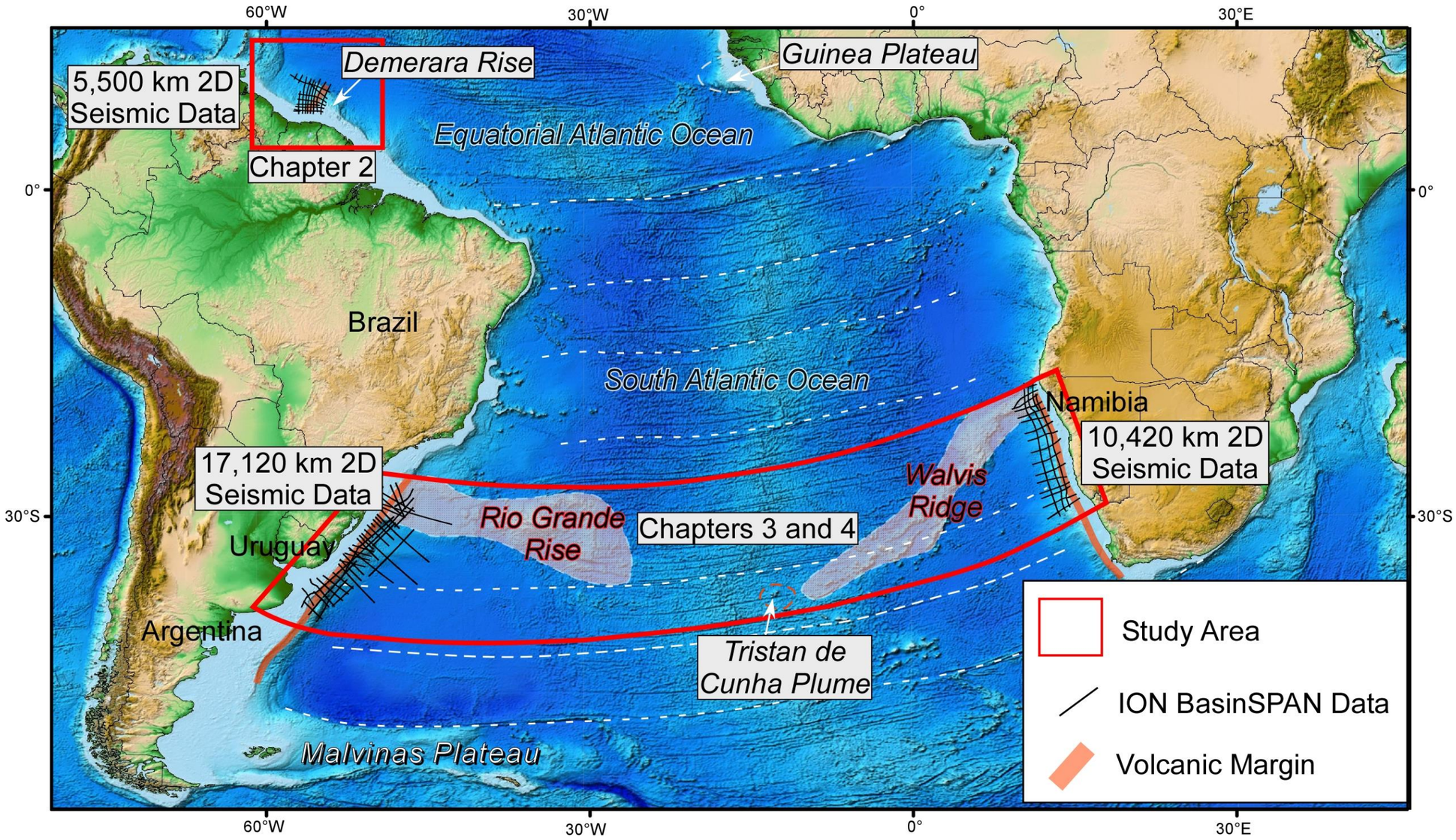

Figure 1.1: Location map of the dissertation areas of study on bathymetry and topography grid. A) The Demerara Rise, offshore Suriname (Chapter 2); B) The conjugate margins of Uruguay/southern Brazil and Namibia (Chapters 3 and 4).

Chapter One: References

Abreu, V.S., Vail, P.R., Bally, A., Wilson, E., 1997, Geologic evolution of conjugate volcanic passive margins: Influence on the petroleum systems of the South Atlantic: Houston Geological Society Bulletin, 40, 10-11.

Basile, C., Maillard, A., Patriat, M., Gaullier, V., Lonke, L., Roest, W., Mercier de Lepinay, M., and Pattier, F., 2013, Structure and evolution of the Demerara Plateau, offshore French Guiana: Rifting, tectonic inversion and post-rift tilting at transform-divergent margins intersection: Tectonophysics, 591, 16-29.

Becker, K., Franke, D., Trumbull, R., Schnabel, M., Heyde, I., Schreckenberger, B., Koopmann, H., Bauer, K., Jokat, W., and Krawczyk, C., 2014, Asymmetry of high-velocity lower crust on the South Atlantic rifted margins and implications for the interplay of magmatism and tectonics in continental breakup: Solid Earth, 5 (2), 1011-1026.

Blaich, O. A., J. I. Faleide, and F. Tsikalas, 2011, Crustal breakup and continent-ocean transition at South Atlantic conjugate margins: Journal of Geophysical Research Solid Earth, 116, 1–36.

Blaich, O.A., Faleide, J.I., Tsikalas, F., Gordon, A.C., and Mohriak, W., 2013, Crustal-scale architecture and segmentation of the South Atlantic volcanic margin. In: Mohriak, W.U., Danforth, A., Post, P.J., Brown, D.E., Tari, G.C., Nemcok, M., and Sinha, S.T. (Eds.),

Franke, D., S. Ladage, Schnabel, M., Schreckenberger, B., Reichert, C., Hinz, K., Paterlini, M., de Abelleyra, J., and Siciliano, M., 2010, Birth of a volcanic margin off Argentina: South Atlantic, Geochemistry, Geophysics, Geosystems, 11, Q0AB04, doi:10.1029/2009GC002715.

Gladczenko, T.P., Hinz, K., Eldholm, O., Meyer, H., Neben, S., and Skogseid, J., 1997, South Atlantic volcanic margins: Journal of Geological Society, 154, 465-470.

Gouyet, S., 1988, Evolution tectono-sédimentaire des marges guyanaise et nordbrésilienne au cours de l'ouverture de l'Atlantique Sud. Ph. D. Thesis, Université de Pau.

Greenroyd, C. J., Peirce, C., Rodger, M., Watts, A.B., and Hobbs, R. W., 2008, Demerara Plateau— the structure and evolution of a transform passive margin: Geophysical Journal International 172, 549–564.

Jackson, M.P.A., Cramez, C., and Fonck, J.M., 2000, Role of subaerial volcanic rocks and mantle plumes in creation of South Atlantic margins: Implications for salt tectonics and source rocks: Marine and Petroleum Geology, 17, 477-498.

Koopmann, H., Schreckenberger, B., Franke, D., Becker, K., and Schnabel, M., 2016, The late rifting phase and continental break-up of southern South Atlantic: The mode and timing of volcanic rifting and formation of earliest oceanic crust. In: Wright, T. J., Ayele, A., Ferguson, D. J., Kidane, T., and Vye-Brown, C. (eds) 2016, Magmatic Rifting and Active Volcanism: Geological Society, London, Special Publications, 420, 315–340.

Mohriak, W.U., Rosendahl, B.R., Turner, J.P., and Valente, S.C., 2002, Crustal architecture of South Atlantic volcanic margins. In: Menzies, M.A., Klemperer, S.L., Ebinger, C.J., Baker, J. (Eds.), Volcanic Rifted Margins: Geological Society of America Special Paper 362, 159-202.

O'Connor, J.M. and Duncan, R.A., 1990, Evolution of the Walvis Ridge-Rio Grande Rise Hot Spot System: Implications for African and South American Plate Motions Over Plumes: Journal of Geophysical Research, 95, 17,475–17,502.

Pindell, J.L., 1985, Alleghanian reconstruction and subsequent evolution of the Gulf of Mexico, Bahamas, and Proto-Caribbean: Tectonics, 4, 1-39.

Stica, J.M., Zalan, P.V. and Ferrari, A., 2014, The evolution of rifting on the volcanic margin of the Pelotas Basin and the contextualization of the Parana–Etendeka LIP in the separation of Gondwana in the South Atlantic: Marine Petroleum Geology, 50, 1–21.

White, R. S., and McKenzie, D., 1989, Magmatism at rift zones: The generation of volcanic continental margins and flood basalts: Journal of Geophysical Research, 94, 7685–7729.

CHAPTER TWO:

DEMERARA RISE, OFFSHORE SURINAME: MAGMA-RICH SEGMENT OF THE CENTRAL ATLANTIC OCEAN, AND CONJUGATE TO THE BAHAMAS HOT SPOT

Chapter Two published as:
Reuber, K., Pindell, J., and Horn, B.W., 2016, Demerara Rise, Offshore Suriname: Magma-Rich Segment of the Central Atlantic Ocean, and Conjugate to the Bahamas Hot Spot: SEG *Interpretation*, 4/3, 31-45.

2.1 Summary

The tectonic histories of volcanic and non-volcanic passive margins are commonly characterized by a discrete period of rifting associated with initial continental extension, followed by a passive margin phase associated with the initiation of sea floor spreading (Wilson, 2001; Geoffroy, 2005; Franke, 2012). However, the Demerara Rise is unique in that its western margin is related to the opening of the Central Atlantic and its northern and eastern flanks are related to the opening of the Equatorial Atlantic (Pindell, 1985; Gouyet, 1988; Greenroyd et al., 2007a; Pindell and Kennan, 2009; Basile et al., 2013). As seismic data acquisition and processing technology improve for deep subsurface studies, new conclusions can be derived that help provide clarity to existing geologic and tectonic models for underexplored frontier regions, such as offshore Suriname.

In this study, I present an interpretation of newly acquired seismic reflection data for the Demerara Rise and deepwater offshore Suriname (Fig. 2. 1 A and B). This deeply penetrating, high resolution dataset was collected as part of a multi-client venture by ION Geophysical in 2013. The GuyanaSPAN

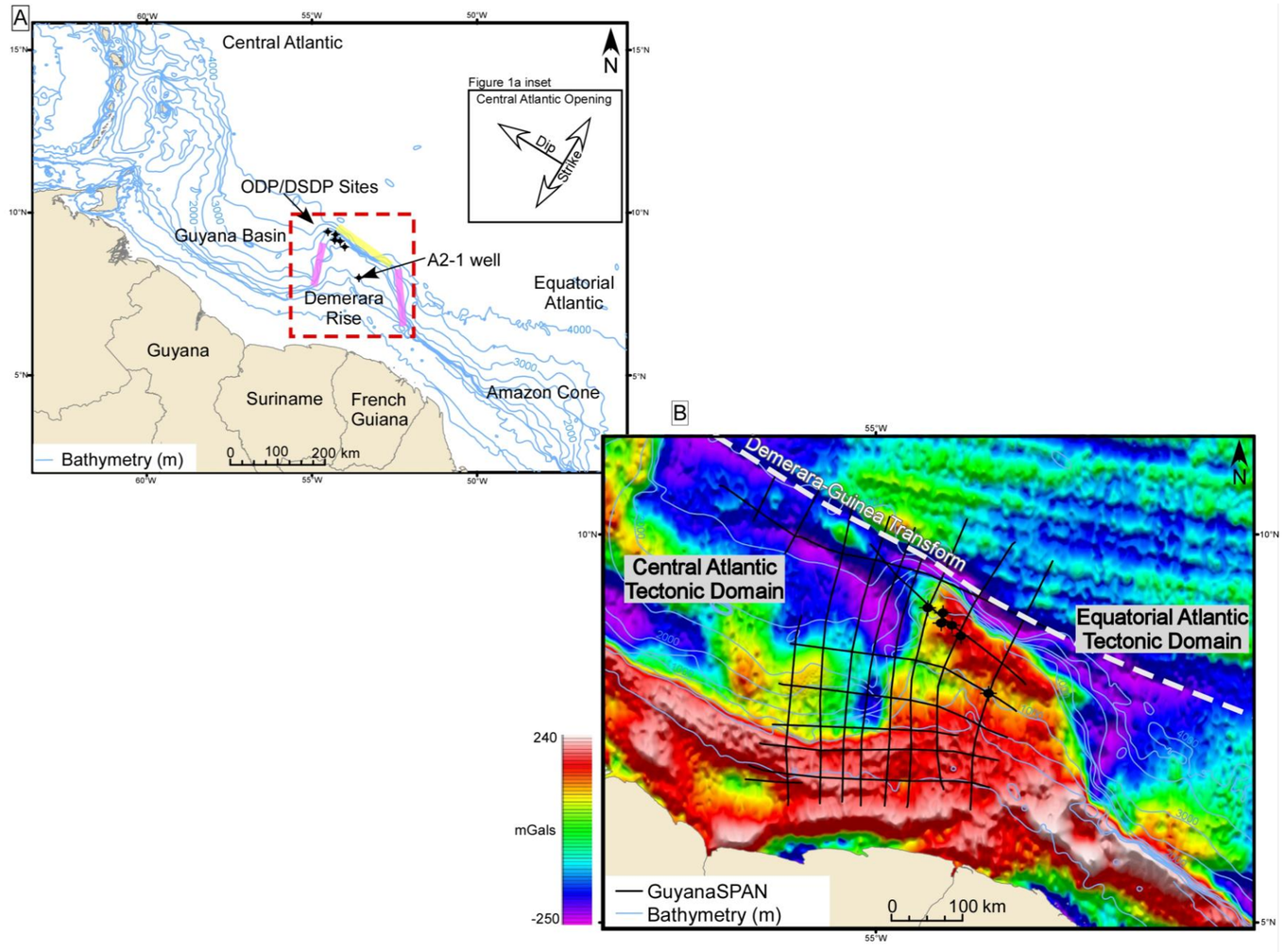

Figure 2.1: A) Regional location map of the Demerara Rise and study area (in red) with bathymetry contours showing the overall geometry of the Demerara Rise and the broad continental shelf to the south. Major features include the Guyana Basin and the Amazon Cone that are present on each of the oceanic domains of the Central and Equatorial Atlantic. Key wells from ODP/DSDP and hydrocarbon exploration (A2-1) are shown and referred to in the text. Given the varied nature of the tectonic phases for the Demerara Rise, divergent margin segments are identified in pink, and sheared margin segment in yellow. Inset) providing dip and strike orientation to the Central Atlantic tectonic phase. B) High resolution free-air gravity image (Sandwell and Smith, 2009) illustrating the location of the Demerara survey across the Demerara Rise (courtesy of Mark Longacre from MLB). Tectonic domains of the Central and Equatorial events are delineated (white line) and an "ocean-ocean boundary" exists where they are adjacent. The Demerara-Guinea Transform separates the tectonic domains. (Free-air anomaly gravity data: reds represent gravity highs; blues represent gravity lows.)

survey was designed to provide a full breadth of coverage for the Demerara Rise in order to better understand the tectonic phases, stratigraphic intervals, and crustal transitions from the continental shelf of Suriname to the various oceanic domains of the Central and Equatorial Atlantic (Fig. 2.1B). The primary goals of this study are to present new observations on the early stages of the tectonic evolution of the Demerara Rise and to test for evidence of hot-spot-related volcanism associated with the opening of the southern Central Atlantic Ocean. Additionally, an important implication for hydrocarbon exploration is that sequences below the Central Atlantic passive margin sediments may be magmatically-derived rather than a large sequence of sedimentary syn-rift. Therefore, Central Atlantic Phase syn-rift source rocks would be sparse or completely absent and prospective intervals are limited to the latest Jurassic or younger. This study will contribute to a better understanding of the geologic history of the Demerara Rise, while also providing critical insights into its conjugate margins of Southern Florida/Bahamas and Guinea in Equatorial West Africa.

2.2 Volcanic and non-volcanic margins

Two end-member classifications exist for giant rifted margins: 1) Volcanic margins and 2) Non-volcanic margins (Franke, 2012). Each type possesses unique elements which are linked to their tectonic evolution. A general geometry of downward and basinward-dipping reflector packages within modern seismic data is a consistent feature shared by both classifications (Planke et al., 2000). Determining the genetic origin of these reflectors is critical to properly classifying

the margin's evolution.

Volcanically rifted margins are observed to have thick packages of magmatically derived material that represent the syn-rift tectonic phase (Hinz, 1981; Mutter et al., 1982; White et al., 1987 Eldholm et al., 1995) and underlie the passive margin sequences (Skogseid, 2001; Menzies et al., 2002). Seismic reflection data of thick volcanic wedges typically reveal sequences of seismic events that are related to voluminous outpourings of magma during the rifting stage (Planke et al., 2000; Franke, 2012). These sequences have internal reflections that dip basinward/seaward and are commonly referred to as Seaward Dipping Reflectors (SDRs) (Planke et al., 2000, Menzies et al., 2002; Pindell et al., 2014). Loss of reflectivity below the SDRs is common on volcanic margins (Geoffroy, 2005). Without physical evidence, determining the origin of these SDRs involves the use of analogs and seismic facies analysis (Planke et al., 2000).

Non-volcanic margins have variable syn-rift sedimentary infill of rotated fault blocks overlying thinned continental crust (Geoffroy, 2005). Basement structure, syn-rift and passive margin sediments have a transparent response in seismic data and therefore are more revealing (Geoffroy, 2005). Basinward and downward dipping reflectors are also present on non-volcanic margins, but they show evidence of depositional responses to sea level fluctuations (Planke et al., 2000). These sequence-stratigraphic units record variations in accommodation and sediment supply (Planke et al., 2000). The presence of these stratigraphic features assists in determining the genetic origin of the dipping reflectors

(Planke et al., 2000; Pindell et al., 2014).

2.3 Regional tectonic setting

The Demerara Rise is a positive bathymetric feature that covers approximately 170,000 km^2 in the offshore Equatorial Atlantic (Fig. 2.1A). It is positioned between the deepwater Guyana Basin offshore Guyana to the west and the offshore region of French Guiana to the east (Fig. 2.1 A and B). Water depths on the Demerara Rise are relatively shallow at the crest (approximately 40 m) and gradually deepen to the respective abyssal plains reaching depths greater than 3,000 m on its eastern and western flanks (Fig. 2.1 A and B).

The tectonic and stratigraphic history of the Demerara Rise encompasses two tectonic phases, the Central Atlantic tectonic phase and the Equatorial Atlantic tectonic phase (Fig. 2.2) (Pindell, 1985; Mascle et al., 1987; Pindell and Kennan, 2001; Greenroyd et al., 2008; Basile et al., 2013). This dual-phase history resulted in a stratigraphic record that provides clues to the role played by the Demerara Rise in Central and Equatorial Atlantic tectonic reconstructions (Fig. 2.2) (Pindell, 1985, Basile et al., 2005; Moulin et al., 2010). Within this study I refer to the Central Atlantic tectonic phase and the Equatorial Atlantic tectonic phase as the first and second tectonic phases, respectively (Fig. 2.2). Figure 2.2 is a generalized stratigraphic column for the Suriname-Guyana Basin (Staatsolie, 2013) illustrating the correlation with the interpreted horizons from this study. The stratigraphy is partially constrained by the A2-1 well which penetrated Jurassic carbonates related to the drift phase of the Central Atlantic

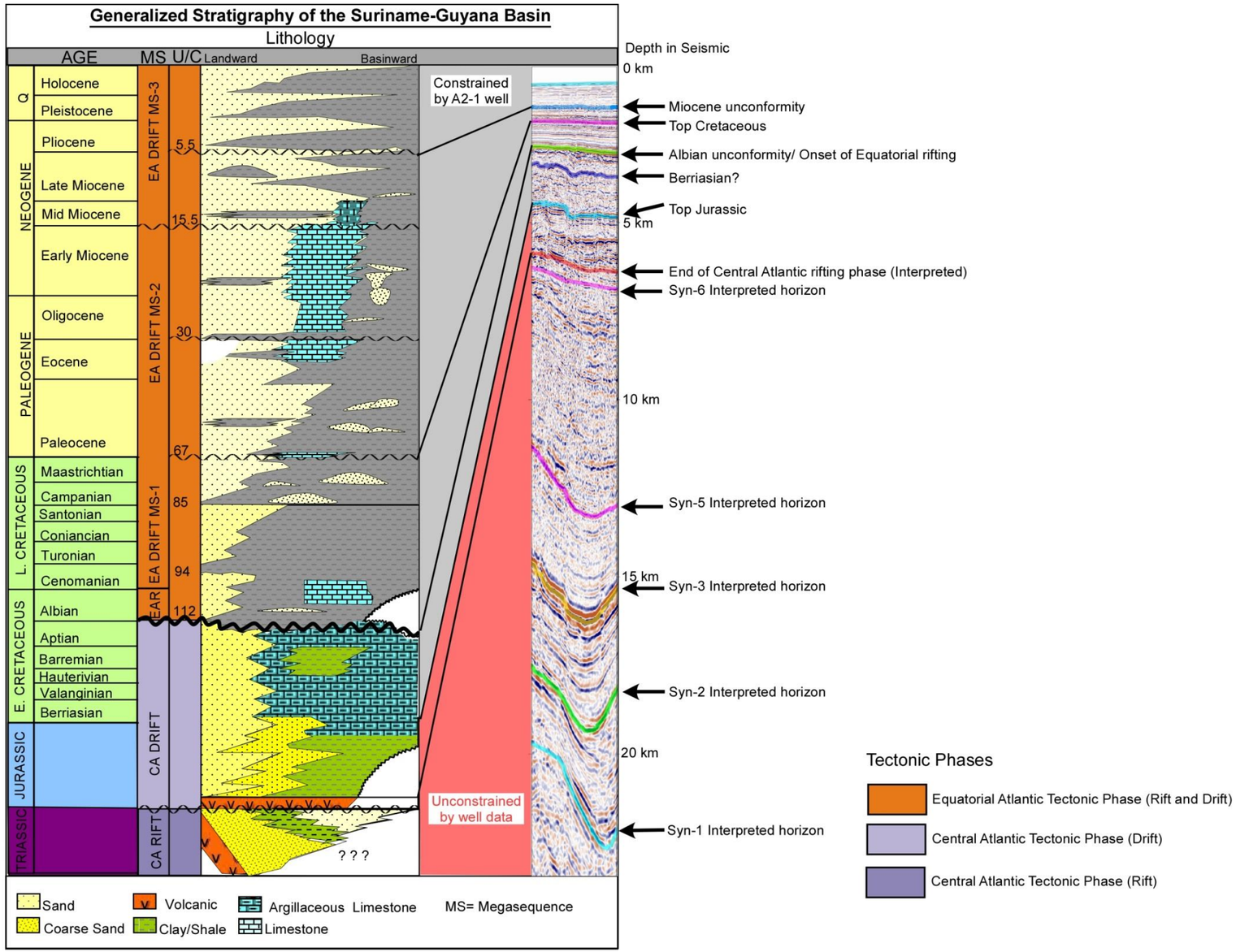

Figure 2.2: A generalized stratigraphic column (Staatsolie, 2013) illustrating the correlation with the recently acquired GuyanaSPAN seismic data. The stratigraphic units below the late Jurassic carbonates are not constrained, as only the A2-1 well (Fig. 1A) has penetrated Jurassic units. Also, illustrated are geologic time divisions for the two major tectonic phases (Central Atlantic and Equatorial Atlantic). Lower interpreted horizons (Syn 1-6), now visible on deep penetrating seismic, are not represented on the stratigraphic column.

(Fig. 2.2) (Staatsolie, 2013).

Previous efforts to reconstruct pre-breakup paleogeographic configurations of the southern Central and Equatorial Atlantic margins have incorporated variable margin overlaps, gaps, and proposed shortening events of the major plates (e.g., Bullard et al., 1965; Rabinowitz and LaBrecque, 1979).

These interpretations are a consequence of the uncertainties in the amount of continental crust beneath the Great Bank of the Bahamas and the Amazon shelf. With the advent of satellite gravity maps of the ocean floors (Fig. 2.1B), Pindell and Dewey (1982) proposed a tighter Equatorial fit that juxtaposed the Guinea and Demerara shelves as an original geometry within Gondwana. Pindell (1985), Moulin et al. (2010), Kneller and Johnson (2011) and Heine et al. (2013) followed this general model and explored adjustments in how the Great Bank, the Demerara Rise and the Guinea Plateau were juxtaposed prior to the opening of the Central Atlantic (Fig. 2.3A). Figure 2.3A shows the relative positions of these key tectonic features at approximately 158 Ma (Late Oxfordian), and is based on the assumption that the Great Bank is largely continental, as well as the association of the approximate lateral extent of the presumed hot-spot volcanism with formation of the southeastern most portions of the Bahamas. Figures 2.3B, 2.3C, and 2.3D show the subsequent displacement of these features and are described in this study as the Central Atlantic or Equatorial Atlantic Tectonic Phases. The apparent underlap of the 2,000 meter isobath at a restored position (Fig. 2.3A-C) indicates an interpreted contractional event for this plate model.

Figure 2.3: Four panel tectonic reconstruction of Meso-America (modified after Pindell and Kennan, 2009). A) Oxfordian plate reconstruction at ~158 Ma showing the recently initiated opening of the Central Atlantic and the location of the Bahamas hotspot that I now believe spilled over into the Demerara Rise during rifting and/or onset of seafloor spreading, and hence was initially an "on-spreading axis" hotspot. B) Berriasian plate reconstruction at 141Ma with all continental crust of South Florida and the western Bahamas in final place, and hence is post-rift for the southern Central Atlantic, although hot-spot volcanism parallel to Atlantic fracture zones continued in the eastern Bahamas, providing a shallow-water foundation for initial reef development. C) Early Aptian plate reconstruction at ~125Ma, near the onset of the Equatorial Atlantic rifting/drifting that produced transpression and peneplanation of the Demerara Rise. D) Middle Albian plate reconstruction estimated at ~104 Ma, illustrating the activation of the Demerara-Guinea Transform, subsequent to all presumed Bahamian hot spot activity, and during the drift stage for the Equatorial Atlantic, following Pindell and Dewey (1982).

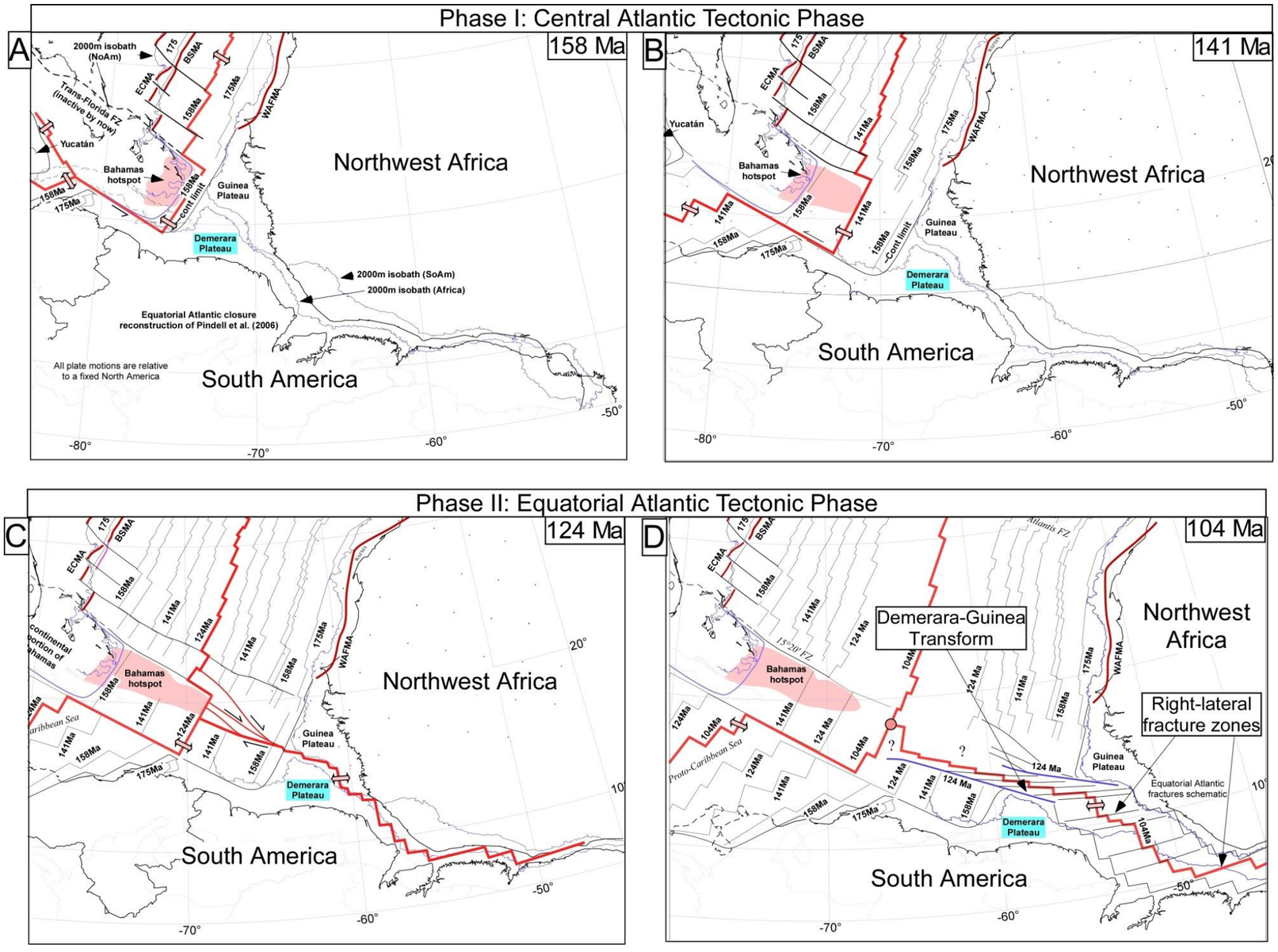
Phase I: Central Atlantic Tectonic Phase
A
158 Ma
2000m isobath (NoAm)
Trans-Florida FZ (inactive by now)
Yucatán
Bahamas hotspot
ECMA
BSMA
175
158Ma
175Ma
WAFMA
Guinea Plateau
Demerara Plateau
Northwest Africa
2000m isobath (SoAm)
2000m isobath (Africa)
Equatorial Atlantic closure reconstruction of Pindell et al. (2006)
All plate motions are relative to a fixed North America
South America
-80°
-70°
-60°
-50°
B
141 Ma
141Ma
Cont limit
Phase II: Equatorial Atlantic Tectonic Phase
C
124 Ma
124Ma
continental portion of Bahamas
Caribbean Sea
20°
D
104 Ma
104Ma
Atlantis FZ
15°20' FZ
Proto-Caribbean Sea
Demerara-Guinea Transform
Right-lateral fracture zones
Equatorial Atlantic fractures schematic

Figure 2.3B illustrates the southern Central Atlantic at 141 Ma (Berriasian) after further separation of Africa and North America, although there is no conclusive evidence that the Guinea Plateau and the Demerara Rise had begun to separate. The Demerara A2-1 well showed that shallow-water carbonate deposition had been established by this time (Fig. 2.2) (Staatsolie, 2013), and thus the western margins of Guinea Plateau and Demerara are shown as a continuous passive margin of the SE Central Atlantic (Pindell, 1985; Erbacher et al., 2004; Pindell, 2014). Mascle et al. (1988) proposed a similar Jurassic Central Atlantic rift and drift phases for the Guinea Plateau.

Figure 2.3C represents the transition from the Central Atlantic Tectonic Phase to the Equatorial Atlantic Phase for the Demerara Rise. The stratigraphy of the Equatorial Atlantic marginal basins suggests that these margins began to rift at 125 Ma-113 Ma (Barremian-Aptian) as a series of alternating dextral transforms and en-echelon pull-apart basins (Fig. 2.3D) (Pindell, 1985; Greenroyd et al., 2007a & 2007b; Basile et al., 2013). This later rifting event, the Equatorial Atlantic Tectonic Phase, is the second tectonic phase where the Demerara Rise was further flanked by transform faults to the north and a N-S rift segment on its eastern flank (Fig.2.3D) (Pindell, 1993; Pindell et al., 2006; Greenroyd et al., 2007a and 2007b; Basile et al., 2013). A series of right-lateral paleo-transform faults, now fracture zones, delineate the relative path of the plates from the conjugate margins of northern South America and Equatorial Africa (Fig. 2.3D) (Pindell et al., 2006; Moulin et al., 2010). The transform faults were locally transpressional and/or transtensional as plate motion proceeded

(Greenroyd et al., 2007a and 2007b; Basile et al., 2013). Folds, inversion features, and thrust faults affecting early marginal strata have been documented along other sheared margins in the Equatorial Atlantic, such as the Ceará Basin in Brazil at the Romanche Fracture (paleo-transform) Zone (Zalan, 1984; Azevedo, 1991, Davison, 2013). The formation of the Demerara-Guinea transform between the once-continuous Demerara Rise and Guinea Plateau resulted in a sheared margin to the north of the Rise (Fig. 2.1A (yellow bar) and Fig. 2.3D), and a divergent eastern flank (Fig. 2.1A (pink bar)) (Benkhelil, et al., 1995; Greenroyd et al., 2007a & 2007b; Basile et al., 2013). Volcanism associated with rifting in the Equatorial Atlantic Tectonic Phase has only locally been documented and appears to be very minor when present (Gouyet, 1988; Azevedo, 1991; Greenroyd et al., 2008).

2.4 Previous studies

The lack of exploration activity in deepwater offshore Suriname and the shallow Demerara Rise has resulted in a limited understanding of the region's earliest geologic history. Despite oil and gas shows within the small number of offshore wells, commercial hydrocarbon production has not been established (Staatsolie, 2013). Previous studies have generally concentrated on the eastern flank or the shallow geologic intervals of the Demerara Rise (Loncke et al., 2009; Mosher et al., 2005). In 2004, the Ocean Drilling Program (ODP) published results of drilling operations and seismic acquisition at the northwest flank of the Demerara Rise (Fig. 2.1A), which were primarily focused on

gathering data related to relatively recent geologic intervals, primarily pertaining to the Equatorial Atlantic tectonic phase (Erbacher et al., 2004). These cores penetrated the Albian unconformity as interpreted by Gouyet (1988), which marks the stratigraphic boundary between the two tectonic phases (Loncke et al., 2009; Mosher et al., 2005).

Greenroyd et al. (2007a) published their model of the crustal architecture at the eastern flank of the Demerara Rise, the obliquely rifted French Guiana margin, and the Foz do Amazonas Basin, which was interpreted using Ocean Drilling Project data. Greenroyd et al. (2007a) modeled rift margin profiles of Suriname, French Guiana, and the Amazon Cone from multi-channel seismic and wide-angle refraction data. The objective of this earlier study was to characterize the Cretaceous Equatorial Atlantic tectonic phase of the easternmost Demerara Rise, as opposed to the older opening of the Central Atlantic at the western margin.

Although our understanding of the Cretaceous equatorial tectonic phase has improved, the Jurassic Central Atlantic tectonic phase of the Demerara Rise remains relatively un-investigated with few constraints on basement and early syn-rift history. Deep seismic intervals below the prominent Albian unconformity have been previously considered to be continental crustal layers that provide the shallow bathymetric expression of the Demerara Rise (Greenroyd et al., 2007a, Basile et al., 2013). The data utilized in this study provides evidence of a deeper, more complex core to the Demerara Rise.

2.5 Data

The data used in this study were sourced from the ION Geophysical GuyanaSPAN multi-client project (Fig. 2.1A and B). The SPAN project is composed of approximately 5,500 km of seismic data in water depths of 40 - 3,500 meters. The source consisted of a bolt and sleeve air-gun with 9 guns per string and 4 strings per array at a depth of 8.5 meters. Seismic reflection data from shot intervals spaced at 50 meters were recorded at 2 millisecond sample rate within 408 channels to 18 seconds. Receiver depth for the acquisition was 15 meters. Data processing from raw stacks to a final pre-stack depth migration (used in this study) included proprietary ION Geophysical applications and processing workflow.

2.6 Observations

Analysis of the 18 second (two-way travel time) / 40 km-deep record seismic data revealed thick seismic successions that extend to depths greater than 35 km below sea level (Fig. 2. 4A and B). Deep seismic reflections are concordant, have medium to high frequency, and are steeply dipping in various directions (Fig. 2.4A and B). Discrete packages of reflectors dip downward and seaward/basinward and have a maximum dip direction to the northwest. The origins of these seismic reflections that underlie the transition from the broad shallow Demerara Rise to the abyssal plain have critical implications for defining the early history of the Demerara Rise.

A)

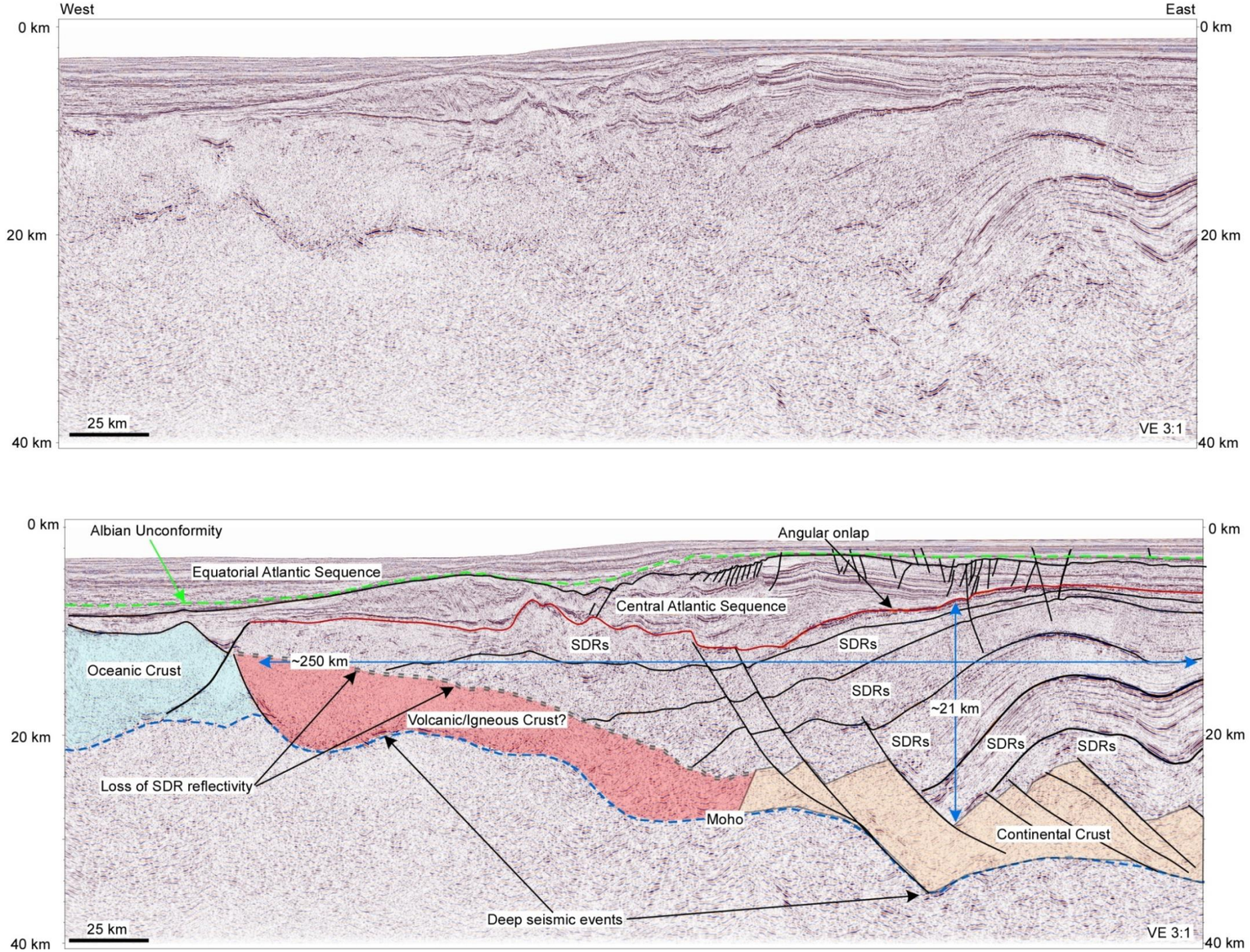

Figure 2.4A: A representative E-W dip line (un-interpreted above interpreted) from the GuyanaSPAN survey positioned atop the Demerara Rise. Crustal domains of continental and volcanic/igneous crusts are identified and subsequent SDRs that transition westerly to oceanic crust.

B)

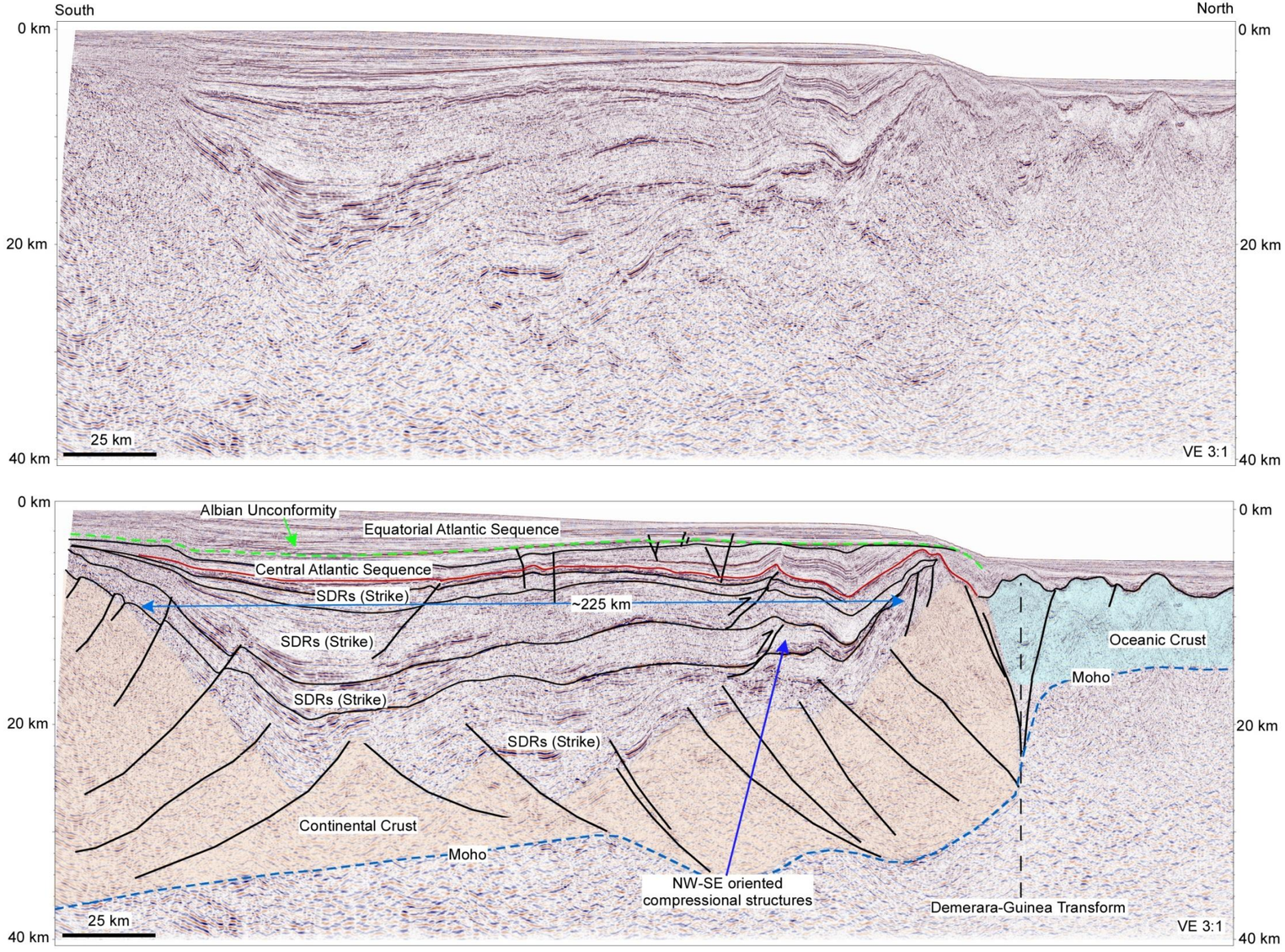

Figure 2.4B: A representative S-N line (un-interpreted above interpreted) showing similar features in the strike orientation and the transition from continental rocks into the northernly bounding oceanic crust.

Figures 2.4A (dip) and 2.4B (strike) are representative lines oriented with respect to the opening of the southern Central Atlantic Ocean (Fig. 2.1A inset). Figure 2.4A shows an unfaulted interval of parallel, continuous reflectors overlying the Albian unconformity horizon (Gouyet, 1988). Below the Albian unconformity, I observe a faulted and deformed succession of reflectors which appear to progressively onlap the underlying unit in an angular fashion (Fig. 2.4A). Below this angular onlap, six individual packages of seaward dipping seismic reflectors (SDRs) are observed. Seaward dipping reflector (SDR) packages lose reflectivity in the west and transition into a 10-12 km- thick zone of nondescripts, unstructured seismic events (Fig. 2.4A). At the western termination of these SDRs, deep seismic events are recognizable and show localized areas of continuity at 20 km below sea level (Fig. 2.4A).

Figure 2.4B illustrates the strike orientation for the same units in the eastern region of the survey. In Figure 2.4B, the uppermost stratigraphic packages are present over the shallow and deepwater regions of the Demerara Rise. The lower six seismic units, spanning South-North, display moderately concordant reflections that possess an undulating seismic character dipping in north and south directions (Fig. 2.4B).

2.6.1 Seismic intervals

Detailed observations of seismic data indicate six unique intervals of SDRs that comprise the majority of reflective units. Overall, the six observed individual SDR packages are convex upward and generally thicken and offlap westward

(Figs. 2.4 and 2.5). The variability between the units is observed in unit thickness, magnitude of dip angle, internal reflection character, and lateral extent (Figs. 2.4 and 2.5). The maximum thickness of the six units reaches approximately 21 km and extends E-W for approximately 250 km (Fig. 2.4A). The dip angles range from 8 to 20 degrees and decrease in the shallower overlying units (Fig. 2.5). Internal amplitudes are highly variable and no consistent trends within units were observed, with the exception of the high amplitudes at the uppermost interval of each unit (Fig. 2.5). Thickness of the individual SDR units generally increases with depth, but their spatial coverage decreases (Figs. 2.4 and 2.5). Each of these units possesses a unique set of geometries and seismic character that are described in the following sections. The oldest unit (Syn-1) is at the base of the seismic succession and the youngest unit (Syn-6) overlies the package of SDRs.

The maximum thickness of Syn-1 unit is 7,300 m and has basal reflectors at 28.7 km below sea level. The uppermost reflector is a continuous high amplitude event in the east that loses continuity to the west (Fig. 2.5). Internal reflections within the Syn-1 unit are disrupted and chaotic. The Syn-2 package is capped by a smooth, high amplitude reflector that has a reduction in amplitude in the west (Fig. 2.5). This SDR unit contains intermittent instances of parallel to sub-parallel reflectors (Fig. 2.5). Maximum thickness of the Syn-2 unit is approximately 2,400 m and the deepest reflector within the package reaches approximately 28.3 km below sea level (Fig. 2.4A). The Syn-3 SDR package is the deepest unit to exhibit highly continuous, and parallel to sub-parallel internal

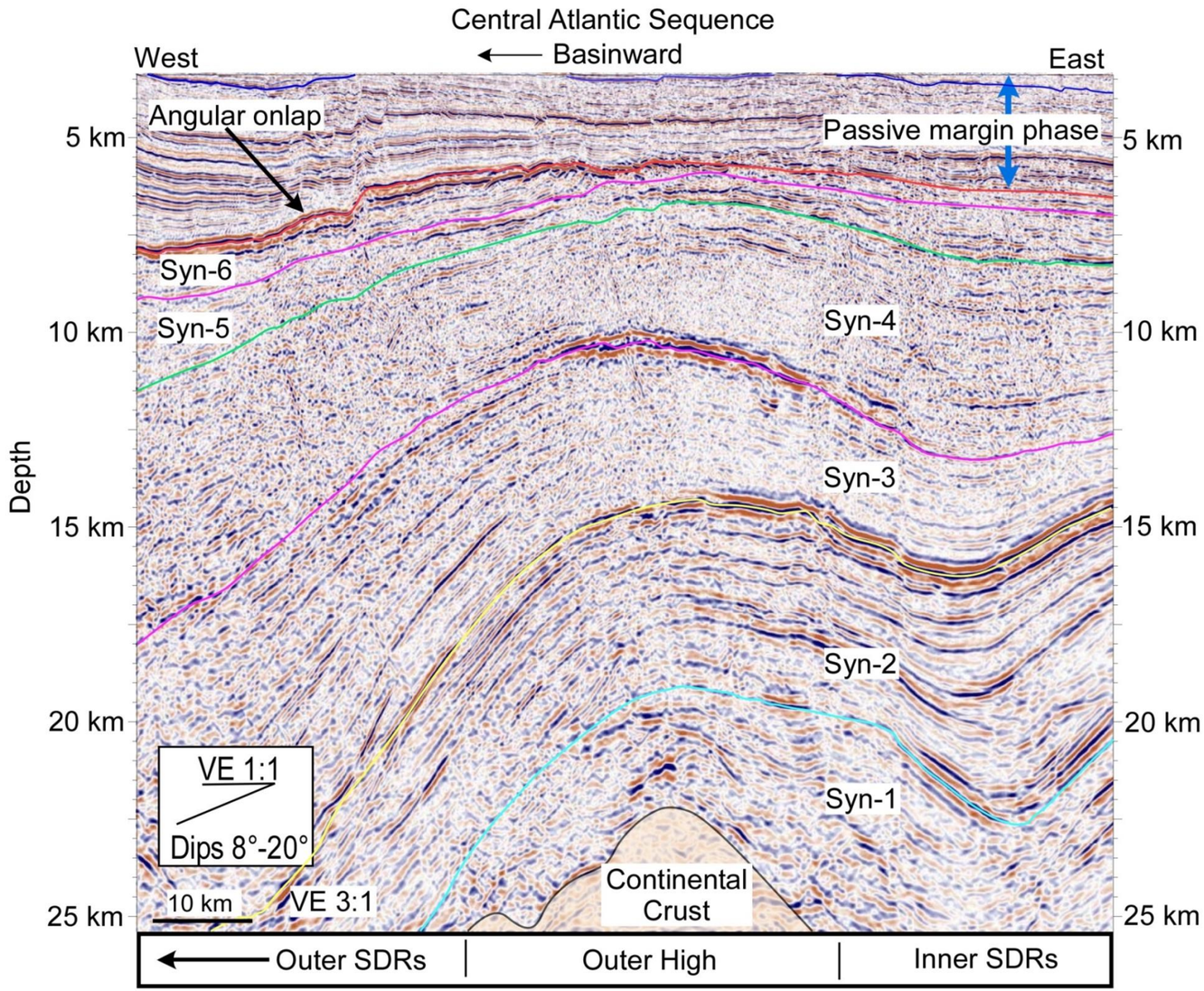

Figure 2.5: A zoomed-in view of the outer high, inner and outer SDRs and the six "Syn-Units." This view illustrates the variations of seismic character (internal and topmost) and high-amplitude reflectors that mark the inferred stagnation of magmatic activity and a likely erosional surfaces, and potential variations of unit composition (Syn1-6).

reflections dipping at approximately 20 degrees (Fig. 2.5). The average thickness of this package is 2,300 m and the deepest units reach 27.2 km in depth. Syn-4 package of SDRs extends for approximately 140 km to the West in the dip-direction. It exhibits parallel reflectors to the east that transition into chaotic, discontinuous events to the west (Fig. 2.4A). In the east, the top reflector for this unit is a smooth, high-amplitude reflector (Figs. 2.4 and 2.5). This unit of SDRs achieves its greatest thickness (8,400 m) at the approximate mid-point of the transect (Fig. 2.4A). Syn-5 is capped by a highly intermittent, but seismically bright, top reflector (Fig. 2.4A and 2.5). This unit has a lateral maximum extent of 235 km and a maximum thickness of 9,300 m (Fig. 2.4A). Maximum thickness was estimated over the approximate mid-point location where the bases of the resolvable SDR events lose reflectivity. Syn-6 is the final observed SDR unit which is composed of a relatively thin (avg. < 2000m), but laterally extensive series of reflectors (Fig. 2.4A and 2.5). The top reflector of this unit is a smooth, high-amplitude reflection that loses coherency in the western region (Fig. 2.4A). In the east, internal reflections are concordant with underlying units (Fig. 2.4A).

A zone of chaotic and unstructured amplitudes underlies the base of reflective SDRs and is present along the entire transect (Fig. 2.4A). The zone appears to range in thickness from 10-15 km, but shows variability east to west (Fig. 2.4A). The boundaries to this zone are deepest to the east and progressively shallow to the west (Fig. 2.4A). This basal zone appears to be segmented into three distinct regions that have an undulating basal reflection

and underlie the SDR units in the east and the layered reflectors in the west (Fig. 2.4A).

2.6.2 SDR units- volcanic sequences

Overall, the six identified downward and seaward dipping units lack any remarkable evidence for a sedimentary origin. The units do not exhibit stratal geometries that are indicative of sedimentary deposition as a response to sea level fluctuations. Alternatively, the six “Syn” SDR units are capped with bright, high-amplitude reflectors and present features that are indicative of volcanic margins outlined by Planke et al. (2000), Blaich et al. (2013) and Pindell et al. (2014). From these observations, I infer that the origin of the SDRs is related to magmatic activity which occurred at the earliest stages of continental break-up at the Demerara Rise (Planke et al., 2000; Geoffroy, 2005; Franke et al., 2012, Pindell et al., 2014). The thickness, dip angles, and geometries of the units are key indicators of large scale volcanism at a rifted continental margin (Planke et al., 2000; Pindell et al., 2014). The apparent lack of faulting and the in-filled nature of the large continental grabens indicate that the SDRs at the base of the section were likely deposited during and after a significant period of continental extension (Franke et al., 2000). Based on the tectonic model employed here, these volcanically derived units (Syn 1-6) (Fig. 2.4A and B) are likely related to the rift phase of the Central Atlantic opening.

The six “Syn-“units are divisible by their prominent high amplitude reflectors. This anomaly between units is most likely a result of weathering, erosion, and

alteration of the material between pulses of magmatic supply (Planke et al., 2000). Although the time intervals between eruptions are unknown, I interpreted that the variations of the various successions are related to periods of volcanic quiescence (Planke et al., 2000). The Syn-1 unit has been interpreted as the initial syn-tectonic unit within a prominent depression, possibly a rift basin, based on its geometry and position with the section (Figs. 2.4B and 2.5). The western seismic reflectors for this unit appear to terminate on a structure that is dipping to the east; interpreted as a fault bounded half-graben. I interpret their emplacement to have occurred at the earliest stages of volcanism, and likely as subaerial flood basalts (Plank et al., 2000). Units Syn-2 and 3, although similar to Syn-1, represent the subsequent flows of basaltic material from the western rift axis. The westerly limit of Syn-3 marks the first unit that does not appear to terminate on a structure, rather displays the loss of reflectivity at a nondescript zone of seismic data. The same transition of reflections can be seen for the remaining three Syn units (4-6) and are interpreted as westerly terminations onto a different crustal domain than the units to the east. Determining the exact boundary between the overlying SDRs and this new crust is not presently clear (Fig. 2.4A), as the contact between them is poorly imaged in seismic. Units Syn-5 and Syn-6 begin to show evidence of a waning magma supply by the reduced thickness overall and more remarkably in the west. In the east, internal reflections of Syn-6 are strongly parallel and exhibit sedimentary features such as stratigraphic pinchouts and wedging (Fig. 2.5). This unit, based on its thickness, reflectivity, and distal-proximal seismic character variations is likely

entirely of sedimentary origin in the east and volcanically sourced in the west.

2.6.3 Crustal domains

Based on seismic character, analysis of analogous margins, and relative position to the continental shelf-slope, three crustal types are interpreted for the study area. Block faulted, thinned continental crust is present in the eastern region of the survey and underlies the Syn 1-3 units. Half-grabens within the crust are infilled with the earliest occurrences of volcanic material. A transitional volcanic/igneous crust that likely possesses a variable composition of unresolvable SDRs, pillow basalts, and an underlying chilled magma chamber is present to the east of the continental domain. To the west I observe oceanic crust that is suggested to be of Jurassic age based on the model employed here (Figs. 2.3 A-D).The transition from SDRs to an absence of seismic reflectors marks the boundary from the volcanic/igneous crust to the oceanic domain.

On the seismic sections, the interpretation of continental crust has been based on the interpreted horizons between semi-layered SDR reflections and the presence of the architecture of an underlying crustal block (Figs. 2.4A and B). The relief presented by the Syn-1 unit indicates that a prominent outer horst of continental crust is present to the east of the underlying rift basin. The Mohorovicic discontinuity (“Moho”) at the base of the continental crust appears to extend eastward to a depth beyond 36 km (Figs. 2.4A and B). The composition of the faulted basement is interpreted to be the Pre-Cambrian Guyana Craton of northern South America, given its relative position to outcrops

on the French Guiana margin (Gouyet, 1988).

Figure 2.4A illustrates a transitional zone of interpreted thick (~10-12 km) volcanic / igneous crust (Pindell et al., 2014) that separates the continental rocks and the more “normal” oceanic crust. In seismic, this intermediate domain is interpreted as being bounded by two distinctly different sets of reflectors: 1) high amplitude, subaerially emplaced SDRs (and probable hyaloclastites) as the upper limit of crust, and 2) an underlying, seismically unstructured, zone floored by the interpreted “Moho” horizon (Fig. 2.4A). The lateral boundaries for this volcanic / igneous crust are: 1) the limit of interpreted continental crust to the east; and 2) the westerly limit of SDRs (Fig. 2.4A). The interpreted Oceanic Crustal domain is likely overlain by deepwater sediments and extends to the west, flooring the deepwater Guyana Basin (Fig. 2.1A). The eastern boundary of oceanic crust is marked by the western termination of SDRs and the transition to chaotic seismic amplitudes that is bounded above by parallel reflectors and below by the Moho.

2.6.4 Gravity modeling approach

In order to constrain the above interpretation, forward gravity modeling was performed for the same transect as Figure 2.4A. Shipborne gravity data was used in this portion of the study and modeled within the Geosoft GM-SYS 2D modeling software. The purpose of this model was to constrain the depth and thickness of the crustal bodies under the Demerara Rise and to validate the interpretation of the lower, Syn 1-6 units. Within this portion of the study, the

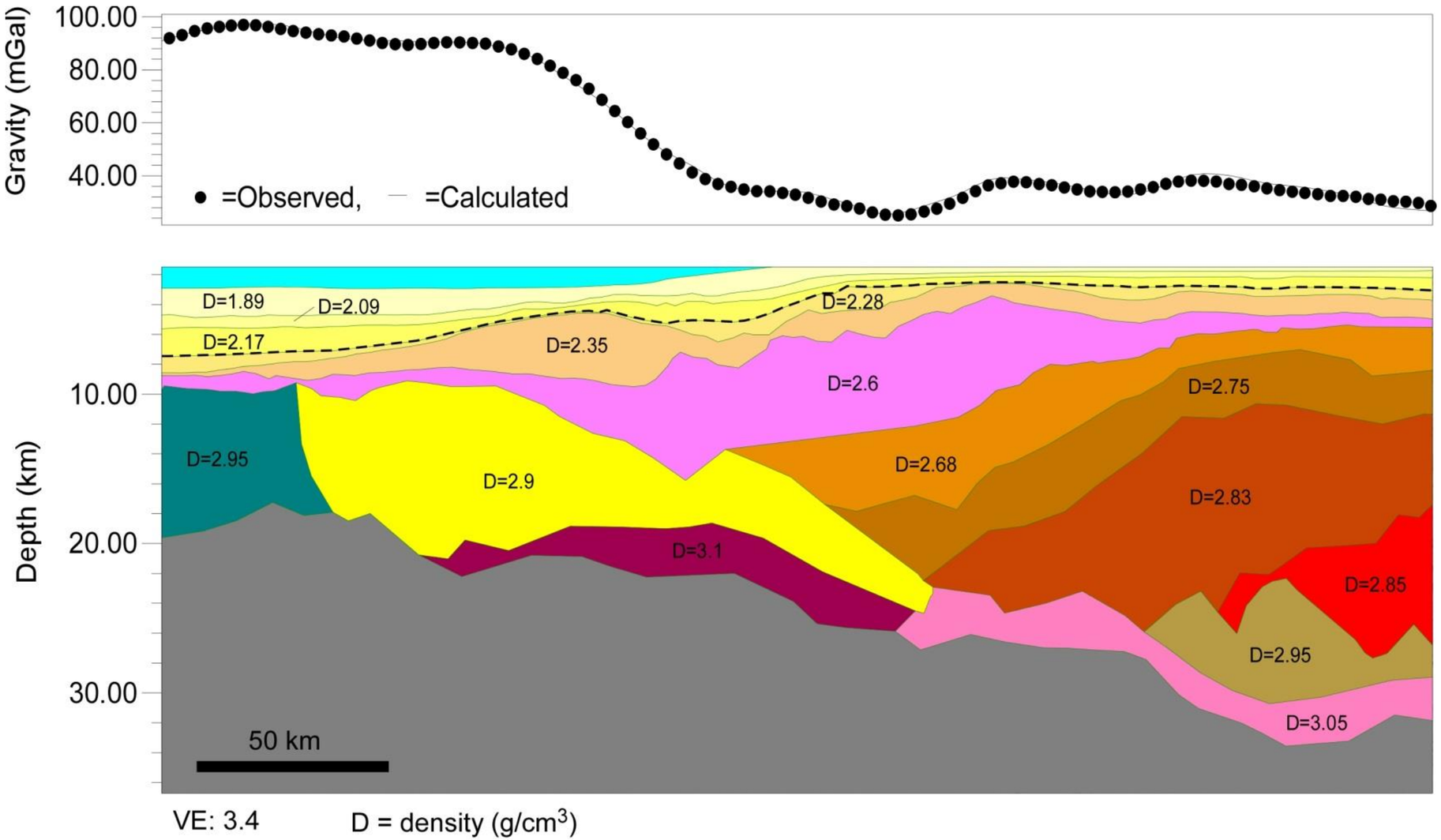

Figure 2.6: The 2D gravity model of figure 4A, illustrating the applied densities for interpreted sedimentary, magmatically-derived material, continental and oceanic crustal domains. The lower panel is a multilayer crustal and stratigraphic cross-section constrained by seismic reflection data and interpretation, the upper panel illustrates observed free-air gravity data, dashed and the calculated model, solid. The gravity data utilized for the model is derived from the ship acquired dataset courtesy of Getech Inc.

gravity response of the proposed model was calculated and iteratively compared to the observed gravity profile (Fig. 2.6). The model was then adjusted until a satisfactory fit between the calculated response and the observed gravity profile was obtained. Densities for apparent sedimentary strata were calculated from the Nafe-Drake (Ludwig et al., 1970) relation. The observed gravity values required that the lower intervals were assigned higher densities typically associated with volcanically-derived material, continental crustal layers, oceanic crust, and mantle (Fig. 2.6) (Blaich et al., 2009; Dragoi-Stavar and Hall, 2009; Blaich et al., 2011; Schiffman et al, 2011; Blaich et al., 2013).

2.6.4.1 2D Modelling-interval densities

Five seismic units were modeled as sedimentary strata, three units younger than the Albian Unconformity and 2 units older than the Albian unconformity that represent the older Central Atlantic passive margin phase (Figs. 2.4A and. 2.6). The sedimentary units of the younger, Equatorial Atlantic phase were assigned increasing densities with depth-- 1.89 g/cm^3 , 2.09 g/cm^3, and 2.17 g/cm^3 (Fig. 2.6). Two sedimentary intervals related to the Central Atlantic passive margin phase were modeled using densities of 2.28 g/cm^3, and 2.35 g/cm^3 (Fig. 2.5). In order to achieve a satisfactory fit between the calculated and observed gravity values, higher densities were required for the SDR units. Layer densities assigned to deeper “Syn” intervals are consistent with the wide range of previously published values at volcanic margins for igneous rocks such as, basalts and gabbros (Fig. 2.6) (Blaich et al., 2009; Dragoi-Stavar and Hall, 2009;

Blaich et al., 2011; Blaich et al., 2013). Blaich et al. (2009) modeled volcanic units emplaced on the rifted margins of the South Atlantic at derived densities of 2.5 -2.66 g/cm^3 at depths of approximately 8 km. Schiffman et al. (2011) reported a significantly broad range of hyaloclastite densities of 2.2-2.8 g/cm^3 sampled from a drill core at a comparatively shallow depth of 3 km. This broad density range, which approaches similar values of upper continental crustal density, was attributed to high degrees of alteration and depth of burial (Schiffman et al., 2011). Therefore, units of seaward dipping reflectors were assigned density values of 2.6 g/cm^3, 2.68 g/cm^3, 2.75 g/cm^3, 2.83 g/cm^3, a2.nd 2.85 g/cm^3 (Fig. 6). Previous gravity modeling studies on volcanic margins have generally placed single density values for SDR or volcanic units. My approach was to integrate a general increase in density with depth, as one might expect from deeply buried, multi-phase emplacement of volcanic rocks. In the context of alteration and compaction, Schiffman et al. (2011) observed an increase in density from 2.2 g/cm^3 to 2.8 g/cm^3 within a 500 m vertical zone of weathered and altered zone of volcanics. I have acknowledged the relationship of increasing density with depth in basalts and have employed a similar approach, accounting for the compaction and alteration of the SDRs within the section.

Fits of the calculated and observed values confirm that such an interpretation is supported by the gravity anomalies on the Demerara Rise. This observation of deep crustal structures and transitions through the integration of 2D potential field data and the deep reflection data permits the analysis of probable and improbable crustal structures. Rifted continental crust is inferred to underlie Syn

units 1-3, by applying upper (2.95 g/cm^3) and lower (3.05 g/cm^3) crustal densities and honoring the interpreted seismic reflections (Fig. 2.6). The high density crust below the SDRs is an indicator of intruded crystalline basement related to the onset of magmatism in the overlying SDRs (Blaich et al., 2009). The gravity model also supports the western extension of this high density (3.05 g/cm^3) lower crustal body under the Syn-3 unit (Fig. 2.6). A lithological change is assumed based on the termination of SDRs in the 2-D reflection data and the fit of the gravity model. This assumption is further extended to the west where the overlying SDRs decrease in thickness and the prominent underlying volcanic/igneous crust increases in thickness. Maintaining previously modeled densities of SDRs, the construction of an acceptable gravity model requires density values of 2.9 g/cm^3 and 3.1 g/cm^3 for the volcanic/igneous transitional-type crust (Fig. 2.6). Similar transitional crustal domains have been observed on other well-known volcanic margins of the South Atlantic (Blaich et al., 2009; Pindell et al., 2014). On these margins, high-density/velocity bodies were modeled and determined to be a common component of typical rifted volcanic margins (Blaich et al., 2009). Thick packages of SDRs were consistently observed as the extrusive component to a two part crustal domain, where a high-density igneous crust served as the basal component (Blaich et al., 2009; Pindell et al., 2014). A distinct transition to oceanic crust is defined from seismic data at the location where SDRs terminate in the west and a higher density (2.9 g/cm^3) is required for an acceptable 2-D gravity model fit. This change in lithology is interpreted to mark the cessation of extrusive magmatic activity and

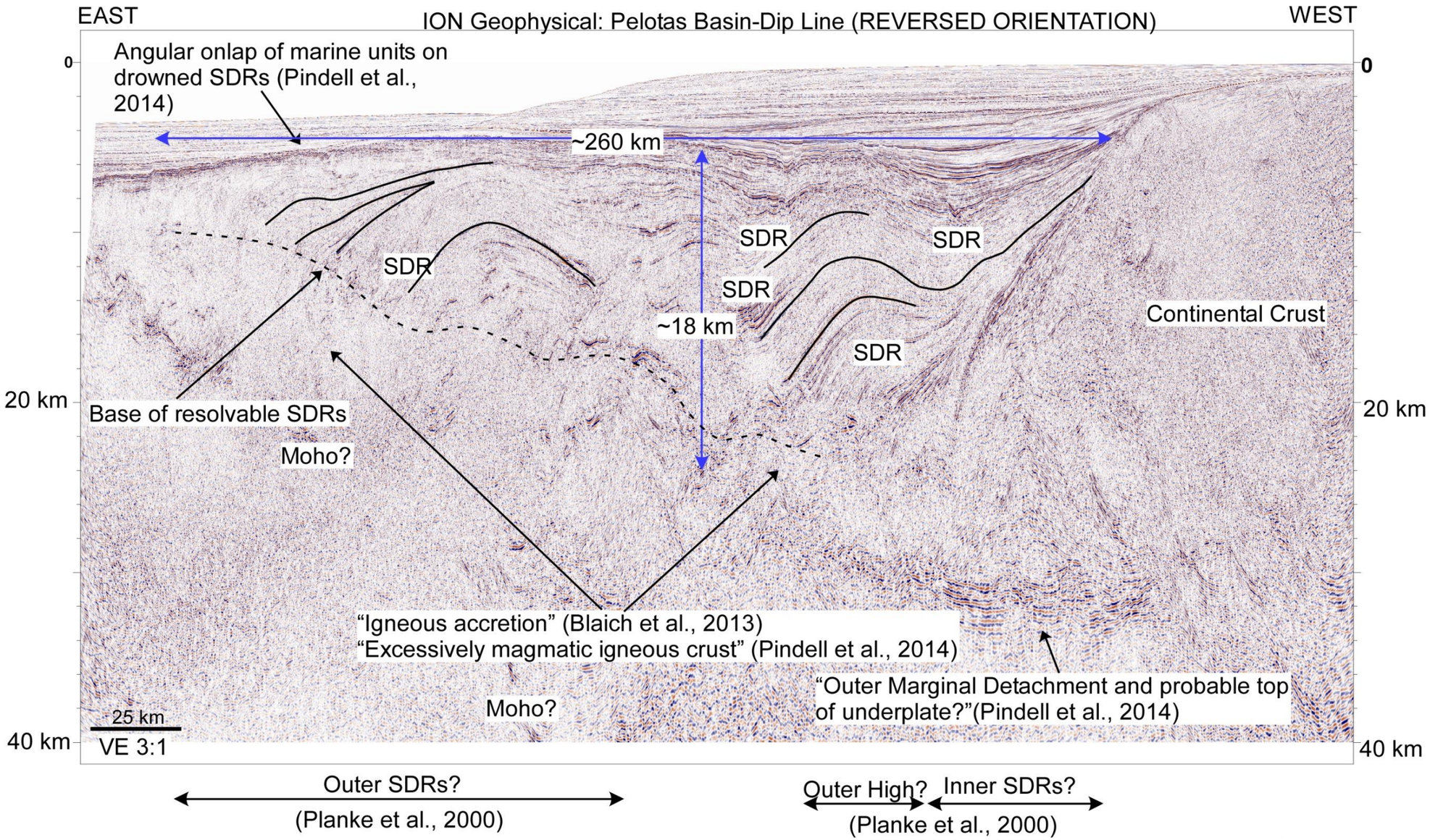

Figure 2.7: An example line from the Pelotas basin (courtesy of ION Geophysical). The data is in a REVERSED orientation in order for a more straightforward comparison to figure 2.4A. Blaich et al., (2013) interpreted and modeled the same line and features presented in their work have been labeled. Pindell et al. (2014) interpreted a similar line and features from that investigation are also labeled. Planke et al. (2000) performed an analysis of volcanostratigraphy on well-known volcanic margins and applied terms to volcanic features (also applied here).

the onset of sea floor spreading.

2.7 Discussion

In order to understand the origin of the deeper sequences within the Demerara Rise, and therefore its evolution, analogs and various geologic processes must be considered. By acknowledging that the deeper section was previously unknown, the starting point to assess the evolution of the crustal domains and SDRs must be broad in scope. Considering the two potential modes of margin evolution (volcanic and non-volcanic) and key features within the data, a volcanic origin for the Central Atlantic Tectonic phase of the Demerara Rise has been hypothesized. Significant correlations exist between analogous volcanic margins and what is observed on the seismic data and gravity modeling. I also rule out a non-volcanic (and therefore stratigraphic) origin on the basis of an overall lack of sedimentary and stratigraphic features in seismic. The presence of pre-rift (pre-Jurassic) strata or folded orogenic material was also considered and dismissed due to the absence of faulted pre-rift units. It is my interpretation that Demerara Rise was the site of intense volcanism during the early stages of rifting and consequently produced a largely magmatically derived basement. Based on the seismic data presented and 2-D gravity modeling, rift-related magmatism is the most plausible process for accumulations of thick sequences of SDRs and an intermediate type crust termed as “volcanic / igneous crust” (Figs. 2.4A, 2.7 ,and 2.8).

For comparison purposes, I have highlighted a representative line (Fig. 2.7)

from the Pelotas basin, a well-known volcanic margin in southern Brazil. In the following section, I will integrate my findings with previous studies of the Pelotas Basin in order to develop an accurate SDR emplacement and crustal model for the Demerara Rise.

2.7.1 Crustal domains

Seismic character, interval densities, and overall geometries were used to evaluate crustal domain models for analogous margins and to develop an appropriate tectonic model for the Demerara Rise. Crustal models previously proposed by Planke et al. (2000), Blaich et al. (2013) and Pindell et al. (2014) exhibit strong correlations with my observations and the interpreted crustal types that core the Demerara Rise. My proposed model for the Demerara Rise includes three primary crustal domains: 1) Continental; 2) Volcanic / Igneous; and 3) Oceanic.

2.7.1.1 Continental crust

The interpreted profiles within Figures 2.4A and 2.4B illustrate large faulted blocks of continental crust at 12-22 km depth that underlie the inner portions of the volcanic SDRs and other possible volcanically-sourced material emplaced during the late stages of rifting (e.g., pillow basalts and hyaloclastites). The apparent lack of continental basement in the western regions of the Demerara Rise is in contrast to previous interpretations on the composition of the broad bathymetric feature (Greenroyd et al., 2007a, Basile et al., 2013). The seismic

data indicate that much of the Rise is not shallow, subsurface continental material, based on the well-layered seismic events recorded to depths of 24 km. In fact, crystalline basement rocks of continental crust are likely a minor component to the overall composition of the Rise. Integration of seismic reflection interpretation and 2-D Gravity modeling indicate the presence of a thin veneer of high-density material (3.05 g/cm^3) below the interpreted thinned continental crust. Pindell et al. (2014) proposed a similar high-density body underlying the “Outer Marginal Detachment” of continental crust for segments of the Pelotas Basin (Fig. 2.7).

2.7.1.2 Volcanic / igneous crust

Within the data, I have interpreted a zone of Volcanic / Igneous Crust that developed as transitional crust between the continental crustal domain and oceanic crust (Fig. 2.4A). The origin of this transitional crust is not well known and has been observed on similar volcanic margins (e.g. Pelotas Basin, deepwater, offshore Argentina) (Fig. 2.7). Within the seismic data, this crust is recognized as a resolvable zone of data having high density (2.9 g/cm^3), as indicated in the 2-D gravity model (Fig. 2.6). The overlying flows and underlying crustal body possess similar densities to crust and therefore serve as an intermediate crustal domain between the limit of continental crust and oceanic crust (Fig. 2.4A). Similar to the proposed underplate at the Pelotas continental margin (Fig. 2.7), this crust also appears to be floored by a higher density zone (Fig. 2.6). Similar zones have been interpreted from seismic reflection

characteristics (Gladczenko et al., 1998) and by velocity intervals indicative of underplating (Bauer et al., 2000). Pindell et al. (2014) arrived at a similar interpretation along the margin when describing the concept of “outer marginal collapse” within the Pelotas Basin (Fig. 2.7). Further, Pindell et al. (2014) cite this zone of less prominent reflection character to be the remnant chilled magma chamber that once sourced the volcanism. The rotation of the SDR units is achieved by the collapse of the chilled magma chamber and the migration of the igneous source away from the rifted margin. Densities of the volcanic / igneous crust have been modeled at 2.9 g/cm^3 and are likely gabbroic in composition (Fig. 2.6). The distribution and thickness of the igneous crust are inferred to be related to volume of magma and duration of supply.

2.7.1.3 Oceanic crust

Figure 4A illustrates a relatively thick (10-12 km) segment of oceanic crust that is present at the western extent of the study area. The above-average thickness is an indicator of a higher than normal supply of melt for production of oceanic crust at the transition from volcanic / igneous crust (Fig. 2.4A). The lack of overlying SDRs indicates that this was the position at which the invasion of shallow marine waters occurred (Planke et al., 2000). It also signifies the cessation of volcanic activity and the onset of passive margin conditions in a deepwater marine environment (Planke et al., 2000).

2.7.1.4 Seaward dipping reflector units

At the Demerara Rise, I observe evidence for multiple units of SDRs that likely relate to variable pulses or geographic shifts of magma supply during the continental breakup. These occurred at the onset of rifting along the continental margin up to the time of oceanic crust production. 2-D gravity modeling performed here employed densities from previously modeled volcanic passive margins (Blaich et al., 2009; Dragoi-Stavar and Hall, 2009; Blaich et al., 2011; Blaich et al., 2013). SDR units display geometric variability that I interpret as different magmatic compositions, or interbedded sedimentary rocks at the newly rifted margin (Fig. 2.4A). I expect the intercalation of terrestrial sediments between basaltic intervals as the magma source migrates distally (Bray, 1999; Planke et al., 2000).

Variability of geometries of the SDR units is present and can be inferred to be related to multiple mechanisms. The contributing factors include composition, volume of magma supply, degree of rotation, and environment of emplacement (e.g., subaerial or sub-aqueous) (Planke et al., 2000). Pindell et al. (2014) suggested that magma and/or magmatic mush (>40% melt) is evacuated basinward from below the outer limit of the continental crustal domain to feed the overlying SDR units, both of which rotate strongly (beyond 20 degrees) basinward. This basinward rotation is evidenced by the angular onlap of subsequent sedimentary intervals (Figs. 2.4A and 2.7). Thick wedge-shaped reflectors with a convex up geometry are present within the initial three SDR units that were the initial manifestations of magma along the rifted margin (Fig.

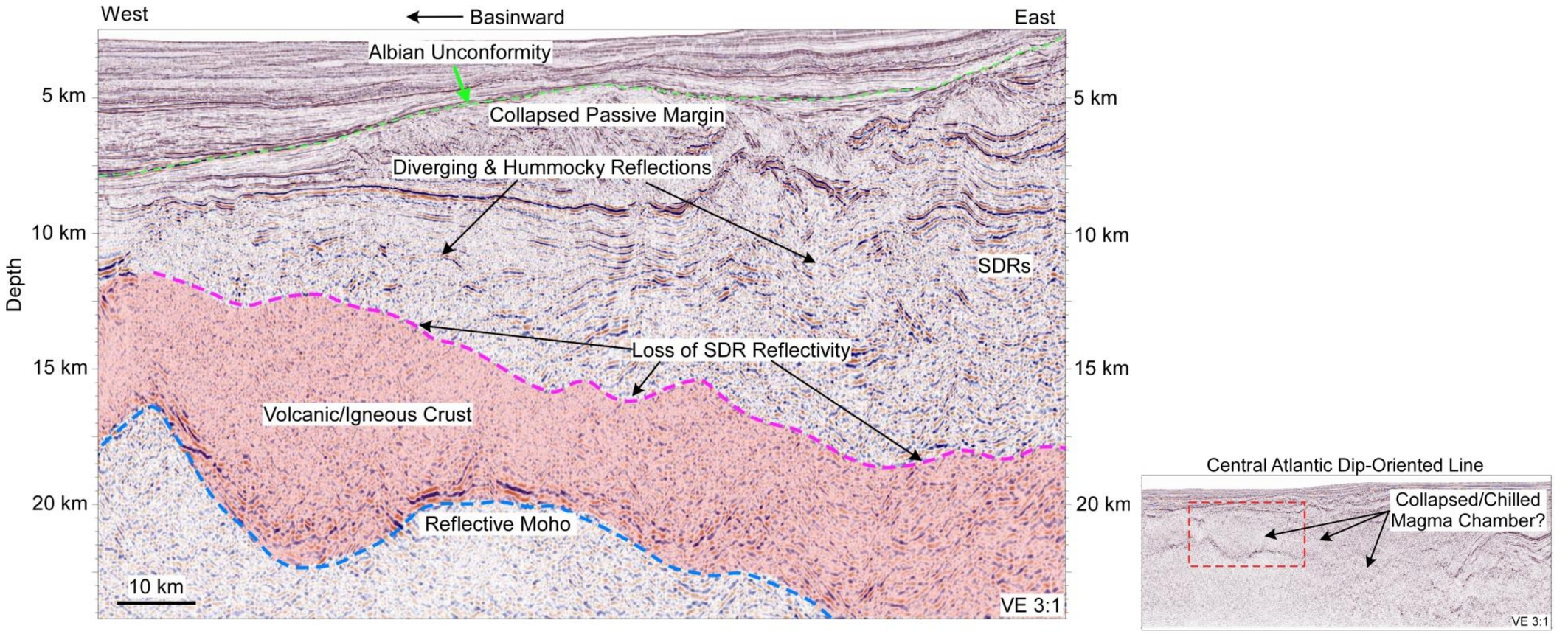

Figure 2.8: Shows the basinward extent of the volcanic material final sub –aerial and/or –marine emplaced volcanic package highlighting the non-systematic, hummocky nature of the seismic character that was potentially emplaced in a shallow-marine environment. Division of resolvable SDRs reflectors and the apparent loss of reflectivity within the volcanic/igneous crust (red) is identified (pink dashed), this interpreted crust is positioned above a series of strong, deep reflectors that have been interpreted as “Moho.“

2.5). These initial SDR units contrast the younger SDR units in the West, as their geometries are strongly divergent at their terminations onto the volcanic/igneous crust (Fig. 2.8). This also is a function of the westerly migrating magma chamber away from the continental margin of the Rise. The final stages of volcanic units, Syn 5-6, present less seismic reflections and more chaotic seismic amplitudes (Fig. 2.8). Similar seismic facies have been identified as occurring in shallowing marine eruptions prior to the initiation of sea floor spreading (Fig. 2.8) (Planke et al., 2000). This systematic transition from SDRs to a marine eruption occurred as the supply to the magma chamber waned, collapse of the chamber initiated, and shallow marine waters invaded the opening basin (Pindell et al., 2014). Thus, I expect that the mottled and hummocky seismic reflections to consist of hyaloclastites and possibly pillow basalts (Fig. 2.8) (Planke et al., 2000). The absence of SDRs at this position is inferred to be the result of a reduced topographic expression of the fissure/volcano at the incipient mid-ocean ridge.

Based on the geographical shift and probable fluctuations of magmatic supply, each of the six SDR units varies in aerial distribution and thickness. Figure 2.9 illustrates the mapped westerly migration of the inner and outer SDRs facies (Syn 1-6) (Planke et al., 2000). The aerial extent of each successive unit grows between each package and is likely the result of separate pulses of magmatism. The coverage of the SDR units 1-6 are: 17,400 km^2, 12,100 km^2, 14,600 km^2, 29,400 km^2, 71,700 km^2, and 77,600 km^2 respectively. These data indicate both a progressively deepening and widening basin in addition to an

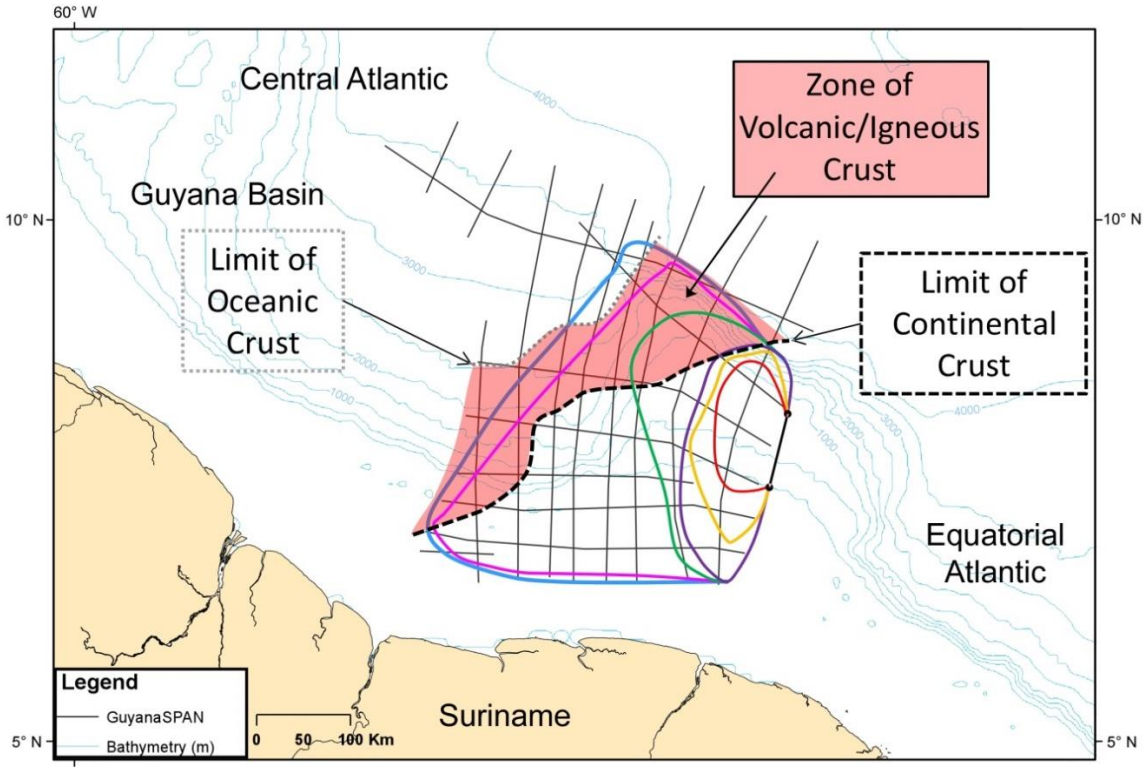

Figure 2.9: Revised crustal domains are highlighted and show the westerly transition from stretched continental crust into a wide zone of volcanic/igneous crust and interpreted Jurassic oceanic crust. Aerial distribution of SDR/volcanic/volcaniclastic syn-rift packages are represented by colored lines and provide evidence of an evolving basin as the Central Atlantic opened to the west. The Bahamas Hotspot was likely the primary source of magma for this poly-phase volcanic margin. (Polygon key: Red) Syn-1, Yellow) Syn-2, Purple) Syn-3; Green) Syn-4, Pink) Syn-5, Blue) Syn-6).

initial voluminous pulse and then subsequent decrease of magmatic supply and extrusive material at the spreading center. Figure 2.9 also presents the revised crustal domains for the Demerara Rise. Inferred Jurassic-aged oceanic crust is the end-member to the Central Atlantic Rift phase on the rise and its occurrence was preceded by the emplacement of a wide zone (70-100 km) of volcanic/igneous crust (Fig. 2.9).

2.8 Plate model implications

The tectonic plate model employed here (Figs. 2.3A -2.3D) suggests that the magmatism is of Jurassic age. However, I acknowledge that choosing between an Early Jurassic syn-rift phases, versus a late Middle Jurassic, late syn-rift phase is dependent upon the plate model invoked. This also determines the potential magmatic source of the volcanic margin as either CAMP (Central Atlantic Magmatic Province) or the suspected Bahamas hot spot-related. The rift model of Kneller and Johnson (2011), which suggested minimal continental crust underlies the Great Bank of the Bahamas would infer the older age, while models presuming a thinned and possibly intruded continental Great Bank (Pindell, 1985; Pindell and Kennan, 2009) would favor the later age, even though the magmatism in either case could relate to the Bahamas hot spot (i.e., the CAMP magmatic outpourings could have been a precursor to the Bahamas hot-spot). The SDR units share similar geometries and seismic properties with SDRs on other volcanic passive margins, such as Southern Brazil, Uruguay and Argentina (Franke et al., 2000; Franke, 2012; Blaich et al., 2013, Pindell et al.

2014). Conjugate margin studies of volcanic margins (Blaich et al., 2009, Blaich et al., 2013) suggested that volumes of magmatic material on opposing margins vary, but both are volcanic in nature. With the observation that rift-related magmatism creates conjugate volcanic margins, the plate model employed here places the continental rocks of the Bahamas as the conjugate to the Demerara Rise. Therefore I can infer that the southern extent of the Great Bank of the Bahamas and the Central Atlantic succession of the Guinea Plateau are also volcanic margins.

2.9 Conclusions

The acquisition of deep-penetration, high-resolution seismic data has resulted in the imaging of geologic intervals linked to the initial stages of the opening of the southern Central Atlantic Ocean. These data are consistent with the model that the Demerara Rise (and most likely the Guinea Plateau) was the site of extensive syn-rift volcanism during the Central Atlantic Phase, which was the first of its two tectonic phases. Seaward dipping reflectors interpreted to be sourced from the Bahamas hotspot are present to depths of 25 km on the Rise. Voluminous magmatic activity was also responsible for the addition of a transitional igneously-derived crustal domain positioned between thinned continental basement in the east and oceanic crust to the west (Fig. 2.9).

This study, based on the integration of high resolution seismic, 2-D gravity modeling, and examination of analogous volcanic margins, has determined that the Demerara Rise is underlain by a thick sequence of SDRs

and passive margin sediments related to the opening of the Central Atlantic Ocean and genetically related to the igneous origin of the Great Bahamas Bank. An implication of this study is that the presumed extent of the southern continental rocks of the Bahamas and the deep composition of the conjugate Guinea Plateau were magmatically derived. This study also confirms the identification of the Central Atlantic margin of the Demerara Rise as a volcanic margin and infers similar classifications for its conjugate margins. As a result of this work, I have gained a better understanding of the formation of igneous/transitional crust, the broad spectrum of possible densities within the volcanic wedge, and the substantial potential for the aerial distribution of SDRs.

Chapter Two: References

Antobreh, A. A., Faleide, J. I., Tsikalas, F., and Planke, S., 2009, Rift-shear architecture and tectonic development of the Ghana margin deduced from multichannel seismic reflection and potential field data: Marine and Petroleum Geology, 26, 345–368.

Azevedo, R. P., 1991, Tectonic evolution of Brazilian equatorial continental margin basins: Unpublished PhD thesis, University of London.

Basile, C., Mascle, J., Sage, F., Lamarche, G., and Pontoise, B., 1996, In: Mascle, J., Lohmann, G.P., Clift, P.D., et al. (Eds.), Pre-cruise and site surveys: a synthesis of marine geologicaland geophysical data on the Côte d'Ivoire–Ghana transform margin: Proc. ODP, Init. Reports, 159, 47–60.

Basile, C., Mascle, J., Benkhelil, J., and Bouillin, J. P., 1998, In: Mascle, J., Lohmann, G.P., Moullade, M. (Eds.), Geodynamic evolution of the Côte d'Ivoire–Ghana transform margin: an overview of Leg 159 results: Proc. ODP, Sci. Results, 159, 101–110.

Basile, C., Mascle, J., and Guiraud, R., 2005, Phanerozoic geological evolution of the Equatorial Atlantic: Journal of African Earth Sciences, 43, 275–282.

Basile, C., Maillard, A., Patriat, M., Gaullier, V., Lonke, L., Roest, W., Mercier de Lepinay, M., and Pattier, F., 2013, Structure and evolution of the Demerara Plateau, offshore French Guiana: Rifting, tectonic inversion and post-rift tilting at transform-divergent margins intersection: Tectonophysics, 591, 16-29.

Bauer, K., and Neben, S., 2000, Deep structure of the Namibia continental margin as derived from integrated geophysical studies: Journal of Geophysical Research, 105, 25, 829–25,853.

Benkhelil, J., Mascle, J., and Tricart, P., 1995, The Guinea continental margin: an example of a structurally complex transform margin: Tectonophysics, 248, 117–137.

Blaich, O. A., Faleide, J. I., Tsikalas, F., Gordon, A.C., and Mohriak, W., 2013, Crustal-scale architecture and segmentation of the South Atlantic volcanic margin, In: Mohriak, W.U., Danforth, A., Post, P.J., Brown, D.E., Tari, G.C., Nemcok, M., and Sinha, S.T. (Eds.), Conjugate Divergent Margins, Geological Society, London, Special Publications, 369.

Blaich, O. A., Faleide, J. I., Tsikalas, F., Franke, D., and Leo´n, E., 2009, Crustal-scale architecture and segmentation of the Argentine margin and its conjugate off South Africa: Geophysical Journal International, 178, 85–105.

Blaich, O. A., Faleide, J. I., and Tsikalas, F., 2011, Crustal breakup and continent–ocean transition at South Atlantic conjugate margins: Journal of Geophysical Research, 116, 1–36.

Bray, R., and Lawrence, S., 1999, Nearby finds brighten outlook: The Leading Edge, May Issue, 806–814.

Bullard, E. C., Everett, J. E., and Smith, A G., 1965, The fit of the continents around the Atlantic: Symposium on continental drift, Royal Society of London, Philosophical Transactions, 258, 41-51.

Cacchione, D. A., Pratson, L. F., and Ogston, A. S., 2002, The shaping of continental slopes by internal tides: Science, 296, 724–727.

Davison, I., 2013, Conjugate transform margins of the Equatorial Atlantic: Similarities and differences: Conjugate Margins 3rd meeting; Dublin, Ireland.

Dragoi-Stavar, D., and Hall, S., 2009, Gravity modeling of the ocean-continent transition along the South Atlantic margins: Journal of Geophysics, 114.

Eldholm, O., Skogseid, J., Planke, S., and Gladczenko, T. P., 1995, Volcanic margin concepts: Rifted Ocean-Continent Boundaries, edited by Banda, E., Torne, M., and Talwani, M., Kluwer Academy, Dordrecht, Netherlands, 1–16.

Erbacher, J., Mosher, D. C., and Malone, M. J., 2004, Demerara Rise; equatorial Cretaceous and Paleogene paleoceanographic transect, western Atlantic; covering Leg 207 of the cruises of the drilling vessel JOIDES Resolution; Bridgetown, Barbados, to Rio de Janeiro, Brazil; Sites 1257-1261; 11 January-6 March 2003: Proceedings Ocean Drilling Program (ODP), Initial Reports, Part A-207, Texas A&M University, College Station, Texas (Ocean Drilling Program)

Franke, D., 2012, Rifting, lithosphere breakup and volcanism: Comparison of magma-poor and volcanic rifted margins: Marine Petroleum Geology, 43, 63–87; doi:10.1016/j.marpet geo.2012.11.0 03.

Gladczenko, T. P., Skogseid, J. and Eldholm, O., 1998, Namibia volcanic margin: Marine Geophysical Research, 20, 313–341.

Geoffroy, L., 2005, Volcanic passive margins: Comptes Rendus Geosciences 337, 1395–1408.

Gouyet, S., 1988, Evolution tectono-sédimentaire des marges guyanaise et nordbrésilienne au cours de l'ouverture de l'Atlantique Sud. Ph. D. Thesis, Université de Pau.

Greenroyd, C. J., Peirce, C., Rodger, M., Watts, A. B., and Hobbs, R. W., 2007a, Crustal structure of the French Guiana margin, West Equatorial Atlantic: Geophysical Journal International, 169, 964–987.

Greenroyd, C. J., Peirce, C., Rodger, M., Watts, A. B., and Hobbs, R. W., 2007b, Crustal structure and evolution of the Demerara Plateau, French Guiana: Geophysical Journal International, 172, 549–564; doi:10.1111/j.1365-246X.2007.03662.x.

Greenroyd, C. J., Peirce, C., Rodger, M., Watts, A.B., and Hobbs, R. W., 2008, Demerara Plateau— the structure and evolution of a transform passive margin: Geophysical Journal International 172, 549–564.

Heine, C., Zoethout, J., and Müller, R. D., 2013, Kinematics of the South Atlantic rift: Solid Earth Discussions 5, 41–116.

Hinz, K., 1981, A hypothesis on terrestrial catastrophes: Wedges of very thick oceanward dipping layers beneath passive margins-their origin and paleoenvironmental significance: Geolisches Jahrbuch, 22, 3–28.

Klitgord, K. D., and Schouten, H., 1986, Plate kinematics of the central Atlantic: The Geology of North America, M, The Western North Atlantic Region, edited by P.R. Vogt and B.E. Tucholke: Geological Society of America 351-378.

Kneller, E. A., and Johnson, C. A., 2011, Plate kinematics of the Gulf of Mexico based on integrated observations from the Central and South Atlantic: Gulf Coast Association of Geological Societies Transactions, 61, 283–299.

Loncke, L., Droz, L., Gaullier, V., Basile, C., Patriat, M., and Roest, W., 2009, Slope instabilities from echo-character mapping along the French Guiana transform margin and Demerara abyssal plain: Marine and Petroleum Geology, 26, 711–723.

Ludwig, W. J., Nafe, J. E., and Drake, C. L., 1970, Seismic Refraction In The Sea: Wiley Interscience, New York.

Mascle, J., and Blarez, E., 1987, Evidence for transform margin evolution from the Ivory Coast–Ghana continental margin: Nature, 326, 378–381.

Mascle, J., Blarez, E. and Marinho, M., 1988, The shallow structures of the Guinea and Ivory Coast-Ghana transform margins: their bearing on the Equatorial Atlantic evolution: Tectonophysics, 188, 193-209

McKenzie, D.P., 1978, Some remarks on the development of sedimentary basins: Earth and Planetary Science Letters, 40, 25–32.

Menzies, M. A., S. L. Klemperer, C. J. Ebinger, and J. Baker, 2002, Characteristics of volcanic rifted margins, in Volcanic Rifted Margins, edited by M. A. Menzies et al.: Special Papers Geological Society of America, 362, 1–14.

Moulin, M., Aslanian, D., and Unternehr, P., 2010, A new starting point for the South and Equatorial Atlantic Ocean: Earth-Science Review, 2040 97, 59–95,

Mosher, D. C., Erbacher, J., Zuelsdorff, L., and Meyer, H., 2005, Stratigraphy of the Demerara Rise, Surname, South America: a rifted margin, shallow stratigraphic source rock analogue: Extended Abstract, American Association of Petroleum Geologists annual meeting, Calgary, Alberta, June 19-22.

Müller, R.D., and Smith, W.H.F., 1993, Deformation of the Oceanic crust between the North American and South American plates: Journal of Geophysical Research 98 (B5), 8275–8291.

Mutter, J. C., M. Talwani, and P. L. Stoffa, 1982, Origin of seaward dipping reflectors in oceanic crust off the Norwegian margin by subaerial seafloor spreading: Geology, 10, 353–357.

Mutter, J., 1985, Seaward dipping reflectors and the continent-ocean boundary at passive continental margins: Tectonophysics, 114, 117-131.

ODP Leg 207 Shipboard Scientific Party, 2004. Leg 207 summary: In: Erbacher, J., Mosher, D.C., Malone, M.J., et al. (Eds.), Proc. ODP, Init. Repts., 207: College Station, TX (Ocean Drilling Program), 1–89.

Pindell, J.L., 1985, Alleghanian reconstruction and subsequent evolution of the Gulf of Mexico, Bahamas, and Proto-Caribbean: Tectonics, 4, 1-39.

Pindell, J. L., 1993. Regional synopsis of Gulf of Mexico and Caribbean evolution, in Pindell, J. L., and Perkins, R.: Gulf Coast Section Society of Economic Paleontologists and Mineralogists Foundation, 13th Annual Research Conference Proceedings, Mesozoic and Early Cenozoic Development of the Gulf of Mexico and Caribbean Region, July 1, 1993, 251-274.

Pindell, J.L., and J.F. Dewey, J.F., 1982, Permo-Triassic reconstruction of western Pangea and the evolution of the Gulf of Mexico/Caribbean Region: Tectonics, 1, 179-211.

Pindell, J.L., Kennan, L., and S.F. Barrett, S., 2000a, A Removal- Restoration Project. Part 3 of a series: Regional Plate Kinematics: Arm Waving, or Underutilized Exploration Tool: AAPG Explorer, August 2000.

Pindell, J.L., Kennan, L., and S.F. Barrett, 2000b, Putting It All Together Again, Part 4 of a series: Regional Plate Kinematics: Arm Waving, or Underutilized Exploration Tool: AAPG Explorer, October 2000.

Pindell, J.L., and Kennan, L., 2001B, Processes and events in the terrane assembly of Trinidad and eastern Venezuela: Transactions, Petroleum systems of deep-water basins: global and Gulf of Mexico experience, GCSSEPM 21st Annual Research Conference, December 2-5: Houston, Texas, GCSSEPM, 159-192.

Pindell, J., Kennan, L., Stanek, K., Maresch, W., and Draper, G., 2006, Foundations of Gulf of Mexico and Caribbean evolution: Eight controversies resolved: Geologica ACTA, 4, 89-128.

Pindell, J. and Kennan, L., 2009, Tectonic evolution of the Gulf of Mexico, Caribbean and northern South America in the mantle reference frame: an update. In: James, K. H., Lorente, M. A. and Pindell, J. L. (eds) The Origin and Evolution of the Caribbean Plate: Geological Society, London, Special Publications, 328, 1-54.

Pindell, J., Graham R., and Horn B. W., 2014, Role of magmatic evacuation in the production of SDR complexes at magma-rich passive margins: GCSSEPM Bob F. Perkins Research Conference, January 2014, 1-16.

Planke S., Symonds P., Alvestad E., and Skogseid J., 2000, Seismic volcanostratigraphy of large-volume basaltic extrusive complexes on rifted margins: Journal of Geophysical Research, 105, 19335–19351

Rabinowitz, P. D. and LaBrecque, J., 1979, The Mesozoic South Atlantic Ocean and evolution of its continental margins: Journal of Geophysics Research, 84, 5975-6002.

Sage, F., Pontoise, B., Mascle, J., Basile, C., and Arnould, L., 1997, Crustal structure and ocean– continent transition at marginal ridge: the Côte d'Ivoire–Ghana marginal ridge: Geo-Marine Letters, 17, 40–48.

Schiffman, P., Watters, R. J., Thompson, N., and Walton, A. W., 2006, Hyaloclastites and the slope stability of Hawaiian volcanoes: Insights from the Hawaiian Scientific Drilling Project's 3-km drill core: Journal of Volcanology and Geothermal Research, 151, 217–228.

Sheridan, R., Musser, D., Glover, III, L., Talwani, M., Ewing, J., Holbrook, W.S., Purdy, G. M., Hawman, R., and Smithson, S., 1993, Deep seismic reflection data of EDGE U.S. mid-Atlantic continental-margin experiment: Implications for Appalachian sutures and Mesozoic rifting and magmatic underplating: Geology, 21, 563-567.

Sleep, N.H., 1971, Thermal effects of the formation of Atlantic continentalmargins by continental break-up: Geophysical Journal of the Royal Astronomical Society, 24, 325–350.

Skogseid, J., 2001, Volcanic margins: Geodynamic and exploration aspects: Marine Petroleum Geology, 18, 457–461.

Staatsolie, Suriname National Oil Company, 2013, Suriname International CompetitiveBidRound2013: http://www.staatsolie.com/pio/images/stories/PDF/suriname_international_bidding_round2013.pdf, accessed July, 2014.

White, R. S., Westbrook, A. N., Bowen, S. R., Fowler, D. P., Spence, C., Prescott, P. J., Barton, M., Joppen, M., Morgan, J., and Bott, M. H. P., 1987, Hatton Bank (northwest UK) continental margin structure: Geophysical Journal of the Royal Astronomical Society, 89, 265–272.

White, R. S., McKenzie, D., and O'Nions, R.K., 1992, Oceanic crustal thickness from seismic measurements and rare earth element inversions: Journal of Geophysics Research, 97(B13), 19683–19715.

Wilson, M., 1997, Thermal evolution of the Central Atlantic passive margins: Continental break-up above a Mesozoic super-plume: Journal of the Geological Society of London, 154, 491-495.

Wilson, R. C., 2001, Non-volcanic rifting of continental margins: a comparison of evidence from land and sea: Geological Society special publication, ISBN 9781862390911, 187.

Van Wagoner, J. C., Posamentier, H. W., Mitchum, R. M., Vail. P. R., Sarg, J. F., Loutit, T. S., and Hardenbol, J., 1988, An overview of the fundamentals of sequence Stratigraphy and key definitions: Wilgus, C. K .Posamentier, H. W., Ross, C. K., and Kendall, C. G. St. C., eds., Sea-level Changes: An integrated approach: Tulsa: SEPM Special Publication 42, 39-45.

Wernicke, B., 1985, Uniform-sense normal simple shear of the continental lithosphere: Canadian Journal of Earth Sciences 22, 108–125.

Zalán, P.V., 1984, Tectonics and sedimentation of the Piauí-Camocim sub-basin, Ceará Basin, offshore northeastern Brazil: Unpublished PhD Thesis, Colorado School of Mines.

CHAPTER THREE:

HOTSPOT ORIGIN FOR ASYMMETRY OF CONJUGATE, VOLCANIC MARGINS OF THE SOUTH ATLANTIC OCEAN AS IMAGED ON DEEPLY-PENETRATING SEISMIC REFLECTION IMAGES

3.1 Summary

I present 27,550 km of deep-penetrating, seismic reflection profiles across the South Atlantic conjugate margins of Uruguay/Southern Brazil and Namibia to illustrate an asymmetrical, lateral and cross-sectional distribution of voluminous, post-rift volcanic material erupted during the Barremian-Aptian (130-120 Ma), early seafloor spreading phase. I mapped the margin-parallel limits of seaward-dipping-reflector complexes (SDR's) based on interpretations of seismic reflection data that were integrated with previous studies using seismic refraction data from both conjugate margins. These conjugate zones of SDRs and their underlying igneous crustal basement are bound by the limit of continental crust (LoCC) and the limit of oceanic crust (LoOC). Subaerially-emplaced and tabular SDR's have rotated downward 20° in the direction of the spreading ridge and are up to 22 km thick near the LoCC. The SDR package is wedge-shaped and thins abruptly basinward towards the LoOC to transition to a normal, 6-8-km thick oceanic crust. Large volumes of continental flood basalts are pre-rift in age (Hauterivian-132 Ma) and are linked spatially to the Tristan de Cunha mantle plume centered during the Hauterivian -Barremian (132-131 Ma) in the Paranà region of southeastern Brazil. My model to explain an approximately 30% greater volume of SDRs/igneous crust on the trailing

Namibian margin than on the leading Brazilian margin during the syn- and post rift phases invokes a combination of diverging tectonic plates and a north-westerly plate motion with respect to a fixed mantle position of the mantle plume. This plate and ridge geometry resulted in the eruption of prolonged and voluminous magmatic material on both conjugate margins in the syn-rift period prior to the nucleation of the mid-oceanic ridge. My proposed model for volcanic margin asymmetry in the South Atlantic does not require simple shear mechanism to produce the observed asymmetrical volcanic material distribution observed both in my data and in seismic refraction studies by previous workers. Understanding the processes and conditions that produce these asymmetries is critical in performing accurate tectonic plate reconstructions and understanding VPM evolution.

3.2 Introduction

The Cretaceous conjugate passive margins of the southernmost - or austral - South Atlantic Ocean include extensive belts of margin-parallel magmatism formed during the initial stages of the breakup of western Gondwana (Hinz 1981; White and McKenzie, 1989; O'Connor and Duncan, 1990; Abreu et al., 1997; Gladczenko et al., 1997; Mohriak et al., 2002; Blaich et al., 2011; Stica et al., 2014). The Early Cretaceous (126-137 Ma) opening of the South Atlantic has been divided by previous workers into three, main stages: 1) pre-rift, voluminous continental flood basalts affecting the diffuse, cratonic rift basins (Rabinowitz and LaBrecque 1979; Unternehr et al. 1988; White and

McKenzie, 1989; O'Connor and Duncan, 1990); 2) break-up-related volcanism affecting the rifted continental crust (Rabinowitz and LaBrecque 1979; Unternehr et al. 1988; White and McKenzie, 1989; O'Connor and Duncan, 1990); and 3) initiation of sea floor spreading along a newly-formed mid-ocean ridge that marks the end of the continental rift phase (Unternehr et al. 1988; White and McKenzie, 1989; O'Connor and Duncan, 1990; Nürnberg and Müller 1991; Gladczenko et al. 1997; Franke et al., 2010).

The volcanic conjugate margins along the coasts of South America and West Africa are presently separated by more than 6,500 kilometers of oceanic crust formed by Barremian (131 Ma) to recent spreading along the Mid-Atlantic ridge (Fig. 3.1A). This extensive ocean basin between South America and Africa contains evidence of prolonged periods of magmatism recorded on the seafloor in the form of seamount chains and linear, volcanic ridges (O'Connor and Duncan, 1990; Gladczenko et al., 1997, Jackson et al., 2000) (Fig. 3.1A). Modern day coastlines and bathymetric features exhibit a strong degree of asymmetry from the spreading center with an overall 4.1% wider zone of oceanic crust on the South American side than on the African side (Fig. 3.1A) (Müller et al., 1998).

I present interpretations of deeply-penetrating seismic lines across the 10-200 km-wide zones of plume- and post-rift related volcanic material in the offshore basins of Uruguay and southern Brazil and their conjugate basins in Namibia (Fig. 3.1A). In this study I use deeply-penetrating seismic reflection images across the conjugate margins to identify and compare similar continental

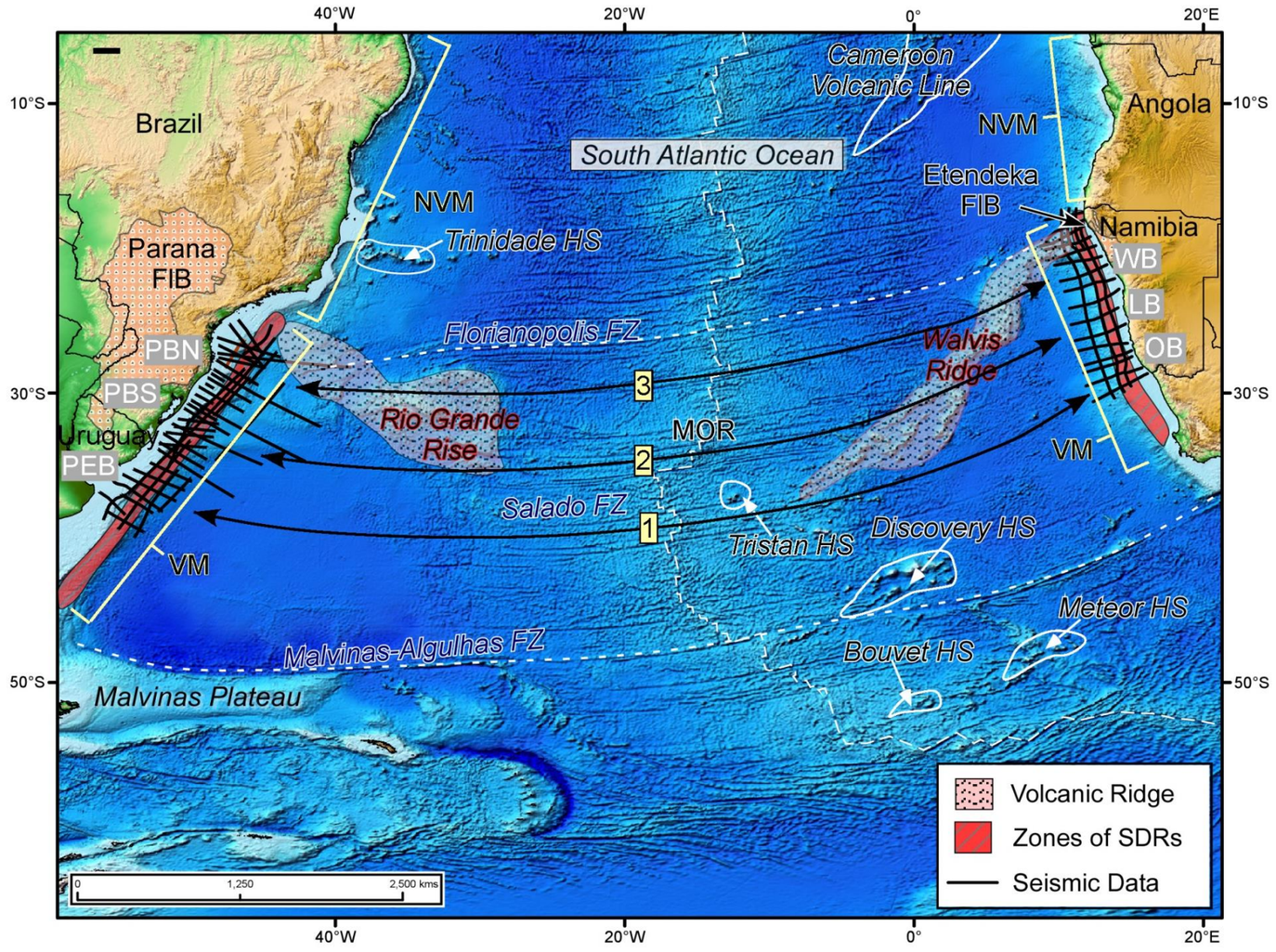

Figure 3.1A:
Regional topographic and bathymetric map of the South Atlantic showing conjugate margins in Uruguay and Namibia described in this study: 1) Punta de Este Basin (PEB); 2) Pelotas Basin South (PBS); 3) Pelotas Basin North (PBN); 4) Orange Basin (OB); 5) Luderitz Basin (LB); and 6) Walvis Basin (WB). Arrowed lines 1 (PEB-OB), 2 (PBS-LB), and 3 (PBN-WB), indicate the conjugate basins identified within the study area and have been chosen for analysis within this investigation. Major oceanic fracture zones (FZ) - including the Malvinas-Algulhas and Florianopolis - allow for precise, plate reconstructions that remove oceanic crust formed at the South Atlantic, mid-ocean ridge (MOR) and realign the rifted, conjugate margins of Uruguay and Namibia. Volcanic margin segments proposed by Franke et al. (2007) and boundaries of the Rio Grande Rise and the Walvis Ridge volcanic complexes are shown. Hotspot-related alignments of volcanoes and seamounts (HS) include these chains: 1) Bouvet; 2) Meteor; 3) Discovery; 4) Tristan; 5) Cameroon; 6) Trinidade.

rift and volcanic features and to infer the relative ages of structural and lithologic features from the seismic images. I use these observations to compare to previous studies mainly based on refraction data and to propose a tectonic, evolutionary history for the rifting to oceanic spreading transition. The primary objective of this study is to integrate these observations and interpretations to establish crustal boundaries for an evaluation of symmetries between conjugate volcanic passive margins.

The mapping and modeling of Cretaceous igneous belts along both conjugate margins has been carried out in the South Atlantic for the past, several decades (Hinz 1981; White and McKenzie, 1989; O'Connor and Duncan, 1990; Abreu et al., 1997; Gladczenko et al., 1997; Blaich et al., 2011; Mohriak et al., 2002; Franke et al., 2007; Hirsch et al., 2009; Blaich et al., 2013; Becker et al., 2014; Koopman et al., 2014; Stica et al., 2014). The contribution of this paper to the topic of magmatism related to South Atlantic rifting includes the use the deeply-penetrating seismic lines to map and quantify the lateral distribution of the igneous zones and crustal transitions on the opposing, conjugate margins (Fig. 3.1A). I use these images to define crustal thicknesses, crustal types (continental, thinned continental, oceanic basement), stacked flows of "seaward-dipping reflectors", and the overlying strata of the sedimentary, passive margin section. I interpret these features in a plate-scale, hotspot and paleogeographic context and present an evolutionary model for the accretion of magmatic material on the conjugate margins that may be applicable to volcanic margins along other conjugate margins.

3.3 Geologic setting

3.3.1 Volcanic margin formation

The creation of large volumes of new mafic crust is commonly associated with volcanic margin formation during the early opening of oceanic basins (White and McKenzie, 1989; O'Connor and Duncan, 1990; Jackson, et al., 2000, Franke et al., 2007; Franke et al., 2011). Evidence of rift- related voluminous magmatism at continental margins is commonly represented by distinctive "seaward-dipping reflectors" composed of stacked, volcanic flows (White and McKenzie, 1989; Hinz, 1981; Mutter, 1984; O'Connor and Duncan, 1990; Gladczenko et al., 1997; Planke et al., 2000; Pindell et al., 2014; Geoffroy, 2015).

Previous studies have identified the continental flood basalts (Hinz, 1981; White and McKenzie, 1989), magmatic underplating, and packages of seaward-dipping reflectors (SDRs) (Mutter, 1984; Geoffroy, 2005; Pindell et al., 2014; Geoffroy, 2015) as common elements of VPMs. Oceanic plateaus (O'Connor and Duncan, 1990; Gladczenko et al., 1997; Jackson et al., 2000) and seamount chains (O'Connor and Duncan, 1990; Müller et al., 1998) (Fig 3.1A and 3.1B) have also been proposed as common components of volcanic activity following the period of normal oceanic crust production (Blaich et al., 2013; Becker et al., 2014; Pindell et al., 2014).

3.3.2 Opening of the South Atlantic

The volcanic passive margin of Uruguay and Southern Brazil began to

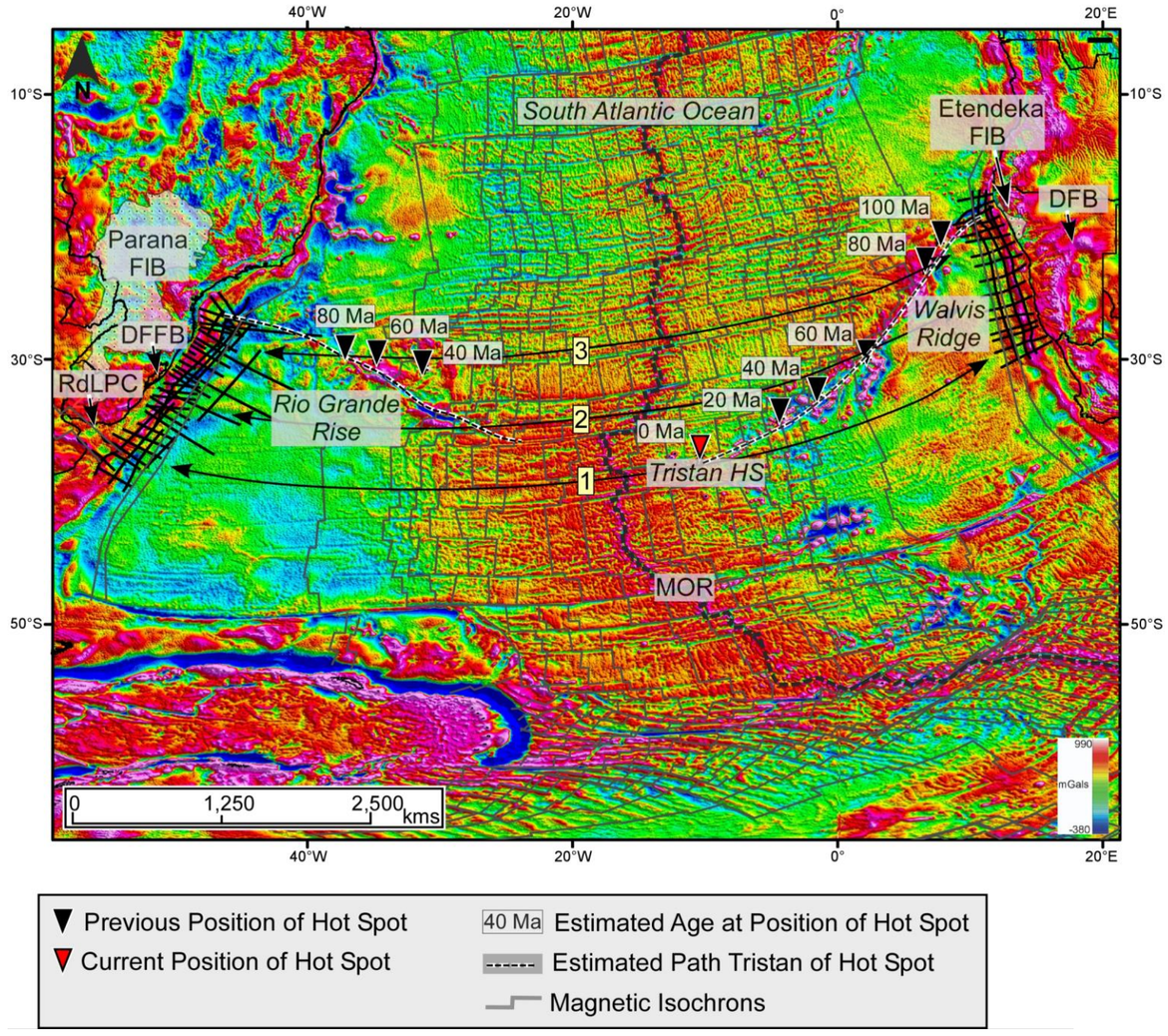

Figure 3.1B:
Regional, satellite free-air gravity data modified from Sandwell and Smith (2014) illustrates the various features associated with the intense volcanic activity that has taken place within the South Atlantic. Continental Rocks of the Rio de la Plata Craton (RdLPC) and the Dom Feliciano Foldbelt (DFFB) are the conjugate members to the Damara Foldbelt (DFB) in Namibia. Magnetic lineation and physical samples from the Rio Grande Rise and the Walvis Ridge provide firm date constraints on the volcanic complexes (O'Connor and Duncan, 1990; Rohde et al., 2013, O'Connor and Jokat, 2015), including the present day location of the Tristan de Cunha Hotspot, formerly a large effusive mantle plume. (Free-air anomaly gravity data: reds represent gravity highs; blues represent gravity lows.)

separate from its conjugate margin in Namibia after the initial opening of the South Atlantic in the Hauterivian (~ 134 Ma) (Rabinowitz and LaBrecque 1979; Unternehr et al. 1988; Nürnberg and Müller 1991; Gladczenko et al. 1997; Franke et al., 2010). From magnetic anomaly investigations, a south-to-north unzippering process is the most widely accepted interpretation for the opening of the South Atlantic Ocean north of the Malvinas-Algulhas Fracture Zone and south of the Florianopolis Fracture Zone (Rabinowitz and LaBrecque 1979; Austin and Uchupi 1982; Uchupi 1989; Jackson et al. 2000) (Fig 3.1A).

During the Hauterivian (132 Ma), onshore continental flood basalts were erupted in the Paranà and Etendeka intracratonic basins (Hoernle et al., 2015) (Fig 3.1A, B). The spatial distribution of the pre-opening flood basalts have been well-mapped and displays a markedly asymmetrical distribution with a larger area of volcanism on the South American plate (Jackson et al., 2000) (Fig 1A and 1B). Two mechanisms have been proposed by previous workers to explain this asymmetrical distribution of continental, flood basalts include: 1) the location of the of the Tristan de Cunha Plume west of the paleo-rift axis (O'Connor and Duncan, 1990); and 2) the presence of a high-relief topographic area that restricted the eastward flow of continental flood basalts from the west to the Etendeka province of Namibia (White and McKenzie, 1989).

Progressive and northward unzipping of the two continental margins followed zones of inherited crustal weakness along late Paleozoic orogenic belts bounding the Rio de la Plata craton and the Dom Feliciano fold belt of South America and the African Damara orogenic belts of west Africa (Chapter 4, this

dissertation) (Fig. 3.1B). These early rifts were followed by voluminous, volcanic eruptions basalts along the main rift axis (White and McKenzie, 1989; O'Connor and Duncan, 1990; Gladczenko et al. 1997; Jackson, et al., 2000; Franke et al., 2010) (Fig 3.1A). In these rifted, volcanic areas, massive zones of SDR complexes up to 24 km in thickness were emplaced along the rift axis and were accreted basinward as the two plates continued to diverge (Hinz, 1981; Gladczenko et al. 1997; Jackson, et al., 2000; Franke et al., 2010). The wide complexes of SDRs show distinct geometries, features, and morphologies on my 2D seismic reflection data used for my study and allow many new interpretations.

Once the pulse of excess magma supply related to the nearby mantle plume was depleted, the initial formation of normal oceanic crust began along the South Atlantic spreading ridge and a north-to-south transgression of marine waters filled the rift valley containing the axial spreading ridge (Rabinowitz and LaBrecque 1979; Austin and Uchupi 1982; Uchupi 1989; Jackson et al. 2000). Maps of high-resolution bathymetry and free-air gravity data illustrate the present-day position of the mid-ocean ridge (MOR), the Rio Grande-Walvis Volcanic Ridges, and the asymmetrical distribution of various hot-spot related features on the ocean floor (Fig 3.1A and 3.1B).

3.3.3 Plate motion

The pre-rift position of the Tristan de Cunha plume in the area of the Paraná-Etendeka continental, flood basalts has been described by previous

workers (O'Connor and Duncan, 1990; White and McKenzie, 1989; Jackson et al., 2000; Hoernle et al., 2015) (Fig 3.1B). Plume-related volcanism following the intra-plate, subaerial emplacement of the Paranà-Etendeka flood basalts is recorded within the Rio Grande Rise-Walvis Ridge volcanic complex and has been dated to show a consistent, west-to-east age progression in the oceanic crust for about 60 million years during the Cretaceous (130-60 Ma) (O'Connor and Duncan, 1990; Rohde et al., 2013, O'Connor and Jokat, 2015) (Fig 3.1b). This migration of locus for the volcanic features is the result of movement over the Tristan de Cunha plume head producing a track on the separating South American and African plates (O'Connor and Duncan, 1990; Mueller et al., 1998, Fairhead and Wilson, 2005)

Ages of the of the marine sediments deposited on the accreted volcanic ridges have been determined by deepsea drilling (Barker et al, 1981a; Barker et al., 1981b; Hay et al., 1982;) and by age interpretations of magnetic stripes in the underlying oceanic crust produced at the spreading ridge (Rabinowitz, 1976; Cande and Rabinowitz, 1978; Cande and Rabinowitz, 1979; LeBrecque at al., 1984; Cande et al., 1988; Shaw and Cande, 1990). These combined drilling and magnetic data reveal a period of 70 Ma (130-60 Ma) of when the underlying mantle Tristan de Cunha plume was directly beneath the young, spreading ridge (O'Connor and Duncan, 1990; Müller et al., 1998, Fairhead and Wilson, 2005) (Fig 3.1B).

The apparent asymmetry of the Rio Grande Rise-Walvis Ridge volcanic complex (wider limb associated with the Walvis Ridge to west, more narrow limb

associated with the Rio Grande Rise to east – Fig. 3.1A) has been attributed to westward migration of the spreading center relative to the plume head in addition to a series of ridge jumps (O'Connor and Duncan, 1990; Müller et al., 1998, Fairhead and Wilson, 2005) (Fig. 3.1B). The continued westward migration of the spreading center relative to a fixed position in the mantle has positioned the Tristan de Cunha Plume head, off-axis of the original spreading center, and approximately 300 km east of the modern, mid-ocean ridge (O'Connor and Duncan, 1990; Müller et al., 1998; Fairhead and Wilson, 2005) (Fig. 3.1B).

3.4 Previous studies

3.4.1 Results from recent South Atlantic conjugate margin studies

Previously proposed asymmetrical elements of the South Atlantic conjugate margins include: 1) conjugate onshore-flood basalts and SDRs (Gladczenko et al., 1997); 2) SDR's (Koopman et al., 2014); and 3) high-velocity lower crust (Becker et al., 2014).

Koopman et al. (2014) studied the variability of the conjugate volcanic margins in the South Atlantic using variable-record-length seismic reflection data. In this study they identified distinctive, along-strike margin segments within the belts of SDRs and the transitions between fracture zones. They integrated dated, magnetic lineation data for age constraints and observed an asymmetrical relationship of SDRs and HVLC underlying the conjugate margins, with an excess amount of igneous material being present on the African plate.

Becker et al. (2014) studied conjugate margin study in the austral region of the South Atlantic using regionally spaced seismic profiles integrated with gravity data. This approach revealed an asymmetrical distribution of HVLC bodies similar to Koopman et al.'s findings (Becker et al., 2014).

Koopman et al. (2014) and Becker et al. (2014) attributed the mechanism for the emplacement of asymmetric conjugate SDR complexes to a simple shear rifting process (Lister et al. 1986). This simple-shear model invokes the presence of a lithosphere-thick detachment within the crust resulting in asymmetric geometries between the diverging plates. Becker et al. (2014) concluded that rifting style was the cause of: 1) the unequal distribution of the Paranà-Etendeka Flood Basalts (wider zone to Paraná); and 2) the wider zone of HVLC bodies is located beneath the West African conjugate margin.

3.4.2 Previous models for SDR formation

Magma-rich continental breakup has been previously studied at many conjugate margins (Hinz, 1981; Mutter, 1984; Planke et al., 2000; Geoffroy, 2005; Pindell et al., 2014; Geoffroy, 2015). Planke et al. (2000), Geoffroy (2005), and Pindell et al. (2014) have established widely accepted models with overlapping elements from the initial stages of break-up to the passive margin phase. From established models cited above, the initial sequences of magmatic activity during the continental break-up stage involves the development of a thick, volcanic pile along the rift axis (Pindell et al.,2014)(Fig. 3.2A). Initial volcanic flows onto rifted, continental crust are faulted along landward-dipping,

normal faults (Geoffroy, 2005; Pindell et al., 2014) (Fig. 3.2A). As plate divergence continues, the once-elevated volcanic flows rotate downwards towards the nucleating spreading ridge (Pindell et al., 2014; Paton et al., 2017).

Continued magmatism and plate divergence includes the progressive accretion and rotation of SDR complexes from the magmatic rift axis as described by Mutter (1984) and Pindell et al. (2014) (Fig. 3.2B). The basinward rotation of SDR's occurs at the flanks of a basinward (sub-SDR) migrating magma body, Pindell et al. (2014). This rotation is also a result of progressive loading of magmatic material atop the magmatic body and the subsequent differential subsidence (Pindell et al., 2014; Paton et al., 2017) (Fig. 3.2C). The system records the progressive loading and rotation of the once-horizontal sheet flows that are isostatically driven towards the magmatic center, where the denser igneous material is located between rifted continental crust (Paton et al., 2017). This process continues until the magma supply is depleted and the accretion of "normal" oceanic crust begins (Pindell et al., 2014) (Fig 3.2D).

Determining the lithologic boundaries between deformed pre-existing continental crust, newly accreted SDRs, and oceanic crust is critical to constrain the conditions of volcanic passive margin (VPM) formation (Fig. 3.2D). McDermott et al. (2015) introduced the terminology of "limit of continental crust" (LoCC) and "limit of oceanic crust" (LoOC) - that I also use in this chapter to identify the crustal boundaries between continental, oceanic, and igneous crust (Fig. 3.2D).

The position of the LoCC at the transition from continental crust to the

igneous crustal domain is marked by the proximal location of the steepest dipping series of SDR's (Pindell et al., 2014) (Fig 3.2D). Planke et al. (2000) described packages of SDR complexes from a volcanostratigraphic perspective and identified "inner-SDRs" as the earliest sets of basaltic flows that overly continental crust and transition to sets of "outer-SDRs" in a more distal position (Fig 3.2D). For all interpreted lines in this study, the term "SDR complexes" refers to both the subaerially-emplaced, steeply-dipping-reflector packages and its underlying igneous crust that occupies the domain between oceanic and continental crusts (Fig. 3.2B-D).

The oldest marine strata of the passive margin onlaps the underlying rotated SDR packages (Fig. 3.2D). This onlap relationship is supportive of the proposal by Pindell et al. (2014) that there is an abrupt transition from a subaerially emplaced SDRs to a submarine setting along thermally-subsiding, conjugate margins.

3.5 Data

The seismic reflection data used in the study total 27,550 km in length and were acquired by ION Geophysical for regional surveys of both conjugate margins in the period of 2009 to 2014 (Fig 3.1A). UruguaySPAN (2012) and PelotasSPAN (2009) (a subset of the BrasilSPAN3 – 2009) were used as my dataset to document the zones of SDRs on the South American volcanic margins, south of the Florianopolis Fracture Zone (Table 3.1). The NamibiaSPAN seismic reflection data (2014) were also used to document the

Figure 3.2
A 4-stage conceptual model for the evolution of a volcanic margin compiled and summarized from previous authors (Hinz, 1981; Mutter, 1984; Planke et al., 2000; Geoffroy, 2005; Pindell et al., 2014; Geoffroy, 2015). The models presented here address the 4-primary tectonic stages that have been identified to determine crustal limits and the kinematics of SDR formation. Stages A through D illustrate the primary features and components present on a typical, symmetric volcanic margin.

A) This model stage represents the earliest stage of volcanic activity as igneous intrusions into thinned continental crust are present and plate divergence occurs away from the rift axis. Also highlighted are the primary subaerial flood basalts outpouring into the flanking half grabens. Note the elevated rift axis away from a normal thickness continental crust and landward-dipping faults as continental crust “sheds” away from axis. Plate divergence is minimal and is only as wide as the zone of rifting and region of intrusions.

B) The second stage illustrates the continued magmatic outpouring onto fully ruptured continental crust, were a large volcanic pile (Pindell et al., 2014) is emplaced with multiple basaltic flows. Half-graben structures are infilled with a variable composition of rift related sediments and extrusive basalt material. Approximate 20 km separates the opposing plates at this stage and continued divergence results in margin subsidence and SDR rotation basinward.

C) The third stage represents a period of prolonged volcanism during plate divergence and the continuous, symmetric accretion of SDRs and underlying igneous crust, on both margins. Rotated arrows indicate progressive basinward rotation of once elevated to flat-lying flows to steeply dipping packages of basalts towards the volcanic center. Zones of SDRs/igneous crust can be a few 10’s of kilometers wide up to 100’s of kilometers. In this profile a typical 32-km-thick continental crust is thinned and separated by approximately 160 km of SDRs/igneous crust approaching 20 km in thickness at the proximal regions. Crustal thinning and fault movement is considered to be negligible at this stage due to the accretion of new crust and the resulting lack of extensional strain on the continental domain. Therefore continental rifting, in its classical definition, has ceased.

D) The fourth and final stage illustrates a typical volcanic passive margin, were: 1) voluminous volcanism has ceased; 2) a mid-ocean ridge is active; 3) margin subsidence has occurred; and 4) marine drift-sequence

stratigraphy overlies the crustal transitions. This stage indicates conjugate volcanic margins with ~300 km of newly added crust now underlying the young ocean basin. Final rotation of the SDR complexes has occurred and infilling drift sequence marine strata onlap the steeply dipping reflectors. Similar to previous authors (McDermott et al., 2015); I have chosen to use the term limit of continental crust (LoCC) and limit of oceanic crust (LoOC) to describe the crustal boundaries. Using the term "continent-oceanic boundary" isn't appropriate in this scenario, given the lack of that particular transition. Inner and outer SDRs indicate the relative position of SDRs to the margin and crustal limits. Outer highs are sometime present at or near the LoCC, but this study finds that to be an inconsistent feature of within the study area. The SDR-oceanic transition is generally observed as a pronounced "notch" in the Moho and the basinward extend the final SDRs.

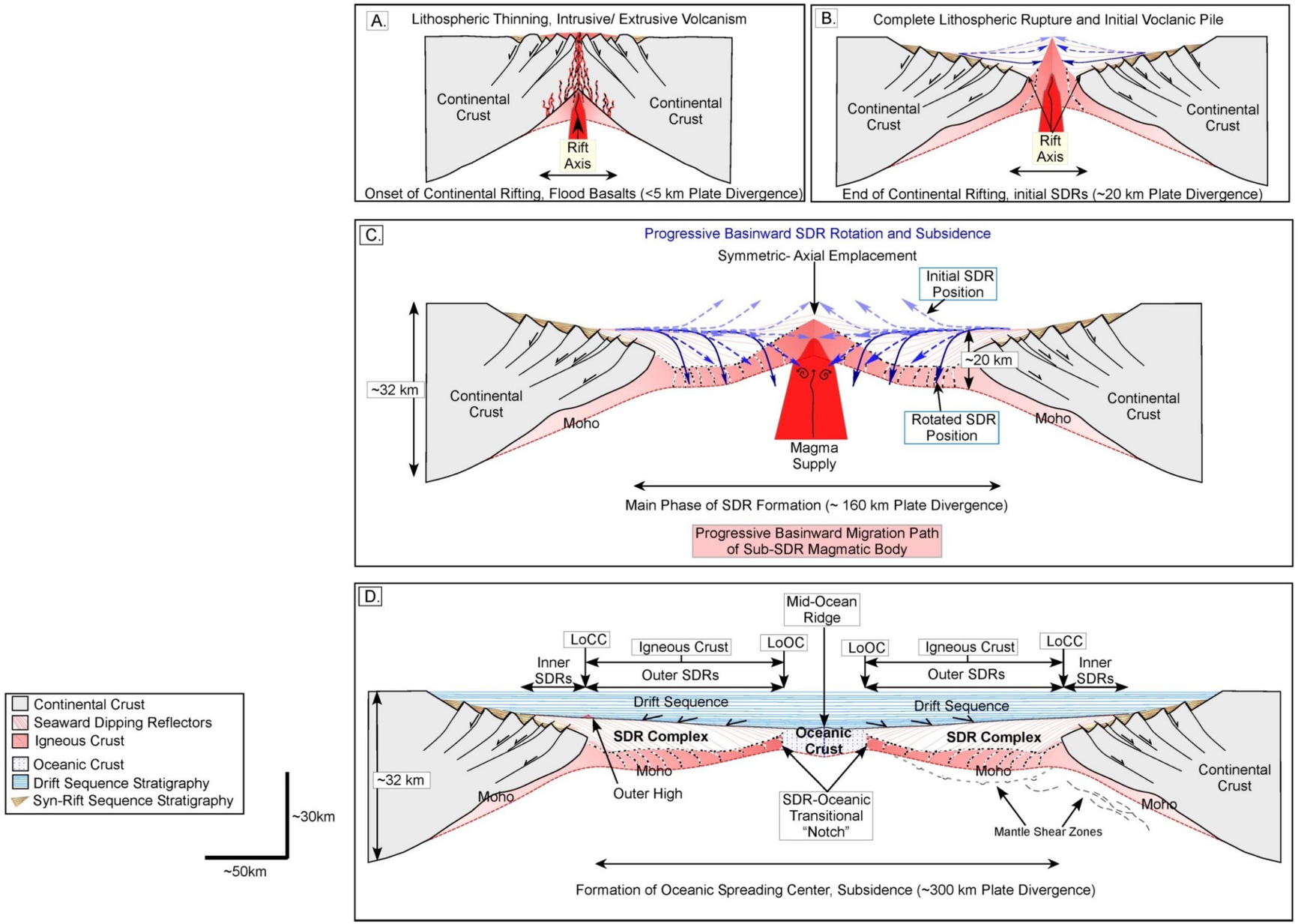
A.
Lithospheric Thinning, Intrusive/ Extrusive Volcanism
Continental Crust
Continental Crust
Rift Axis
Onset of Continental Rifting, Flood Basalts (<5 km Plate Divergence)
B.
Complete Lithospheric Rupture and Initial Voclanic Pile
Continental Crust
Continental Crust
Rift Axis
End of Continental Rifting, initial SDRs (~20 km Plate Divergence)
C.
Progressive Basinward SDR Rotation and Subsidence
Symmetric- Axial Emplacement
Initial SDR Position
~32 km
~20 km
Continental Crust
Moho
Magma Supply
Rotated SDR Position
Moho
Continental Crust
Main Phase of SDR Formation (~ 160 km Plate Divergence)
Progressive Basinward Migration Path of Sub-SDR Magmatic Body
D.
Mid-Ocean Ridge
LoCC
Igneous Crust
LoOC
LoOC
Igneous Crust
LoCC
Inner SDRs
Outer SDRs
Outer SDRs
Inner SDRs
Drift Sequence
Drift Sequence
SDR Complex
Oceanic Crust
SDR Complex
~32 km
Moho
Moho
Outer High
Moho
Continental Crust
SDR-Oceanic Transitional "Notch"
Mantle Shear Zones
Moho
Formation of Oceanic Spreading Center, Subsidence (~300 km Plate Divergence)
Continental Crust
Seaward Dipping Reflectors
Igneous Crust
Oceanic Crust
Drift Sequence Stratigraphy
Syn-Rift Sequence Stratigraphy
~30km
~50km

Figure 3.2 (A-D)

Seismic Survey	Country	Year Acquired	Record Length (s)	Receiver Depth (m)	Cable Length (m)	Total (km) (used in this study)	
UruguaySPAN	Uruguay	2012	18	9.5.	10,200	2,818	
PelotasSPAN	Brazil	2009	18	9.5	10,200	10,667	
BrasilSPAN	Brazil	2009	18	8.5	10,200	3,638	
NamibiaSPAN	Namibia	2014	18	10	10,200	10,421	
						27,544	Total

Table 3.1: Seismic data acquisition parameters (ION GXT)

west African volcanic margin. The total line kilometers of the surveys are 2,818 km, 10,667 km, 3,638 km, and 10,421 km, respectively (Table 3.1).

Seismic lines were recorded to 18 seconds two-way-travel time and were depth-migrated to 40 kilometers (Table 3.1). Data processing from raw stacks to the final pre-stack depth migration shown in this study included proprietary ION Geophysical applications and processing workflow.

Acquisition specifications from survey to survey had varied air-gun source depths varied (8.5-10 m), but a uniform cable length of 10,200 m (Table 3.1). Survey orientation and spacing was designed at right angles to the extension direction of the rifts with orthogonal dips lines connecting the strike lines (Fig. 3.1A).

3.6 Interpretation of deep-penetration seismic reflection lines

Seismic profiles from three conjugate basin pairs along the margins of Uruguay/Sothern Brazil and Namibia were interpreted to show the along- and across-strike variability of volcanism within the study area, including asymmetry on the two margins (Fig. 3.1A and 3.1B). I have defined the three conjugate basin pairs as: 1) the Punta de Este – Orange basins; 2) the Pelotas South-Luderitz Basins; and 3) Pelotas North- Walvis Basins (Fig. 3.1A and 3.1B). These divisions were made based on geographic basin terminology from the Namibian margin (Fig. 3.1A and 3.1B). In this section, I identify the recurring features from the seismic data that permit the identification of crustal transition zones. Despite the high degree of variability between the transitional zones,

distinct seismic elements from facies described here form the basis for defining crustal boundaries.

3.6.1 Conjugate basins

Determining the limits of the thick igneous crust with overlying SDRs that separates the rifted continental domain from the normal oceanic domain requires the identification of specific and repeated features on the seismic profiles. Conjugate similarities and differences can be identified once a consistent framework for interpretation has been established.

For this study, the LoCC is positioned beneath the oldest, most proximal sets of steeply-dipping SDR's where the seismic facies are not dipping or layered, and are interpreted as rifted continental crust (Fig. 3.2D). The LoOC position interpretation was placed at the location where the angle of the dipping SDR's diminishes to a sub-horizontal position and where the seismic Moho generally exhibits a downward-facing concavity or "notch" in the transition zone to typical oceanic crust (Fig. 3.2D). In this position, I also observe a change in seismic character from the smooth-top SDRs to a rugose-top oceanic seismic event that defines the top of the SDR units. This change would infer the transition to the sheeted dike emplacement related to normal oceanic crust production at a mid-ocean ridge.

3.6.1.1 Reflection lines from Punta del Este-Orange Basins

Seismic profiles from the southern region of the study area: the Punta de Este (Fig. 3.3A and 3.3B) and Orange Basins (Fig. 3.3C and 3.3D) illustrate the

Figure 3.3A-3.3D: Seismic profiles and interpretation for the conjugate Punta de Este and Orange basins (inset).

- **A)** A 40-km-deep record seismic line from the Punta de Este Basin of offshore Uruguay.
- **B)** The interpreted version of the Punta de Este Basin line shows a west to east crustal transition from: 1) 32-km-thick continental crust; to 2) initially 13-km-thick SDR/igneous crust; to 3) ~6-km-thick oceanic crust in the east. Continental crust shows evidence of extensive thinning from its original thickness and then transitions to a ~175-km-wide zone of SDRs/igneous crust. The LoCC has been determined based on the location of the westernmost rotated packages and located at the former rift axis. The LoOC is observed by the pronounced concave-don Moho expression at the SDR-oceanic transition and the "step-down" at a seismically bright Top-SDR seismic event. Deeper within the section, seismic events are present and are likely evidence of shear zones deep within the mantle. These events do not represent Moho reflectivity.
- **C)** An un-interpreted deep record seismic line from the Orange Basin of offshore southern Namibia.
- **D)** This interpreted Orange Basin seismic profile illustrates an east to west ~28-km-thick continental transitions to a wide ~135 km zone of SDRs/Igneous crust and then to an ~8.5-km-thick section of oceanic crust. The LoCC has been determined based on the location of the easternmost rotated packages, where the LoOC is observed by the pronounced "notch" of the SDR-oceanic transition.

A.

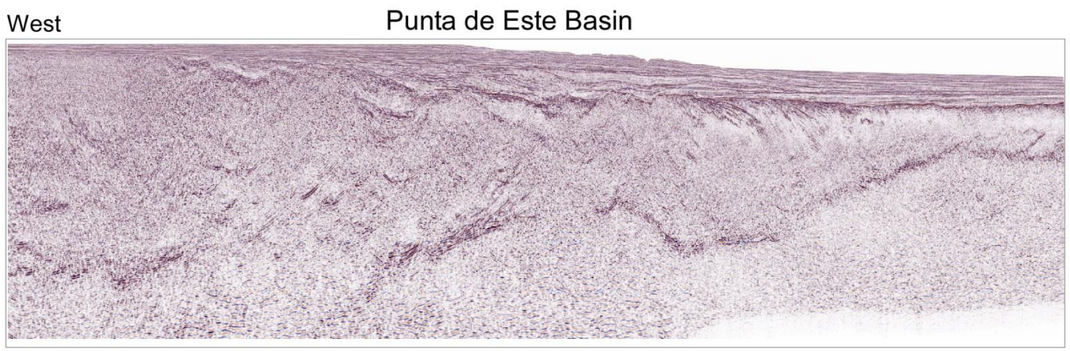

C.

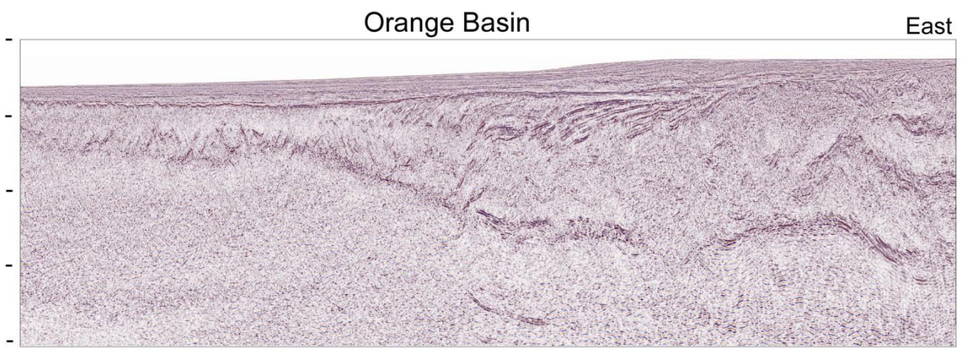

B.

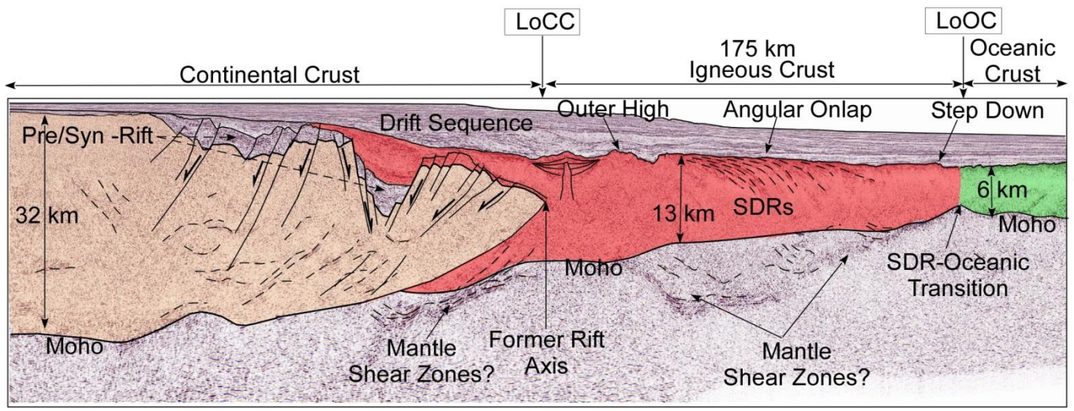

D.

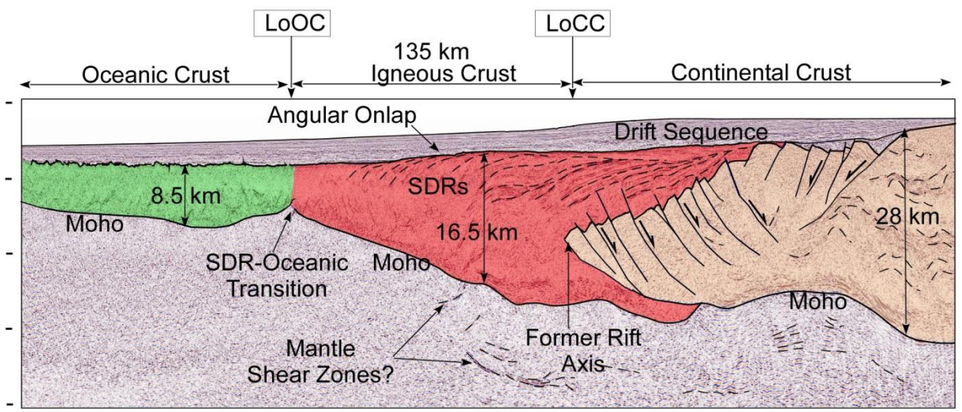

- 0 km -
-10 km -
-20 km -
-30 km -
-40 km -

50 km
VE 3:1

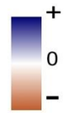

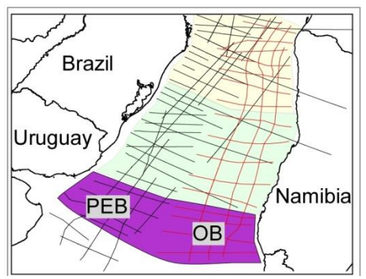

Crustal Domains
Continental Crust
SDR/Igneous Crust
Oceanic Crust

broad nature of SDRs present on the VPMs. The South American seismic profiles both show a broad area of 32-km-thick continental crust that is thinned across a series of horsts and grabens towards the LoCC and the former rift axis (Fig. 3.3A and 3.3B). Beyond the distal limits of the continental crust and extending to the LoOC, there are a series of outer SDR complexes that reach a thickness of 13 km and occupy a belt that is 175-km-wide (Fig. 3.3B). This zone of igneous crust is underlain by a series of mantle seismic events inferred to represent mantle shear zones (Planert et al., 2016) (Fig. 3.3B). The SDR-Oceanic crustal transition at the LoOC is marked by the prominent concave-down “notch” at the in the seismic Moho and a distinctive, crustal step-down coinciding with faint sets of inferred SDRs (Fig. 3.3B). An oceanic crust of ~6 km thickness is present seaward of this transition (Fig. 3.3B). The various crustal domains are floored by a relatively continuous and mappable Moho that is overlain by passive margin strata that onlap the underlying igneous basement (Fig. 3.3B).

Seismic reflection lines from the Namibian margin that show similar volcanic and igneous features to the conjugate Punta de Este seismic profile (Figs. 3.3C and 3.3D). The crustal profile also shows a continuous transition from un-thinned continental crust (28 km), to igneous crust (16.5 km), to oceanic crust (8.5 km) (Fig. 3.3D). In contrast to the conjugate Uruguayan- Punta de Este profile, the early SDR’s on the Namibian margin onlap the distal boundary of the continental crust over a distance of 40 km. The SDRs within the zone of igneous crust reach a thickness of approximately 16.5km and extend across a

135-km-wide zone separating the LoCC and LoOC (Fig. 3.3D). SDR-oceanic transition is defined by the transition from the zone of igneous crust to an 8.5-km-thick oceanic crust is marked by the concave down section of Moho at the base of the crust. There is a smooth and continuous transition from sub-horizontal SDRs to the top oceanic crust (Fig. 3.3C and 3.3D).

The Moho reflector is a high-amplitude, 1-2 km-thick package of reflectors underlying the continental, igneous, and oceanic domains (Fig. 3.3C, 3.3D). At a depth of 36 km below the Moho, there is a series of mantle seismic events that are inferred to be mantle shear zones as a result of rheological alteration of the mantle from intense magmatism (Planert et al., 2016) (Fig. 3.3B and 3.3D). Passive margin strata overlie and angularly onlap the zone of SDR's (Fig. 3.3D and 3.2D).

3.6.1.2 Reflection lines from Pelotas South and Luderitz Basins

The seismic lines shown in Figures 3.4 are from the VPMs of the Pelotas South and Luderitz Basins. Consistent with the lines from the Punta de Este line to the south, Figure 3.4A and 3.4B crossing the Uruguayan margin show full-thickness (32 km), continental crust with a much more abrupt (65 km) transition to the volcanic sequences in the east (Fig. 3.4A and 3.4B) than seen on the previous lines from the Punta del Este Basin (Figs. 3.3A and 3.3B). The interpreted zone of thinned continental crust in this position is 140 km less in width compared to the Punta del Este basin line in Figure 3.3A. The proposed LoCC in Figure 3.4B is located along the former rift axis and marks the transition

Figure 3.4A-4D: Seismic Profiles and interpretation for the conjugate Pelotas South and Lüderitz basins (inset).

- **A)** An un-interpreted deep record seismic line located in the Pelotas South Basin of the offshore southern Brazil and Uruguay region.
- **B)** The interpreted seismic profile from Fig 4A where a relatively narrow zone (~70 km) of SDRs/igneous crust occupies a region between an abruptly rifted continental crust and a section of typical thickness (~6.5 km) oceanic crust. Clear onlap is present on the upper-seismically bright Top SDR horizon as a relatively flat transition is present in the east to oceanic crust. The SDR-oceanic transition is subtle for this example.
- **C)** An un-interpreted deep record seismic line from the Luderitz Basin of Namibia and a conjugate image from Figure 4 A and B.
- **D)** This interpreted section shows an extensively rifted zone of continental crust with a high density of internal seismic events, likely evidence of previous deformation. West of the LoCC, a 90-km-wide/ 14-km-thick zone of SDRs/igneous crust transitions to a thick ~8.5-km-thick oceanic crust in the West.

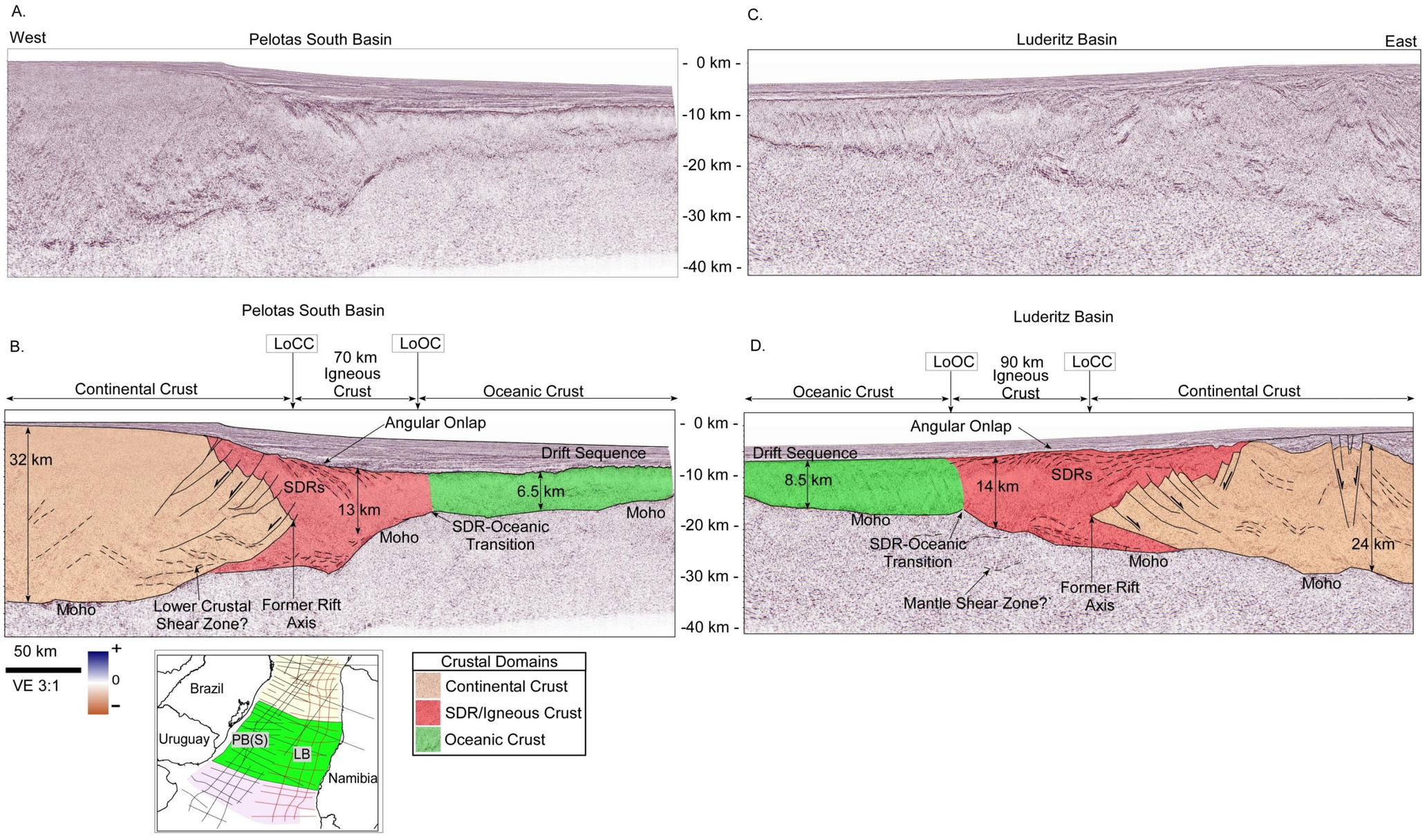
A.
West
Pelotas South Basin
C.
Luderitz Basin
East
- 0 km -
-10 km -
-20 km -
-30 km -
-40 km -
Pelotas South Basin
B.
LoCC
LoOC
70 km
Igneous
Crust
Continental Crust
Oceanic Crust
Angular Onlap
Drift Sequence
32 km
SDRs
13 km
6.5 km
Moho
SDR-Oceanic
Transition
Moho
Lower Crustal
Shear Zone?
Former Rift
Axis
Luderitz Basin
D.
LoOC
90 km
Igneous
Crust
LoCC
Oceanic Crust
Continental Crust
Angular Onlap
Drift Sequence
8.5 km
14 km
SDRs
Moho
SDR-Oceanic
Transition
Mantle Shear Zone?
Former Rift
Axis
Moho
24 km
Moho
50 km
VE 3:1
+
0
–
Brazil
Uruguay
PB(S)
LB
Namibia
Crustal Domains
Continental Crust
SDR/Igneous Crust
Oceanic Crust

to the basinward igneous domain consisting of SDR complexes that extends to a width of 70 km and reaches a thickness of 13 km (Fig. 3.4B).

The transition from SDRs to a 6.5-km-thick oceanic crust across the Uruguayan margin is interpreted at a concave down “notch” of the Moho (Fig. 3.4A and 3.4B). The SDR-oceanic crust transition for this profile shows distinctly sub-vertical and planar seismic events, characteristic of oceanic crust production, east of the dipping reflectors of the SDRs (Fig. 3.4B). The interpreted Moho is a continuous reflective event underlying all the crustal domains (Fig. 3.4A and 3.4B).

The interpreted, highly-deformed, continental crust of Paleozoic age in Figure 3.4D occupies a 180-km-wide zone of crustal thinning characterized a series of horsts and grabens. Seismic facies within the interpreted upper- and mid-crustal levels reflect the folded and thrusted units of the late Paleozoic Damara orogenic belt (Fig. 3.1B and 3.4D). The thickest section of continental crust imaged within this profile reaches 34 km in the east and thins to ~5.5 km in the west (Fig. 3.4D).

The rifts in continental crust at the western end of the line are overlain by the oldest SDR’s which extend beyond the LoCC for a distance of 90 km towards the ocean basin (Fig. 3.4D). The SDR complex is thickest at the LoCC at 19 km and tapers down to a thickness of 14 km near the LoOC (Fig. 3.4D). The basinward limit of the SDR complex marks the LoOC and oceanic crust of a thickness of 8.5 km lies to the west (Fig. 3.4D).

The oceanic domain on this profile of the Namibian margin exhibits

distinctive, sub-vertical seismic events within the lower crust inferred to represent large-scale dikes from an increasing volume of magmatic supply during the Albian (113-100 Ma) - but is still lacking the excessive volcanic material necessary to produce SDR's (Fig. 3.4D). The Moho interpreted on this profile consists of a 1-3-km-wide band of seismic reflections, rather than a single-isolated event, and underlies all continental and oceanic crustal domains (Fig. 3.4D). As observed on previous profiles in Figures 3.3B and 3.3D, a prominent concave-downward geometry on the Namibian margin marks the transition to oceanic crust from the SDR complexes (Fig. 3.4D). The top reflector between the oceanic and SDR domains is seismically smooth and conformable from east to west (Fig. 3.4C and 3.4D).

3.6.1.3 Reflection lines from Pelotas North and Walvis Basins

Near-conjugate margin profiles through the Pelotas North and Walvis Basins illustrate the wide zones of SDRs related to the intense breakup magmatism at the continental margin (Fig 3.5A - 3.5D). Seismic facies packages from these seismic profiles match previously established VPM features from Figure 3.2 A-D. This pair of seismic profiles of these conjugate margins does not image the transition to a non-SDR-composed oceanic crust (Fig. 3.5A and 3.5B).

The western limit of the Pelotas North line is consists of un-thinned, 27.2-km-thick continental crust that transitions to a 24-18 km-thick series of SDR complexes that extend over an across-margin distance of 280 km (Fig 3.5B).

Figure 3.5A-5D: Seismic profiles and interpretation for the conjugate Pelotas North and Walvis basins (inset).

- **A)** An un-interpreted seismic profile located in the Pelotas North Basin
- **B)** The interpreted section for the Pelotas North Basin shows high angle dips of SDRs at an abrupt LoCC spanning a zone of greater than 280 km. An abrupt transition occurs from the 27-km-thick continental crust to the SDR/igneous domain, indicating that the process of crustal thinning was replaced by the addition of magmatic material. Within the SDR/Igneous crust, five distinct packages of SDRs can be observed and have an onlapping relationship to the older package.
- **C)** An un-interpreted seismic profile from the Walvis Basin
- **D)** The interpreted version of Figure 4C illustrating the 300+-km-wide zone of SDRs from the Walvis Ridge complex. The undulating Moho is at the base of the interpreted igneous crust that varies in thickness from 25- 19 km. The LoCC is interpreted to be located at the eastern-most package of resolvable SDRs.

A.

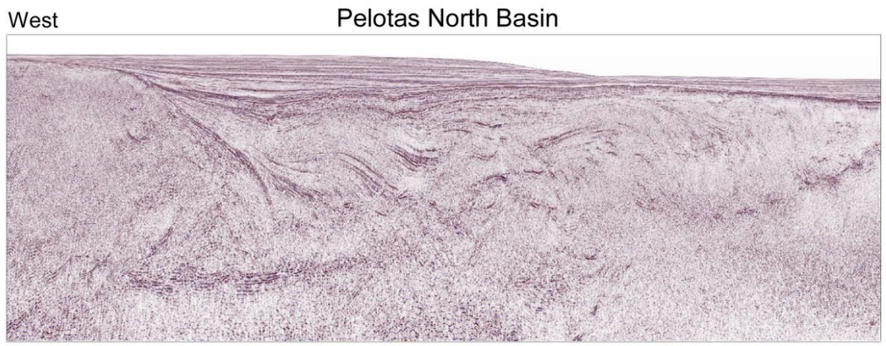

- 0 km -
-10 km -
-20 km -
-30 km -
-40 km -

C.

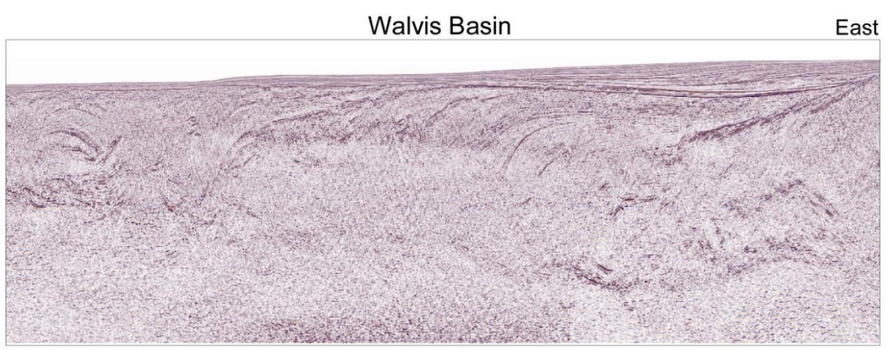

B.

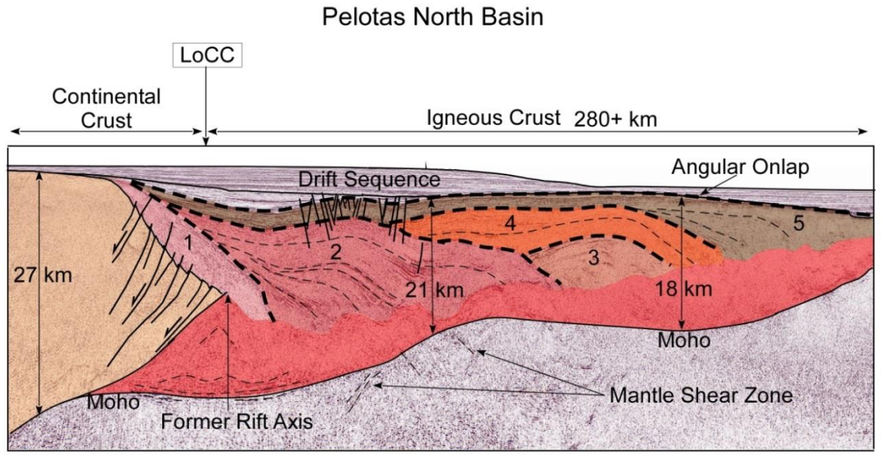

D.

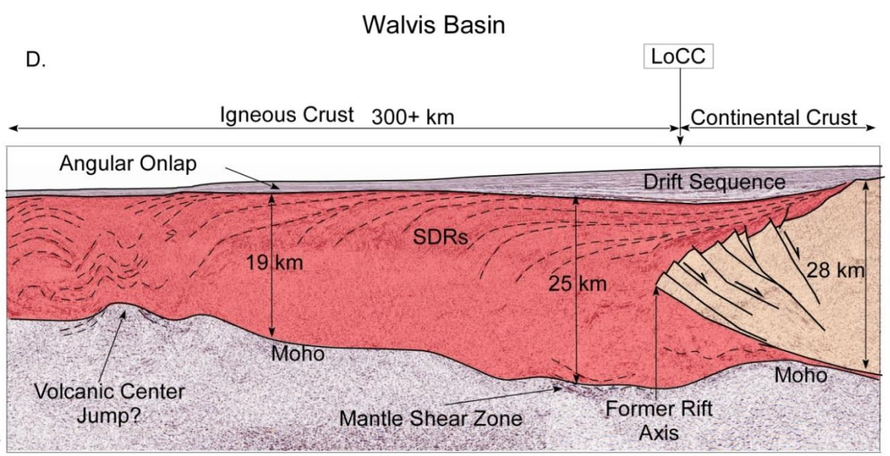

50 km
VE 3:1

+
0
–

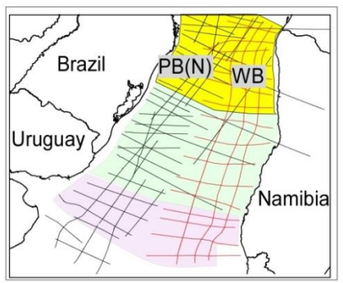

Crustal Domains
Continental Crust
1 SDR Package
2 SDR Package
3 SDR Package
4 SDR Package
5 SDR Package
Igneous Crust

Five distinct packages of SDR's are observed on the southern Brazil margin with younger and basinward-dipping packages onlapping the previous flows (Fig 3.5B). The earliest sets of SDR's emplaced on continental crust on the southern Brazil margin reach maximum dip angles of 20° and transition to sub-horizontal dips on the most distal eastern end of the profile (Fig. 3.5A and 3.5B). SDR sets 1, 2, and 3 are inferred to represent a basinward-migrating magmatic center with expelled volumes of magma that onlap the previous sets of SDRs (Fig. 3.5B). For example, set 4 overlies set 3, that in turn onlaps set 2, and, finally, with set 5 overlying the entire SDR complex (Fig. 3.5B). All these sets indicate a highly voluminous SDR complex which indicates a variability of supply and duration given their onlapping relationship with the older, rotated packages (Fig 3.5B).

The line shown in Figure 3.5C and 3.5D are the near-conjugate line to the line shown in Figure 3.5A and illustrates extensive amounts of SDR's on the Namibian margin. The Walvis Basin profile images the Walvis Ridge volcanic complex and the transition from the continental crustal domain to the entirely igneous domain of the SDR complexes (Fig. 3.5D). In the east, the 28-km-thick continental crust displays an abrupt transition from westward-dipping SDR's (Fig. 3.5D). The 25 to 16-km-thick-zone of SDR complexes likely extend beyond the western limit of the data in this location (Fig. 3.5D). SDR's reach a maximum thickness of 25 km at the former rift axis and average 19 km in thickness in the western area (Fig. 3.5D). On the western part of the line, westward-dipping reflectors converge with a zone of eastward-dipping reflectors

(Fig. 3.5D). These converging packets of SDR reflectors occur above a zone of chaotic events that are floored by a concave-downward geometry of the Moho and could be related to westerly jump in the volcanic center (Fig. 3.5D). Kumar (1979) noted similar events on the conjugate volcanic ridge and igneous domain of the Pelotas North Basin.

SDR complexes appear to progressively prograde westward in a repeating geometry with little variation until they appear to have a convergent relationship with packages in the west (Fig. 3.5D). This convergence may indicate a volcanic center jump, similar to an oceanic spreading ridge jump. The interpreted Moho horizon at this location appears to be the deepest along the rift axis and gradually shallows under 25-16 km SDR's (Fig. 3.5D). The Moho horizon appears as a variable thickness band of seismic events for the entirely of the profile with a wide region of faint to non-existent reflectivity under the SDR complexes (Fig. 3.5C and 3.5D).

3.6.2 Determining SDR complex limits from reflection data

Determining the proximal and distal limits of the SDR complexes within the study area is critical estimating the volumes of SDR's and igneous rocks on both conjugate margins (Figs. 3.2-3.5). The seismic reflection profiles show variable types of transitions between the LoCC and LoOC that complicate the location of the exact limits of the SDR complexes (Figs. 3.2A-3.2D). In the following sections I provide additional description of the interpreted crustal boundaries based on the common seismic facies and the reflector geometries.

Figure 3.6: Seismic profile and interpretation for the Pelotas South basin (inset) illustrating the typical LoCC and SDR transition over a narrow zone of continental rifting.

A) An un-interpreted seismic profile example from the Pelotas South Basin.
B) The interpreted seismic profile is from the Pelotas-South Basin (highlighted in inset) and interpreted elements from a typical volcanic margin are labeled to define the LoCC. Older, outer SDRs are present beyond the LoCC and are present in conjunction with the igneous crust.

A.

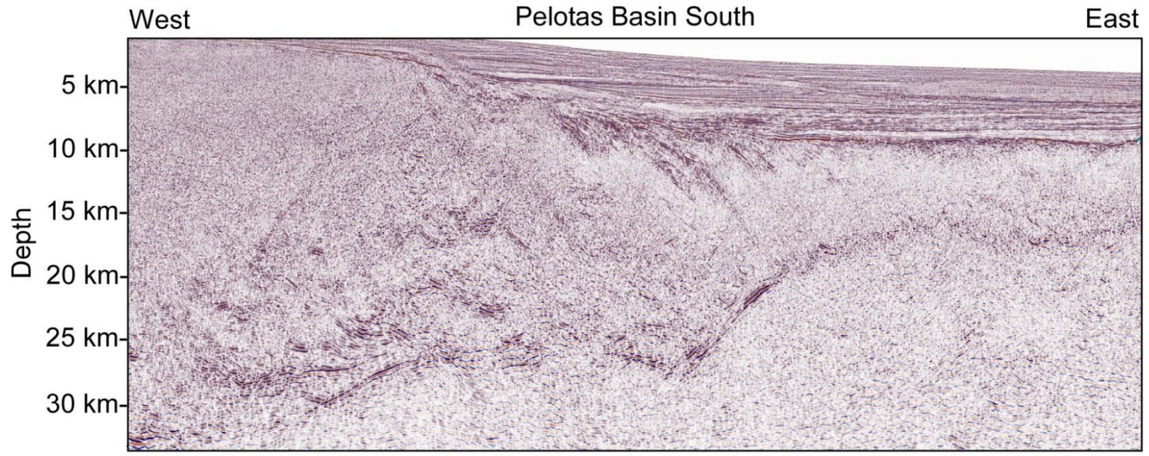
West
Pelotas Basin South
East
Depth
5 km
10 km
15 km
20 km
25 km
30 km

B.

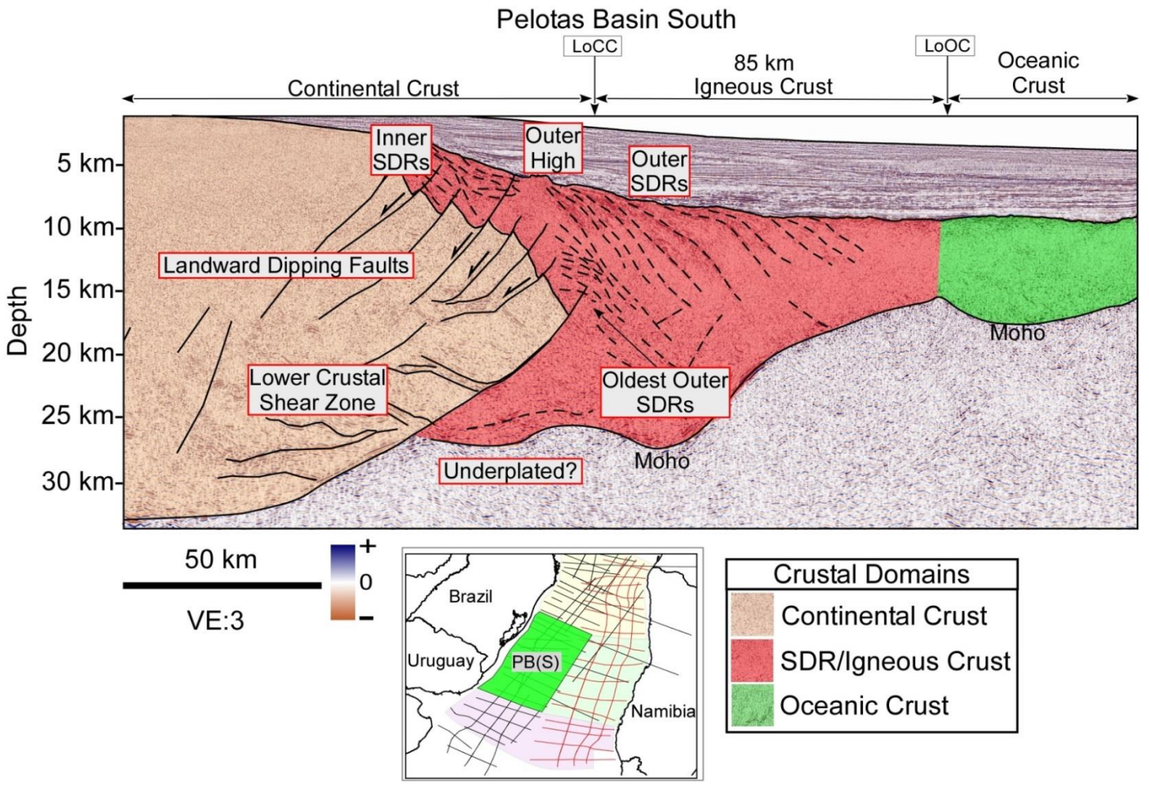
Pelotas Basin South
LoCC
LoOC
Continental Crust
85 km
Igneous Crust
Oceanic
Crust
Inner
SDRs
Outer
High
Outer
SDRs
Landward Dipping Faults
Lower Crustal
Shear Zone
Oldest Outer
SDRs
Moho
Underplated?
Moho
Depth
5 km
10 km
15 km
20 km
25 km
30 km
50 km
VE:3
+
0
−
Brazil
Uruguay
PB(S)
Namibia
Crustal Domains
Continental Crust
SDR/Igneous Crust
Oceanic Crust

3.6.3 Defining the Limit of Continental Crust (LoCC) from reflection data

The basinward limit of rifted continental crust (LoCC) on volcanic margins has been studied intensively by many groups of previous workers (Hinz, 1981, Mutter et al., 1982; Smythe, 1983; Roberts et al., 1984; Geoffroy, 2005; Pindell et al., 2014; Geoffroy, 2015; Paton et al., 2017). Pindell et al. (2014) proposed that the apparent absence of continental crust beneath SDR complexes was required due to the large (>20°), seaward rotation observed for SDR's on conjugate margins in the Gulf of Mexico and South, Central, and North Atlantic (Figs. 3.2B-C). In this investigation I also maintain, similar to Pindell et al. (2014), the required absence of continental crust beyond the initial packages of SDRs in order to achieve the dip angles associated with the final degree of rotation at the LoCC (>20°) (Pindell et al., 2014) (Figs. 3.2B-3.2C).

Pindell et al. (2014) and Geoffroy (2015) also describe landward-dipping normal faults within the continental crust adjacent to the rift axis, this structural style is also observed in profiles from this study (Figs. 3.2A-3.2D). Seismic imaging of the oldest sequences of basalt emplacement atop of continental crust is quite rare and has been interpreted based on seismic events related to the Moho and the landward limit of parallel-, offlapping SDRs reflective seismic facies (Figs. 3.2A-3.2D).

The Southern Pelotas Basin illustrates an example of an abrupt transition from un-thinned, 33-km-thick continental crust to an 18-km-thick (85-km-wide) zone of SDRs and igneous crust (Fig. 3.6). This transition occurs over a 45-km-wide zone of rifting. The oldest magmatic activity present on this profile is

represented by a discrete package of inner SDRs and a prominent outer high (Fig. 3.6). Reflective events within the continental crust and basinward wedging of the inner SDR packages support the interpreted landward dipping faults (Figs. 3.2 and 3.6). Packages of seismic reflections are present in the east underlying the base of the interpreted continental crust and could indicate the presence of underplating at the rift axis in addition to intrusive bodies into the continental crust (Fig. 3.6). The LoCC for this profile has been located at the position where the oldest- outer SDRs lose seismic reflectivity into the underlying igneous crust (Fig. 3.6 and 3.2B-3.2D).

Seismic data in Figure 3.7 is an example of a transition from thinned continental crust to outer SDRs from the Orange Basin on the West African margin. In contrast to the profile in Figure 6, this profile shows a 100-km-wide zone of thinned continental crust that has been thinned to 7 km at the LoCC (Fig. 3.7). Similarly, I observe landward dipping faults that are present under the Inner SDR packages (Fig. 3.7 and 3.2A-3.2D). A seismically bright package (125 km-wide, 3 km-thick) of reflectors is present at the LoCC that have been interpreted to be underplated continental crust at the rift flank (Fig. 3.7). In the western region of the profile in Figure 3.7, I interpret the packages of outer SDRs to extend basinward and overly the new mafic crust below (Fig. 3.7 and 3.2A-3.2D). I also note the absence of an outer high as described by Planke et al. (2000); therefore I have grouped the SDRs that overlie the distal edges of continental crust as Inner SDRs which indicate the earliest presence of

Figure 3.7: Seismic profile and interpretation for the Orange basin (inset) illustrating the typical LoCC and SDR transition over a wide zone of rifting.

A) An un-interpreted seismic profile crust example from the Orange Basin of southern offshore Namibia.

B) The interpreted version illustrates the transition from a wide zone of rifted continental domain to the 95+-km-wide zone of igneous crust underlying progressive SDRs. Inner SDRs are highlighted over a zone of rifted continental domain and the outer SDRs extend basinward overlying igneous crust.

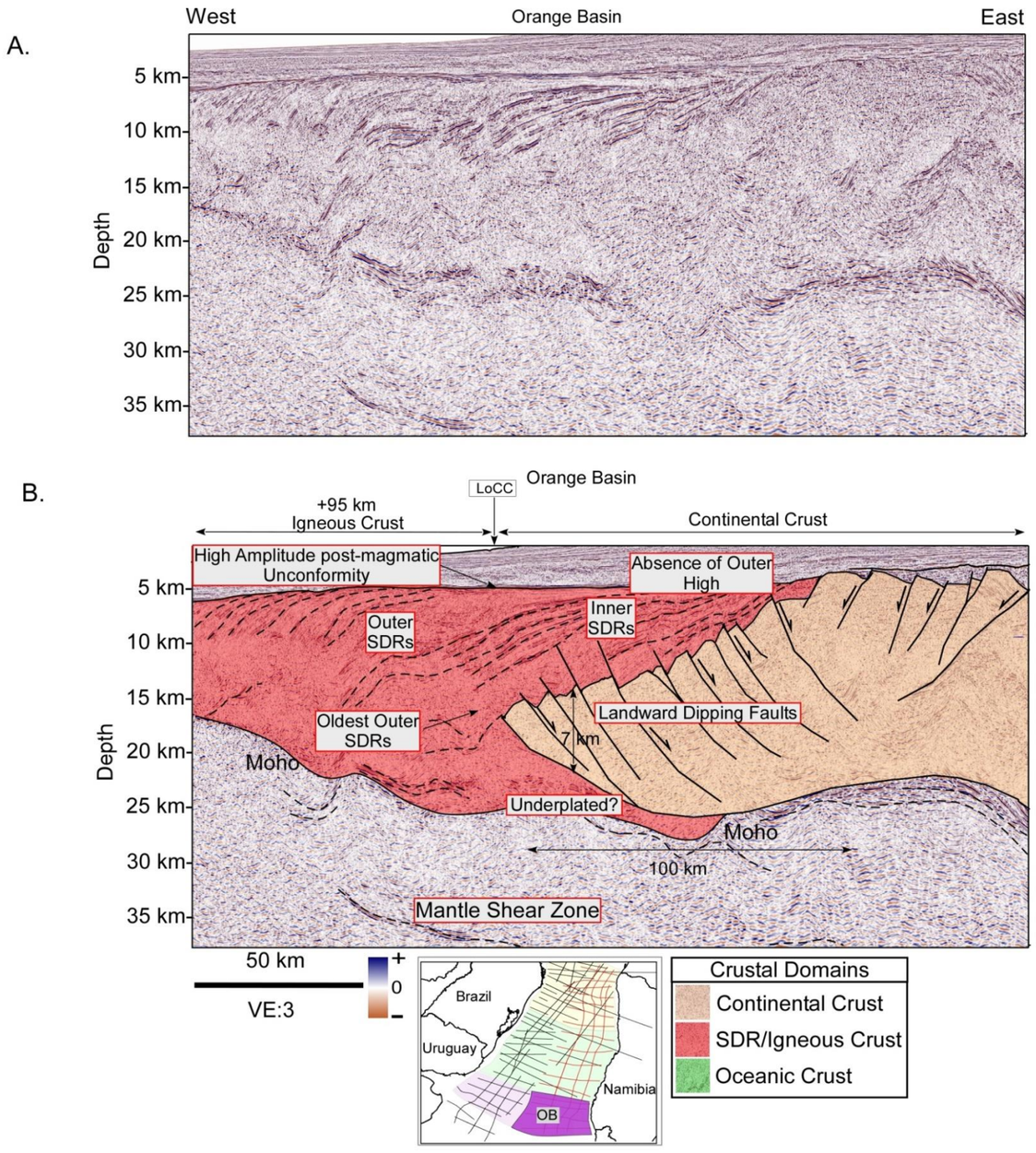
A.
West
Orange Basin
East
Depth
5 km
10 km
15 km
20 km
25 km
30 km
35 km
B.
LoCC
Orange Basin
+95 km
Igneous Crust
Continental Crust
High Amplitude post-magmatic
Unconformity
Absence of Outer
High
Outer
SDRs
Inner
SDRs
Landward Dipping Faults
7 km
Oldest Outer
SDRs
Moho
Underplated?
Moho
100 km
Mantle Shear Zone
50 km
VE:3
+
0
–
Brazil
Uruguay
Namibia
OB
Crustal Domains
Continental Crust
SDR/Igneous Crust
Oceanic Crust

active volcanism as it was subaerially extruded onto the rifted continental crust (Fig. 3.7 and 3.2B). The observed presence of outer highs (Planke et al., 2000); within the data is not observed in my data. It can be concluded that outer highs are not a standard element of SDR volcanostratigraphy.

3.6.4 Defining the Limit of Oceanic Crust (LoOC) from reflection data

The position of the lateral transition from the voluminous emplacement of SDR's to the onset of the accretion of oceanic crust has been identified on lines from both conjugate margins (Figs. 3.8-3.10). This transition line has been interpreted using the underlying and overlying seismic facies along each 2D profile (Figs. 3.8-3.10). In this section, the criteria is explained for identifying this transition based on the depth of the interpreted Moho horizon, reflections within the interpreted crustal domains, and the nature of the top reflector for the igneous and oceanic crust (Figs. 3.8-3.10).

Figures 3.8, 3.9, and 3.10 illustrate the lateral transition from SDR seismic facies to the oceanic crustal domain. I propose that this change in seismic character is gradational as the exact processes do not appear to be replicated in the same manner at each LoOC boundary as observed on other seismic profiles (Figs. 3.8-3.10). The most prominent feature in each section is the presence of a concave-down geometry of the Moho at the LoOC/SDR transition (Figs. 3.2D, 3.8 and 3.9). This 10-15 km-wide and distinctive notch in the Moho is marked by a

Figure 3.8: Seismic profile and interpretation for the Punta de Este basin (inset) illustrating the typical LoOC and SDR transition on the South American Plate.

A) An un-interpreted seismic section of the SDR-oceanic transition example from the Punta de Este Basin from offshore Uruguay.
B) The interpreted seismic section illustrating a gradual decrease in dip angle for the overlying SDRs is an indicator of decreasing magmatic supply prior to the onset of oceanic crust production. This profile shows the transition of dip angles from 16 degrees to 8 degrees followed by a period of magma-water interaction. Figure 3.8 inset schematically represents the gradual transition of SDRs to oceanic crust production.

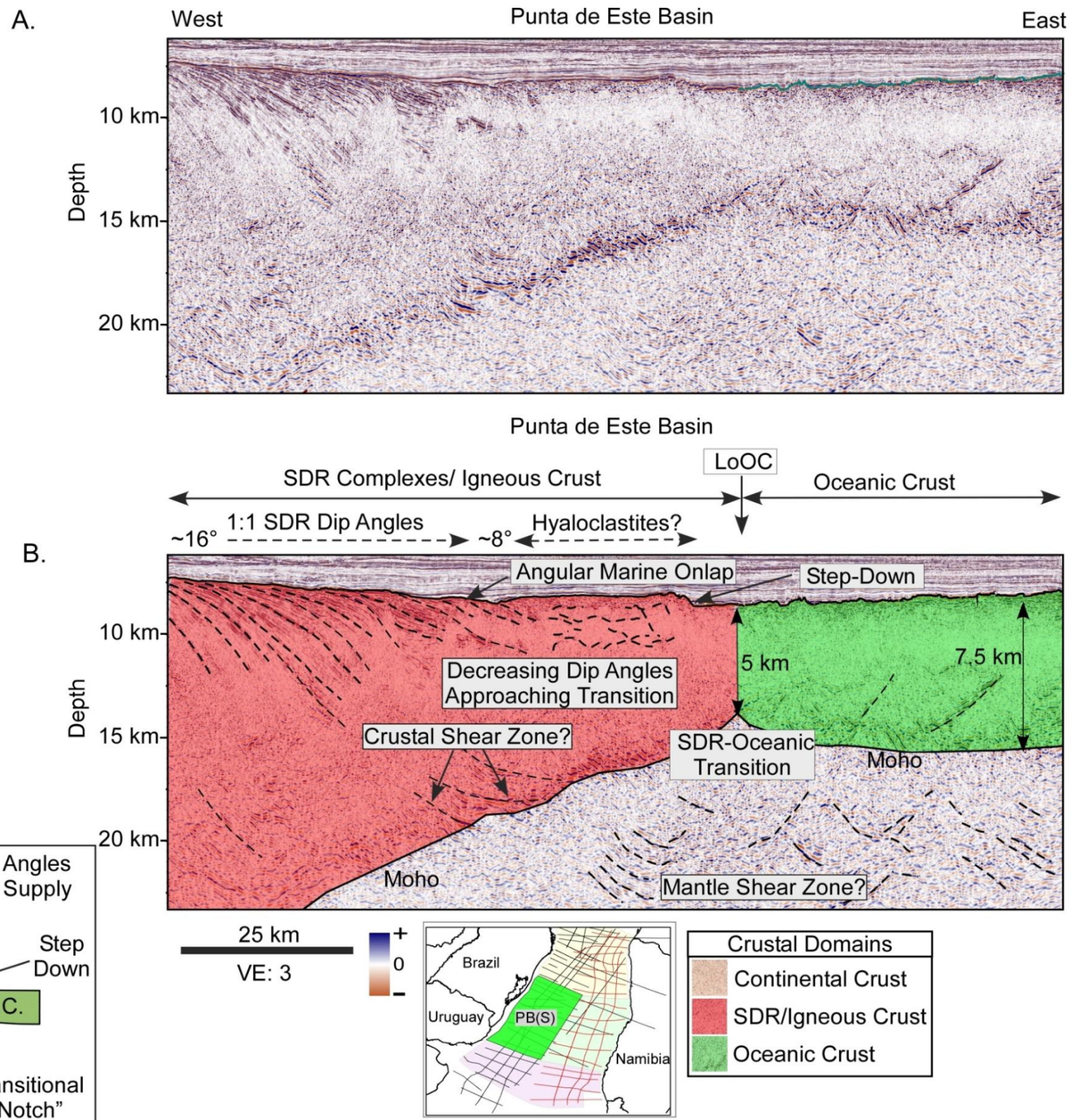

Figure 3.8 Inset

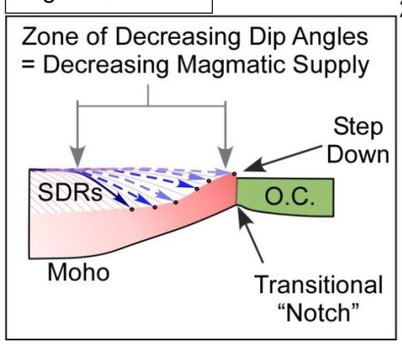

band of reflectors that vary from high- to low- amplitudes (Figs. 3.8-3.10). The transition varies from a smooth, high-amplitude top-SDR package to a rugose top-oceanic event (Figs. 3.8-3.10). A distinct change in internal reflectivity of the crusts also occurs at this location, where proximal dipping events cease and the internal seismic character is more sub-vertical in nature. This transition marks the onset of normal oceanic crust production thought dike accretion at a spreading ridge.

Figure 3.8 illustrates a second example of an SDR-oceanic transition in the Southern Pelotas Basin of Uruguay where more details of the final stages of the outermost SDR's are present (Fig. 3.8). Individual SDRs reach dip angles of 16° in the westernmost position of the line and lose their reflectivity at depths of 12-15 km within the igneous crust (Fig. 3.8). Arcuate and divergent dipping reflectors gradually decrease in dip angle to 8° prior to loosing reflectivity at depths of 7 km (Fig. 3.8).

A package of chaotic and near-opaque reflectors extends to the LoOC east of the shallowest dipping SDRs (Fig. 3.8). I predict this zone to be composed primarily of hyaloclastites that were deposited during a period of transition from subaerial environment rich in ash deposits to a marine setting characterized by larger amounts of basaltic lavas (Planke et al., 2000). Calvés et al. (2011) and Reuber et al. (2016) observed similar seismic facies at the transitional locations and where there were water-extrusive-lava interaction (Fig. 3.8).

The uppermost reflector of the SDR complex is a high-amplitude, smooth

event which contrasts to the rugose reflector of “normal” oceanic crust. The rugosity of normal oceanic crust stems from generation of sub-vertical dike emplacement, the primary mode of oceanic crust emplacement at a slow-spreading, mid-ocean ridge (Fig. 3.8). The rugosity of normal oceanic crust is related to the variable magmatic budget, but remains in contrast to a smooth top-SDR reflector. Also present at the transition in this area is a prominent, basinward-offlapping surface of the SDRs (Fig. 3.2 and 3.8). The notched Moho is present east of the interpreted LoOC where I observe a normal thickness of oceanic crust of 7.5 km (Fig. 3.8).

Seismic data in Figure 3.9 illustrates the zones of crustal transitions within the Lüderitz Basin of Namibia. SDR packages reach dip angles of 14° in a concave down geometry to the east and flatten their arcuate shapes to achieve dip angles of less than 5° at the position of the LoOC (Fig. 3.9). Onlapping, divergent, and planar events are present to the western limit of the SDR complex within this section (Fig. 3.9). The previously described (Fig. 3.8) zone of discordant disrupted and opaque events at the LoOC is not observed on this profile (Fig. 3.9).

The 7.5 km-thick zone of crust at the LoOC and the shallowing Moho forms the boundary between the voluminous SDRs and the oceanic domain (Fig. 3.9). Oceanic crust initially increases in thickness to 8.25 km away from the transition area. Extensive tilted to sub-vertical (~80°) seismic events are present within the upper and lower regions of the crust (Fig. 3.9). A prominent basinward, step-down divides the smooth amplitude of the SDRs and the mildly-

Figure 3.9: Seismic profile and interpretation for the Lüderitz basin (inset) illustrating the typical LoOC and SDR transition on the African Plate.

A) An un-interpreted seismic section of the SDR-oceanic transition example from the Lüderitz Basin from offshore Namibia.
B) An interpreted profile from the Namibian margin showing the abrupt transition of SDRs/igneous crust to the oceanic domain. This transition is illustrated by a decrease in dip angles from 14 to 5 degrees over the distance of 75 km prior to the notable “step-down” above the concave down Moho expression. The clear and significant change in seismic expression is observed as the transition from SDRs/igneous crust to oceanic crust. An abrupt transition at the observed “step down” and concave-down geometry of the underlying Moho.

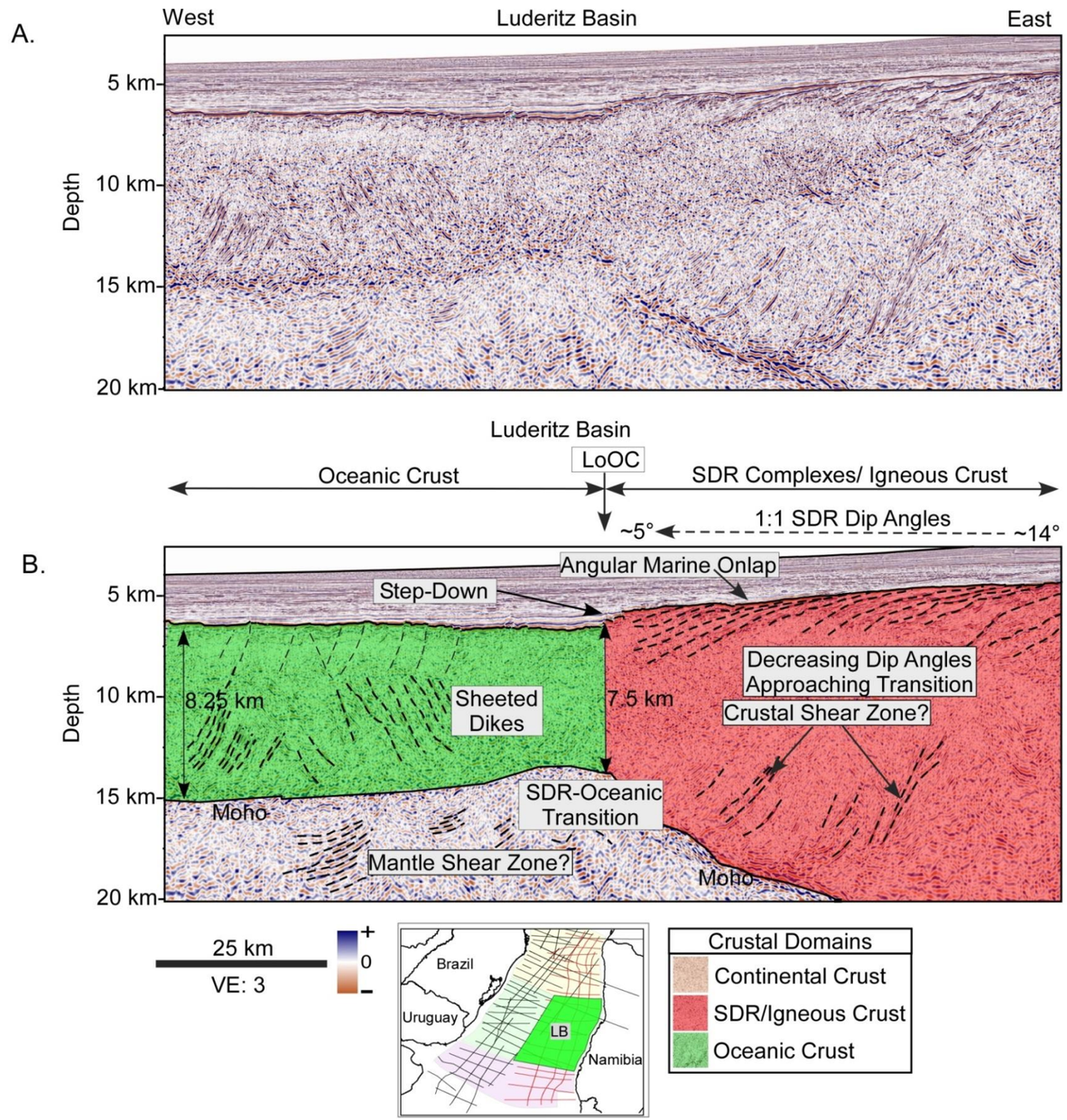
A.
West
Luderitz Basin
East
5 km
10 km
15 km
20 km
Depth
Luderitz Basin
LoOC
Oceanic Crust
SDR Complexes/ Igneous Crust
1:1 SDR Dip Angles
~5°
~14°
B.
Angular Marine Onlap
Step-Down
8.25 km
Sheeted Dikes
7.5 km
Decreasing Dip Angles Approaching Transition
Crustal Shear Zone?
SDR-Oceanic Transition
Moho
Mantle Shear Zone?
Moho
25 km
VE: 3
+
0
−
Brazil
Uruguay
LB
Namibia
Crustal Domains
Continental Crust
SDR/Igneous Crust
Oceanic Crust

rugose oceanic crust (Fig. 3.9). This abrupt change from dipping to sub-horizontal reflectors to the LoOC is inferred to represent a rapid transition from subaerial SDR emplacement of basalts to the incursion of marine waters along the volcanic spreading axis as a result of rapid subsidence and rotation (Planke et al., 2000). The lack of hyaloclastite seismic facies indicates the minor magma-water interaction at the time SDR-producing magmatic activity waned (Planke et al., 2000).

SDR-oceanic crust transitions occur as smooth, high-amplitude events of the outer SDRs to the highly rugose surface of oceanic crust (Fig. 3.10). Seaward-dipping events decrease in dip angle from 14° to horizontal and the underling basement is not well defined (Fig. 3.10). A series of dikes are present within the basal igneous crust and were emplaced into both the pre- and post-rotated SDR packages (Fig. 3.10). This distinction has been made based on the orientation of the intrusion and the cross-cutting nature (Fig. 3.10).

Similar relationships of SDR's and intrusive dikes have been observed on the Norwegian margin by Abdelmalak et al. (2015). The 18 km-wide-zone of oldest oceanic crust is 6 km-thick and shows an early infilling of 0.6 km of sediments overlying a faulted zone (Fig. 3.10). The recurring nature of the elements and seismic facies described from these profiles (Figs 3.8-3.10) add to the evidence of the high degree of variability at the transition between the two domains along margin segments (Figs 3.8-3.10).

Figure 3.10: Seismic profile and interpretation for the Lüderitz basin (inset) illustrating the faulted LoOC and SDR transition on the African Plate

A) An un-interpreted section of seismic from the Lüderitz Basin showing the SDR/Igneous crust to oceanic crust transition.
B) The interpreted profile seismic profile showing the abrupt transition between SDRs and oceanic crust where early faulting has occurred at the transition, west of the “step-down” and above the brief rise in the Moho expression below the transition. Similar to figure 9, a dramatic decrease in SDR dip angle occurs from 14 to 3 degrees.

A.

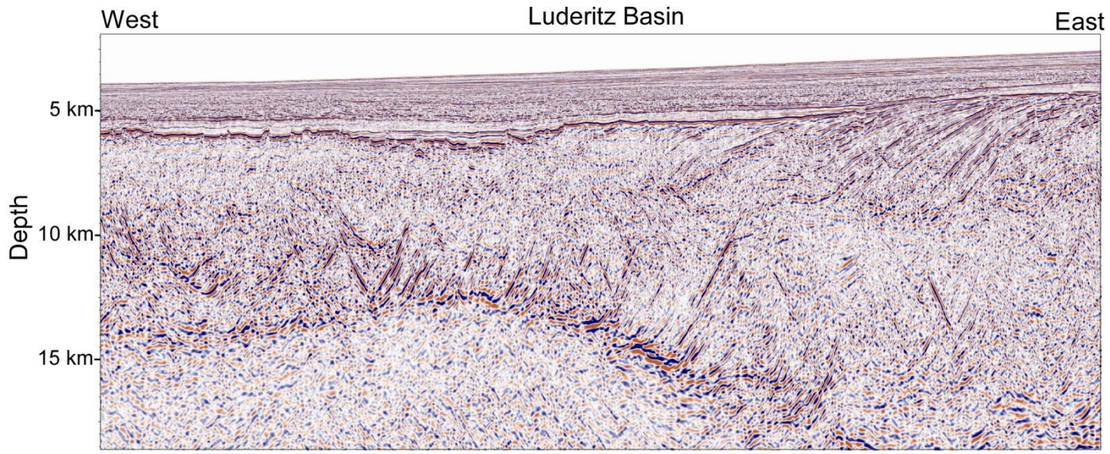

B.

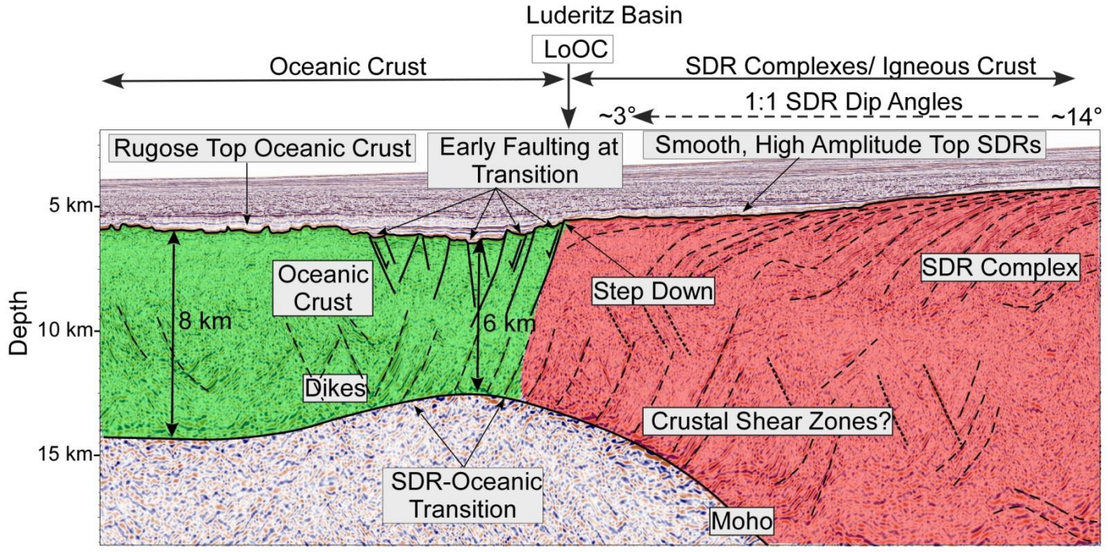

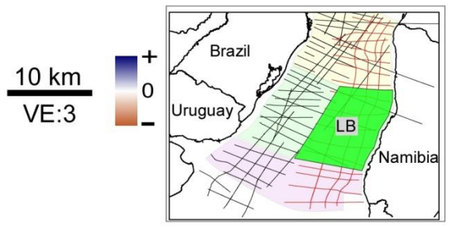

10 km
VE:3

\+
0
–

Crustal Domains
Continental Crust
SDR/Igneous Crust
Oceanic Crust

3.6.5 Mechanism for faulting observed within SDR's

A distinctive, high-amplitude seismic event that represents the boundary between igneous SDRs and overlying strata was used to identify the top of the SDR units on all lines in this study (Figs. 3.2-3.5). Seismic evidence of internal faulting within SDR complexes is generally rare, as subsidence and a basinward migrating volcanic center are thought to be the main mechanisms for SDR rotation (Pindell et al., 2014). In the following section, I describe two areas of widespread, normal faulting within the upper sequences of SDR's. These same normal fault geometries are also expressed in the older, underlying SDRs (Figs. 3.11-3.12). Similar normal faults are also observed on the Rio Grande Rise and the Walvis Ridge volcanic ridge complexes, and are interpreted to be related to the massive volumes of magmatic material or the proximity to the Tristan de Cunha hotspot, as inferred by their absence on margins with less magmatic addition (Figs. 3.1, 3.2, and 3.11-3.12).

The lines in Figures 3.11 and 3.12 provide evidence for faulted SDR's in different marginal settings. The example from the southern Brazil margin of South America shows apparent symmetrical extensional faulting about a prominent convex-upward package of outer SDRs to the east of the continental domain (Fig. 3.11). A proximal sediment-filled graben was created as a result of the localized subsidence and subsequent faulting as shown by basinward onlap of strata against the underlying SDR complexes (Fig. 3.12).

Complex normal faulting of SDR's is also observed within the Walvis basin and includes a series of landward-dipping faults adjacent to a region of

Figure 3.11: Seismic profile and interpretation for the Pelotas North basin (inset) illustrating the faulted TOP SDR surface on the South American Plate

A) An un-interpreted section of seismic from the Pelotas North Basin on the Rio Grande Rise
B) An interpreted seismic profile showing a faulted Top SDR surface that underlies the drift sequence strata. Bold, black-hachured lines delineate the multiple magmatic flows in this area that formed during variable rates of magmatic supply and a migrating spreading center.

A.

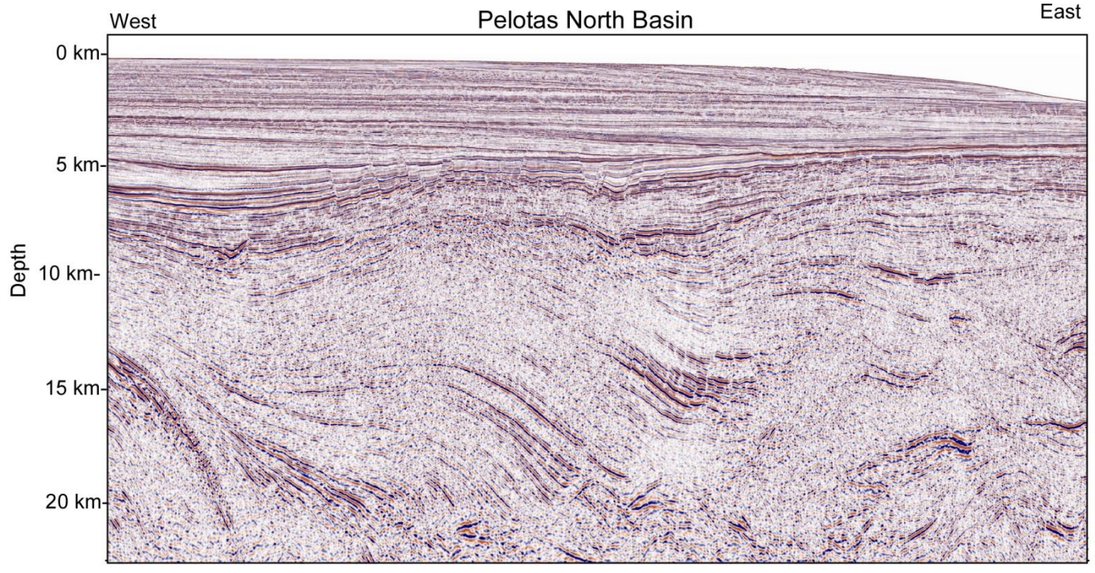
West
Pelotas North Basin
East
0 km
5 km
10 km
15 km
20 km
Depth

B.

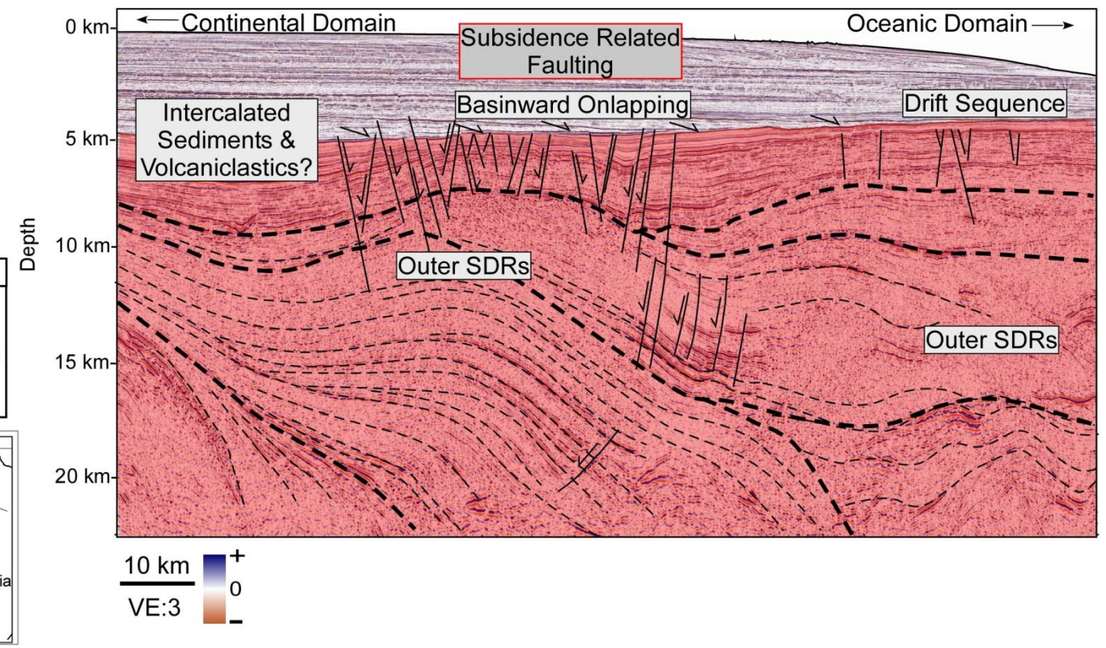
Continental Domain
Oceanic Domain
Subsidence Related Faulting
Basinward Onlapping
Drift Sequence
Intercalated Sediments & Volcaniclastics?
Outer SDRs
Outer SDRs
0 km
5 km
10 km
15 km
20 km
Depth
10 km
VE:3
+
0
−

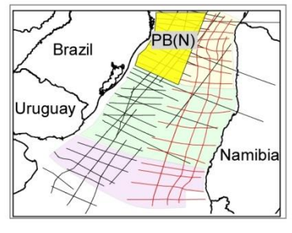
Crustal Domains
Continental Crust
SDR/Igneous Crust
Oceanic Crust
Brazil
PB(N)
Uruguay
Namibia

Figure 3.12: Seismic profile and interpretation for the Walvis basin (inset) illustrating the faulted TOP SDR surface on the African Plate.

A) An un-interpreted section of seismic from the Walvis Basin on the Walvis Ridge volcanic complex
B) A interpreted seismic profiles showing landward-dipping normal faults deforming the upper ~7 km of the SDR complex ,

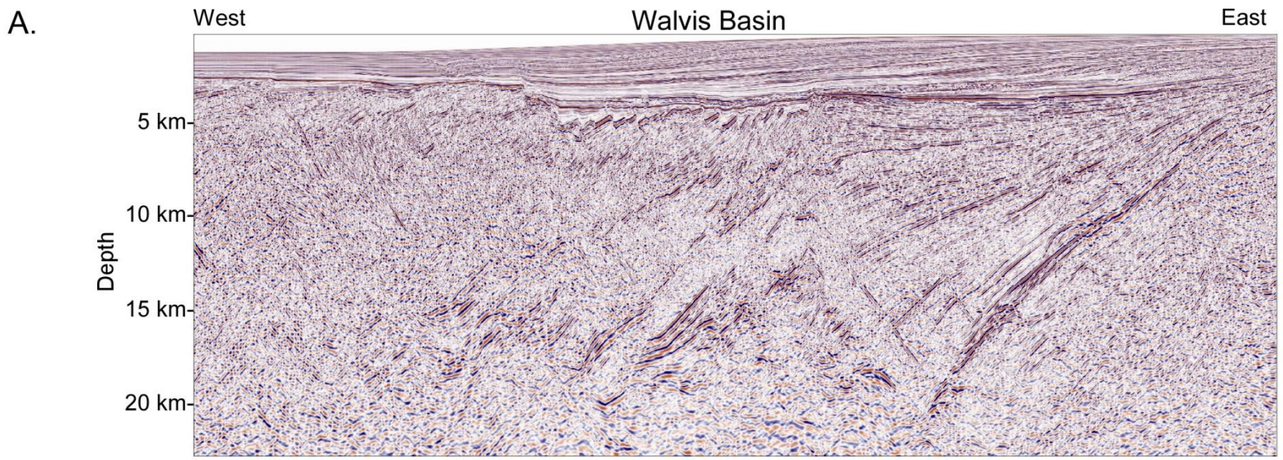
A.
West
Walvis Basin
East
5 km
10 km
15 km
20 km
Depth

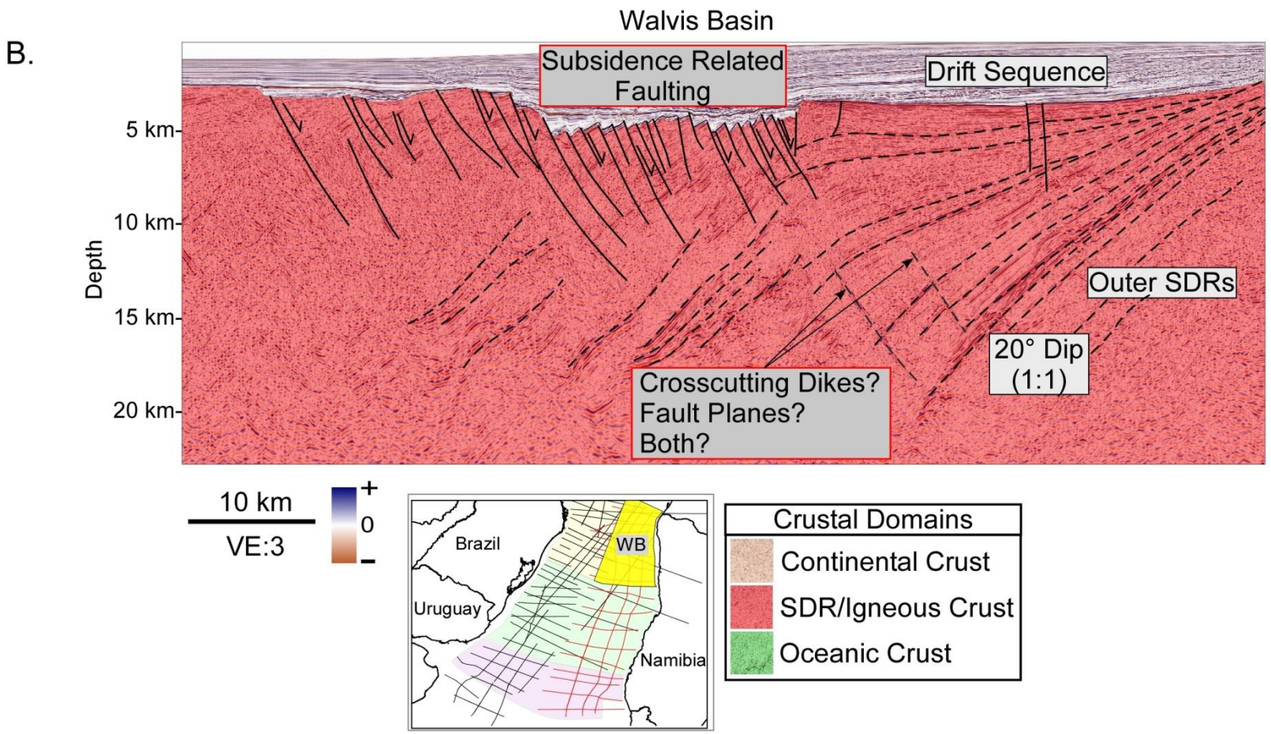
B.
Walvis Basin
Subsidence Related Faulting
Drift Sequence
5 km
10 km
15 km
20 km
Depth
Outer SDRs
20° Dip (1:1)
Crosscutting Dikes? Fault Planes? Both?
10 km
VE:3
+
0
–
Brazil
WB
Uruguay
Namibia
Crustal Domains
Continental Crust
SDR/Igneous Crust
Oceanic Crust

steeply-dipping SDRs (>20°) (Fig. 3.12). The resulting rift zone was subsequently filled by the overlying, clastic sediments of the passive margin (Fig. 3.12). As proposed for the line in Figure 3.5B, the likely mechanism for the normal faulting seen on Figure 3.11 is thermal subsidence overlying a basinward-migrating volcanic center. The faulted SDRs in both locations are located at the oldest position of SDRs for each location and might be a result of greater subsidence related to the initial site of rifting. Normal faulting on the broad scales identified within Figures 3.11 and 3.12 was not observed south of these locations which are further away from the location of the Tristan de Cunha plume and consequently contain less voluminous, volcanic eruptions.

3.6.6 Mapping the Mohorovicic Discontinuity (Moho) and deep igneous events

Deep seismic events related to the Mohorovicic Discontinuity (Moho) are generally well-imaged from both conjugate margins (Figs. 3.3-3.10). Pindell et al. (2014) note the presence of a seismically-well-defined Moho as a key indicator of a magmatic margin versus an amagmatic rifted margin. This characteristic is likely a key process related to the addition of crust at the rifted margin, similar to oceanic crust generation. The Moho discontinuity underlies the unstructured zone below the SDRs and gabbroic igneous crust (Sheridan et al., 1993; Pindell et al., 2014) (Fig. 3.13).

The shallowing basal reflector(s) of this igneous crust is inferred to represent progressive basinward migration of the once-active magma chambers

Figure 3.13: Seismic profile and interpretation for the Pelotas North basin (inset) illustrating the variable Moho expression on the South American Plate.

A) An un-interpreted section of seismic from the Pelotas North Basin on the Rio Grande Rise.

B) The interpreted profile illustrating a highly variable expression of Moho underlying an SDR complex and/or igneous crustal domain.

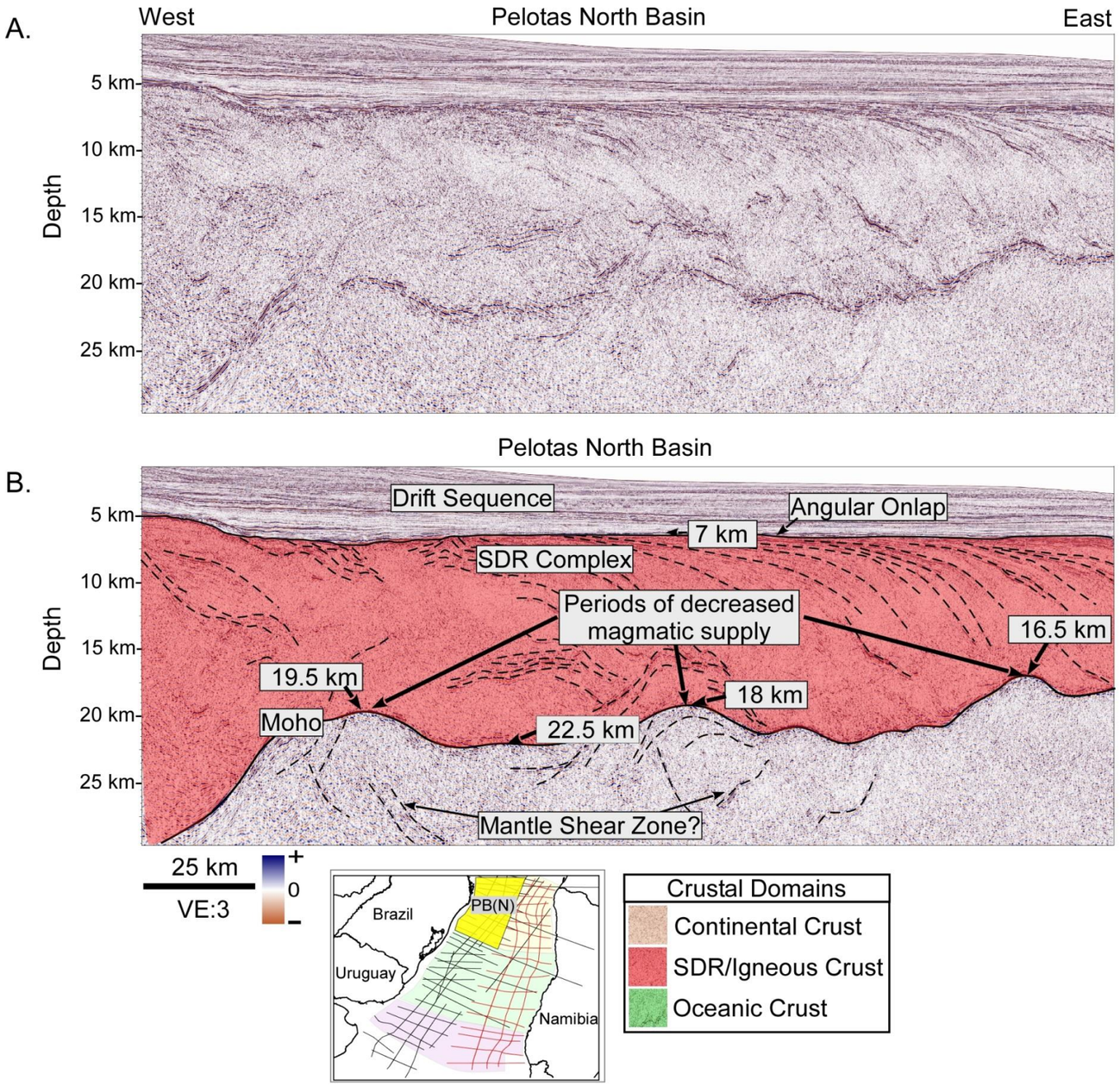
A.
West
Pelotas North Basin
East
Depth
5 km
10 km
15 km
20 km
25 km
B.
Pelotas North Basin
Drift Sequence
Angular Onlap
7 km
SDR Complex
Periods of decreased magmatic supply
16.5 km
19.5 km
18 km
Moho
22.5 km
Mantle Shear Zone?
25 km
VE:3
+
0
−
Brazil
PB(N)
Uruguay
Namibia
Crustal Domains
Continental Crust
SDR/Igneous Crust
Oceanic Crust

that supplied the overlying SDRs (Fig. 3.2). Variations in magmatic supply or spreading rates are likely mechanisms for generating relief along the Moho of the SDR complex that separates the continental and oceanic domains. The interpreted Moho horizon in this study area occurs as wide bands of seismic events or bright and continuous reflectors, similar to VPM observations of Calvés et al. (2011) and Pindell et al. (2014) (Figs 3.3-3.10, 3.13).

An example of the rugosity present along the seismic Moho is illustrated in Figure 3.13 from the Northern Pelotas Basin and the Rio Grande Rise. The Moho has been interpreted from a generally-consistent band of seismic events that underlie the SDRs/igneous crust (Fig. 3.13). The average depth to the top of the SDR complex is approximately 7 km along this profile, illustrating a consistent supply of magmatic material (Fig. 3.13). The Moho varies in depth beneath the angular onlap of the SDRs and has a maximum range from 22.5 km to 16.5 km in depth (Fig. 3.13). This characteristic is in contrast with the described basinward-shallowing trend on other profiles in this study.

For this location, a variability of Moho depths can be explained by changes in the magma supply during the accretion of the SDR complexes. I propose that the mechanism for Moho shallowing is a decrease in the volume of magma supply at the volcanic center. This interpretation corresponds with the regularly observed shallowing of the Moho at the LoOC and its concave down geometry. It is also at this position where the voluminous magmatic supply is greatly reduced and the onset of normal oceanic spreading is initiated. In the case where the Moho deepens again under the SDR complex, I interpret this as a

localized increase in the magmatic supply (Fig. 3.13). I interpret this control of this Moho depth variability to be related to the proximity of the Tristan de Cunha Plume to this location with a variable magmatic supply (Fig. 3.1B).

3.7 Synthesis of main observations in this study and proposed model for South Atlantic volcanic margins

The interpretation of the LoCC, SDR complexes/igneous crust, and the LoOC using deep crustal 2D-seismic reflection data provides new constraints for the spatial distribution and volumes of the volcanic/igneous crustal domain related to continental breakup in the South Atlantic (Figs. 3.1, 3.3-3.13). The evolution of a volcanic margin is marked by the onset of rift-related volcanism, breakup-related magmatic activity, and finally by the onset of oceanic crust accretion along a spreading ridge (Fig. 3.2).

The spatial boundaries (LoCC and LoOC) were mapped using criteria from previous workers described in the previous sections that are summarized in the conceptual model in Figure 3.2D. Figure 3.14 is a plate tectonic reconstruction at Aptian times (115 Ma) shows the spatial relations of the volcanic margin crustal domains after the onset of oceanic crust production in the late Aptian (126-113 Ma).

The stippled pattern on the plate reconstruction of conjugate volcanic margins in Figure 3.14 shows the reconstructed-overlap area of the Early- to Late-Cretaceous (120-60 Ma) Rio Grande Rise and the Early Cretaceous to Miocene (120-10 Ma) Walvis Ridge volcanic complexes that formed as the

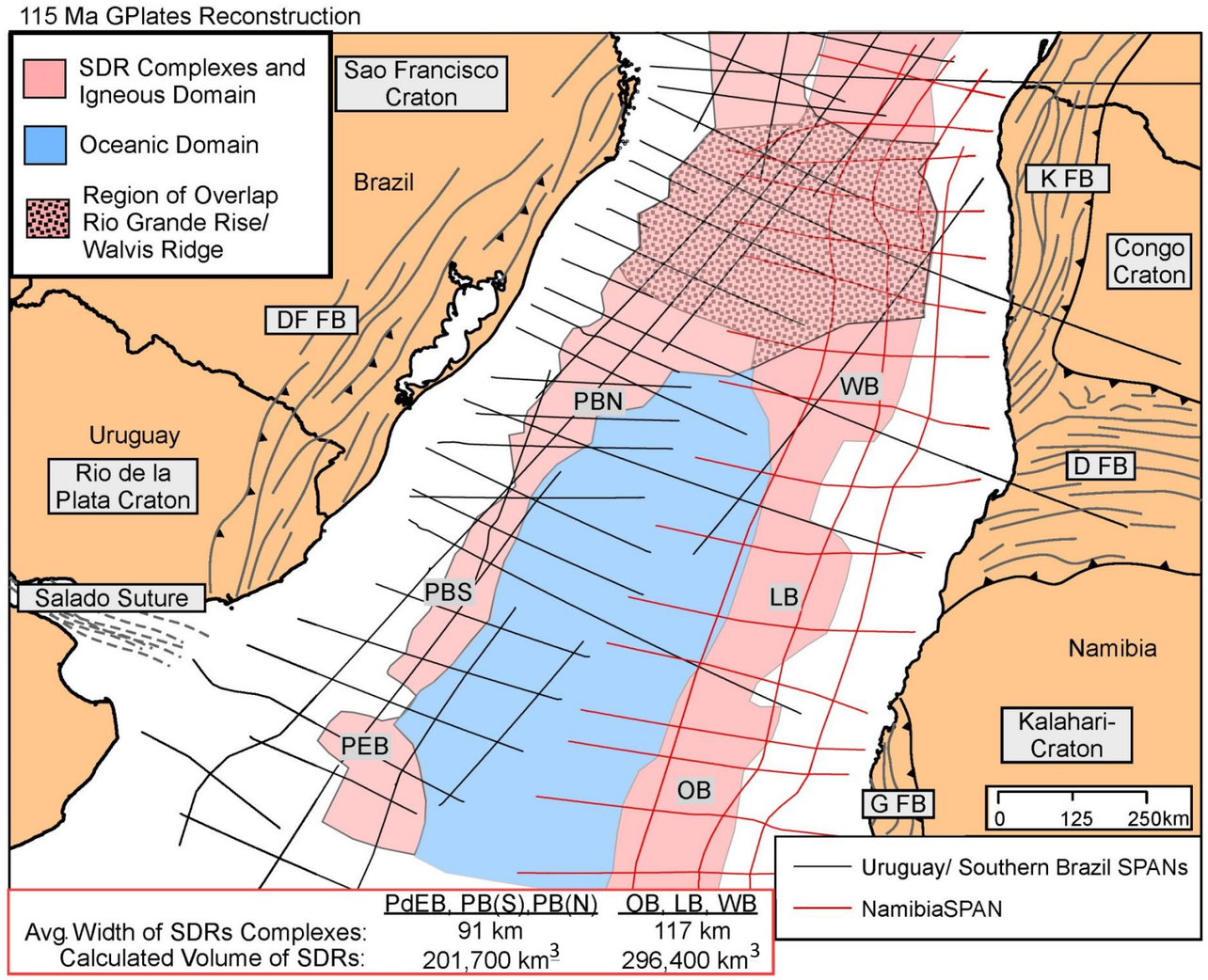

Figure 3.14:
Aptian (115 MA) reconstruction of the South Atlantic (Seton et al., 2012) showing locations of conjugate margins of this study: 1) Punta de Este Basin (PEB); 2) Pelotas Basin South (PBS); 3) Pelotas Basin North (PBN); 4) Orange Basin (OB); 5) Lüderitz Basin (LB); and 6) Walvis Basin (WB). The extent of SDRs/igneous crust is asymmetrical with a wider zone (~70 - 170 km) present in west African than found in South America (0-147 km).

result of the long-lived position of the plume center at the spreading ridge after the ridges formation in the Aptian (115 Ma) (O'Connor and Duncan, 1990; Müller et al., 1998). The average widths of the igneous zones located between the LoCC and LoOC on the South American margins of the study area are 91 km, while the average width of the wider, Namibian margin is 117 km (Fig. 3.14).

Based on the seismic reflection profiles described in this chapter, I estimate that the volcanic margins of Uruguay and Southern Brazil contain a total area of 81,100 km^2 of igneous material (SDR's and igneous crust) and that the volcanic margins of Namibia cover an area of 110,800 km^2 (Fig. 3.14). My volumetric calculation for the study area south of the Rio Grande Rise and Walvis ridge complexes and is 201,700 km^3 for the South American margin and 296,400 km^3 for the Namibian margin (Fig. 3.14). Volumes were calculated using a right triangle geometry method similar to the method proposed by Franke et al. (2010). This method assumes a rough fit triangle at the margin where the LoOC is considered the apex of the triangle and a vertical boundary at the LoCC is the considered the triangle base. My estimates do not include the volume of SDRs/basalts that are from the volcanic ridge depicted by overlap/stippled region in Figure. 3.14.

3.8 Discussion

3.8.1 Comparison of this study to previous refraction study of the same margins

Recent studies by Becker et al. (2014) and Koopman et al. (2014) used

seismic refraction methods for these same South Atlantic conjugate margins to observe similar asymmetrical distributions of magmatic materials and internal elements associated with volcanic passive margins. Becker et al. (2014) mapped the distribution of high-velocity lower crust (HVLC) using seismic refraction data from the Argentine, Uruguayan, Namibian and South African margins.

From this overlay shown in Figure 3.15, I observe close correlations between the Becker et al. (2014) refraction model and the seismic reflection data for the eastern expression of Moho, top oceanic crust, and the seafloor surface. However, there are significant differences in the limits of the interpreted SDRs in the Becker et al. (2014) model and the basinward extent of the seismic facies related to SDRs as observed on my seismic reflection data. In the same location I interpret SDRs extending 50 km east of the observed, seismic limit of the SDR's seen on refraction data (Fig. 3.15). One additional dissimilarity between my reflection data and Becker et al.'s refraction line is that the outer-high modeled by Becker et al. is shown to protrude upward into the overlying passive margin sediments (Fig. 3.15A).

The southern profile (profile 6) from Becker et al. (2014) (Fig. 3.15) is more problematic to correlate with the interpretation of a reflection line from the Orange Basin (Fig. 3.15D) considering the near-exact match in position between the refraction model and the seismic reflection data. An acceptable match between the Becker et al. (2014) "refraction model profile 6" and the seismic reflection data utilized here could not be achieved. Although a fair match for the

Figure 3.15: Comparison of interpreted refraction profiles from Becker et al. (2014) and seismic data used in this study.

A) A refraction cross section (Profile #1) from Becker et al. (2014) located on the Uruguay volcanic margin.
B) A comparison image of a collinear (inset), ION seismic line in the on the Uruguay margin and is overlain onto the refraction line in A. The comparison of seismic refraction and reflection also show an overall “fair” fit of crustal horizons (i.e.-Moho, Top SDRs).
C) A refraction cross section (Profile #6) from Becker et al. (2014) on the Namibian margin.
D) A comparison image of a collinear (inset), ION seismic line in the on the Namibian margin and is overlain onto the refraction line in C. The comparison of seismic refraction and reflection also show an overall poor fit of crustal horizons (i.e.-Moho, Top SDRs).

A.

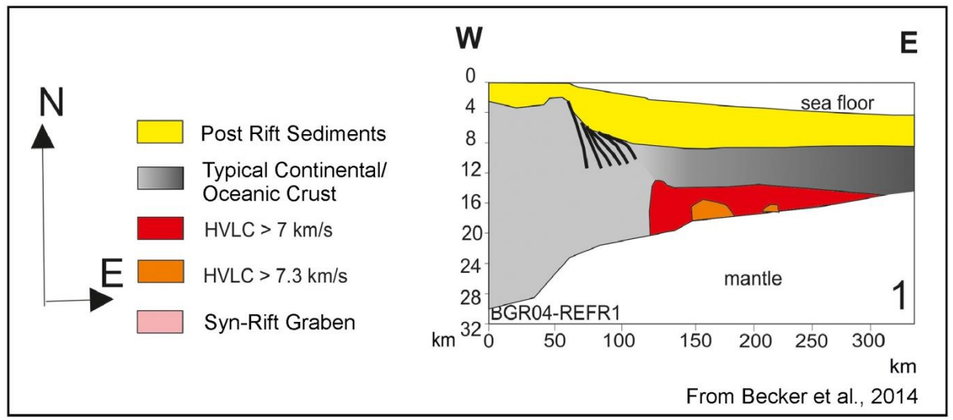
N
E
Post Rift Sediments
Typical Continental/
Oceanic Crust
HVLC > 7 km/s
HVLC > 7.3 km/s
Syn-Rift Graben
W
E
0
4
8
12
16
20
24
28
32
km
sea floor
mantle
1
BGR04-REFR1
0
50
100
150
200
250
300
km
From Becker et al., 2014

B.

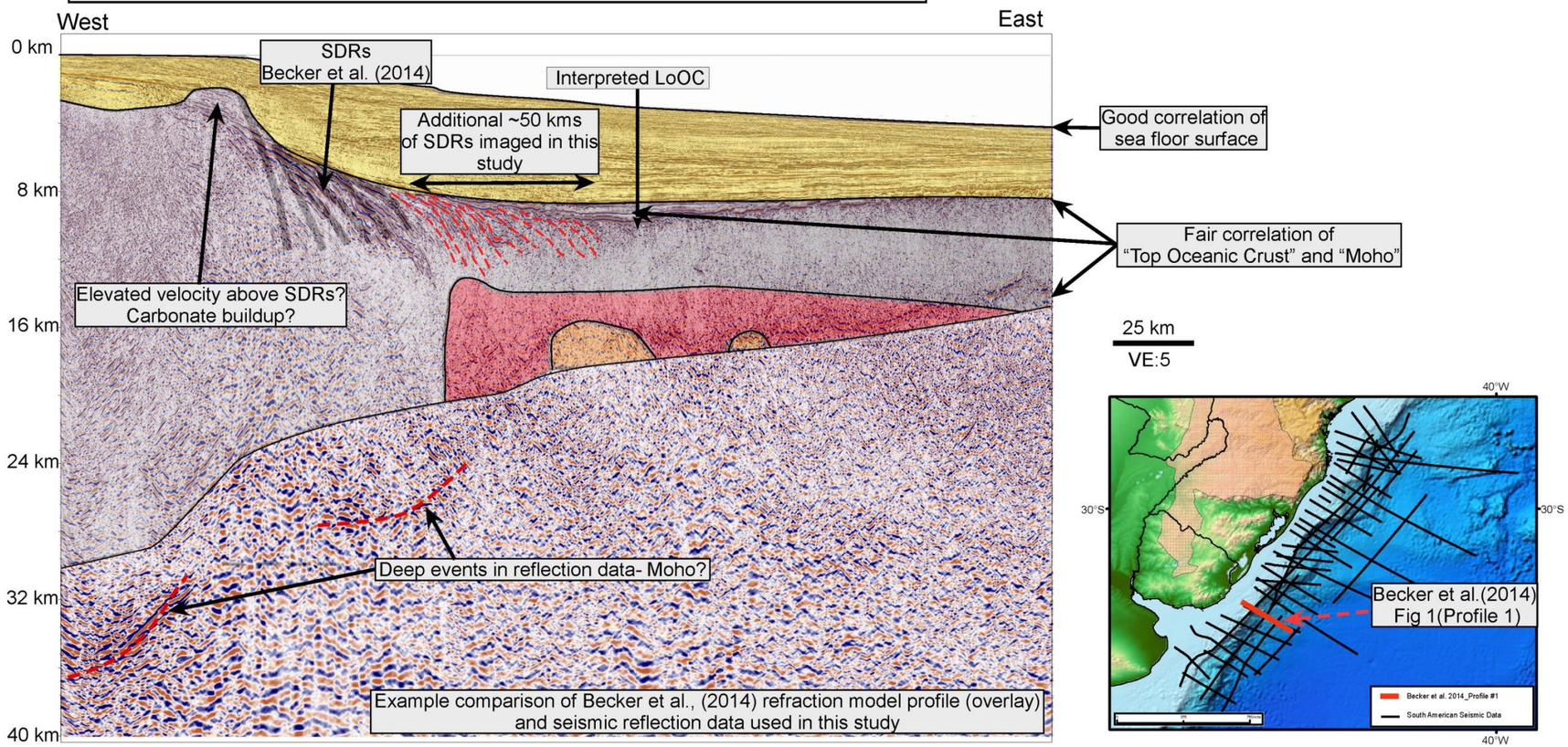
West
East
0 km
8 km
16 km
24 km
32 km
40 km
SDRs
Becker et al. (2014)
Interpreted LoOC
Additional ~50 kms
of SDRs imaged in this
study
Elevated velocity above SDRs?
Carbonate buildup?
Deep events in reflection data- Moho?
Example comparison of Becker et al., (2014) refraction model profile (overlay)
and seismic reflection data used in this study
Good correlation of
sea floor surface
Fair correlation of
“Top Oceanic Crust” and “Moho”
25 km
VE:5
40°W
30°S
Becker et al.(2014)
Fig 1(Profile 1)
Becker et al. 2014_Profile #1
South American Seismic Data

C.

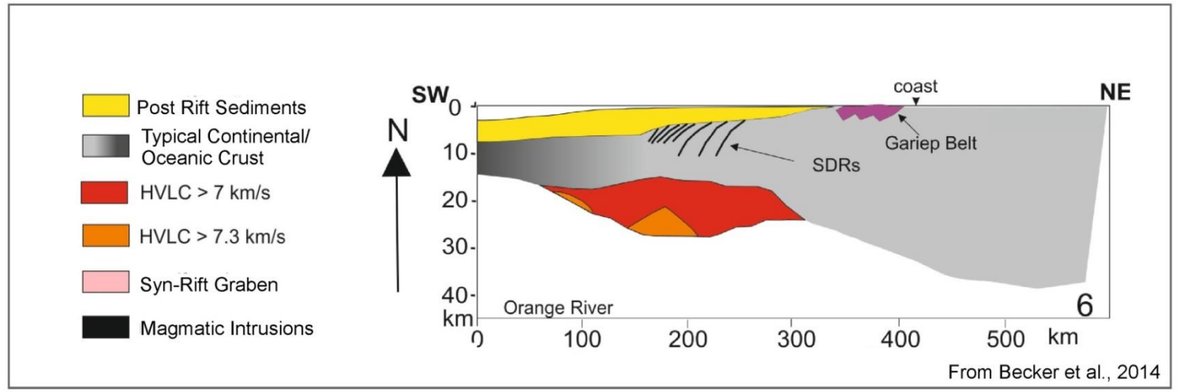
Post Rift Sediments
Typical Continental/ Oceanic Crust
HVLC > 7 km/s
HVLC > 7.3 km/s
Syn-Rift Graben
Magmatic Intrusions
N
SW
NE
coast
Gariep Belt
SDRs
Orange River
6
0
10
20
30
40
km
0
100
200
300
400
500
km
From Becker et al., 2014

D.

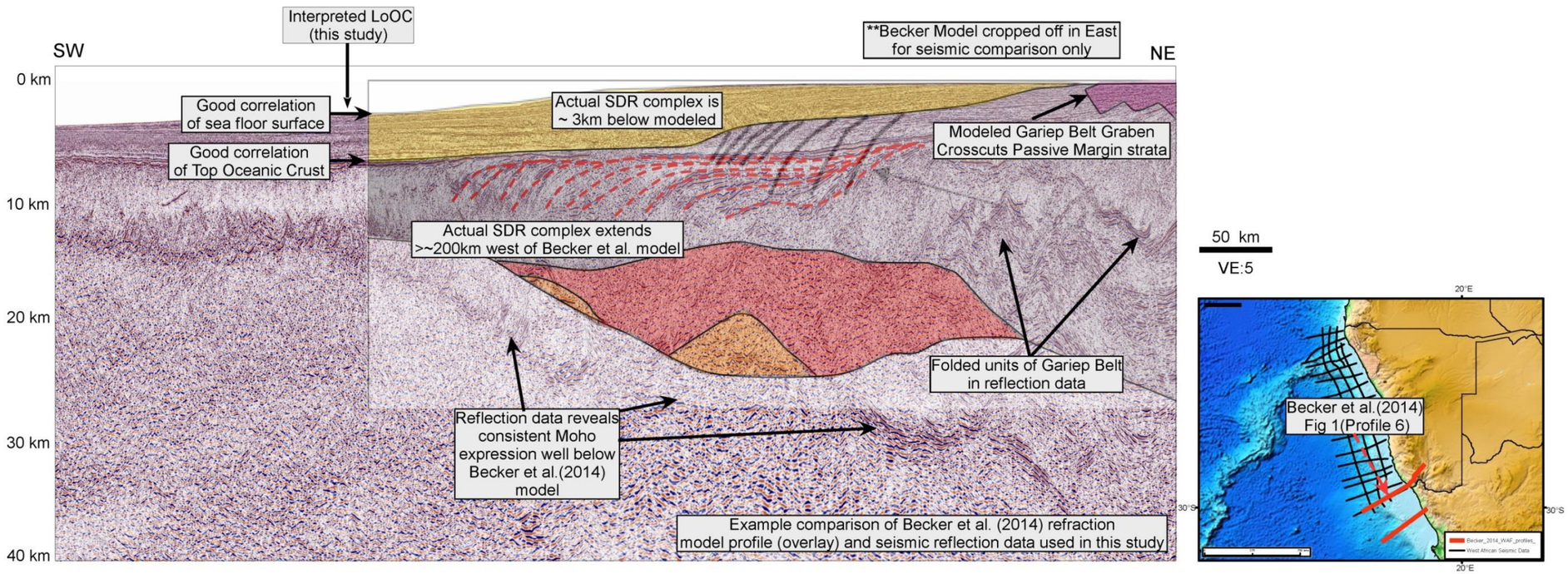
Interpreted LoOC (this study)
**Becker Model cropped off in East for seismic comparison only
SW
NE
0 km
10 km
20 km
30 km
40 km
Good correlation of sea floor surface
Good correlation of Top Oceanic Crust
Actual SDR complex is ~ 3km below modeled
Modeled Gariep Belt Graben Crosscuts Passive Margin strata
Actual SDR complex extends >~200km west of Becker et al. model
Folded units of Gariep Belt in reflection data
Reflection data reveals consistent Moho expression well below Becker et al.(2014) model
Example comparison of Becker et al. (2014) refraction model profile (overlay) and seismic reflection data used in this study
50 km
VE:5
20°E
30°S
Becker et al.(2014) Fig 1(Profile 6)
Becker_2014_WAF_profiles_
West African Seismic Data

seafloor was made, the boundaries between the crustal units and the overlying stratigraphic units are not in agreement. Seismic reflection data shows that the Moho is far deeper (29 km) than modeled on the seismic refraction lines (23 km); the westward extent of SDR's extends ~200 km beyond the modeled location; and the thickness of the continental crust is greater (24 km) than observed from the refraction data (20 km).

The difference in my reflection and refraction observations is significant for interpreting the early rifting processes of this margin. Based on refraction, Becker et al. (2014) concluded that the asymmetrical distribution of their modeled HVLC is a result of asymmetrical rifting and simple-shear extension with hanging wall and footwall components (Fig. 3.16A). This proposed interpretation of conjugate, structural asymmetry could only be possible if the entire section of rift and volcanic sections overlay thinned continental crust (Fig. 3.16). However, I know from accepted models of SDR's on volcanic margins, discussed earlier in this paper, that the syn-rift phase on volcanic passive margins is complete after the basinward rotation of the oldest packages of SDRs. From this point onward, extension occurs by the accretion of new igneous crust to the margin (Pindell et al., 2014) and not by a simple-shear process.

My observations here require that the observed asymmetry must be the result of another mechanism related to a spreading ridge, where excess material is emplaced preferentially on one plate over the other. The process of accreting new material at a volcanic spreading center no longer is driven by the processes

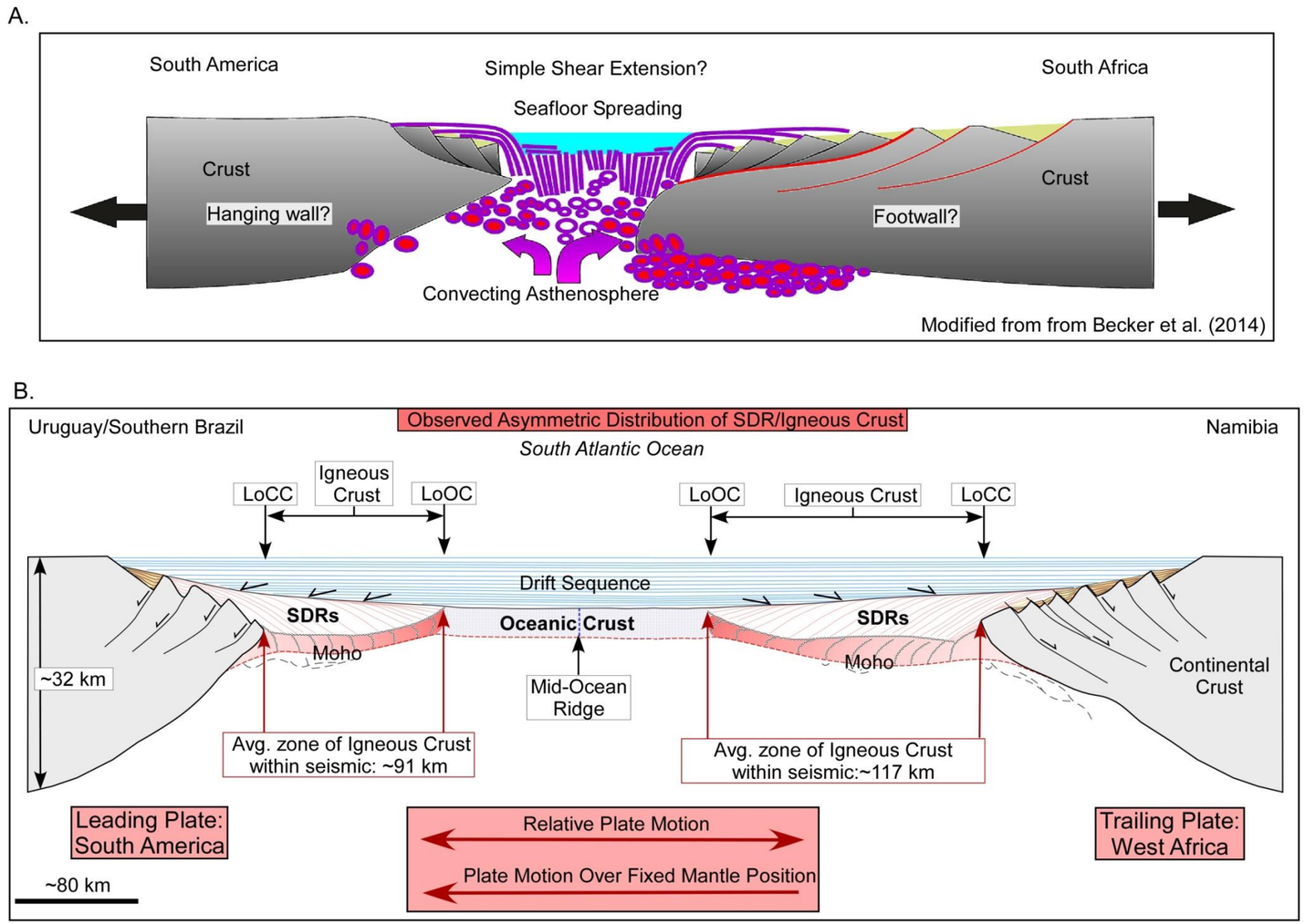

Figure 3.16: A comparison of models for SDR asymmetry.

A) Seismic refraction-based interpretation by Becker et al. (2014) with zones of asymmetrical distribution of high-velocity lower crust (HVLC) and underplated, magmatic material on the conjugate, volcanic margins of southern South America and southern West Africa. B) Seismic reflection-based interpretation based on seismic interpretations shown in this paper with asymmetrical zones of SDRs. Average widths of SDRs are approximately 30% wider on the African margin.

of simple- or pure- shear rifting and is more likely a product plate and ridge interaction. A generic SDR-spreading ridge model with features similar to that of an oceanic spreading ridge forming in a subaerial setting has also recently been proposed by Paton et al. (2017).

3.8.2 Asymmetric-conjugate SDR model

An idealized model for the asymmetrical distribution of SDRs on my seismic reflection observations invokes regional elements of plate motion and velocity to explain the excess accretion of SDRs on the slower, trailing plate relative to a fixed mantle position (Fig 3.16B).

To address the asymmetry of the volcanic zones, I integrate several key points of evidence: 1) the asymmetrical distribution of continental flood basalts of 132 Ma age that are found in Paranà and Etendeka (White and McKenzie, 1989; O'Connor and Duncan, 1990; Gladczenko et al., 1997; Hoernle et al., 2015); 2) the asymmetrical distribution of SDR complexes with a wider zone in Africa than South America (Fig. 3.14 and 3.16B); 3) a well-documented past and present-day position of the Tristan de Cunha Hotspot (O'Connor and Duncan, 1990) (Fig. 3.1B). These three documented features of the South Atlantic are related to the plate motion relative to a fixed mantle position and magma-rich continental break up (Fig. 3.1B).

3.8.3 Plate motion controls on asymmetry of volcanic passive margins

Prior to the onset of Barremian (~132 Ma) rifting in the study area, the Rio de la Plata Craton, Dom Feliciano, and Damara Foldbelts were fused

Figure 3.17: Sequential opening of South Atlantic conjugate margins from Hauterivian (130 Ma) to Middle Miocene (20 Ma) based on GPlates reconstructions of present-day bathymetry and topography (Seton et al., 2012) showing the controls of Tristan de Cunha plume and plate motion for production of asymmetrical volcanic margins (wider volcanic margin is on the African conjugate margin).

A) Hauterivian (130 Ma) early-opening, rift phase, reconstruction with Tristan de Cunha plume-head, continental flood basalts of the Parana-Etendeka Flood Basalt Provinces and the location the schematic cross section shown in A2. **A1)** Schematic cross section showing the closed fit, pre-rift reconstruction of the South American and African plates and preexisting orogenic belts of varying strike that will be reactivated during extension: RLPC = ~130 km; DFFB = ~65 km; DFB = ~180 km. **A2)** Schematic cross section with arrival and intrusion of the Tristan de Cunha Plume head into continental crust and subaerial extrusion of overlying, Parana-Etendeka continental flood basalts.

B) Aptian (120 Ma) volcanic margin and SDR formation phase south of the volcanic ridge complexes of the Rio Grande Rise and Walvis Ridge and the location the schematic cross section shown in B1. **B2)** Schematic cross section at 120 Ma showing the relative position of the South American and African plates during the emplacement of SDRs with a wider and more voluminous accretion of SDRs on the slower African plate.

C) Campanian (80 Ma) reconstruction showing SDRs on the volcanic margins and the volcanic ridge complexes of the Rio Grande Rise and the Walvis Ridge and location of the schematic cross section shown in C1. **C1)** Schematic cross section at 80 Ma with Tristan de Cunha Plume underlying the symmetrically-spreading, South Atlantic spreading ridge.

D) Middle Miocene (20 Ma) reconstruction zones of SDRs on both conjugate, volcanic margins, the direction of plate motion relative to a fix position, and the hotspot-related Rio Grande Rise and Walvis Ridge. The center of the modern Tristan de Cunha hotspot is now 300 east of the active, South Atlantic spreading ridge. The location of the schematic cross section shown in D1. **D1)** Schematic cross section at 20 Ma showing the asymmetrical lengths of both volcanic margins and the location of the modern Tristan de Cunha 300 km west of the active spreading ridge.

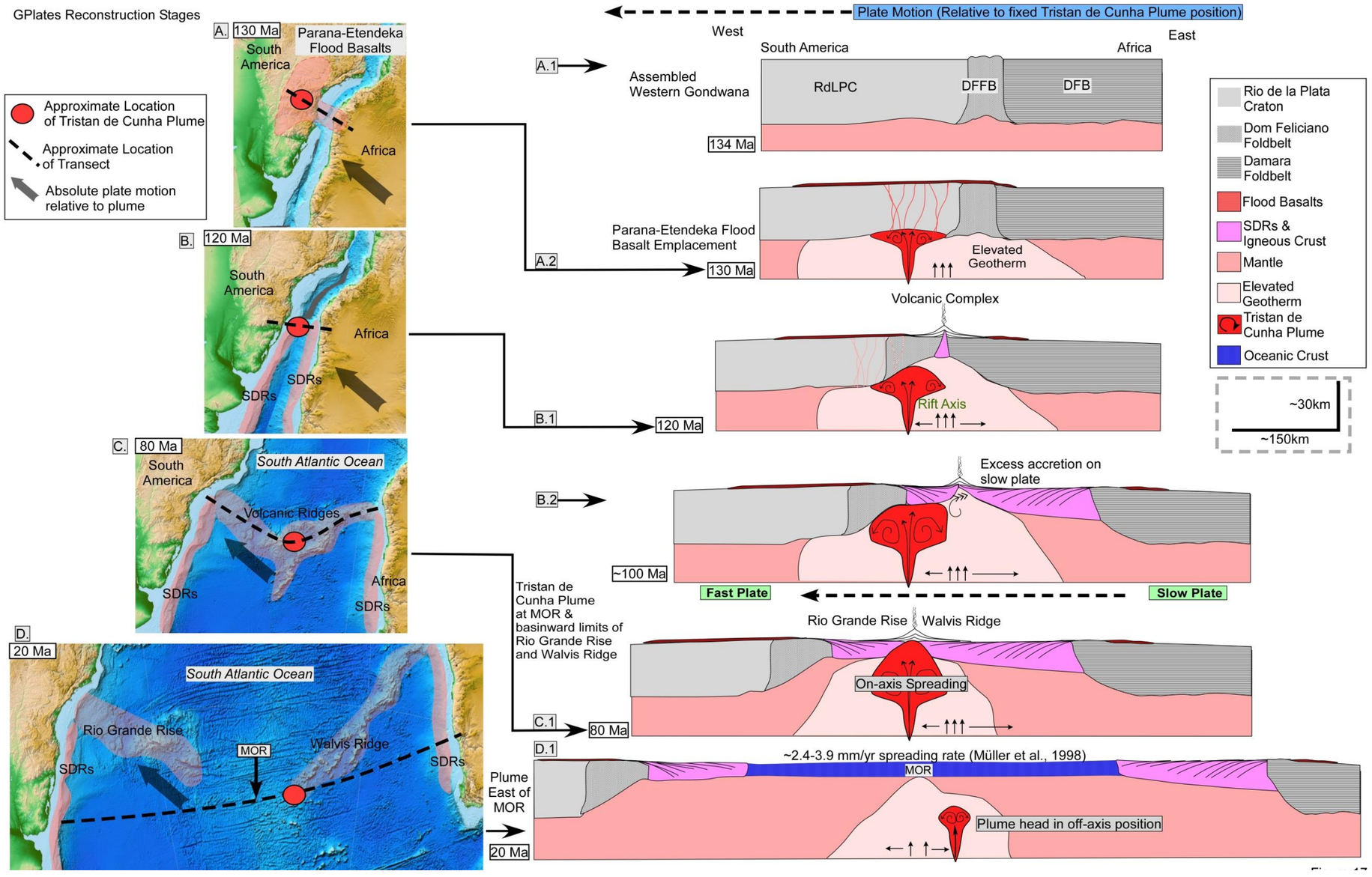
GPlates Reconstruction Stages
Approximate Location of Tristan de Cunha Plume
Approximate Location of Transect
Absolute plate motion relative to plume
A. 130 Ma
Parana-Etendeka Flood Basalts
South America
Africa
B. 120 Ma
South America
Africa
SDRs
SDRs
C. 80 Ma
South America
South Atlantic Ocean
Volcanic Ridges
Africa
SDRs
SDRs
D. 20 Ma
South Atlantic Ocean
Rio Grande Rise
MOR
Walvis Ridge
SDRs
SDRs
Plate Motion (Relative to fixed Tristan de Cunha Plume position)
West
East
South America
Africa
A.1
Assembled Western Gondwana
RdLPC
DFFB
DFB
134 Ma
A.2
Parana-Etendeka Flood Basalt Emplacement
Elevated Geotherm
130 Ma
Volcanic Complex
B.1
120 Ma
Rift Axis
B.2
Excess accretion on slow plate
~100 Ma
Fast Plate
Slow Plate
Tristan de Cunha Plume at MOR & basinward limits of Rio Grande Rise and Walvis Ridge
Rio Grande Rise
Walvis Ridge
On-axis Spreading
C.1
80 Ma
D.1
~2.4-3.9 mm/yr spreading rate (Müller et al., 1998)
MOR
Plume East of MOR
Plume head in off-axis position
20 Ma
Rio de la Plata Craton
Dom Feliciano Foldbelt
Damara Foldbelt
Flood Basalts
SDRs & Igneous Crust
Mantle
Elevated Geotherm
Tristan de Cunha Plume
Oceanic Crust
~30km
~150km

together to form part of Western Gondwana craton (White and McKenzie, 1989) (Fig 3.17-A1). The initiation of the Tristan de Cunha Plume during the Hauterivian (132 Ma) caused an elevated geotherm that extended 2000 km outward from the plume head (White and McKenzie, 1989) (Fig. 3.17A, 3.17A2). The area of the elevated geotherm and extrusive continental flood basalts overlay a broad, sub-lithospheric, “plume pancake” (O’Connor and Duncan, 1990; Fairhead and Wilson, 2005) that began to expand radially and encroach on the rifting, conjugate margins of the austral South Atlantic (Fig. 3.17A-A2). During the Aptian (~120 Ma), the interaction between the northwesterly path of the South American and African plates and the stationary position of the plume began to shift the two plates eastward away from the initial sites of the Hauterivian continental flood basalts and towards the South Atlantic rift axis and the sites of its volcanic margins (Fig. 3.17B and 3.17B1).

Following this rifting event, my model proposes the establishment of an extensive zone of volcanic complexes along or near the rift axis (Fig. 3.17B1). At this stage, the model derived from my observations of seismic data would predict a period of crustal thinning, the emplacement of Inner SDRs in the topographic lows of half-grabens, and the potential for underplating of high-velocity materials beneath the zone of thinned continental crust. After continued divergence of the continental domain during the Albian, a ~12 km-thick zone of mafic crust overlain by SDRs accumulates at the plate margins in a subaerial setting (Fig. 3.17B2). During this stage the South American plate is established as the faster plate and Africa as the slower plate, as a result of increased plate

velocity (Brune et al., 2016)(Fig. 3.17B2).

This plate motion, relative to a fixed mantle position, permits greater accretion of new, igneous crust and SDR complexes on the Namibian margin (Fig. 3.17B2). Stein et al. (1977) modeled this asymmetric plate accretion in their study of seafloor spreading and the relationship to absolute plate motion relative to the oceanic spreading ridge between the Indian and Antarctic plates. They developed a fluid mechanical model which predicted the faster accretion on the trailing ridge flank Stein et al. (1977). Fujita and Sleep (1978) reported a higher susceptibility of dyke intrusion on the hotter and weaker flanks of a spreading ridge system, creating asymmetry at the axis. They also noted that, in a hot spot scenario, the slower plate would be hotter and weaker in comparison to the faster plate (Fujita and Sleep, 1978). This plate motion concept was further discussed by Müller et al. (1998). Muller et al. (1998) compared the Stein et al. model with their calculated, global ocean age maps. They agreed that minimum spreading rates could accompany greater magmatic addition on the slower plate provided that the rate of spreading remained high (30-80 mm/yr.) relative to a fixed mantle position.

Spreading rates for the emplacement SDRs/igneous crust were investigated by Armitage et al. (2010) and a correlation was proposed between spreading rates during magmatism (40-50 mm/yr.) and thicknesses of the SDRs/igneous crust (15-20 km). From my study I can determine the lateral extent of SDRs and crustal thickness from the seismic data. Paleo-extensional velocities from the South Atlantic rifted margins were calculated by Brune et al.

(2016) and indicate a rapid increase from the Barremian (128 Ma) through the Mid-Aptian (118 Ma). The calculated 40-50 mm/yr. extensional velocity for this time period supports the boundary criteria for the emplacement of thick igneous crust (Armitage et al., 2010; Brune et al., 2016). The relationship of SDR/igneous thickness and spreading rates proposed by Armitage et al. (2010) can be integrated with Brune et al.'s findings to support a rapid (>30mm/yr.) spreading rate during the emplacement of SDRs. By linking the spreading rate, SDR/Igneous crust thickness, and plate motion, the model for asymmetric accretion of SDRs can be confirmed.

From the Cenomanian (100 Ma) to the Early Eocene (40 Ma), the Tristan de Cunha Plume was underlying the Mid-Atlantic Ridge (MAR) (O'Connor and Duncan, 1990; Müller et al., 1998) (Fig. 3.17-C-C1). This plume-ridge interaction produced a symmetrical on-axis geometry, where the two plates recorded plume-related magmatism at the spreading ridge (O'Connor and Duncan, 1990).

South of the conjugate volcanic ridge complexes and during the period of the Aptian ("126-120 Ma"), the supply of melt from the mantle plume declined; the production of thick igneous crust eventually ceased; and the onset of oceanic crust formation at the spreading ridge began by the Aptian ("~120 Ma") (Fig 3.17D). The lack of a recognizable, morphologic junction along the modern MOR between the ENE-trending Rio Grande Rise and the WSW-trending Walvis Ridge (Fig. 3.1B and 3.17D) can be explained by the proposed westward migration of the spreading axis and its depleting magmatic supply (O'Connor

and Duncan, 1990) (Fig. 3.17D1). Evidence for a shift from an on-axis to intraplate hotspot in the Late Cretaceous – Early Paleogene (70-60 Ma) is observed by the series of seamounts chains and volcanic edifices of early Eocene (40 Ma) to present age (O'Connor and Duncan, 1990; Müller et al., 1998; Hoernle et al., 2015) along the western limit of the Walvis Ridge and approximately 300 km from the MOR (Fig. 3.71D and D1).

3.9 Conclusions

On our seismic reflection data, the conjugate margins of Uruguay/ Southern Brazil and Namibia both exhibit wide, asymmetrical zones of SDRs in 10->220 km-wide transition between the LoCC and LoOC (Figs. 3.3-3.7). SDR complexes have distinctive seismic character (Figs. 8-10), internal structures (Figs. 3.6-3.10), Moho reflector (Fig. 3.13), crustal velocities (Fig. 3.15), and relation to overlying strata (Figs. 3.8-3.13) - which all distinguish the recognition for the areas of igneous crust formed during the rifting phase from adjacent areas of oceanic and continental crust.

The Uruguay/Southern Brazil margin south of the Rio Grande Rise has 30% less volume of rift-related igneous rocks compared to the conjugate margin of Namibia (Fig. 3.14 and 3.16B). The greater volume of volcanic addition to the African plate is related to the north-westward direction of plate motion of the South American and African plates and increased spreading velocity. These combined elements produced a fast South American plate and a slower African plate, relative to a fixed mantle position. From the point of continental

separation and formation of the mid-oceanic spreading ridge, a greater amount of SDR-related igneous material accumulated on the hotter, weaker, and slower African plate (Fig. 3.14).

Interpretations by previous workers that have invoked simple- and/or pure-shear mechanisms to explain the observed asymmetries cannot explain the lack of continental crust underlying SDR's – a relationship that is shown on several seismic images (Figs. 3.3-3.10, 3.13). Simple and pure rifting models imply lithospheric thinning and prior to the onset of oceanic formation or SDR crustal accretion. Findings from this study and previously established models indicate that the continental rifting process is no longer active during the emplacement of SDRs basinward of the LoCC. In this position, a volcanic spreading ridge is present where magmatic addition takes place by accretion at a spreading axis. In my model, I propose that the observed asymmetry can be explained by the accretion of thick, igneous crust underlying the SDRs, and a divergent setting of plate motions over a fixed mantle position that involves a faster, South American plate and a slower, African plate.

Chapter Three: References

Abreu, V.S., Vail, P.R., Bally, A., Wilson, E., 1997, Geologic evolution of conjugate volcanic passive margins: Influence on the petroleum systems of the South Atlantic: Houston Geological Society Bulletin, 40, 10-11.

Abdelmalak, M., Andersen, T., Planke, S., Faleide, J., Corfu, F., Tegner, C., Shephard, G., Zastrozhnov, D., and Myklebust, R., 2015, The ocean-continent transition in the mid-Norwegian margin: Insight from seismic data and an onshore Caledonian field analogue: Geology, 43(2), 1011-1014.

Armitage, J.J., Collier, J.S. and Minshull, T. A., 2010, The importance of rift history for volcanic margin formation: Nature 465, 913-917.

Austin, J. A. and Uchupi, E., 1982, Continental-oceanic crustal transition of southwest Africa: American Association of Petroleum Geologists Bulletin, 66, 1328 – 1347.

Barker, P.F., Buffler, R.T., and Gamboa, L.A., 1981a, A seismic reflection study of the Rio Grande Rise. In: Barker P.F., Carlson R.L., Johnson D.A. (Eds.), Initial Reports of the Deep Sea Drilling Project, 72, pp. 499-517.

Barker, P.F., Carlson, R.L., and Jonhson, D.A., 1981b, Site 515: Rio Grande Rise. In: Initial reports, DSDP, 72: 155-338.

Becker, K., Franke, D., Trumbull, R., Schnabel, M., Heyde, I., Schreckenberger, B., Koopmann, H., Bauer, K., Jokat, W., and Krawczyk, C., 2014, Asymmetry of high-velocity lower crust on the South Atlantic rifted margins and implications for the interplay of magmatism and tectonics in continental breakup: Solid Earth, 5 (2), 1011-1026.

Becker, K., Franke, D., Schnabel, M., Schreckenberger, B., Heyde, I., and Krawczyk, C.M., 2012, The crustal structure of the southern Argentine margin: Geophysical Journal International, 189, 1483-1504.

Blaich, O. A., J. I. Faleide, and F. Tsikalas, 2011, Crustal breakup and continent-ocean transition at South Atlantic conjugate margins: Journal of Geophysical Research Solid Earth, 116, 1–36.

Blaich, O.A., Faleide, J.I., Tsikalas, F., Gordon, A.C., and Mohriak, W., 2013, Crustal-scale architecture and segmentation of the South Atlantic volcanic margin. In: Mohriak, W.U., Danforth, A., Post, P.J., Brown, D.E., Tari, G.C., Nemcok, M., and Sinha, S.T. (Eds.), Conjugate Divergent Margins, Geological Society, London, Special Publications, 369, 167-183.

Calvès, G., Schwab, A. M., Huuse, M., Clift, P.D., Gaina, C., Jolley, D., Tabrez, A.R., and Inam, A., 2011, Seismic volcanostratigraphy of the western Indian rifted margin: The pre-Deccan igneous province: Journal of Geophysical Research, Solid Earth, 116, B01101.

Cande, S.C., and Rabinowitz, P. D., 1978, Mesozoic sea floor spreading bordering conjugate continental margins of Angola and Brazil: Proceedings Annual Offshore Technology Conference, 3, 1769-1776.

Cande, S.C., and Rabinowitz, P. D., 1978, Magnetic anomalies of the continental margin of Brazil, Offshore Brazil Map Series: American Association of Petroleum Geologists Tulsa, Oklahoma.

Cande, S., LaBrecque, J.L., and Haxby, W.F., 1988, Plate kinematics of the South Atlantic: Chron C34 to present, Journal of Geophysical Research, 93(13),479-,492.

Fairhead, J.D., and Wilson, M., 2005, Plate tectonic processes in the South Atlantic Ocean: Do we need deep mantle plumes?, In: Foulger, G.R., Natland, J.H., Presnall, D.C., and Anderson, D.L., eds., Plates, plumes, and paradigms: Geological Society of America Special Paper 388, 537–553.

Franke, D., Neben, S., Ladage, S., Schreckenberger, B., and Hinz, K., 2007, Margin segmentation and volcano-tectonic architecture along the volcanic margin off Argentina/Uruguay: South Atlantic Marine Geology, 244, 46-67.

Franke, D., S. Ladage, Schnabel, M., Schreckenberger, B., Reichert, C., Hinz, K., Paterlini, M., de Abelleyra, J., and Siciliano, M., 2010, Birth of a volcanic margin off Argentina: South Atlantic, Geochemistry, Geophysics, Geosystems, 11, Q0AB04, doi:10.1029/2009GC002715.

Fujita, K. and Sleep, N. H., 1978, Membrane stresses near mid-ocean ridge-transform intersections: Tectonophysics, 50, 207-221.

Geoffroy, L., 2005. Volcanic Passive Margins: Geoscience, 337, 1395–1408.

Gladczenko, T.P., Hinz, K., Eldholm, O., Meyer, H., Neben, S., and Skogseid, J., 1997, South Atlantic volcanic margins: Journal of Geological Society, 154, 465-470.

Hay, W.W., Sibuet, J.-C., Barron, E.J., Boyce, R.E., Brassell, S.C., Dean, W.E., Huc, A.Y., Keating, B.H., McNulty, C.L., Meyers, P.A., Nohara, M., Schallreuter, R., Steinmetz, J.C., Stow, D., and Stradner, H., 1982. Sedimentation and accumulation of organic carbon in the Angola Basin and on the Walvis Ridge: preliminary results of Deep Sea Drilling Project Leg 75. *Geol. Soc. Am.*

Bull., 93:1038-1050.

Hinz, K., 1981, A hypothesis on terrestrial catastrophies: Wedges of very thick oceanward- dipping Layers beneath passive continental margins and their origin and paleoenvironmental significance: Geophysics, Schweizerbart Pub., 22, 3-28.

Hirsch, K.K., Bauer, K., and Scheck-Wenderoth, M., 2009, Deep structure of the western South African passive margin - results of a combined approach of seismic, gravity and isostatic investigations: Tectonophysics 470 (1–2), 57–70.

Hinz, K., Neben, S, Schreckenberger, B., Roeser, H.A., Block, M., Gonzalvez de Souza, K., and Meyer, H., 1999, The Argentine continental margin north of 48°S: Sedimentary successions, volcanic activity during breakup: Marine and Petroleum Geology, 16, 1-25.

Hoernle, K., Rohde, J., Hauff, F., Garbe-Schonberg, D., Homrighausen, S., Werner, R., and Morgan, J., 2015, How and when plume zonation appeared during the 132 Myr evolution of the Tristan Hotspot: Nature Communications, 6 7799.

Humphris,S . E, and Thompson, G., 1982, A geochemical study of rocks from the Walvis Ridge, South Atlantic: Chemical Geology, 36, 253-274.

Humphris, S. E, and Thompson, G., 1983. Petrology and geochemistry of rocks from the Angola Basin adjacent to the Walvis Ridge: Deep Sea Drilling Project leg 75, site 530, Initial Report Deep Sea Drilling Project, 75, 1099-1105.

Jackson, M.P.A., Cramez, C., and Fonck, J.M., 2000, Role of subaerial volcanic rocks and mantle plumes in creation of South Atlantic margins: Implications for salt tectonics and source rocks: Marine and Petroleum Geology, 17, 477-498.

Koopmann, H., Schreckenberger, B., Franke, D., Becker, K., and Schnabel, M., 2016, The late rifting phase and continental break-up of southern South Atlantic: The mode and timing of volcanic rifting and formation of earliest oceanic crust. In: Wright, T. J., Ayele, A., Ferguson, D. J., Kidane, T., and Vye-Brown, C. (eds) 2016, Magmatic Rifting and Active Volcanism: Geological Society, London, Special Publications, 420, 315–340.

LaBrecque J. L., Phillips, J., and Austin, J.A., 1984. The crustal age and tectonic fabric at the Leg 73 sites, In: Histi, K.J., and LaBrecque, J.L., et al., Initial Reports Deep Sea Drilling Project., US Government Printing Office, Washington, D.C., 73, 791-798.

Lister, G.S., Etheridge, M.A., and Symonds P.A., 1986, Detachment faulting and

the evolution of passive continental margins: Geology, 14, 246-250.

McDermott, K., Gillbard, E., and Clarke, N., 2015, From basalt to skeletons - the 200 million-year history of the Namibian margin uncovered by new seismic data: First Break, 33, 77-85.

Mohriak, W.U., Rosendahl, B.R., Turner, J.P., and Valente, S.C., 2002, Crustal architecture of South Atlantic volcanic margins. In: Menzies, M.A., Klemperer, S.L., Ebinger, C.J., Baker, J. (Eds.), Volcanic Rifted Margins: Geological Society of America Special Paper 362, 159-202.

Müller, R. D., Roest, W. R., and Royer, J., 1999, Asymmetric sea-floor spreading caused by ridge-plume interactions, Nature, 396, 455–459,

Mutter, J. C., 1985, Seaward-dipping reflectors and the continent-ocean boundary at passive continental margins: Tectonophysics, 114, 117–131.

Mutter, J. C., Talwani, M., and Stoffa, P. L., 1982, Origin of seaward-dipping reflectors in oceanic crust off the Norwegian margin by 'subaerial sea-floor spreading': Geology, 10, 353–357.

Nürnberg, D., and Müller, R. D., 1991, The tectonic evolution of the South Atlantic from Late Jurassic to present: Tectonophysics, 191, 27–53.

O'Connor, J.M. and Duncan, R.A., 1990, Evolution of the Walvis Ridge-Rio Grande Rise Hot Spot System: Implications for African and South American Plate Motions Over Plumes: Journal of Geophysical Research, 95, 17,475–17,502.

O'Connor, J., and Jokat, W., 2015. Age distribution of Ocean Drill sites across the Central Walvis Ridge indicates plate boundary control of plume volcanism in the South Atlantic, Earth Planetary Science Letters, 424, 179-190, doi: 10.1016/j.epsl.2015.05.02.

Paton, D.A., Pindell, J., McDermott, K., Bellingham, P., and Horn, B., 2017, Evolution of seaward-dipping reflectors at the onset of oceanic crust formation at volcanic passive margins: Insights from the South Atlantic, Geology, 45(5), 439-442.

Pindell, J. L., Graham, R., and Horn, B.W., 2014, Role of magmatic evacuation in the production of SDR complexes at magma-rich passive margins: Proceedings of the GCSSEPM Bob F. Perkins Research Conference, 1–16.

Planert, L., Behrmann, J., Jokat, W., Fromm, T., Ryberg, T., Weber, M., and Haberland, C., 2016, The wide-angle seismic image of a complex rifted margin,

offshore North Namibia: Implications for the tectonics of continental breakup: Tectonophysics, (article in press).

Planke, S., Symonds, P.A., Alvestad, E., and Skogseid, J., 2000, Seismic volcanostratigraphy of large-volume basaltic extrusive complexes on rifted margins: Journal of Geophysical Research, Solid Earth 105, 19335-19351.

Rabinowitz, P.D., 1976, Geophysical Study of the continental margin of southern Africa: Geological Society of America Bulletin, 87, 1643-1653.

Rabinowitz, P. D. and LaBrecque, J., 1979. The Mesozoic South Atlantic and evolution of its continental margins: Journal of Geophysical Research, 85, 5973–6002.

Rohde, J.K., Hoernle, K., Hauff, F., Werner, R., O'Connor, J., Class, C., Garbe-Schönberg, D., and Jokat, W., 2013, 70 Ma Chemical Zonation of the Tristan-Gough hotspot Track, Geology, 41(3), 335-338, doi:10.1130/G33790.1

Richardson, S. H., Erlank, A. J., Duncan, A. R., and Reid, D. L., 1982, Correlated Nd, Sr and Pb isotope variations in Walvis Ridge basalts and implications for the evolution of their mantle source: Earth Planet, Science Letters, 59, 327-342.

Sandwell, D. T. and. Smith, W. H. F, 2009, Global marine gravity from retracked Geosat and ERS-1 altimetry: Ridge segmentation versus spreading rate: Journal of Geophysical Research, 114, B01411, doi:10.1029/2008JB006008.

Shaw, P., and Cande, S.C., 1990, High-resolution inversion for South Atlantic plate kinematics using joint altimeter and magnetic anomaly data, Journal of Geophysical Research., 95, 2625-2644.

Sheridan, R.E., Musser, D.L., Glover, L. Iii, Talwani, M., Ewing, J., Holbrook, W.S., Purdy, G.M., Hawman, R., and Smithson, S., 1993, Deep seismic reflection data of EDGE U.S. Mid-Atlantic continental margin experiment: Implications for Appalachian sutures and Mesozoic rifting and magmatic underplating: Geology, 21, 563–567.

Smythe, D.K., 1983, Faroe-Shetland Escarpment and continental margin of the Faroes. In: Bott, M.H.P., Saxov, S., Talwani, M., Thiede, J. (Eds.), Structure and Development of Greenland-scotland Ridge, NATO Conference Series IV: Marine Sciences, 8, 109-119.

Stein, S., Melosh, H. J. and Minster, J. B., 1977, Ridge migration and asymmetric sea-Floor spreading: Earth Planetary Science Letters, 36, 51-62.

Stica, J.M., Zalan, P.V. and Ferrari, A., 2014, The evolution of rifting on the volcanic margin of the Pelotas Basin and the contextualization of the Parana–Etendeka LIP in the separation of Gondwana in the South Atlantic: Marine Petroleum Geology, 50, 1–21.

Uchupi, E. 1989, The tectonic style of the Atlantic Mesozoic rift system: Journal of African Earth Sciences, 8, 143 – 164.

Unternehr, P., Curie, D., Olivet, J. L., Goslin, J. and Beuzart, P., 1988, South Atlantic fits and intraplate boundaries in Africa and South America: Tectonophysics, 155, 169-179.

White, R. S., and McKenzie, D., 1989, Magmatism at rift zones: The generation of volcanic continental margins and flood basalts: Journal of Geophysical Research, 94, 7685–7729.

Chapter Four:

Control of Paleozoic basement orogenic trends on along-strike variations of Cretaceous continental stretching and formation of South Atlantic volcanic passive margins

4.1 Summary

Early Cretaceous (134-131 Ma) continental rupture of Western Gondwana to form the South American and African plates closely paralleled the elongate trends of Precambrian and Paleozoic basement orogenies. These orogenic belts were produced as a result of the Neoproterozoic convergent and strike-slip assembly of Gondwana that were later re-deformed by later Paleozoic orogenic events. Subsequent Early Cretaceous (132-130 Ma) continental rifting to form the South Atlantic Ocean produced conjugate volcanic passive margins (VPM's) whose widths vary from 55-180 km. Along-strike variations in crustal stretching, measured from deep-penetration, depth-migrated seismic reflection profiles, can be correlated with the orientation of the rift relative to the trend of the older, basement fabric. Where basement fabric trends parallel to the north-south South Atlantic rift direction in the Dom Feliciano Uruguay/Brazil and Kaoko orogenic belt of Namibia, narrow (55-90 km) rift zones with modest continental stretching factors of 2.5-3.5 are measured as smaller amounts of rifting were needed to stretch the weaker, parallel, orogenic fabric. Where basement fabric trends near--orthogonally to the north-south South Atlantic rift direction in the Salado suture of Southern Uruguay and the Damara belt of Namibia, wider (185-220 km) rift zones with higher stretching factors of 4.3-5 are

observed as greater amounts of stretching were needed to extend the stronger, orthogonal, orogenic fabric. The rift-oblique Gariep belt intersects the South Atlantic continental rupture at an intermediate angle (30°) and an intermediate stretching factor (4). A compilation of published stretching factors from other rifted margins worldwide confirms the same relationship described, with rift-parallel margins having lower stretching factors in a range of 1.3-3.5 and rift-orthogonal or oblique-margins have higher stretching factors in a range of 4-8.

4.2 Introduction

Pre-existing structures and anisotropic tectonic fabrics within the continental lithosphere have been proposed by many groups of previous workers to influence the structural architecture of rifted, continental margins (Sykes, 1978; Dunbar and Sawyer, 1989; Tommasi and Vauchez, 2001; Autin et al., 2013; Chenin, 2015). The variable orientation of crustal fabrics adjacent to large ocean basins have been proposed to control the locations of continental transfer faults connecting normal faults and oceanic fracture zones (Wilson 1965; Sykes, 1978; Vink et al., 1984; Dunbar and Sawyer, 1989; Benkhelil et al. 1995; Mascle et al. 1997; Tommasi and Vauchez, 2001; Mohriak and Rosendahl, 2003; de Castro et al. 2012). Rift propagation preferentially occurs along rift-parallel orogenic fabrics, but in some locations rifts crosscut orthogonally- and obliquely-oriented, basement fabrics (Sykes, 1978; Vink et al., 1984; Dunbar and Sawyer, 1989; Tommasi and Vauchez, 2001; 2013; Chenin, 2015).

Compilation of onshore geologic data by previous workers have shown that basement orogenic trends on the conjugate VPM's of the South Atlantic Ocean were both rift-parallel and rift-orthogonal to the Barremian-Aptian (132-125 Ma) paleo-spreading center (Tommasi and Vauchez, 2001; Frank et al., 2007; Gray et al., 2008; Blaich et al., 2013). The net result of the interaction between the northward-propagating lithospheric rupture across pre-existing crustal fabrics was expressed as both wide and narrow rifted margins. These variations in the width of the margin are thought to reflect variations in the amount of crustal stretching, measured as a beta factor (β), the ratio between the initial crustal thickness/final and stretched crustal thickness as defined by the zone of crust and underlying lithosphere (McKenzie, 1978; Davison, 1998). Low beta-factor rifts are characterized by lower amounts of crust and lithospheric stretching, and narrower zones of extension, and high- to moderate-angle normal faults bounding half-grabens and tilted fault blocks. High beta-factor rifts are characterized by wider zones of extension, lower-angle normal faults, and a greater degree of fault block rotation along these lower-dipping normal faults.

4.2.1 Main features of continental rifting and oceanic spreading of the South Atlantic Ocean

The breakup of the Western Gondwana continent by early Cretaceous opening (134-130 Ma) of the South Atlantic Ocean initiated along the east-west-striking Malvinas-Algulhas transfer zone and propagated northward (Rabinowitz

and LaBrecque 1979; Austin & Uchupi 1982; Nürnberg and Müller 1991; Chang et al. 1992; Blaich et al., 2011; Blaich et al., 2013) (Fig. 4.1). The tectonic evolution of the South Atlantic, conjugate VPM's and non-volcanic margins of the northern South Atlantic was the result of continued, northward propagation of the rift towards the Equatorial Atlantic (Rabinowitz and LaBrecque 1979; Austin and Uchupi 1982; Nürnberg and Müller 1991; Chang et al. 1992; Gladczenko et al., 1997; Blaich et al., 2011; Blaich et al., 2013). The conjugate VPM's of the southernmost - or austral segment - of the South Atlantic Ocean are now separated by more than 6,500 km of oceanic crust formed from the Aptian (132-120 Ma) to present-day along the Mid-Atlantic Ridge (Fig. 4.1) (Moulin et al., 2010; Blaich et al., 2011; 2013).

Extensive plume-related, pre-break-up volcanism is recorded on South Atlantic VPM's from the onshore Hauterivian (132 Ma) Paranà flood basalts of southern Brazil and Etendeka volcanic area of the same age in northern Namibia (Wilson 1965; Sykes, 1978, Gladczenko et al., 1997; Tommasi and Vauchez, 2001; Geoffroy, 2005; Blaich et al., 2011, 2013; Geoffroy et al., 2015) (Fig. 4.1). Voluminous break-up related magmatic activity continued after lithospheric thinning as recorded by wide zones of Barremian-Aptian (131- 125 Ma) SDR's along the conjugate VPM's (Fig 4.1). Aptian (130 Ma) oceanic crust production followed the extrusive magmatism and continues at the presently active Mid-Atlantic Ridge (Wilson 1965; Franke et al., 2007; Blaich et al., 2011; Blaich et al., 2013; Koopman et al., 2014) (Fig. 4.1).

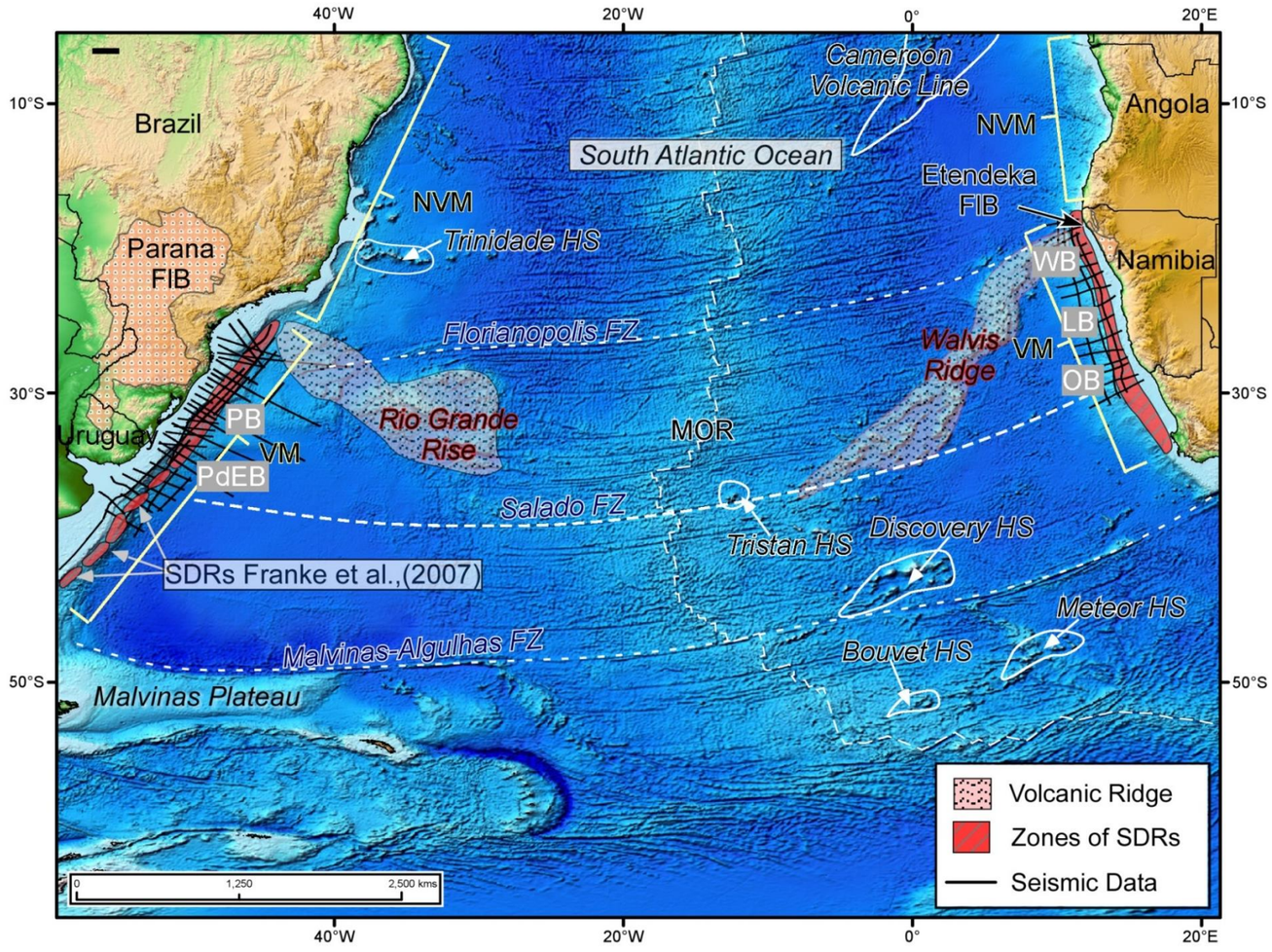

Figure 4.1: Regional topographic and bathymetric map of the South Atlantic showing conjugate margins in Uruguay and Namibia described in this study: 1) Punta de Este Basin (PdEB); 2) Pelotas Basin(PB); 4) Orange Basin (OB); 5) Lüderitz Basin (LB); and 6) Walvis Basin (WB). Oceanic fracture zones (FZ) - including the Malvinas-Algulhas, Salado, and Florianopolis – are flow lines that allow for restoration of conjugate margins. Volcanic margin segments and discreet zones of SDR packages proposed by Franke et al. (2007) are highlighted in the austral South Atlantic on the South American margin. The Early Cretaceous opening of the South Atlantic Ocean basin was accompanied by effusive volcanism emplaced at the rifted continental margins and continued hotspot activity has been recorded in the ocean floor as seamounts and volcanic ridges. The post-rift Rio Grande Rise and the Walvis Ridge volcanic complexes associated with the Tristan de Cunha hotspot are shown. Younger hotspot-related features of sub-marine volcanoes and seamounts (HS) include these chains: 1) Bouvet; 2) Meteor; 3) Discovery; 4) Tristan; 5) Cameroon; 6) Trinidade.

rifting and magmatic processes (Franke et al., 2007, Blaich et al., 2013, Koopman et al., 2014) (Fig. 4.1).

The east-west-trending Salado oceanic fracture zone links the conjugate basins of the Punta del Este and Orange Basins (Franke et al., 2007; Koopman et al., 2014) (Fig. 4.1). The east-west-trending Florianopolis oceanic fracture zone forms the northern boundary of the VPM's of the austral South Atlantic and connects the Northern Pelotas and Walvis Basins of Brazil (Franke et al., 2007, Blaich et al., 2013, Koopman et al., 2014). The Barremian-Eocene (131-40 Ma) Rio Grande Rise and the Barremian – Miocene (131-10 Ma) Walvis Ridge Volcanic Complexes provide evidence of long- lived volcanism associated with the Tristan de Cunha Plume (O'Connor and Duncan, 1990; Planert et al., 2016) (Fig. 4.1).

4.2.2 Plate reconstructions of the opening of the South Atlantic Ocean

Figures 4.2A and 4.2B show plate reconstructions of the South Atlantic at Maastrichtian (67 Ma) and Aptian (120 Ma) modified from reconstructions by Seton et al. (2012). Satellite free-air gravity data present evidence for variable gravity expressions of structural domains onshore and at the Barremian (130 Ma) rifted margins (Fig. 4.2). These boundaries onshore can also correlate with prominent east-west-trending, oceanic fracture zones (Franke et al., 2007; Sandwell and Smith, 2009; Koopman et al, 2014) (Fig. 4.2). Tectonic plate reconstructions permit the restoration of major tectonic domains to their pre-

67 Ma GPlates Reconstruction

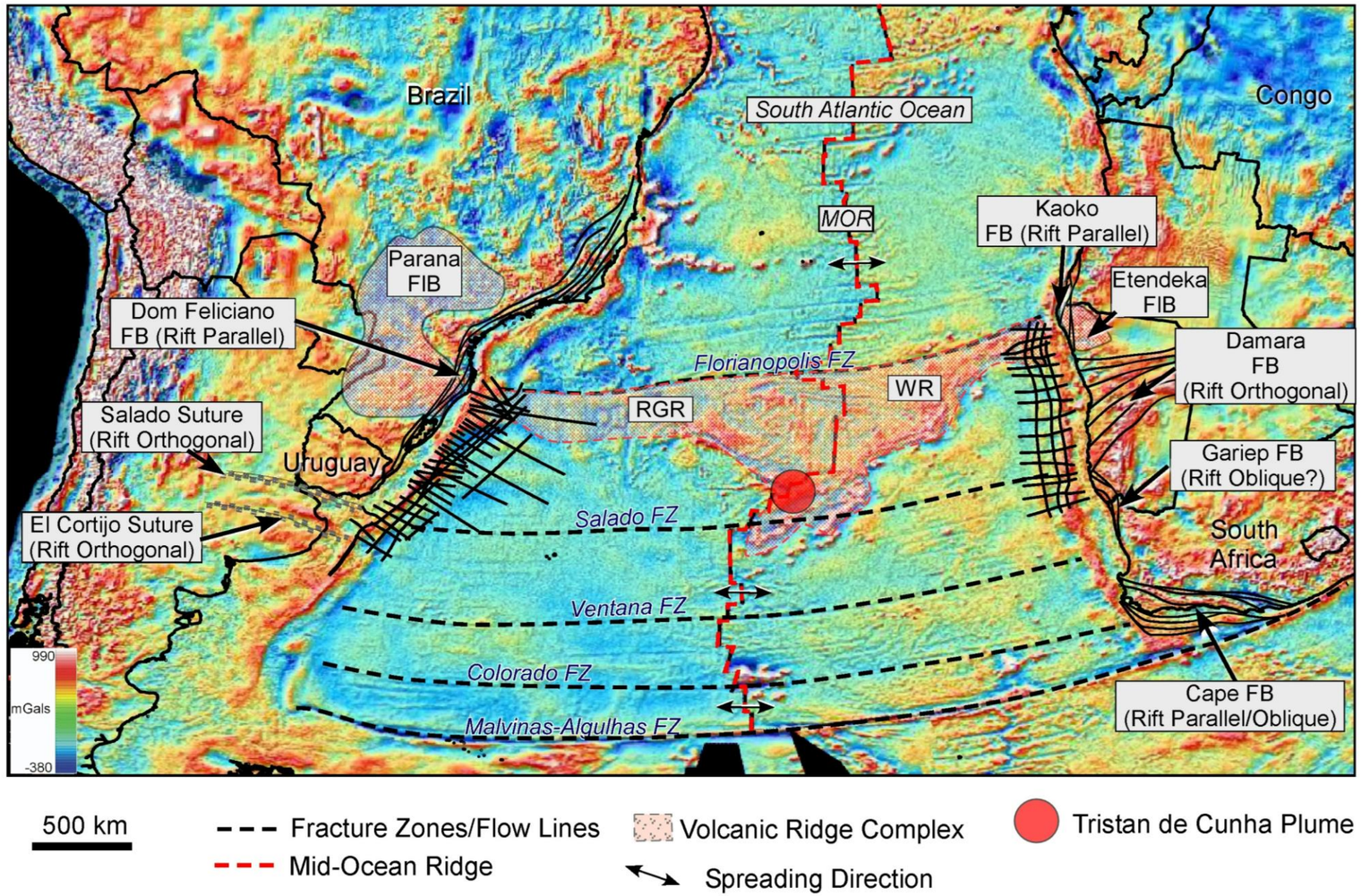

Figure 4.2: A) A 67Ma GPlates reconstruction of the South Atlantic show a conjugate relationship between the volcanic passive margins of Uruguay and Namibia (Seton et al., 2012) and major geologic features of the region. Fracture zones, divided by the mid-ocean ridge, act as flow lines within the satellite free-air gravity data (Sandwell and Smith, 2009) and can be used to retrace the path of the diverging plates since continental rupture. Seismic data used in this study is also highlighted on the conjugate margins of Namibia and Uruguay/Southern Brazil. Major tectonic and orogenic foldbelts (FB) and their structural orientation to the rift axis are labeled on the opposing conjugate margins: South American Plate: Dom Feliciano FB, Salado Suture, El Cortijo Suture; African Plate: Cape FB, Gariep FB, Damara FB, and Kaoko FB. (Free-air anomaly gravity data: reds represent gravity highs; blues represent gravity lows.)

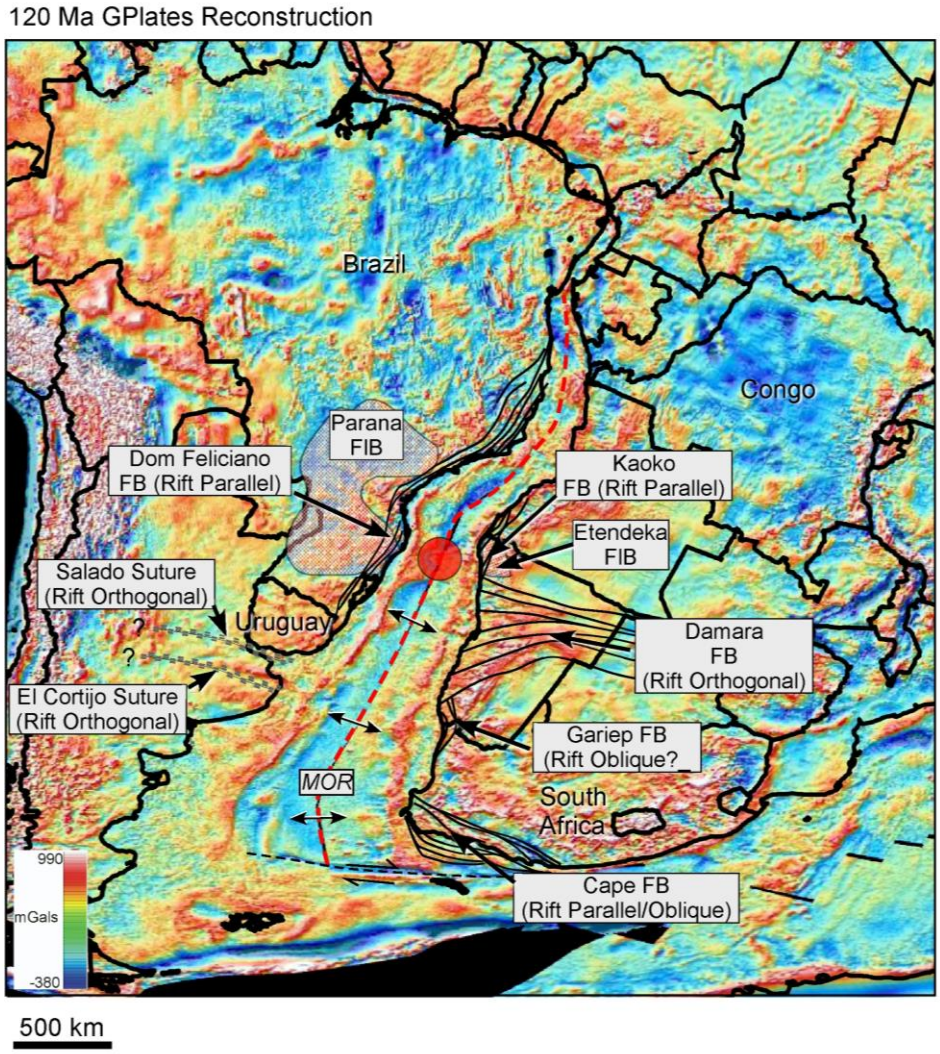

Figure 4.2: A 120 Ma tectonic reconstruction using free-air gravity data
B) The South American margin has 3 notable tectonic features and foldbelts (FB): 1) the El Cortijo Suture; 2) the Salado Suture; and 3) the Dom Feliciano Foldbelt. Their orientations to the paleo-rift axis of the South Atlantic are rift-orthogonal, rift-orthogonal, and rift-parallel respectively. The West African margin is flanked by four prominent foldbelts: 1) the Kaoko; 2) the Damara; 3) the Gariep; and 4) the Cape FBs. These have orientations of rift-parallel, rift-orthogonal, rift-oblique, rift-parallel/oblique respectively. (Free-air anomaly gravity data: reds represent gravity highs; blues represent gravity lows.)

break-up, Barremian (131 Ma), locations and allow for a better understanding of the paleogeography at the time of the formation of the conjugate VPM's of the South Atlantic (Fig. 4.2A) (Moulin et al., 2010; Seton et al., 2012; Blaich et al., 2013).

4.2.3 Overview of Precambrian to Paleozoic orogenic belts surrounding the Cretaceous South Atlantic Ocean

Precambrian to Paleozoic intra-cratonic, orogenic belts and their related suture zones have been previously mapped on the onshore regions of the South American and African plates (Figs. 4.2A, B) (Coward, 1983; Tommasi and Vauchez, 2001; Gray et al., 2008, Blaich et al., 2013, Chernicoff et al., 2014). The onshore continental rocks of the South American plate contain three, distinctive orogenic belts and suture zones: 1) El Cortijo suture formed at 2050-2300 Ma (Moulin et al., 2010; Chernicoff et al., 2014); 2) Salado suture formed 2050-2300 Ma (Chernicoff et al., 2014); and 3) the Dom Feliciano orogenic belt formed 580-620 Ma (Gray et al., 2006; Blaich et al, 2013, Chernicoff et al., 2014) (Figs. 4.2A, B). The 1200-km-long Dom Feliciano orogenic belt is considered rift-parallel with respect to the north-south-trending rift axis of the early South Atlantic Ocean (Tommasi and Vauchez, 2001; Gray et al., 2006; Heilbron et al., 2008) (Fig. 4.2B). In contrast, the sutures to the south of the Dom Feliciano FB have a relatively narrow exposure of 50-90 km at the margin.

The conjugate margin of Namibia has three margin orogenic foldbelts that flank the Cretaceous rifted margin (Gray et al., 2006; Heilbron et al., 2008; Blaich et al., 2013) (Fig. 4.2B). The north-south-trending Kaoko orogenic belt - formed at 580-655 Ma - is conjugate to the northern regions of the South American N-S Dom Feliciano FB (580-620 Ma) and shares a similar rift-parallel orientation to the rift axis for 450 km at the modern coastline (Goscombe et al., 2003, Gray et al., 2006; Heilbron et al., 2008) (Fig. 4.2B).

South of the Kaoko belt is the rift-orthogonal Damara belt (505-530 Ma) which has a mostly right-angle orientation to the modern coastline of Namibia (Gray et al., 2006; Heilbron et al., 2008) (Fig. 4.2B). This tectonic feature intersects 715 km of the present day Namibian coast (Fig. 4.2B). The rift-oblique Gariep belt (535-545 Ma) is located in the southern coastal region of Namibia and has an arcuate shape with respect to the Barremian (130 Ma) rifted margin and therefore has an oblique component the paleo-rift axis of the South Atlantic (Frimmel and Frank, 1998; Gray et al., 2006; Heilbron et al., 2008) (Fig. 4.2B). This Paleozoic belt occupies approximately 220 km of the southern Namibian coast (Fig. 4.2B).

4.3 Geologic setting of South Atlantic continental rifting

The early Cretaceous, Barremian (131 Ma) continental break-up occurred within a framework of heterogeneous tectonic domains that made up Western Gondwana (Kröner and Cordani, 2003; Gray et al., 2008; Heilbron et al., 2008)

(Fig. 4.3). This preexisting framework consists of a mosaic of: 1) thick, Pre-Cambrian cratons; 2) reworked basement terranes; 3) magmatic arc assemblages; and 4) mixed terranes of Paleoproterozoic basement and back-arc successions (Heilbron et al., 2008) (Fig. 4.3).

Pan-African-Brasiliano (870-550 Ma) mobile foldbelts situated amongst the cratonic domains compose much of Western Gondwana (Gray et al., 2008; Heilbron et al., 2008) (Fig. 4.3). The tectonic fabrics and various structural orientations are a result of multi-orogenic deformation as the ages of the deformation zones vary widely (Gray et al., 2008) (Fig. 4.3). It is from this setting of orogenic belts and tectonic fabrics that structural inheritance - and therefore variable amounts of stretching - would be affected during the Barremian (131 Ma) rifting (Tommasi and Vauchez, 2001; Mohriak and Rosendahl, 2003; de Castro et al. 2012; Blaich et al., 2013).

4.3.1 South Atlantic crustal fabrics

Gray et al. (2008) investigated the orogenic processes of the Brasiliano and Pan-African orogenic systems (870- 550 Ma) and the amalgamation of the intra-cratonic components to confirm the Pan-African-Brasiliano cratonic assemblage by 550 Ma (Fig. 4.3). In a pre-rift, restored position, the orientation of the structural fabrics to the South Atlantic rift basin is apparent (Gray et al., 2008; Heilbron et al., 2008) (Fig. 4.3A). Gravimetric response from satellite derived free-air gravity data (Sandwell and Smith, 2013) of the Gondwanan

Figure 4.3: Previous works featuring a Gondwana reconstruction and associated profiles of major orogenic belts between South America and Africa.

A) A western Gondwana reconstruction highlighting the regional Brasiliano-Pan-African mobile foldbelts and sutures within the area of investigation. Prominent orogenic foldbelts (FB) are positioned between major cratons on both the South American and African plates The El Cortijo (ECS) and Salado Sutures (SS) and Damara FB are orientated rift-orthogonal with respect to the rift axis. In contrast, the Dom Feliciano and Kaoko FBs are observed to be oriented in a rift-parallel position.

B) The inset shows the approximate location of the zoomed-in western Gondwana area (A) within a reconstructed, free-air gravity image of Gondwana. (Free-air anomaly gravity data: reds represent gravity highs; blues represent gravity lows.)

C) Four profiles of Conjugate Margin Tectonic Belts from previous works (Gosscombe and Gray, 2007; Gray et al., 2008; Chernicoff et al., 2014)

Profile 1) The conjugate, rift-parallel, N-S trending Dom Feliciano (DFFB) and NNW- trending Kaoko FBs (KFB) share a mirror-like structural geometry with respect to shear direction and thrust vergence. They share similar ages of deformation that ranges from ~ 580 to 655 Ma. These foldbelts are adjacent to the Rio de la Plata Craton (RdlP) on South American and the Kaoko FB is at the western limit of the Congo Craton. These belts are both dominated by NNW-trending lithospheric shear zones. Age of deformation from DFFB - Basei et al., (2000), KFB- Gosscombe et al., (2005).

Profile 2) The E-W trending thrusted zones within Damara FB (DFB) are positioned rift-orthogonal to the South Atlantic Rift axis. The origin of the foldbelt stems from the convergence between the Rio de la Plata, Congo, and Kalahari Cratons (Gray et al., 2006). The northern and southern limits of the Damara FB are doubly-vergent with inwardly dipping thrusts from the flanks of the bounding cratons. It should be noted that based on the near-coast change in geometry, the northern and southern arms of the Damara FB take on a less-orthogonal orientation at the rift axis, while the core of the foldbelt remains strongly orthogonal. Age of deformation from Jung and Mezger, 2003.

Profile 3) The structural fabric of the Gariep FB, on the west African margin has arcuate shaped zones with respect to the rift axis and therefore likely has both a parallel and oblique component along strike within the Gariep domain. The Gariep FB ranges in age from ~535-545 Ma and is generally younger than the foldbelts to the west and north. The Kalahari Craton borders the Gariep FB to the west where a thrust nappe is present on the craton. Age of deformation from Frimmel et al., (2000).

Profile 4) The Rhyacian age WNW trending El Cortijo and Salado Sutures are related to the Transamazonian Orogeny and fall within a region of that continually re-worked during Paleozoic orogen. The Salado Suture is the northern limit of the orogenic domains and is positioned at the southern boundary of the Rio de la Plata Craton. These suture zones are separated by the Tandil High (TH) and are oriented rift-orthogonal to the future propagation of the South Atlantic opening. Age of deformation from Chernicoff et al., (2014).

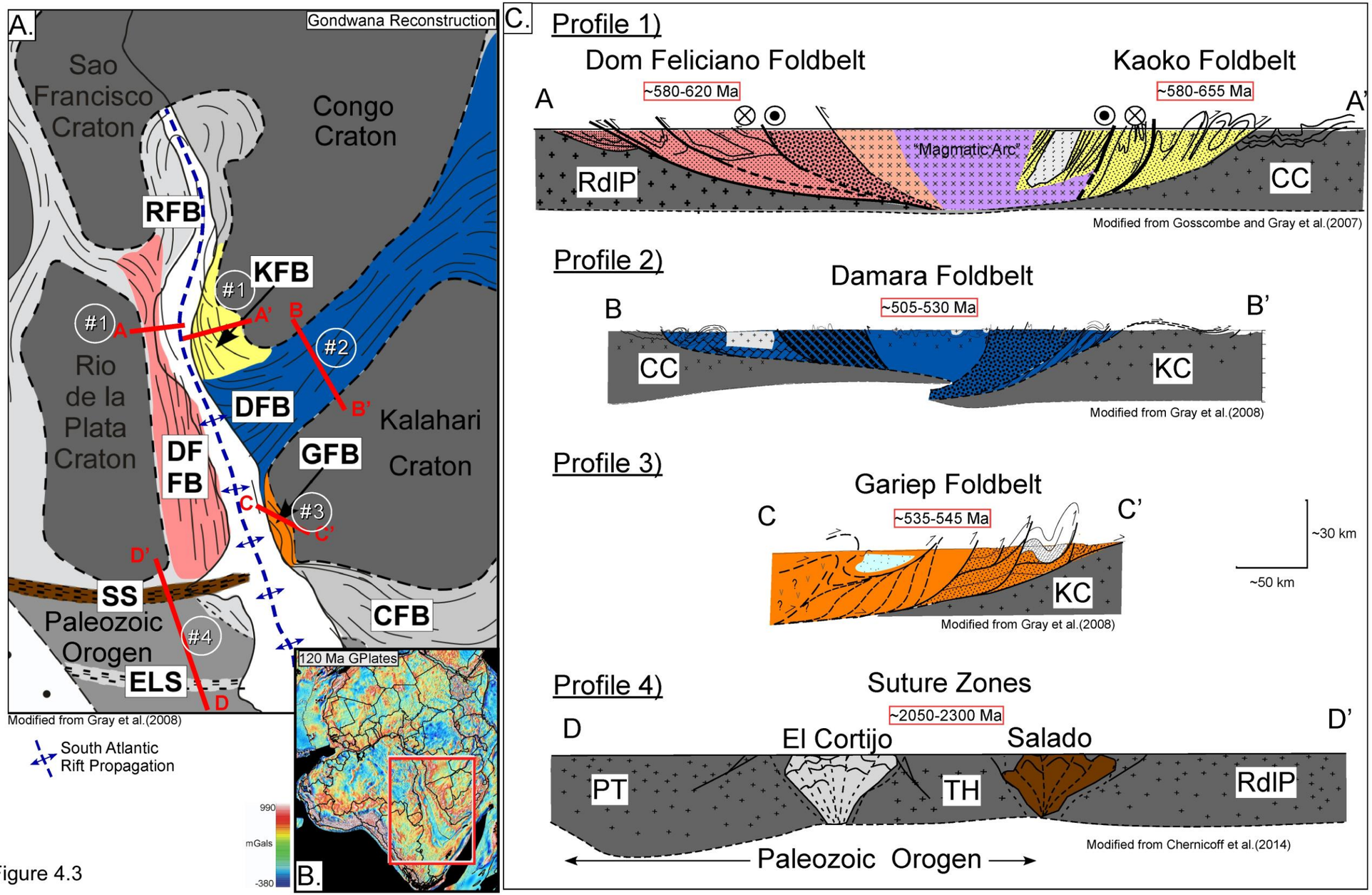
A.
Gondwana Reconstruction
Sao Francisco Craton
Congo Craton
RFB
KFB
#1
#1
A
A'
B
#2
B'
Rio de la Plata Craton
DFB
DF FB
GFB
Kalahari Craton
C
#3
C'
D'
SS
Paleozoic Orogen
#4
CFB
ELS
D
Modified from Gray et al.(2008)
South Atlantic Rift Propagation
120 Ma GPlates
990
mGals
-380
B.
C.
Profile 1)
Dom Feliciano Foldbelt
Kaoko Foldbelt
A
~580-620 Ma
~580-655 Ma
A'
"Magmatic Arc"
RdlP
CC
Modified from Gosscombe and Gray et al.(2007)
Profile 2)
Damara Foldbelt
B
~505-530 Ma
B'
CC
KC
Modified from Gray et al.(2008)
Profile 3)
Gariep Foldbelt
C
~535-545 Ma
C'
KC
~30 km
~50 km
Modified from Gray et al.(2008)
Profile 4)
Suture Zones
~2050-2300 Ma
D
El Cortijo
Salado
D'
PT
TH
RdlP
Paleozoic Orogen
Modified from Chernicoff et al.(2014)

Figure 4.3

assembly illustrates structural boundaries of the orogenic fabrics along the once-fused supercontinent (Gray et al., 2008) (Fig. 4.3B). Along strike- variables from the data used here can be correlated with the orogenic boundaries observed in gravity data.

Plate reconstructions show that conjugate orogenic trends are either complementary (parallel-parallel) or create apparent intersections (parallel-orthogonal) with respect to their opposing plate (Gray et al., 2008; Heilbron et al., 2008) (Fig. 4.3A). The Damara belt is rift-orthogonal and contrasts with the Dom Feliciano belt on the South American Plate (Gray et al., 2008; Heilbron et al., 2008; Blaich et al, 2013) (Fig 4.3A). The Salado and El Cortijo sutures are orientated approximately orthogonal to the paleo-rift axis and contrast the oblique rift-axis orientation of the Gariep and Cape Foldbelts (Chernicoff et al., 2014) (Fig. 4.3A). The Barremian (131 Ma) rift propagation through these zones of various orientations led to the opening of the South Atlantic Ocean basin (Rabinowitz and LaBrecque, 1979; Austin and Uchupi, 1982; Nürnberg and Müller 1991; Chang et al. 1992; Tommasi and Vauchez, 2001; Moulin et al., 2010; Blaich et al., 2011; Blaich et al., 2013) (Fig. 4.3A). The locus of the rift axis was influenced by the structural boundaries between these major orogenic trends (Austin and Uchupi, 1982; Tommasi and Vauchez, 2001; Moulin et al., 2010; Blaich et al., 2013).

The Dom Feliciano and Kaoko conjugate-pair foldbelts are both rift-parallel and show evidence of shearing during the course of deformation

(Gosscombe and Gray, 2007; Gray et al., 2008; Heilbron et al., 2008;) (Fig. 4.3C, Profile 1). The Kaoko belt of northern Namibia is composed of four distinct structural zones that are separated by sinistral-oblique shear zones that extend into the deep lithosphere (Goscombe and Gray, 2007). Westward-dipping thrusts are observed at shallow depths and major faults dip in a listric fashion to deeper crustal zones (Goscombe and Gray, 2007) (Fig. 4.3C). The Brasiliano-Dom Feliciano belt on the conjugate margin of South American shares a mirror-like structural deformation history within the high-grade metamorphic units and magmatic arc units, in dextral shear regime of the Kaoko FB (Gray et al., 2008; Passerelli et al., 2010) (Fig. 4.3C, Profile 1). Similar to the Kaoko belt, the surface exposures of the Dom Feliciano belt are characterized by high-angle N-S shear zones that have westerly dipping listric faults at deeper, crustal levels (Passerelli et al., 2010) (Fig. 4.3C, Profile 1).

The Pan-African Damara foldbelt is positioned between the Congo and Kalahari Cratons of Africa (Goscombe and Gray, 2007, Gray et al., 2008) (Fig. 4.3A). The origin of the Pan-African Damara foldbelt is considered to be a result of the convergence of the three primary cratons that bound it: 1) Congo Craton; 2) Kalahari Craton; and 3) Rio de la Plata Craton (Fig. 4.3A). This east-west-trending orogenic system has been defined as one branch of a collisional triple-junction with doubly-vergent bounding faults (Coward 1981; Coward, 1983; Hoffman et al., 1994) (Fig. 4.3A). The internal fabric of the Damara belt trends east-west and contrasts to the adjacent, north-south- trending structural fabrics

of the Kaoko and Gariep foldbelts belts Gray et al., 2008) (Fig. 4.3A). At the coast, the Damara belt has been described to have sinistral-transpressional boundaries that parallel the Kaoko and Gariep belts. The central exposure at the margin indicates that the Damara's coastal terranes remain rift-orthogonal (Gray et al., 2008) (Fig. 4.3A). East-west-trending internal shear zones of the Damara belt are dominated by craton-vergent, imbricate thrust shear zone systems (Gray et al., 2008) (Fig. 4.3C, Profile 2).

The rift-oblique Gariep belt is the southern branch of the collisional triple-junction on the West African Margin (Coward 1981; Coward, 1983; Hoffman et al., 1994) (Fig. 4.3A). This orogenic belt has internal structural deformation trends that vary from north to south and are positioned in parallel and oblique geometries to the paleo-spreading center of the early South Atlantic (Frimmel and Frank, 1998) (Fig. 4.3A). The arcuate "bend" in the Gariep Belt is considered to be a result of the pre-existing geometry of the Neoproterozoic continental margin at the time of continent-continent collision (Frimmel and Frank, 1998) (Fig. 4.3A). High angle (>60°) thrust nappes from the Gariep belt were emplaced onto the western region of the Kalahari Craton (Gray et al., 2008) (Fig. 4.3C Profile 3). High-angle, westward-dipping thrusts with listric geometries at- depth divide the major zones of the Gariep belt (Gray et al., 2008) (Fig. 4.3C Profile 3).

The Salado and El Cortijo Sutures of northern Argentina have been described by Chernicoff et al. (2014) as structural belts formed during the

Rhyacian (2050-2300 Ma), Trans-Amazonian Orogeny (Fig. 4.3A). The Salado Suture defines the maximum northern extent of deformation related to Paleozoic Orogenic deformation (Gray et al., 2008) (Fig. 4.3A and 4.3C, Profile 4). The orientation of the east-west suture zones described here and the east-west trending limit of Paleozoic orogens are oriented rift-orthogonal to the paleo-spreading axis of the early South Atlantic (Gray et al., 2008; Chernicoff et al., 2014). (Fig. 4.3A and 4.3C, Profile 4).

4.4 Previous ideas on the control of crustal fabrics on the style of continental rifting

The investigation of rifted margin architecture geometries as a result of pre-existing features has been examined by previous workers using several methods (Sykes, 1978; Dunbar and Sawyer, 1989; Tommasi and Vauchez, 2001; Autin et al., 2013; Chenin, 2015). Tommasi and Vauchez (2001) conducted modelling of the preferential and systematic reactivation of pre-existing features within the continental lithosphere at sites of intense magmatic activity associated with mantle plumes. In this study, I analyze the interactions of the trends of rifting with the orogenic fabrics of the southern segment of the South Atlantic (Fig. 4.3).

Franke et al. (2007) and Koopman et al. (2014) observed margin segments with discrete packages of SDR's within South Atlantic VPM's that varied along-strike (Fig. 4.1). These previous studies cited "distinct along-margin

variations in architecture" as a mechanism to influence the presence of seaward-dipping reflectors (SDR's), volume variability in magma volumes, and margin segmentation (Franke et al., 2007; Koopman et al., 2014).

I investigate the structural influence of along-strike, pre-existing tectonic fabrics on the Uruguay/Southern Brazilian and conjugate Namibian Margins. I analyze regional, deep-record, high resolution seismic reflect data to determine the variable-width zone of continental stretching. I calculate apparent crustal thinning factors or "Delta c" (Δ_c) for the South Atlantic margins analyzed from seismic reflection profiles in order for a quantitative comparison of these values with global values at rift basins with adjacent tectonic fabrics of varying rift-axis orientation. From this we can predict wide and narrow continental passive margins as they relate to pre-existing zones of weakness at the paleo-rift axis.

4.5 Seismic reflection data used in this study

The seismic reflection data used in the study total 27,550 km in length and were acquired by ION Geophysical during their various regional, or "SPAN", surveys of both conjugate margins from 2009 to 2014 (Fig 4.1A). UruguaySPAN (2012) and PelotasSPAN (2009) (a subset of the BrasilSPAN3 – 2009) were used as the dataset to document the South American VPM's (Table 4.1). The NamibiaSPAN seismic reflection data (2014) were used to document their conjugate, west African VPM. The total line kilometers for each of the three

Seismic Survey	Country	Year Acquired	Record Length (s)	Receiver Depth (m)	Cable Length (m)	Total (km) (used in this study)	
UruguaySPAN	Uruguay	2012	18	9.5.	10,200	2,818	
PelotasSPAN	Brazil	2009	18	9.5	10,200	10,667	
BrasilSPAN	Brazil	2009	18	8.5	10,200	3,638	
NamibiaSPAN	Namibia	2014	18	10	10,200	10,421	
						27,544	Total

Table 4.1: Seismic Data Acquisition Parameters (ION Geophysical)

surveys are: UruguaySPAN = 2,818 km; PelotasSPAN = 10,667 km, BrasilSPAN = 3,638 km, and NamibiaSPAN = 10,421 km (Table 4.1).

Seismic lines were recorded to 18 seconds two-way-travel time and were migrated to a depth of 40 km (Table 4.1). The data processing flow from the raw stacks to the final pre-stack depth migration shown on the seismic images shown in this chapter are based on geophysical industry standard applications and processing workflow at ION Geophysical. Acquisition specifications remained constant from survey to survey with air-gun source depths varying from 8.5-10 m and cable lengths fixed at 10.2 km (Table 4.1). Survey design and spacing was designed to take capture elements of the regional tectonic setting from the paleo rift and fracture zone orientation between the conjugate VPM margins of South America and west Africa.

4.6 Observations of rifted continental crust from deep-penetration seismic reflection profiles of South Atlantic VPM's

Analysis of the seismic reflection data shown in this chapter confirms a variability of crustal stretching at orogenic structured zones on the conjugate VPM's of the South Atlantic Ocean. In order to compare the various degrees of continental stretching, I have measured crustal stretching factors for seven, 2D seismic profiles (Figs. 4.4-4.10). The seismic profiles are representative examples from each onshore tectonic structural domain as described in Figure

4.3A-4.3C. Constraining the crustal limits and thicknesses is a key factor in determining the true degree of deformation that took place on the rifted continental margin. The 40-km-deep record of the seismic reflection data permits a simple assessment of the un-thinned, maximum continental crust thickness which ranges from 32-24 km (Figs. 4.4-4.10). The smaller values of 24-km-thick continental crust may indicate a wider zone of rifting that is not possible to completely define because of the lengths of the available seismic lines (Figs. 4.4-4.10). Thinning factors were calculated using a simple stretching factor calculation similar to Steckler and Watts (1978), where I determine the factor of thinning as a relationship of: "Delta c" (Δ_c) = initial crustal thickness (km) / final thickness (km).

Until recently, determining the "Limit of Continental Crust" (LoCC) (McDermott et al., 2015) along passive margins was not well understood. Pindell et al., (2014) and Geoffroy et al., (2015) provide a similar set of criteria to determine the location of the LoCC on VPM's based on several assumptions about the emplacement and kinematics of the SDR complexes at VPM's. Both these studies recognized the existence of landward-dipping normal faults at VPM's and proposed that the landward-dipping, normal fault planes were initiated during the early rift phase by gravitational shedding from an initially-elevated, volcanic center (Pindell et al., 2014; Geoffroy et al., 2015). These details of rifted VPM are essential to establish in order to constrain the crustal boundaries and therefore the total amount of crustal stretching.

Figure 4.4: A south-north strike profile illustrating the rift-orthogonal El Cortijo and Salado Sutures.

A) The profile location map (heavy black line) within the South Atlantic, GPlates reconstruction at 115 Ma.

B) The un-interpreted, south–north, deep record seismic line from the continental shelf of offshore Argentina and Uruguay.

C) The interpreted seismic profile from Figure 4.4B where deep seismic events indicate lithospheric scale deformation in the form of thrusts dipping to the south within the tan-shaded region identified as continental crust. The El Cortijo and Salado sutures are separated by an area of thick, un-structured continental crust. Crustal thinning reaches 18km thick at the Salado Suture and reaches a maximum thickness of 31 km. The apparent brittle-ductile transition (B-D T) is identified from internal crustal - seismic facies. The continental crust is floored by a rugose Moho expression. Seismic data at the rifted margin indicates that the structure of the Salado Suture is dominated by southward dipping thrusts at the Argentine-Uruguay border.

D) Enlargement of a section of the section from Figure 4C illustrating the deformed and rotated pre-rift fabric at the Salado Suture.

A.

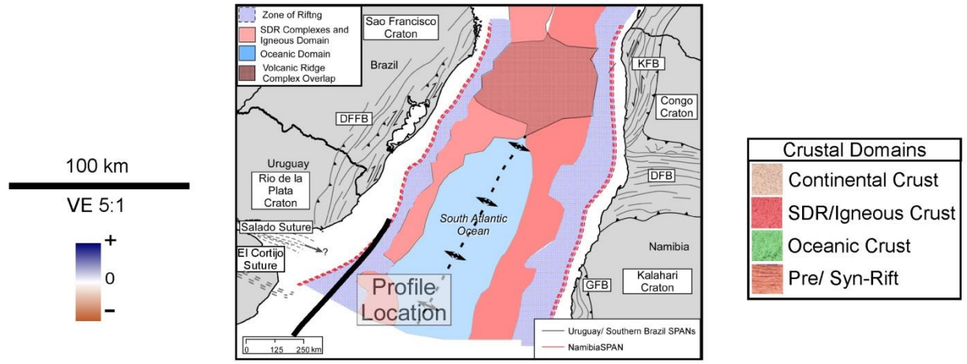
100 km
VE 5:1
+
0
–
Zone of Riftng
SDR Complexes and Igneous Domain
Oceanic Domain
Volcanic Ridge Complex Overlap
Sao Francisco Craton
Brazil
DFFB
Uruguay
Rio de la Plata Craton
Salado Suture
El Cortijo Suture
South Atlantic Ocean
Profile Location
KFB
Congo Craton
DFB
Namibia
GFB
Kalahari Craton
Uruguay/ Southern Brazil SPANs
NamibiaSPAN
0 125 250 km

Crustal Domains
Continental Crust
SDR/Igneous Crust
Oceanic Crust
Pre/ Syn-Rift

B.

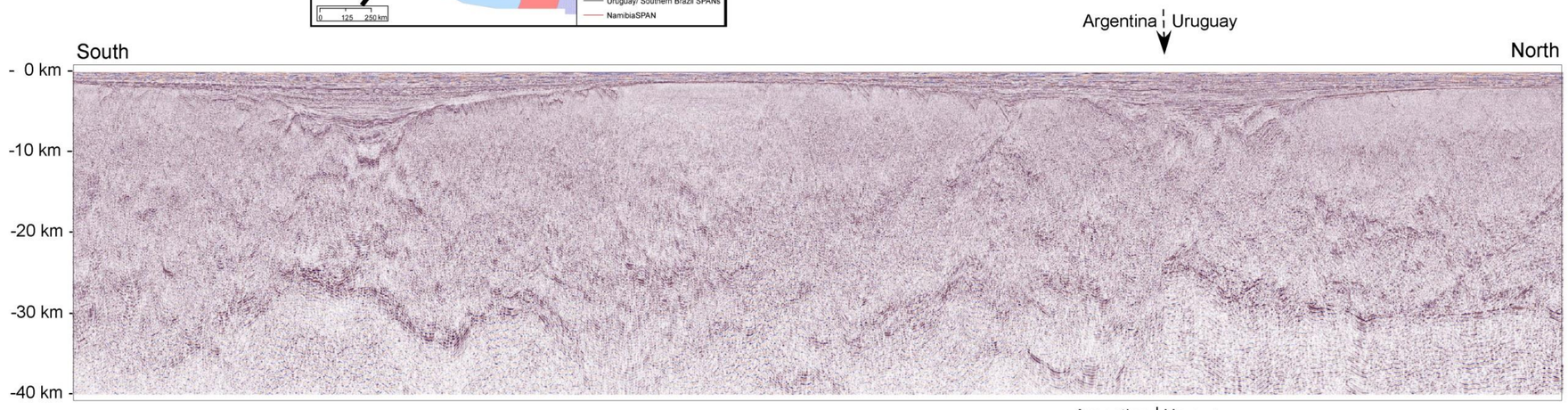
Argentina | Uruguay
South
North
- 0 km -
-10 km -
-20 km -
-30 km -
-40 km -

C.

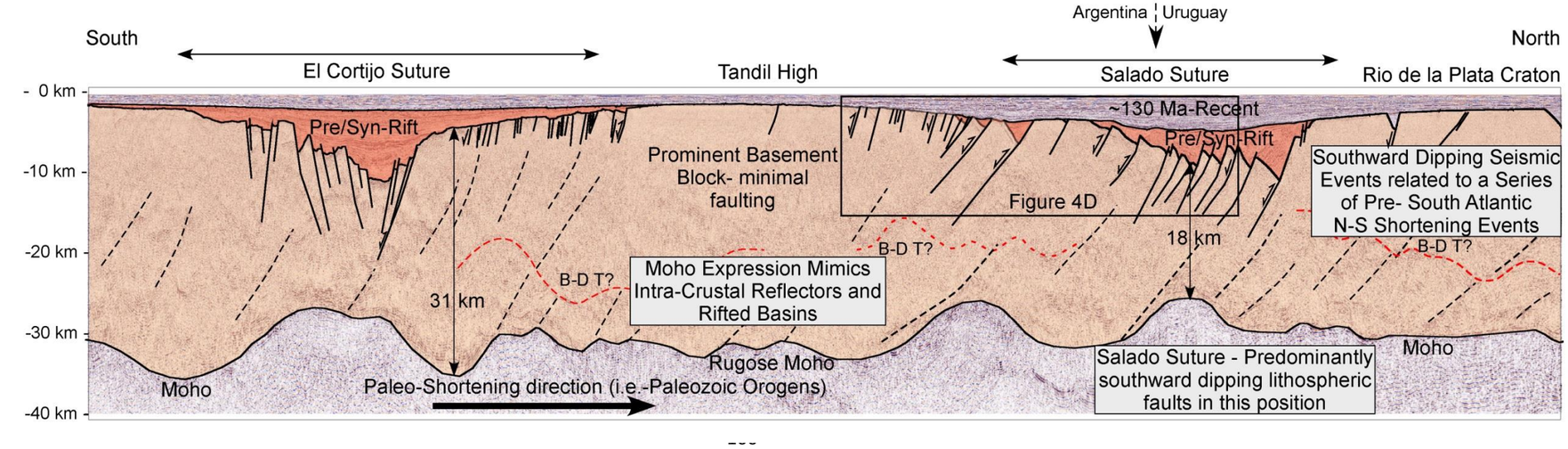
Argentina | Uruguay
South
North
El Cortijo Suture
Tandil High
Salado Suture
Rio de la Plata Craton
- 0 km -
-10 km -
-20 km -
-30 km -
-40 km -
Pre/Syn-Rift
Prominent Basement Block- minimal faulting
~130 Ma-Recent
Pre/Syn-Rift
Figure 4D
Southward Dipping Seismic Events related to a Series of Pre- South Atlantic N-S Shortening Events
B-D T?
B-D T?
B-D T?
31 km
18 km
Moho Expression Mimics Intra-Crustal Reflectors and Rifted Basins
Rugose Moho
Moho
Moho
Paleo-Shortening direction (i.e.-Paleozoic Orogens)
Salado Suture - Predominantly southward dipping lithospheric faults in this position

D.

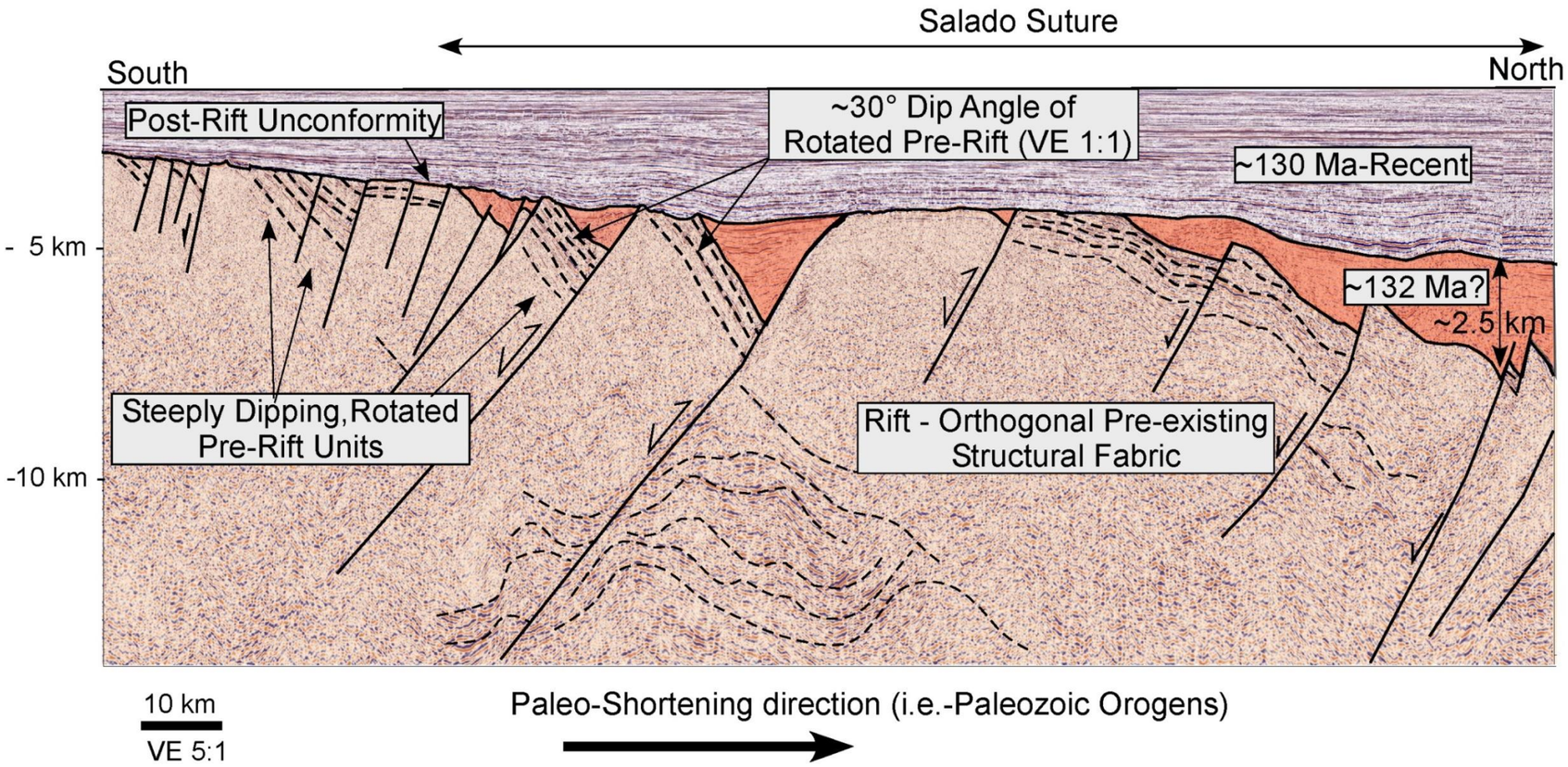
Salado Suture
South
North
Post-Rift Unconformity
~30° Dip Angle of
Rotated Pre-Rift (VE 1:1)
~130 Ma-Recent
- 5 km -
~132 Ma?
~2.5 km
Steeply Dipping, Rotated
Pre-Rift Units
Rift - Orthogonal Pre-existing
Structural Fabric
-10 km -
10 km
VE 5:1
Paleo-Shortening direction (i.e.-Paleozoic Orogens)

4.6.1 Zones of Pre-Existing Weaknesses

4.6.1.1 Rift-orthogonal, Salado suture zone (Argentina and Uruguay)

Figures 4.4A is a north-south, mega-regional strike-oriented seismic reflection line along the continental shelf of Argentina and southern Uruguay shows abundant evidence of variations in Paleozoic, orogenic basement trends and intensity of both Paleozoic shortening and Cretaceous rift-related deformation. The continental crust along this line extends southward from the southern limit of the Rio de la Plata Craton in Argentina to Uruguay where Cretaceous rifting has overprinted the older Paleozoic crustal fabric is present (Fig. 4.4B, C).

The rugose Moho at the base of the South American continental crust is attributed to the combined effects of multiple pre-Cretaceous, north-south shortening events accommodated along a series of southward-dipping thrust faults (Fig. 4.4B, C). Many of these shallow faults are reactivated thrust faults from previous orogens (Fig. 4.4C). The Moho (Mohorovicic discontinuity) expression exhibits a close correlation with the lithospheric scale faulting seen here, in addition to shallowing at the thinned zones of continental crust (Fig. 4.4C). Along-strike crustal thickness ranges from ~18 km to 31 km (Fig. 4.4C).

The Rhyacian (2050 – 2300 Ma) El Cortijo and Salado Suture zones are separated by the Tandil High, a relatively undeformed basement dome that shows little evidence of faulting (Fig. 4.4C). Figure 4.4D highlights a zoomed in

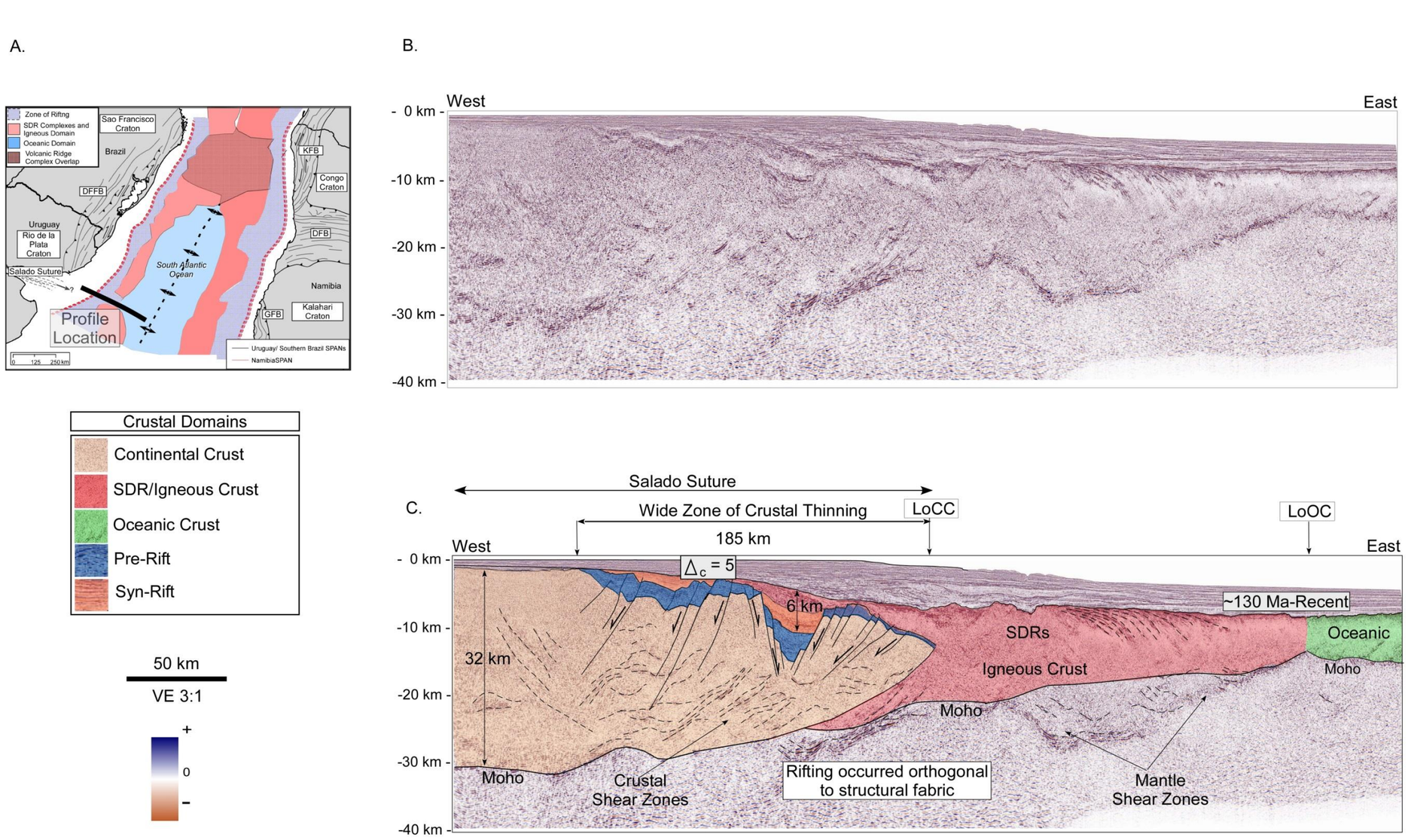

Figure 4.5: An example profile from the Punta del Este Basin. A) The profile location (black line) map within the South Atlantic, GPlates reconstruction at 115 Ma. B) An un-interpreted deep record seismic line from Salado Suture zone located in the Punta del Este Basin of the offshore Uruguay. Seismic amplitudes are variable and range from steeply dipping, offlapping packages to laterally continuous and flat lying events in the shallow section. C) The interpreted section of Figure 4.5B where a wide zone (~185 km) of horsts and grabens are present within rifted continental crust. In the West, the interpreted continental crust is ~32km in thickness which is then thinned to the east until final continental rupture. A crustal thinning factor (Δ_c) of 5.0 has been calculated. This continental crustal domain limit (LoCC) is present west of the onset of SDRs/igneous crust and oceanic crust.

section of the southern Salado Suture Zone and demonstrates the highly rotated pre-rift (Paleozoic?) units (Fig. 4.4D). Deep crustal reflective events are the seismic expression for the rift-orthogonal oriented Salado Suture (Fig. 4.4D). Faulted units to the south in Figure 4D illustrate the high angle of the units that remain unaffected by the South Atlantic rifting phase and record the amount of structural deformation prior to the opening of the ocean basin (> 134 Ma) (Fig. 4.4D).

Punta del Este Basin seismic data, in the dip-oriented position, provides evidence of a 185-km-wide zone of crustal thinning of the Salado Suture prior to the onset of Barremian (132 Ma) SDR's and igneous crust (Fig. 4.5C and 4.5B). The wide zone of crustal stretching suggests that the crust was highly resistant to rupture because the direction of extension was orthogonal to the zone of pre-exiting weakness.

The zone of horsts and grabens from an along-strike position has a narrow exposure at the margin of ~165 km, where the Salado Suture intersects the rift margin. The resistance to lithospheric break-up produced a wide margin (185 km) consisting of horsts and grabens east of full-thickness continental crust. Break up was followed by the emplacement of SDR's and igneous crust in the east (Fig. 4.5C). Using the stretching factor calculation described in section 4.6, 32-km-thick crust was eventually thinned by a factor of 5 (Fig. 4.5C). Intra-crustal reflectivity is high for this seismic section and might represent extensive shearing within the crust related to pre-existing deformation events

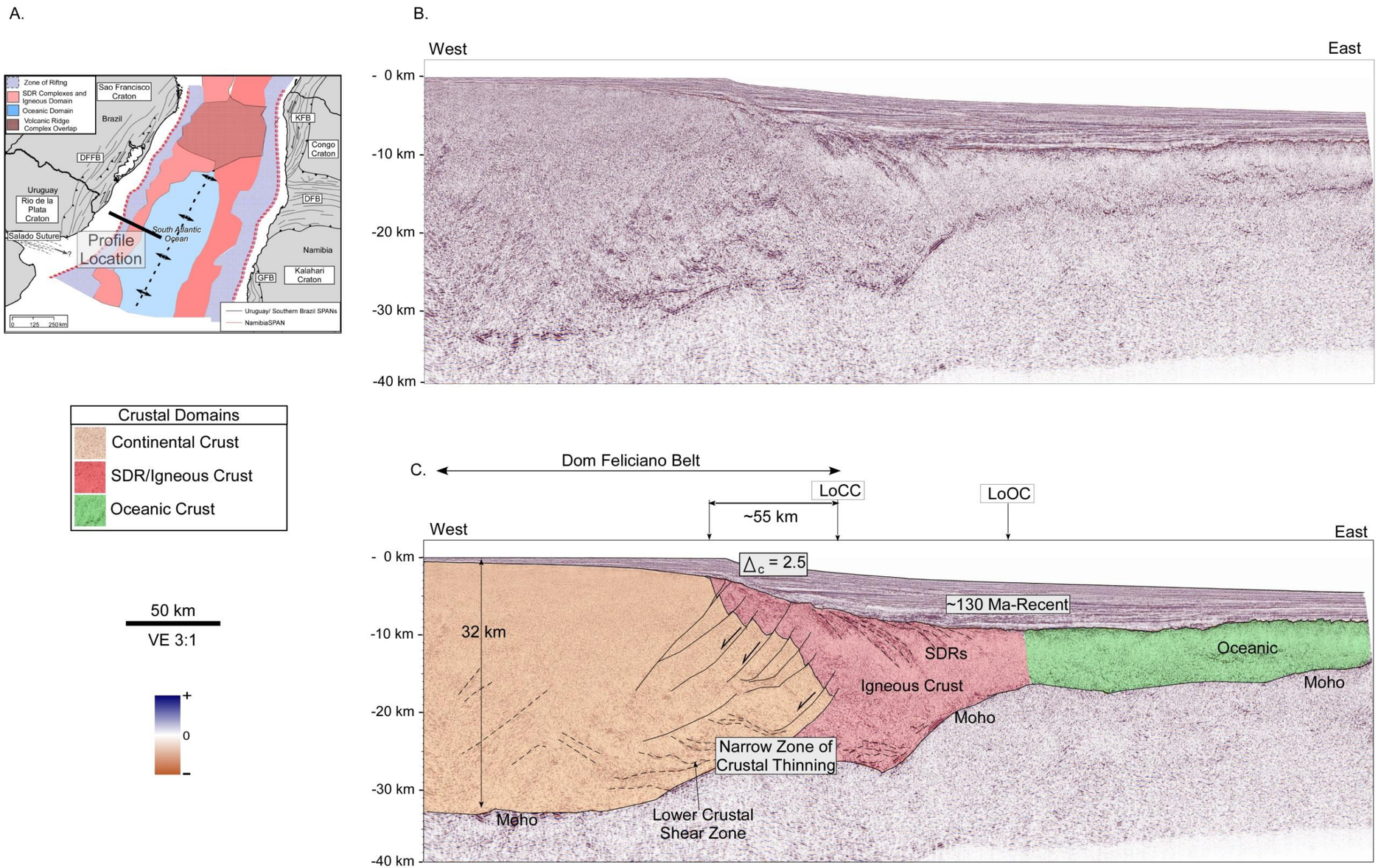

Figure 4.6: An example profile from the Pelotas Basin. A) The profile location (black line) map within the South Atlantic, GPlates reconstruction at 115 Ma. B) An un-interpreted deep record seismic line from the rift-parallel Dom Feliciano FB located in the Pelotas Basin of the offshore southern Brazil. C) An interpreted profile from Figure 4.6A illustrating the narrow zone (~55 km) of rifted continental crust within the rift-parallel fabric of the foldbelt. A crustal thinning factor (Δ_c) of 2.5 has been calculated. Oceanic domain is present to the east of the SDRs/ igneous crust.

and crustal stretching associated with the Barremian (132 Ma) rifting in the South Atlantic (Fig. 4.5C). This 185-km-wide zone of deformation and the eastern position of the SDR complexes illustrate that the rifting period delayed the onset of a volcanic ridge development at this location, whereas it less resistant zones progressed to crustal rupture with less stretching and allowed the volcanic center to propagate at a more rapid rate.

4.6.1.2 Rift-parallel, Dom Feliciano orogenic belt (Uruguay and southern Brazil)

The rift-parallel, Dom Feliciano belt intersects at the modern passive margin of Uruguay and southern Brazil along 1,200 km (Fig. 4.6A). The opening of the South Atlantic at the Dom Feliciano belt occurred by reactivation of pre-

existing planes of weakness (Tommasi and Vauchez, 2001). This narrow, 55-km-wide zone of crustal thinning represents the rapid onset of the volcanic center from which voluminous igneous material was produced for the subsequent SDR's and igneous crust (Fig. 4.6C). Apparent shear zones are present within the lower crust at the margins flank (Fig. 4.6C). The seismic data confirms that a full-thickness, 32-km-thick continental crust was present prior to extension and resulted in apparent crustal thinning factor calculations of 2.5 for this section and for the rifted Dom Feliciano belt (Fig. 4.6C).

4.6.1.3 Rift-orthogonal Damara and Gariep orogenic belts (Namibia)

A north-south, mega-regional strike, seismic reflection line along the Namibian margin illustrates zones of intra-cratonic zones of Paleozoic deformation (Fig. 4.7A, B). The Moho expression is rugose, as observed from the conjugate VPM in Uruguay (Fig. 4.7A, B), and reflects Paleozoic (2300-2050 Ma) orogenic deformation prior to Barremian (132 Ma) rifting in South Atlantic (Fig. 4.7C). The Moho geometries match seismically-bright events in the lower crust interpreted as lower crustal shear zones. Paleozoic (2300-2050 Ma) north-south shortening occurred across this domain and created the doubly-vergent thrust features as previously described (Fig. 4.3).

A brittle-ductile transition can be traced at the base of the series of interpreted folds and thrusts that bound the Damara belt to the north and south, and are similar to the geometries that have been described onshore (Gray et al., 2008) (Fig. 4.7C). The thickness of continental crust ranges from 32 km (Damara belt), 17 km in the north (Kaoko belt), and 21 km (Gariep belt) in the south. The thinned nature of the crust in the north is likely an offshore expression of the Kaoko belt, where the pre-existing orogenic fabrics of the Damara and oblique Gariep belt are more resistant to stretching, and remain thicker (Fig. 4.7C).

The pre-existing structural trends of the Gariep Belt are considered to be oblique as a result of their varied orientations with respect to the South Atlantic paleo-spreading axis (Fig. 4.3A). Their arcuate geometry indicates that most of

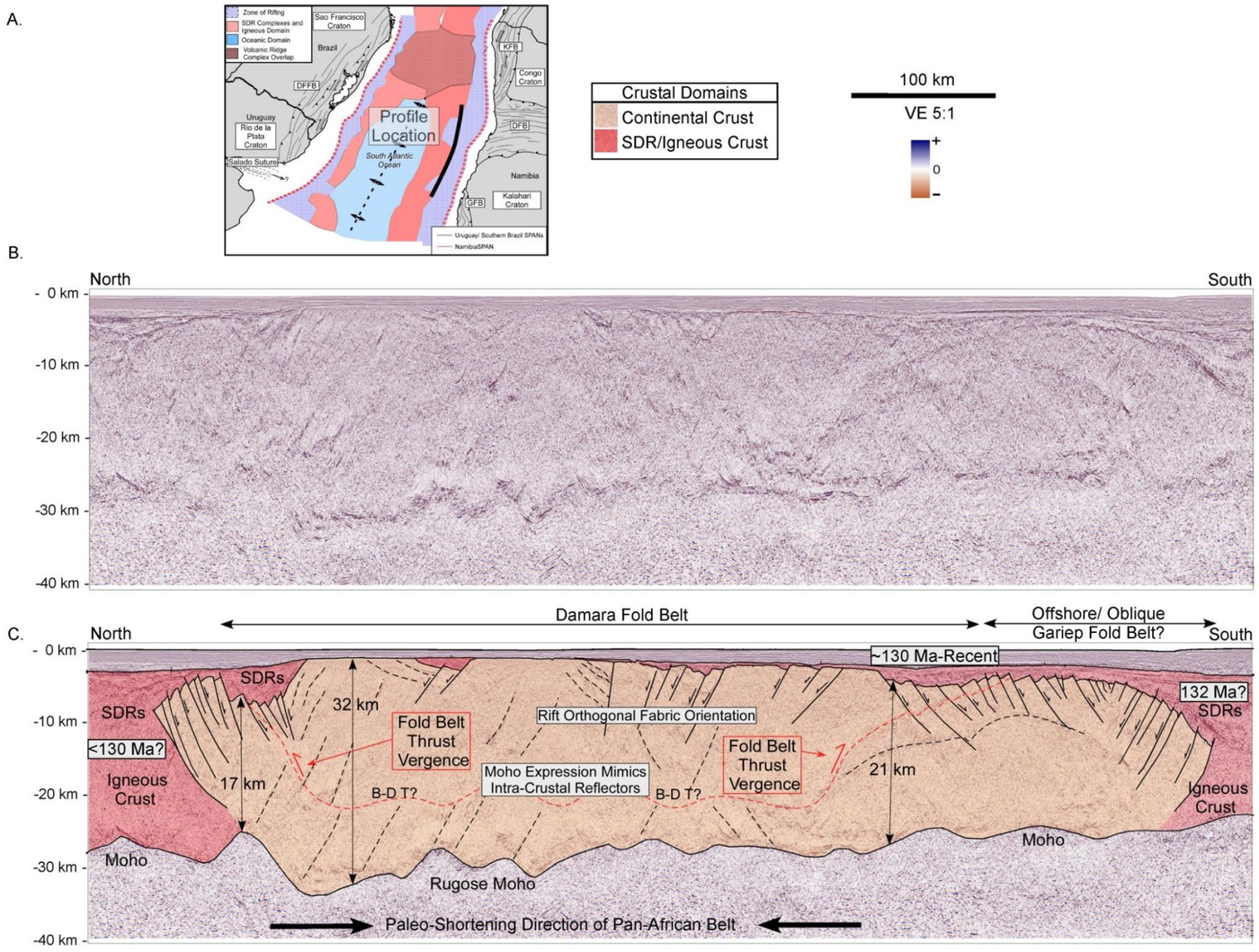

Figure 4.7: An example strike line profile from the Namibia. **A)** The profile location (black line) map within the South Atlantic, GPlates reconstruction at 115 Ma. B) An un-interpreted North-South strike-line profile from the Namibian margin, capture in the shelfal domain of the rift-orthogonal Damara and ~rift parallel/oblique Gariep FBs. C) The interpreted version of Figure 4.7A illustrates the along-strike variation of the continental crust on the margin that is bounded by zones of SDRs to the north and south. Centered within the profile is the Damara FB which remains relatively un-thinned in this position and presents a thick, ~28-30 km-thick crustal thickness. Internal seismic events suggest intense pre-rift deformation within the foldbelt. From the north, SDRs transition into the continental domain over a region of thinned continental crust with pre-existing high-angle thrust faults. Internal seismic character indicates a relationship between apparent faults within the crust and the Moho expression that is present at the base of the continental crust.

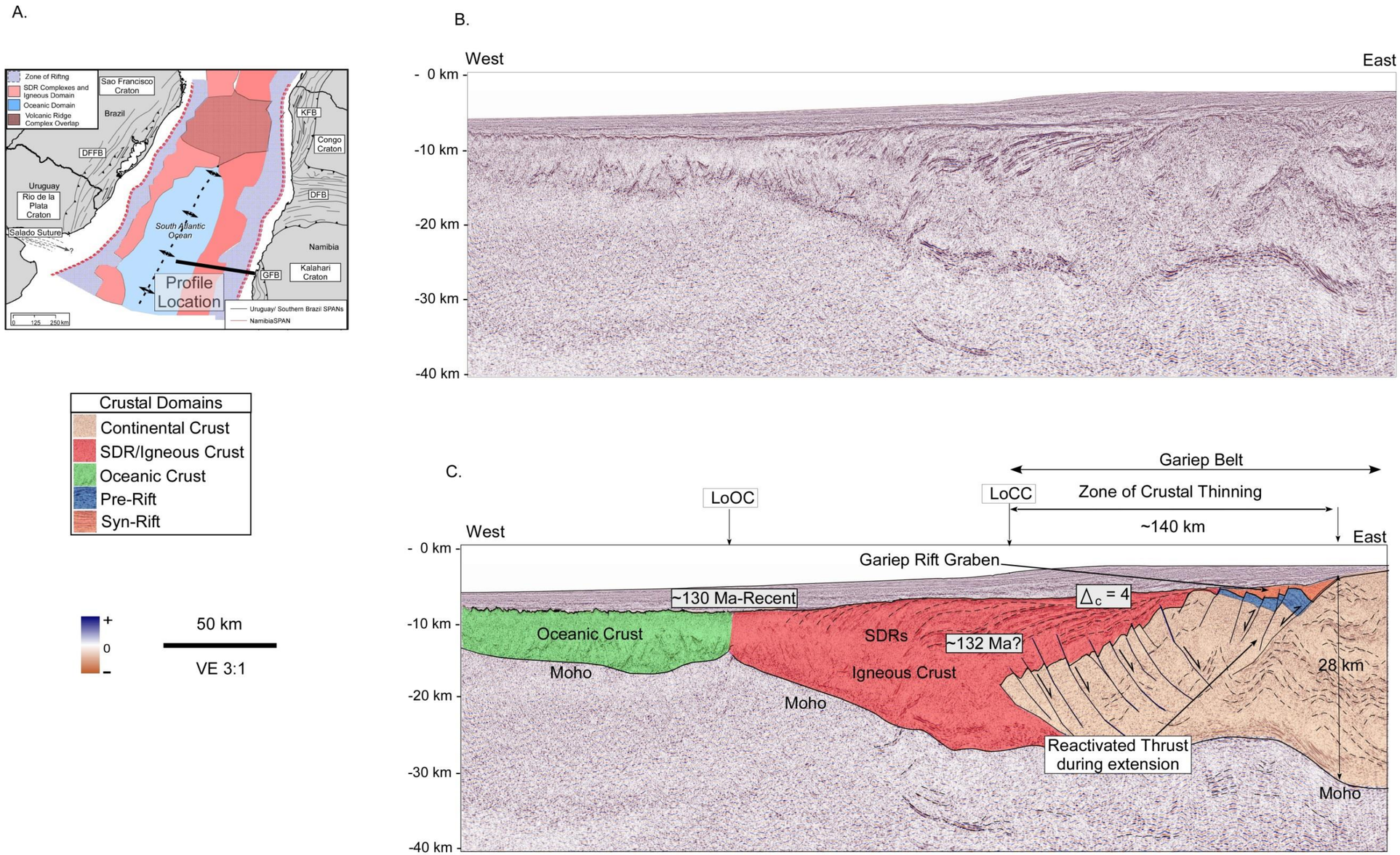

Figure 4.8: An example profile from the Gariep Basin, Namibia. A) The profile location (black line) map within the South Atlantic, GPlates reconstruction at 115 Ma. B) An un-interpreted West-East dip oriented line profile from rift-oblique oriented Gariep FB on the Namibian margin of West Africa. C) The interpreted profile shows a ~ 140 km zone of rifted continental crust from an original thickness of 28 km. A high density of internal seismic events is imaged east of the large-scale, basinward-dipping normal fault. A crustal thinning factor (Δ_c) of 4.0 has been calculated for this profile

the Gariep belt is oblique to the margin in the offshore position (Fig. 4.3A). Seismic data from the west African margin at the Gariep belt provides evidence of crustal thinning over a zone of 140 km (Fig. 4.8C).

The interpreted Moho shows a pronounced concave-down geometry directly below the basinward dipping, reactivated thrust (Fig. 4.8C). Figure 4.8C shows a zone of half-grabens west of the 28-km-thick continental crust as a response to the reversal of the westward-dipping Paleozoic thrust fault (Fig. 4.8C). This reversal is the reactivation of the nappe features that were described in Figure 4.3C, where the Gariep Units (535-545Ma) were over-thrusted onto the Kalahari Craton (Figs. 4.3C and 4.8C). Following this reversal, the landward-dipping faults were created at the volcanic spreading center at the rift axis. A thinning factor of 4 was calculated for the Gariep belt that had an initial, pre-rift crustal thickness of 28 km (Fig. 4.8C).

The rift-orthogonal E-W Damara FB has approximately 715 km of intersection with the 220-km-wide, rifted continental margin (Fig. 4.9A). Aptian (131 Ma) rifting resulted in cross-cutting of this ancient domain across a 220-wide-zone of crustal stretching, that was followed by an intense phase of magmatic activity from a volcanic spreading axis (Fig. 4.9C). The 2D seismic profile contains well-imaged intra-crustal reflections that reflect both Paleozoic deformation (505-530 Ma) and of lower crustal shear from rifting at more distal locations (Fig. 4.9C).

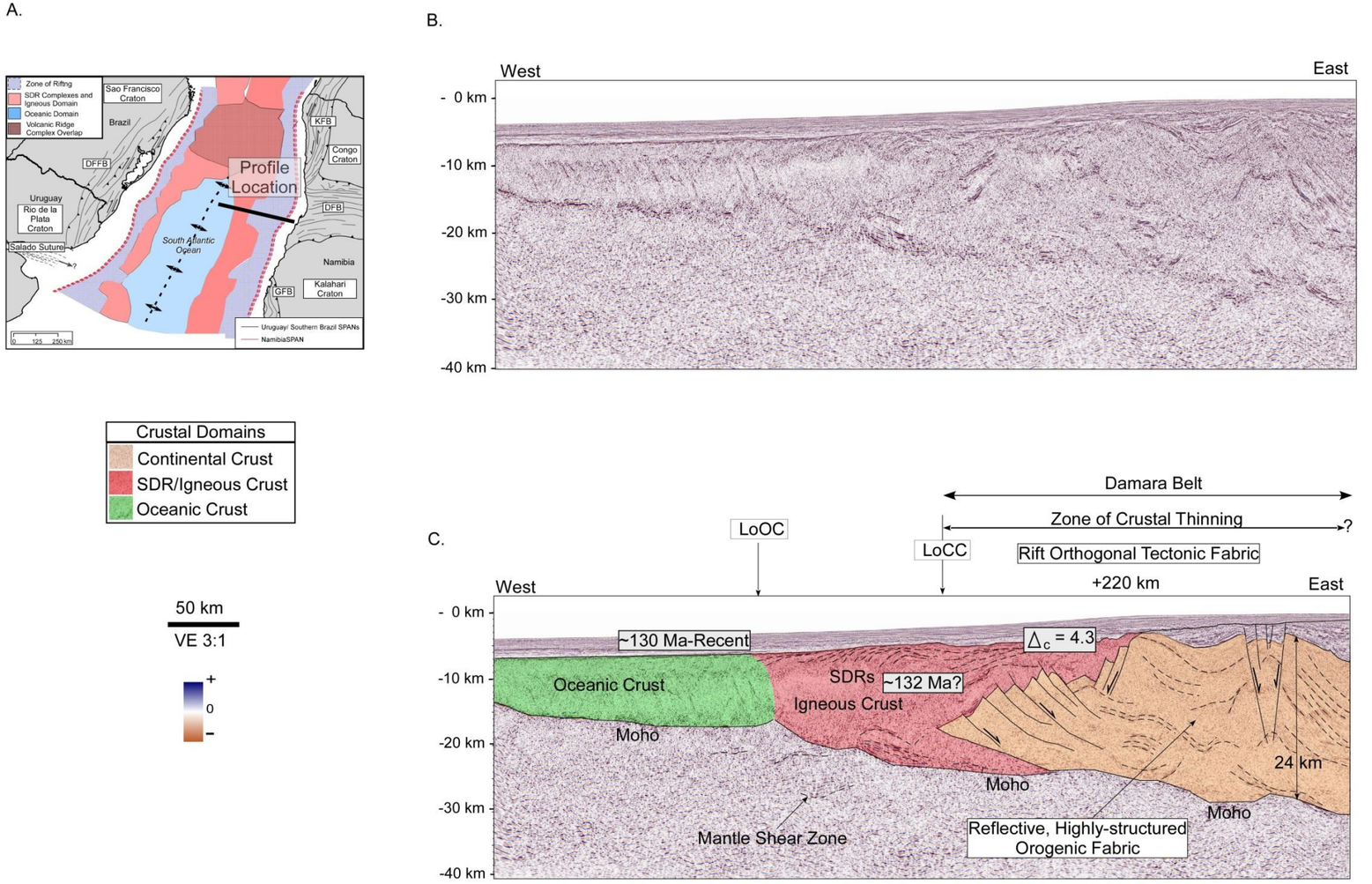

Figure 4.9: An example profile from the Luderitz Basin, Namibia. **A)** The profile location (black line) map within the South Atlantic, GPlates reconstruction at 115 Ma. B) An un-interpreted West-East dip oriented line profile from rift-orthogonal oriented Damara FB on the Namibian margin of West Africa. C) The interpreted seismic section for Figure 4.9A presenting a wide zone (~+220km) of horsts and grabens in the east within highly structured continental crust. A stretching value (Δ_c) of 4.3 was calculated for this profile. The true eastern limit of thinning is not constrained within the seismic data, where the eastern limit of this line presents thinned continental crust at ~24 km. A high-density zone of seismically-bright reflectors is present within the interpreted continental crust.

from east to west the Moho rises gradually to the oceanic domain (Fig. 4.9C). The initial thickness of continental crust in this position is 24 km; however, the true eastward extent of stretching related to the South Atlantic is not constrained from this study. Therefore, I assume that the pre-rift crustal thickness was 24 km with some amount of overlying Paleozoic cover related to the intra-cratonic deformation (Fig. 4.9C). Using 24 km as original crustal thickness results in a calculated crustal thinning factor of 4.3. Additional seismic refraction data indicates that the non-rifted orogenic collisional belt reaches a thickness of 40 km, 191 km to the east of the seismic data from the Damara FB (Baier et al., 1983). Although I am unable to constrain the true eastern extent of rifting in the foldbelt, a deeper base of crust would result in a higher crustal thinning factor for the Damara belt (Fig. 4.9C).

4.6.1.4 Rift-parallel, Kaoko orogenic belt (Namibia)

The Kaoko belt is conjugate to the Dom Feliciano belt and possesses a similar parallel and complimentary tectonic fabric (Figs. 4.3C and 4.10A). The rift-parallel orientation allowed full continental rupture and rapid development of the volcanic spreading ridge

The development of landward-dipping faults across the basinward-dipping, pre-existing fabric was likely enhanced by an elevated thermal regime from the Tristan de Cunha Plume where the thinning crust was weakened and lithospheric rupture was accelerated (Tommasi and Vauchez, 2001). Crustal

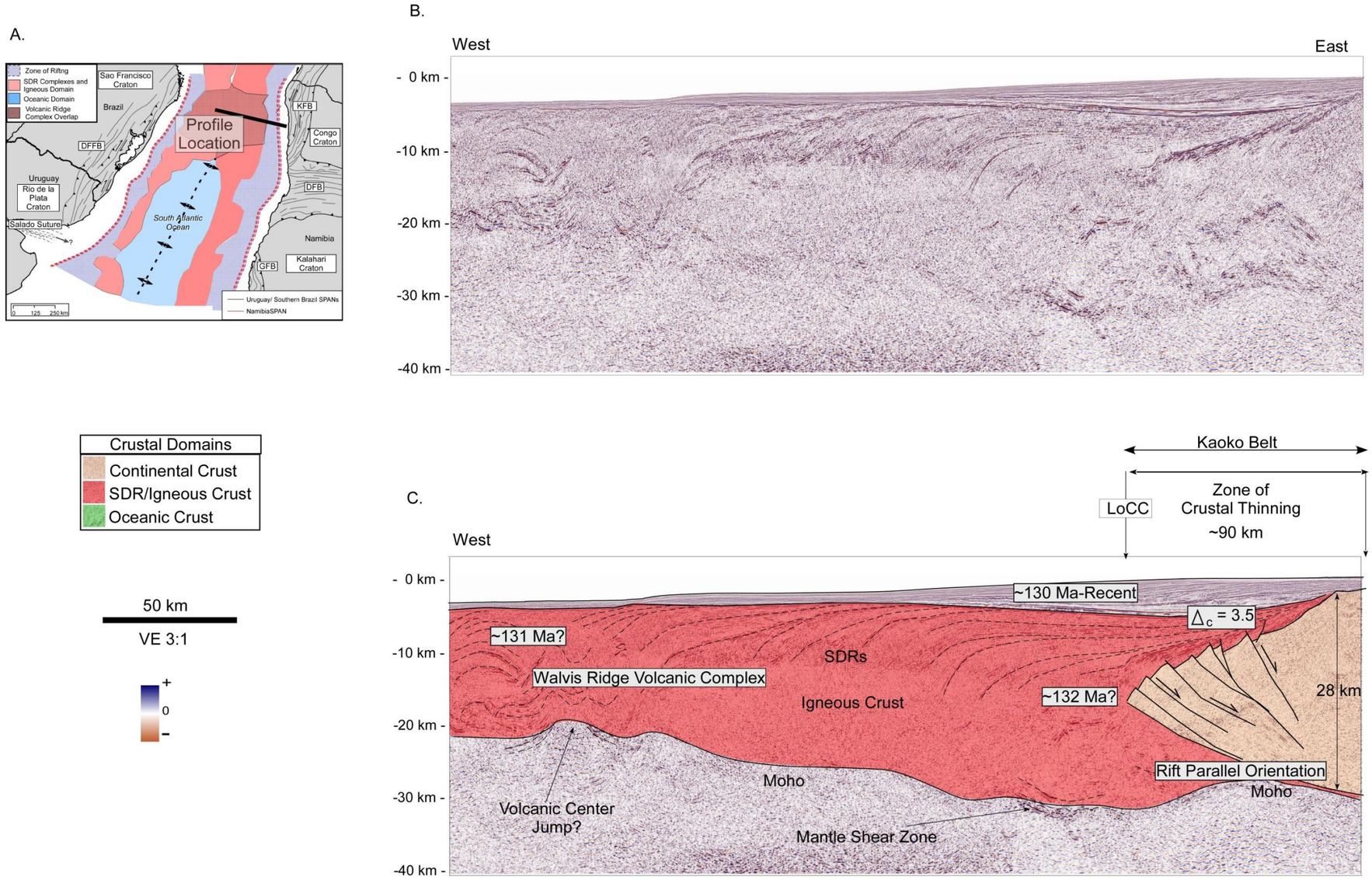

Figure 4.10: An example profile from the Kaoko Basin, Namibia. **A)**The profile location (black line) map within the South Atlantic, GPlates reconstruction at 115 Ma. B) An un-interpreted West-East dip oriented line profile from rift-parallel oriented Kaoko FB on the Namibian margin **of** West Africa. This seismic profile also contains data from the Walvis Ridge volcanic complex. C) The interpreted seismic data from Figure 10A illustrates a narrow zone (~90km) of rifted continental crust underlying the initial set of SDRs on the continental margin. A calculated thinning factor (Δ_c) of 3.5 has been determined for this profile.

stretching took place over a zone of 90 km as the pre-rift Paleozoic tectonic fabric was reactivated (Fig. 4.10C). Internal seismic facies at the LoCC is related to lower crust shear zones or a reflection of pre-existing tectonic fabric from the Paleozoic (Fig. 4.10B and 4.10C). The apparent initial crustal thickness in the continental domain is 28 km which results in a calculated thinning factor (Δ_c) of 3.5 (Fig. 4.10C).

4.7 Discussion

4.7.1 Two modes of South Atlantic rifting controlled by pre-rift orogenic grain

The south-to north-propagation of Early Cretaceous (134-130 Ma) rifts to form the proto-South Atlantic Ocean did not result in a uniformly wide zone of rifting (Fig. 4.5, 4.6,4.8-4.10, 4.11). My interpretations of the seismic lines shown in this paper indicate the rift propagation between Uruguay/Southern Brazil and Namibia occurred as two primary responses to extension: 1) the first mode was to reactivate and follow the north-south-trending, rift-parallel, orogenic fabrics to produce a more narrow (55-90 km), less extended, margin with observed thinning factors (Δ_c) in the lower range of 2.5-3.5; and 2) the second mode was to crosscut east-west-trending, rift-orthogonal or oblique orogenic fabrics to produce a wider, more extended, margin with observed thinning factors (Δ_c) in the higher range of 4.3-5 (Figs. 4.5-4.6, 4.8-4.10).

4.7.1.1 Simple shear vs. pure shear models for VPM's

Geoffroy et al. (2015) concluded from their study of South Atlantic VPM's that these margins are the result of symmetrical, pure shear deformation (i.e., lacking upper and lower plates). Here I support the findings of Geoffroy et al. (2015) where their work concluded that continental breakup at volcanic passive margins are predominantly the result of pure-shear style extension at the rift axis. My observations of the seismic data show a lack of evidence to suggest large scale asymmetries that would be the result of simple-shear rifting of the continental margin. My calculated crustal thinning factors indicate that onshore, structural anisotropies from the pre-existing zones of weakness are first-order controls for the margin's structural inheritance.

Seismic data illustrate that pre-rift configurations of the South American and West African tectonic plates would likely reveal near full-thickness continental crust (~32 km) - with some variability (Fig. 4.4C and 4.7C). A simple thinning factor (Δ_c) calculation is used here to quantify the magnitudes of rifting along-strike at the various tectonic domains (Fig. 4.11A). The quantification of crustal stretching permits the comparison of the thinning factors (Δ_c) from the belts that flank the rift margins (McKenzie, 1978).

4.7.1.2 Crustal fabric controls on wide versus narrow rifted margins

The Aptian (120 Ma) Gondwanan reconstruction shows the along-strike conjugate relationships and spatial distribution of the pre-rift orogenic belts (Fig.

4.11B). I have developed three cross-sectional profiles that illustrate the conjugate relationships between continental rift zones, thinning factors, and associated tectonic trends along the rift flank (Fig. 4.11C). Conjugate, rift-parallel orogenic fabrics from the north-south-trending Dom Feliciano and Kaoko belts have relatively low thinning values of 2.5 and 3.5, respectively (Fig. 4.11C - Profile 1). These conjugate margin profiles are narrow and likely exhibit similar strain rates and thermal regimes (Davison, 1997) (Fig. 4.11C Profile 1).

The seismic examples shown in Figures 4.6 and 4.10 illustrate the narrow zone of crustal thinning that shows an abrupt transition to the SDRs and igneous crust. This abrupt transition may indicate a faster spreading rate during breakup at these areas. The abrupt failure of continental lithosphere is reasonable as the addition of new magmatic material can be considered the substitute for stretching (I. Davison, pers. comm., 2016).

The rifted Dom Feliciano belt maintains a similar thinning factor (Δ_c) of 2.5 and a narrow zone of extension (55 km), which is in contrast to the higher factor of 4.3 from the wide zone of rifting (220+ km) on the Damara belt (Fig. 4.11C, Profile 2). The north-south and east-west opposing orientations of tectonic fabrics suggest that the rift axis bisected the two structural domains, and that the observed structural inheritance is highly asymmetric (Fig. 4.11C, Profile 2). Finally, the conjugate margins of Punta del Este and the Orange Basins show a middle-member scenario as the rifting of the E-W Salado Suture fabric resulted

Figure 4.11: Thinning factor overview and South Atlantic profile cartoons
A) A schematic representation of the varying thinning factor values and margins width results. From original crustal thicknesses, low thinning factor (Δ_c) values will result in narrow continental rift zones, while high thinning factor (Δ_c) values will result in wide continental rift zones (Modified from Kusznir and Park (1987).
B) A Western Gondwana reconstruction highlighting the regional Brasiliano-Pan-African mobile foldbelts and sutures within the area of investigation
C)
Profile 1) Transect A-A' illustrates the predicted relationship of a pre-lithospheric breakup between the Dom Feliciano and Kaoko FBs where the bisection of the pre-existing structural fabric is occurring and results in conjugate low thinning factor (Δ_c) values This type of rifting between two rift-parallel tectonic domains results in conjugate, narrow zones of deformation on each margin.
Profile 2) Transect B-B' illustrates the predicted relationship of the pre-lithospheric break-up between the rift-parallel and rift-orthogonal foldbelts of the South American, Dom Feliciano FB and the West African, Damara FB. The Dom Feliciano FB experienced a brief period of rifting and resulting in a low thinning factor value of 2.5. In contrast, the rift-orthogonal Damara FB experienced a longer, more resistant-to-rupture rifting episode and resulted in a thinning factor (Δ_c) value of 4.3
Profile 3) Transect C-C' illustrates the predicted geometry of the pre-lithospheric break up between the South American region of the Salado Suture and the Namibian Gariep FB. The continental thinning of the rift-orthogonal Salado suture resulted in a wide zone of thinned and structured crust and a high thinning factor value of 5. The geometry and arcuate orientation to the rift axis of the Gariep FB provided for a resulting factor (Δ_c) value of 4 and a moderately narrow margin.

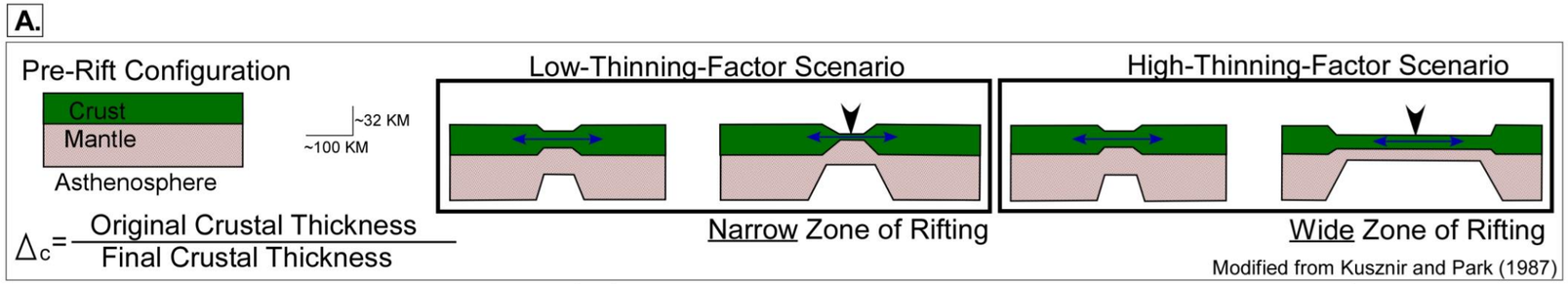

$$\Delta_c = \frac{\text{Original Crustal Thickness}}{\text{Final Crustal Thickness}}$$

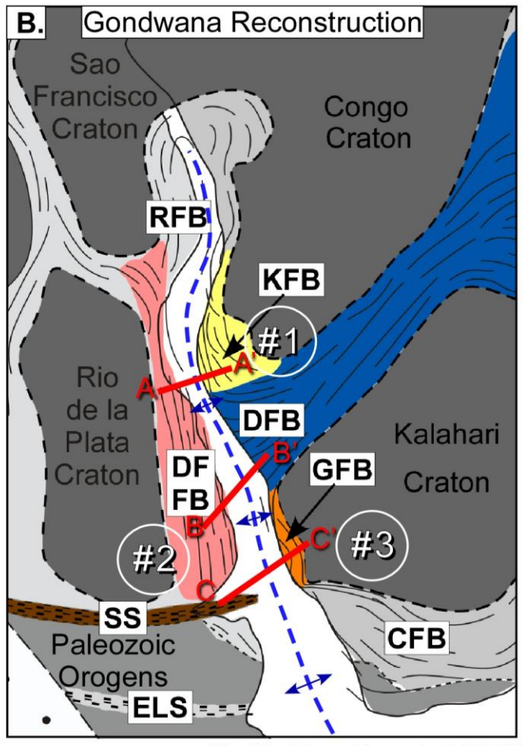

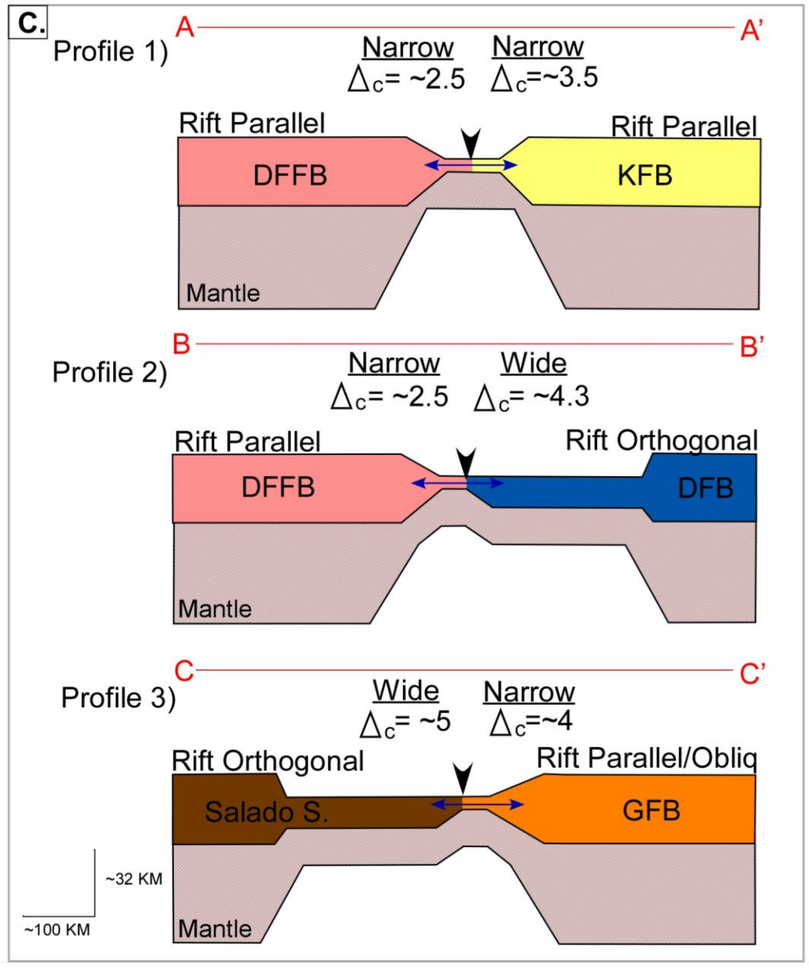

in a wide margin profile and the obliquely oriented Gariep belt shows thinning between the two extremes presented here (Fig. 4.11C, Profile 3).

4.7.1.3 Comparing zones of stretched crust along the South America VPM's

The Albian (115 Ma) plate reconstruction by Seton et al. (2012) (Fig. 4.12) illustrates the spatial relationships between the various crustal domains: 1) continental crust – rifted and un-deformed; 2) SDRs/igneous crust; and 3) oceanic crust. By 115 Ma (Albian), large-scale, the absence of rift--related faults in the SDR complexes indicates that continental stretching would have ceased. At this time SDRs and the transition domain of igneous crust were emplaced, and divergence continued at the mid-ocean spreading ridge (Rabinowitz and LaBrecque 1979; Austin and Uchupi 1982; Nürnberg and Müller 1991; Chang et al. 1992; Gladczenko et al., 1997; Blaich et al., 2011; Blaich et al., 2013) (Fig. 12).

On the South American Margin, two pre-existing fabrics imposed structural inheritance on the geometry and most likely the style and rate of extension: 1) the N-S Dom Feliciano orogenic belt; and 2) the east-west-trending Salado Suture (Dunbar and Sawyer, 1989; Kusznir and Park, 1987; Davison, 1987; Blaich et al., 2009) (Fig. 4.2A, B). The map in Figure 4.12 provides support for the strong influence of the rift-parallel, north-south-trending

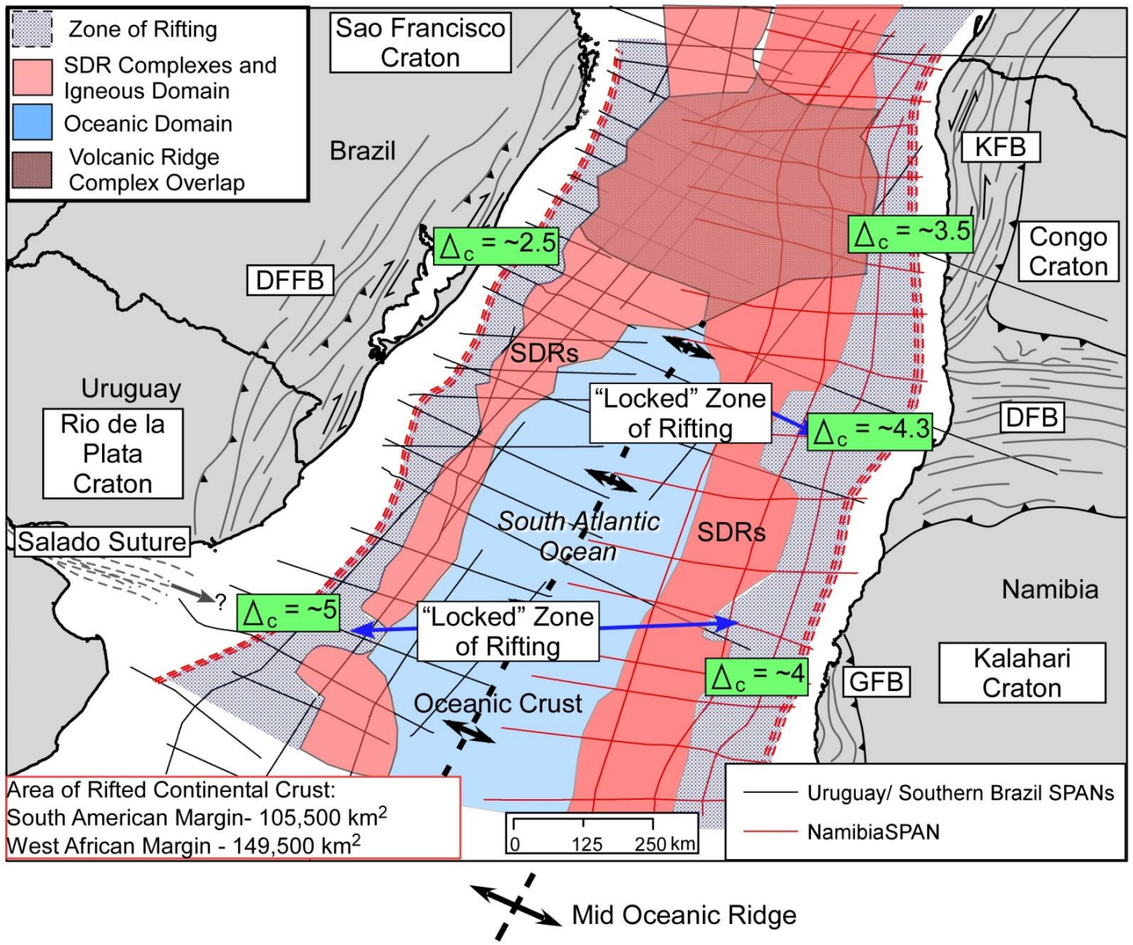

Figure 4.12: 115 Ma Tectonic Reconstruction
Aptian (115 MA) reconstruction of the South Atlantic (Seton et al., 2012) showing locations and structural trends of onshore tectonic domains as they relate to the rifted passive margins of the South Atlantic. The gray, stippled region illustrates the mapped zone of interpreted zone of rifted continental crust that is present between full thickness (~28-32 km) continental crust and the igneous domain and oceanic crust. Specifically the offshore regions of the Damara FB and the Salado Suture exhibit wide zones of continental thinning, with high thinning factors (Δ_c). Regions of narrow continental thinning are associated with zones of low thinning factor values from exploitation of pre-existing rift-parallel fabrics.

Dom Feliciano belt on the smaller amount of continental rifting that produced a relatively, narrow margin (55 km).

The north-south-trending, strike-parallel Dom Feliciano belt an average thinning factor (Δ_c) of 2.5 to the west of the igneous crustal domain (Fig. 4.12). North of the east-west-trending, rift-orthogonal Salado suture, the zone of SDR's maintains a constant width of 100-125 km, - but increases significantly in width to the north and towards the Rio Grande Rise (Fig. 4.12).

South of the Dom Feliciano belt, the rifted Salado Suture exhibits a 185-km-wide zone of extension with an average thinning factor of 5 with a margin width of approximately 165 km (Fig. 4.12). This area appears to behave as a "locked zone of rifting," where the lithosphere has resisted rupture it the form of horsts and grabens as described in Figures 4.5 and 4.12 (Courtillot, 1982). The concept of locked zones was introduced by Courtillot (1982) and described as zones that continued to rift while oceanic crust (in this case SDRs) developed at the rift tip. This increased resistance to rupture was the result of extension across the E-W rift-orthogonal suture zone tectonic fabric, and thus a wide margin scenario (Kusznir and Park, 1987; Davison, 1987).

The Namibian margin has three major orogenic belts that were all affected by the South Atlantic rifting phase: 1) rift-oblique Gariep belt; 2) east-west-trending Damara belt; and 3) Kaoko belt (Fig. 4.12). They variations in styles and rates of extension were likely controlled by the structural anisotropies

within the various, orogenic belts (Dunbar and Sawyer, 1989; Kusznir and Park, 1987; Davison, 1987; Blaich et al., 2009).

Published references on the structural orientation of the Gariep belt indicate an arcuate trend with respect to the margin; and therefore was more oblique to the trends of the paleo-rift axis of the South Atlantic (Coward 1981; Coward, 1983; Hoffman et al., 1994; Frimmel and Frank, 1998). The Gariep belt has an approximate 220 km of intersection area of its margin with the Atlantic rift (Fig. 4.2A, B). This orientation resulted in the extensional stresses being applied across oblique fabrics within the Gariep belt with a moderately-wide zone of rifting and a thinning factor of 4 (Fig. 4.12).

Between the conjugate margins in this area, I see two zones that appeared to have been "locked" across the rift axis (Fig. 4.12). This may have been the result of a change in orientation from the east-west-trending Damara belt to the north from the structural fabric of the obliquely-trending Gariep belt in the south (Fig. 4.12). No data is present to constrain their actual boundaries in the offshore region; however the Damara belt has been estimated to flank the margin for approximately 715 km (Gray et al, 2008).

Thinning factor values for the east-west-trending, rift-orthogonal Damara belt average 4.3 for the area where the trend appears to be perpendicular to the paleo-rift axis of the South Atlantic and responsible for producing the wide-margin configuration (Fig. 4.12). Similar to the east-west-trending Salado suture,

the extensional stresses across the pre-existing structural fabric created the resistance to full continental rupture and therefore have resulted in a wide zone of horsts and grabens.

The coastal branch of the east-west-trending Damara belt appears to turn obliquely at the margin (Gray et al., 2008) and therefore exhibits a lower thinning factor than the core region. This region was also likely a “locked” zone of rifting (Courtillot, 1982) during extension and is strongly asymmetric to the conjugate zone of rift at the Dom Feliciano belt (Fig. 4.12). These opposing asymmetries support the interpretation that the rift axis bisected the opposing tectonic fabrics and thereby influenced the structural inheritance and style and rate of extension between the two plates (Fig. 4.12). Continuing northward, the narrow margin along the Kaoko belt has an average thinning factor of 3.5 and decreases to the north towards the Walvis Ridge along its 450 km long zone of intersection with the rifted margin.

4.7.1.4 Comparison of this study to previous concept of “locked zones” along propagating rifts

Previous work by Courtillot (1982) attempted to conceptually explain along strike-variations in a propagating rift by invoking the idea of a “locked zones” produced by thicker crustal areas envisioned as zones of thickened, plate overlap in a closed-fit, plate reconstruction (Fig. 4.13A). Courtillot (1982) did not elaborate on why the plates would overlap to form the locked zones

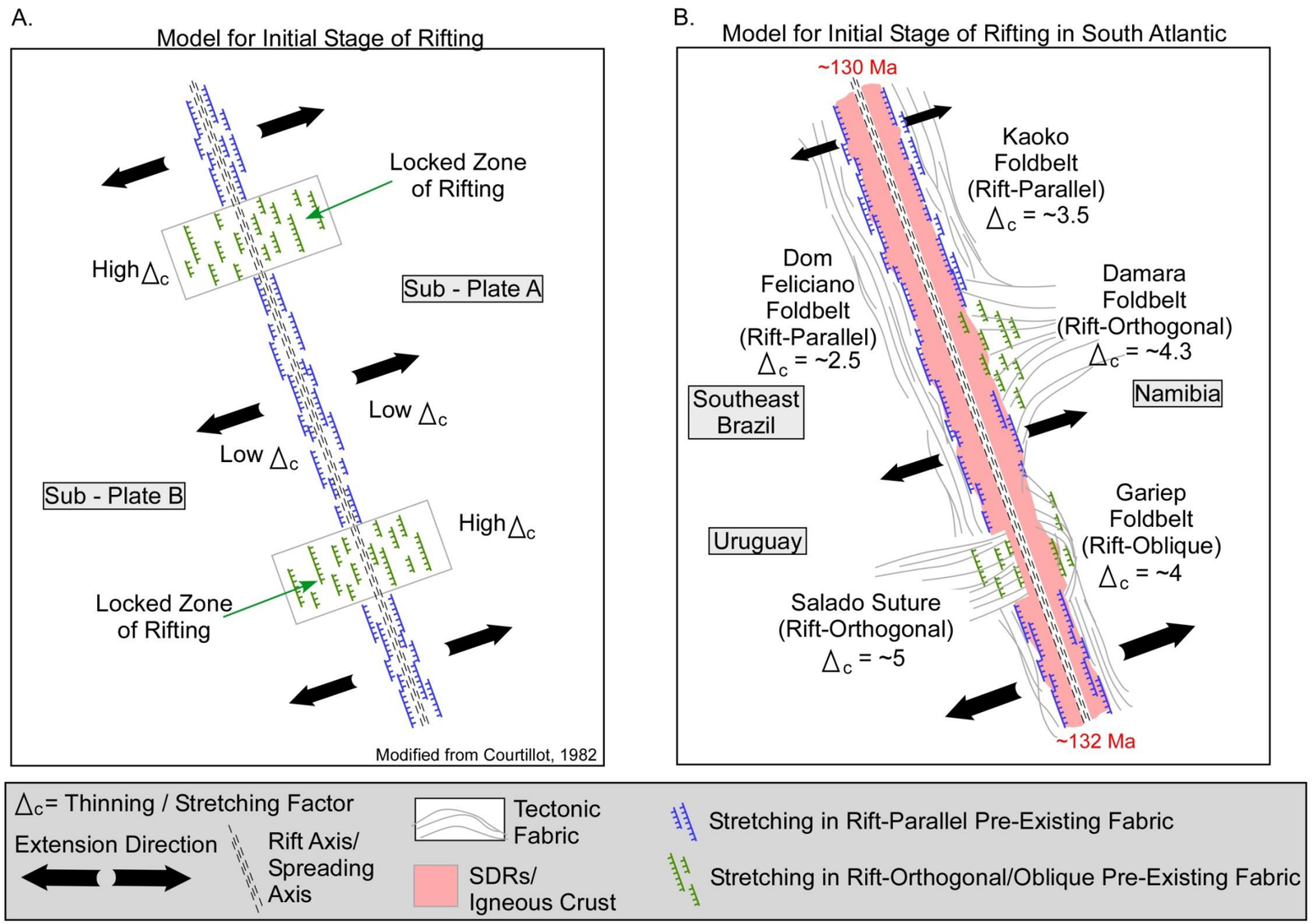

Figure 4.13: A comparative stretching model with locked zones ad this study's thinning factors**. A)** A modified schematic model from Courtillot (1982) illustrating along strike zone of locked continental extension between two plates. B) A schematic model derived from the observations in this study where I observe wide and narrow zones of rifted that would have been similar to Courtillot's findings. I observe varying thinning factor (Δ_c) values, where large values are present at orogenic trends with an angular relationship to the rift axis (Salado Suture and Damara FB) and lower values at parallel orientations (Dom Feliciano and Kaoko FBs). Generalized pre-existing structural fabric is traced along the margins (gray lines).

along the trend of the rift - but my model would predict the locked zones would correspond to areas of orogenic basement fabric that are orthogonal to the direction of rift propagation and act as wider, “locked zones” of stronger crust that requires greater amounts of extension to rupture (Fig. 4.13B).

4.7.2 Global compilation of data to test the link between orientation of orogenic basement fabric and amount of rift stretching

4.7.2.1 Case of low-stretch rifts along parallel, basement trends

Previous workers have noted that a major rift system that is likely to propagate in the direction of pre-existing zones of weakness. This occurs in regions of anisotropy along older, stable orogenic belts like the Appalachians (Fig. 4.14A), the Hercynian belt and Caledonides (Fig. 4.14B), and orogenic belts previously described in the South Atlantic region (Tommasi and Vauchez, 2001) (Fig. 4.14C). This observation implies that the direction of rift development is not random, but instead can be predicted based on the regional, extension direction, the trends of mapped, orogenic basement fabrics, and the locations of major plume heads that thermally weaken the crust and focus extension (Tommasi and Vauchez, 2001). In the Appalachian and Variscan case, rifting is parallel to orogenic grains and exhibit low thinning factors (Table 4.2). In the areas on the maps in Figure 4.14 where orogenic basement trend was orthogonal to rifting, the rift ultimately failed in higher thinning factor settings

Location	Thinning Factor Min	Thinning Factor Max	Orientation to Rift (degrees)	Margin Type	Source
North Sea basin - Central Graben	1.55	1.9	10	Non Volcanic	Kuznir and Park, 1987
North Sea basin - Flanks	1.2	1.3	5	Non Volcanic	Kuznir and Park, 1987
Wessex Basin	1.1	1.25	10	Non Volcanic	Kuznir and Park, 1987
Bass Basin	1.25	1.5	20	Non Volcanic	Kuznir and Park, 1987
Gippsland Basin, S Australia (Tasman Units)	-	1.8	10	Non Volcanic	Kuznir and Park, 1987
Labrador Margin	5	7.5	80	Non Volcanic	Reston, 2009
Ligurian Sea	3.6	5.3	65	Non Volcanic	Reston, 2009
Galicia Bank West	5	6	75	Non Volcanic	Reston, 2009
S Newf Basin (avalon uplift)	4	5	90	Non Volcanic	Reston, 2009
Rio Muni (Eq Guinea)	-	4	20	Non Volcanic	Reston, 2009
Ross Sea- Central Trough	-	4	65	Non Volcanic	Trey et al., 1999
Lake Baikal (*Baikal Rift Zone)	-	1.7	5	Non Volcanic	Thybo and Nielsen, 2009
Guinea Plateau(Baraka Fault)	-	1.39		Non Volcanic	Edge 2015
Galicia Bank (Easternmost CC)	-	4.3	5	Non Volcanic	Whitmarsh et al., 1996
ERAS Western Branch- Lake Malawi	1.2	1.3	5	Non Volcanic	Morley et al., 1999
Otway basin	-	6	80	Non Volcanic	Ball et al., 2013
Bight Basin	-	8	85	Non Volcanic	Ball et al., 2013
Porcupine Basin	5	6	75	Non Volcanic	Welford et al. 2012
Laptev Sea (Taimyr Foldbelt)	-	6	85	Non Volcanic	Mazur et al., 2015
Lusitanian Basin (West Iberia)	1.5	2	25	Non Volcanic	Teixeira et al., 2012
Paris Basin	-	1.3	5	Non Volcanic	Brunet and Pichon 1992
Congo	-	1.3	10	Non Volcanic	Karner et al. 1997
Red Sea (at Aden)		4	85	Volcanic	Bosworth, 2015
WGreenland	-	3.5	40	Volcanic	Reston, 2009
Rockall	-	3	40	Volcanic	Reston, 2009
Goban Spur	-	4.3	90	Volcanic	Reston, 2009
Porcupine Median Ridge	-	6	60	Volcanic	O'Sullivan et al., 2010
Nova Scotia	1.7	2	5	Volcanic	Luheshi et al., 2012
Blake Plateau	-	3	30	Volcanic	Pindell, 1985
Northern Kenya Rift turkana	-	4	40	Volcanic	Morley et al., 1999
Oslo Graben	-	2.3	15	Volcanic	Stratfor and Thybo, 2011
Morroco (Coastal Meseta)	-	1.4	15	Volcanic	Le Roy et al., 1997
Campos basin (Avg of 3 Zones)	-	1.4	20	Volcanic	Muniz and Bosence, 2016
Santos Basin, Brazil	2.7	4.6	20	Volcanic	Jensen and Teasdale, 2010
US East Coast Avg	1.3	2.6	15	Volcanic	Wyers and Watts, 2006
Pelotas Basin -Dom Feliciano Foldbelt	-	2.5	10	Volcanic	(This Study)
Punta del Este Basin -Salado Suture	-	5	80	Volcanic	(This Study)
Orange Basin -Gariep Fold Belt	-	4	30	Volcanic	(This Study)
Luderitz Basin -Damara Foldbelt	-	4.3	85	Volcanic	(This Study)
Walvis Basin -Kaoko Fold Belt	-	3.5	20	Volcanic	(This Study)

Table 4.2: Worldwide compilation of thinning factors from published literature.

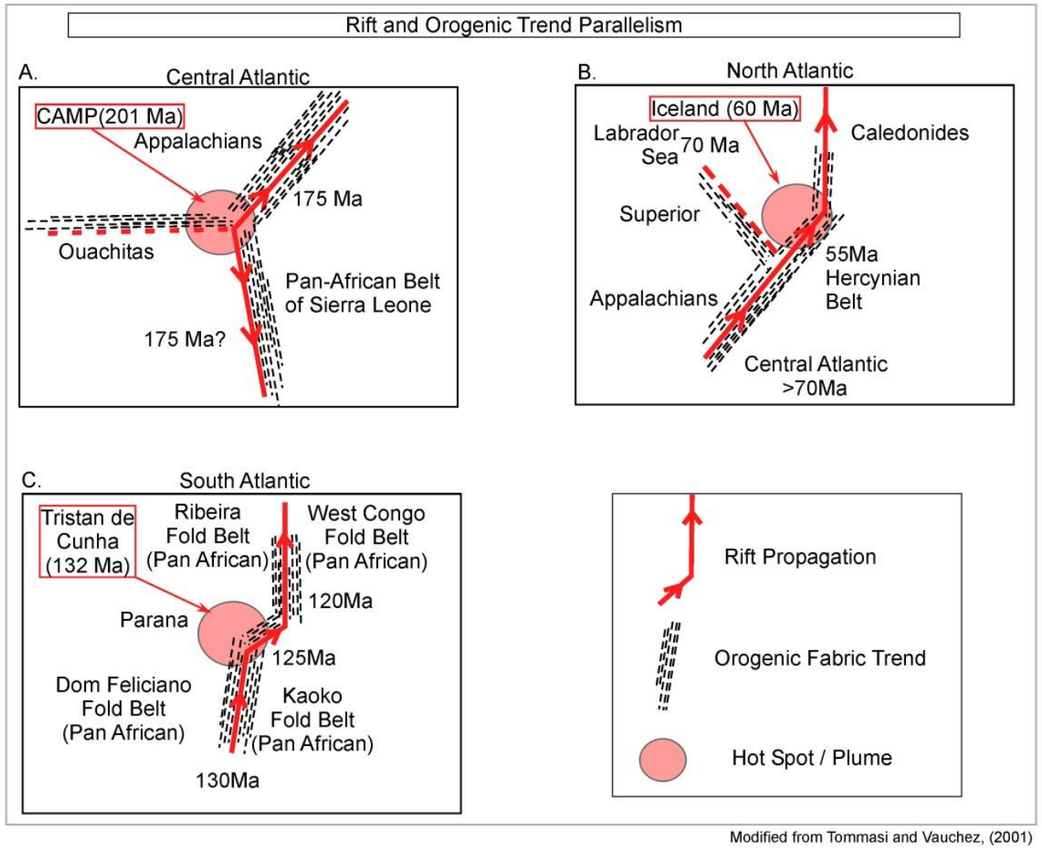

Figure 4.14: Rift and orogenic trend parallelism. Figures A-C represent modified schematic examples (Tommasi and Vauchez, 2001) of rift and orogenic trend parallelism at major continental rifting events of the Central Atlantic, Northern Atlantic, and the Southern Atlantic.

- **A)** A schematic representation of the Central Atlantic Magmatic Province (CAMP) illustrating the preferential rift propagation along rift-parallel structural fabrics of the Pan-African Belts to the south away from the magmatic source and to the north along the Appalachian structural fabric. Rift propagation occurs by reactivation of structural fabrics within the zone of rifting, radiating from the magmatic center.
- **B)** A schematic representation of northward rift propagation along the Hercynian Belts and the Appalachians in the south and bisecting the Caledonides to the north of the Icelandic Hotspot. Rift propagation occurs by exploitation of rift-parallel fabrics within the zone of rifting, initiated from the south to the north radiating from the magmatic center.
- **C)** A schematic representation of a northward rift propagation along rift-parallel orogenic trends and foldbelts from the South American Dom Feliciano FB and the Kaoko FB to the Ribeira FB. Rift propagation occurs by reactivation of structural fabrics in the zone of rifting, initiated from the south to the north through the magmatic center of the Tristan de Cunha Plume.

(Table 4.2) - as in the case of the areas of the Ouachitas in the southern USA (Fig. 4.14A) and the Labrador Sea in eastern Canada (Fig. 4.14B).

4.7.2.2 Cases of high-stretch rifts crossing orthogonal or oblique basement trends

Two other examples of high-stretch rifts attempting to crosscut orogenic fabric include the Rhine Graben of the northern Europe (Fig. 4.15A) and the Rukwa shear zone of the East African Rift System (EARS) (Fig. 4.15B). The east-west-trending, structural trends of the Upper Main Rhine High and the Northern Black Forest High are oriented at 45° to the current direction of extension. Because these basement trends are more resistant to stretching they have localized higher strain rates than observed in the areas that are oriented parallel to the structural fabric (Bhen et al., 2002). The northwest-trending Rukwa shear zone is also oblique to the current extensional direction (~50°). This section of the East African rift system and has developed more extensive, higher thinning factors, extensional fabrics (Rosendahl, 1987) (Fig. 4.15B).

4.7.2.3 Comparison of rifting processes in the North, Central and South Atlantic

Recent work by Chenin et al., (2015) discusses the impact of structural inheritance of the Caledonian and other orogenic fabrics on the opening of the North and Central Atlantic Ocean (Fig. 4.14A, B). Chenin et al. (2015) proposed that magma-rich VPM's of the North Atlantic were a consequence of reactivation

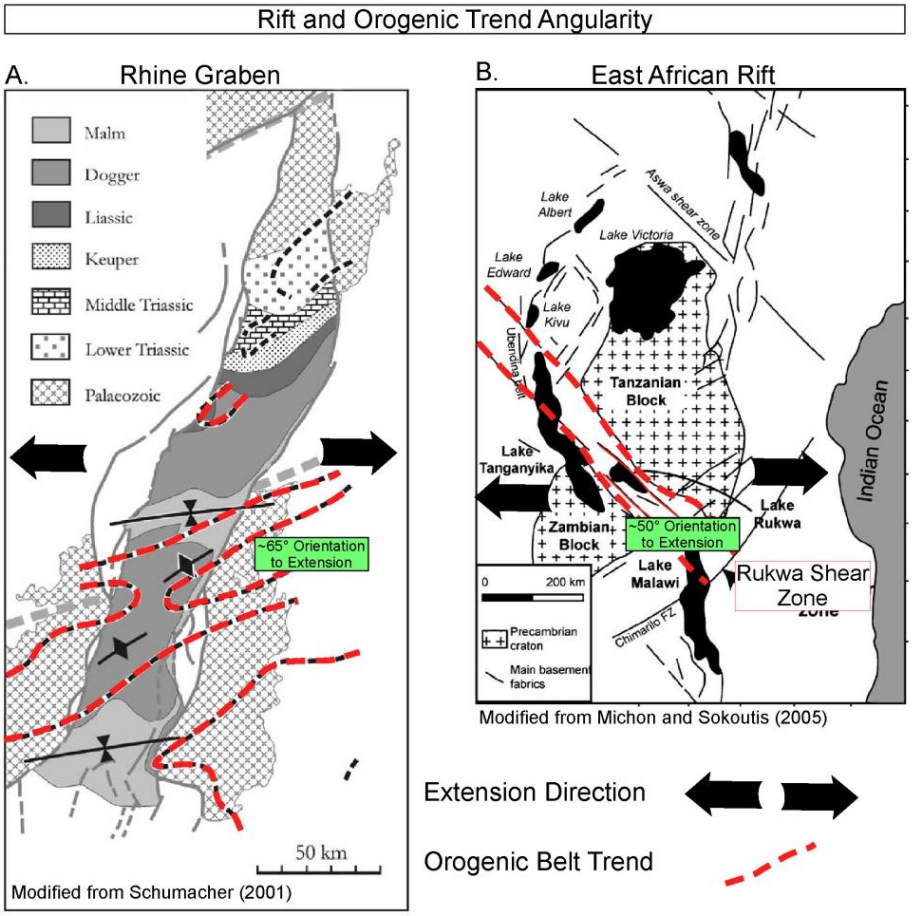

Figure 4.15: Rift and orogenic trend angularity to the rift axis. Foldbelts oriented at angles to the extensional directional inhibit continental rupture in contrast to rift parallel orogenic fabrics.

A) E-W Extension within the Rhine Graben region is present at a near-orthogonal relationship to pre-existing lithospheric fabrics resulting higher Beta where the material is resistant to continental rupture, and produces a wide zone of present day deformation.

B) E-W extension across the obliquely oriented Rukwa shear zone have resulted in a resistance of continental thinning and a wider zone of grabens and depositional basin deepening.

of the Caledonian rift-parallel, orogenic trends and that magma-poor rifting was the result of the rift crosscutting the fabric of the Variscan orogenic tectonic belt. They also propose that the North Atlantic VPM resulted from a long duration extensional event (60 Ma) while the non-volcanic margins of the Central Atlantic resulted from a shorter-lived, extensional event. Chenin et al. (2015) do not comment on Beta Factors as influenced by structural inheritance, but a few elements are in contrast from the investigation presented in this South Atlantic study. These differences are likely to have a significant impact on the correlation between the investigation performed here and the work performed by Chenin et al. (2015).

The definition for necking and final lithospheric breakup at a magma-rich margin is dependent upon the model used to determine crustal limits. The distal extent to which continental domain is interpreted in an VPM will influence the characterization of a short or long lived extensional event. Also, the ages of these orogenic trends are substantially younger than the ages of the tectonic belts investigated in the South Atlantic (~600 Ma). The Caledonian Orogeny was active as early as 290 Ma and the Variscan as early as 280 Ma (Chenin et al., 2015). As Tommasi and Vauchez indicated, the age of the orogenic trend with respect to the age of rifting might have an influence on final structural inheritance. The relative age of deformation will dictate important factors such as the state of isostatic equilibrium, amount of erosion of the topography, and potential erosion of the orogenic root (Tommasi and Vauchez, 2001). Rifting of

a younger tectonic structural trend might have significantly dissimilar results compared to the same processes occurring on a tectonic trend with twice the age of deformation.

4.7.2.4 Worldwide comparison of rift stretching factors to the orientation of basement fabric

A table of compiled crustal thinning factors from rifts along volcanic and non-volcanic margins shows a direct relationship between the orientation of orogenic fabric to the rift axis and the amount of crustal stretching (Table 4.2). For the South Atlantic VPM's, my estimation of thinning factors (Δ_c) is based on the identification and assignment of the exact limits of un-thinned continental crust, thinned, continental crust, igneous crust and SDR's, and oceanic crust. Deep-penetration seismic images described in this paper provided a uniform basis for my measurements especially the definition of the LoCC (Figs. 4.5, 4.6, 4.8-4.10, 4.12) .

My compilation in Table 4.2 shows that more stretching (higher thinning factors in the range of 4.5-8) is required to rift continental crust in regions where the trend of the rift is orthogonal to the orogenic grain because this this crust is more resistant to breakup and requires more extension to rift apart. Less stretching (lower thinning factors (Δ_c) in the range of 1.3-3.5) is required to rift continental crust where the trend of the rift is parallel to orogenic grain because this crust is weaker and requires less extension to rift part. These two end

members also are reflected in the width of the extended zone: in the case of a low thinning factor.

Figure 4.16 illustrates the results from a distribution plot of Table 4.2, where crustal stretching factors from published literature from many volcanic and non-volcanic margins/basins were compared. This plot illustrates a consistent relationship of the stretching factor to the angle of pre-existing zones and the rift axis. The calculated high thinning factors (4.3-5) for crustal stretching observed at the rift-orthogonal Damara and Salado belts match other volcanic and non-volcanic margins where the orientation of the pre-existing tectonic fabric is a high angle to the direction of extension (Figs. 4.12, 4.16). The resulting structural interaction between the rift and the orogenic fabric produces a wide, high-thinning factor, rifted margin. Conversely, the rift-parallel, north-south-trending Dom Feliciano and Kaoko belts have lower thinning factors and narrow margins because of their low-angle orientation relative to the paleo-spreading axis of the South Atlantic (Figs. 4.12, 4.16). As predicted the intermediate case of the rift-oblique Gariep belt falls in a moderate thinning factor due to its intermediate angle to the original direction of extension (Figs. 4.12, 4.16).

From the results presented here, it is possible to predict crustal thinning factors based on the orientation of the pre-existing structural fabrics at rifted margins. The structural inheritance is independent of the margin type i.e. - volcanic, non-volcanic.

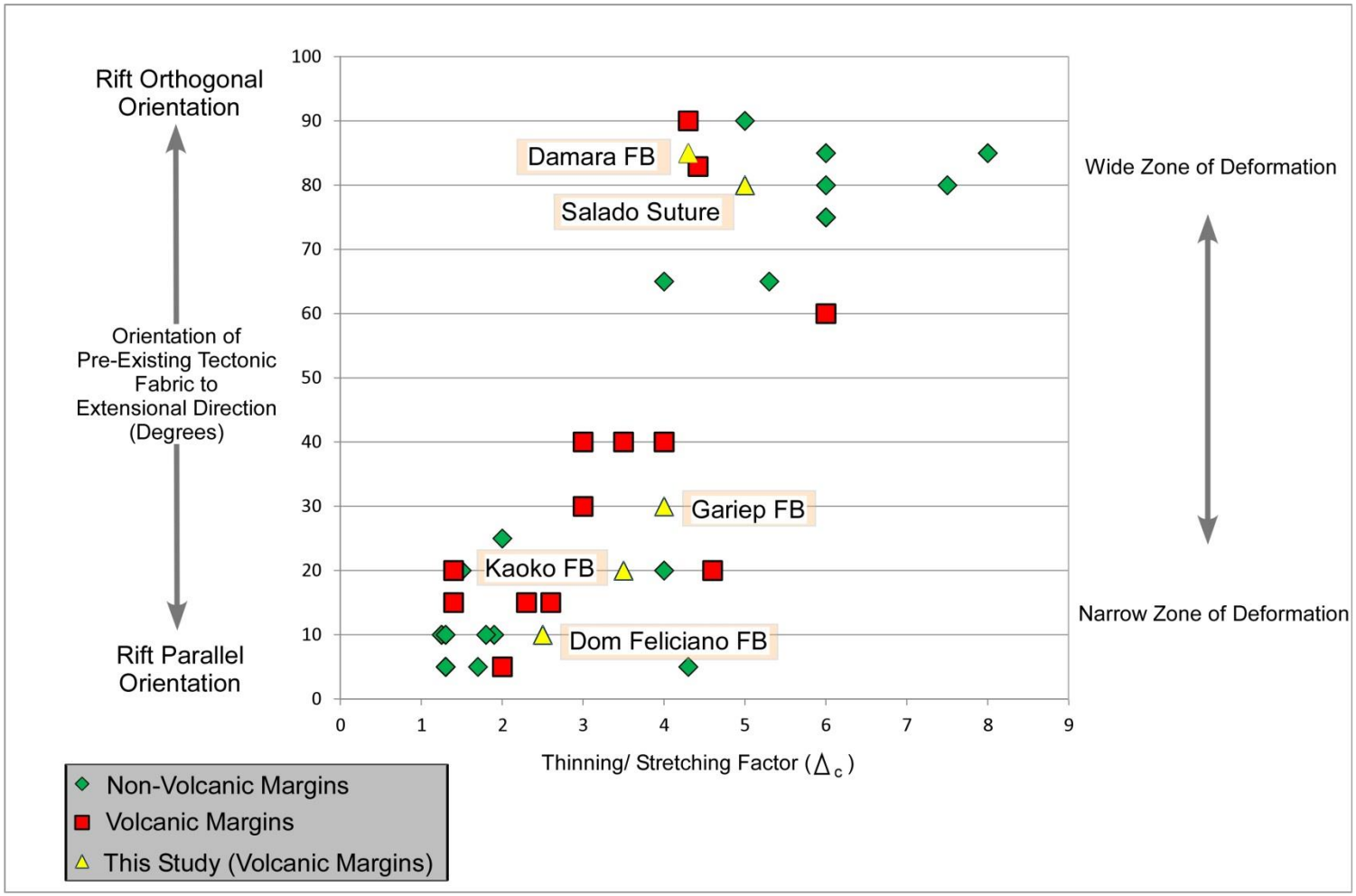

Figure 4.16: A schematic cross plot of thinning factor (Δ_c) values versus angle of orientation from Table 1 to illustrate the relationship of Δ_c to the structural orientation of orogenic belts on volcanic and non-volcanic margins.

4.8 Conclusions

Along-strike variations in crustal stretching measured from deep-penetrating, depth-converted seismic reflection profiles can be correlated with the orientation of the rift relative to the various trends of the Precambrian to Paleozoic, orogenic fabric. Where basement fabric trends parallel to the north-south South Atlantic rift direction in the Paleozoic Dom Feliciano and Kaoko orogenic belts, narrow (55-90 km) rift zones with modest thinning factors of 2.5-3.5 are measured as smaller amounts of rifting were required to stretch the weaker, parallel, orogenic fabric. Where basement fabric trends orthogonal to the north-south South Atlantic rift direction in the Salado suture of Uruguay/Argentina and the Damara belt of Namibia, wider (185-220 km) rift zones with higher stretching factors of 4.3-5 are observed as greater amounts of stretching were required to extend the stronger, orthogonal, orogenic fabric.

The rift-oblique Gariep belt intersects the South Atlantic continental rupture at an intermediate angle (30°) and an intermediate stretching factor (4). A compilation of published stretching factors from other rifted margins worldwide confirms the same relationship described from the South Atlantic VPM's of rift-parallel margins having lower stretching factors in a range of 1.3-3.5 and rift-orthogonal or oblique-margins have higher stretching factors in a range of 4.5-8.

Chapter Four: References

Austin, J. A. J., and Uchupi, E., 1982, Continental–oceanic crustal transition off southwest Africa: American Association of Petroleum Geologists Bulletin, 66, 1328–1347.

Autin J., Bellahsen N., Leroy S., Husson, L., Beslier, M-O., and d'Acremont, E., 2013, The role of structural inheritance in oblique rifting: insights from analogue models and application to the Gulf of Aden: Tectonophysics 607, 51–64.

Baier, B., Berckhemer, H., Gajewski, D., Green, R.W., Grimsel, C., and Prodehl, C., 1983, Deep seismic sounding in the area of the Damara Orogen, Namibia, South West Africa. In: Intracontinental Fold Belts, case studies in the Variscan belt and in the Damara belt in Namibia, edited by H. Martin and F.W. Eder, Springer-Verlag, 885-900.

Ball, P., Eagles, G., Ebinger, C., McClay, K. and Totterdell, J., 2013, The spatial and temporal evolution of strain during the separation of Australia and Antarctica: Geochemistry, Geophysics, Geosystems, 14, 2771–2799.

Benkhelil, J., Mascle, J. and Tricart, P., 1995. The Guinea Continental Margin: An Example of a Structurally Complex Transform Margin: Tectonophysics, 248, 117–137.

Blaich, O. A., Faleide, J. I., Tsikalas, F., Franke, D. and Leo´n, E., 2009, Crustal-scale Architecture and Segmentation of the Argentine Margin and its Conjugate off South Africa: Geophysical Journal international, 178, 85–105.

Blaich, O. A., J. I. Faleide, and F. Tsikalas, 2011, Crustal breakup and continent-ocean transition at South Atlantic conjugate margins: Journal of Geophysical Research Solid Earth, 116, 1–36.

Blaich, O.A., Faleide, J.I., Tsikalas, F., Gordon, A.C., and Mohriak, W., 2013, Crustal-scale architecture and segmentation of the South Atlantic volcanic margin. In: Mohriak, W.U., Danforth, A., Post, P.J., Brown, D.E., Tari, G.C., Nemcok, M., and Sinha, S.T. (Eds.), Conjugate Divergent Margins: Geological Society, London, Special Publications, 369, 167-183.

Bosworth, W., 2015, Geological Evolution of the Red Sea: Historical Background, Review and Synthesis. In The Red Sea: It's Origin, Structure and Environment. N.M. Rasul and I.C.F. Stewart Eds: Springer-Verlag, Berlin, 45–78.

Brunet, M.F., and Le Pichon X., 1982, Subsidence of the Paris basin: Journal of Geophysical Research, 87, 8547—8560.

Chang, H. K., Kowsmann, R. O., Figueiredo, A.M. F., and Bender, A. A., 1992, Tectonics and stratigraphy of the East Brazil Rift System: an Overview: Tectonophysics, 213, 97–138.

Chenin, P., Manatschal, G., Lavier l., and Erratt, D., 2015, Influence of the architecture of magma-poor hyperextended rifted margins on orogens produced by the closure of narrow versus wide oceans: Journal of the Geological Society, 172, 711–720.

Chernicoff, C.J., Zappettini, E.O., and Peroni, J., 2014, The Rhyacian El Cortijo suture zone: Aeromagnetic signature and insights for the geodynamic evolution of the southwestern Rio de la Plata craton, Argentina: Geoscience Frontiers, 5, 43–52.

Choi, E., Lavier, L., and Gurnis, M., 2008, Thermomechanics of mid-ocean ridge segmentation: Physics of the Earth and Planetary Interiors, 171, 374–386.

Coward, M.P., 1981, The junction between Pan African Mobile Belts in Namibia: its structural history: Tectonophysics 76, 59-73.

Coward, M.P., 1983, The tectonic history of the Damaran Belt, In: Miller, R.G. ed, Evolution of the Damara Orogen of South West Africa/ Namibia: Geological Society South Africa Special Publication 11, 409-421.

Courtillot, V., 1982, Propagating rifts and continental breakup: Tectonics 1, 239–250.

Davison, I., 1997, Wide and narrow margins of the Brazilian South Atlantic: Journal of Geological Society, 154, 471–476.

De Castro, D.L., Bezerra, F.H.R., Sousa, L., and Fuck, R.A., 2012, Influence of Neoproterozoic Tectonic Fabric on the Origin of the Potiguar Basin, Northeastern Brazil and its Links with West Africa Based on Gravity and Magnetic Data: Journal of Geodynamics, 54, 29–42.

Dunbar, J.A., and Sawyer, D.S., 1988, Continental rifting at pre-existing lithospheric weaknesses: Nature, 333, 450-452.

Edge, R., 2014, Rifting Of The Guinea Margin In The Equatorial Atlantic From 112 To 84 Ma: Implications Of Paleo-Reconstructions For Structure And Sea-Surface Circulation: Doctoral Thesis, The University of Arizona, 1-181.

Franke, D., Neben, S., Ladage, S., Schreckenberger, B., and Hinz, K., 2007, Margin segmentation and volcano-tectonic architecture Along the Volcanic Margin off Argentina/Uruguay: South Atlantic Marine Geology, 244, 46-67.

Frimmel, H.E., and Frank, W., 1998, Neoproterozoic tectono-thermal evolution of the Gariep Belt and its basement, Namibia and South Africa: Precambrian Research, 90, 1-28.

Geoffroy, L., 2005, Volcanic Passive Margins: Geoscience, 337, 1395–1408.

Geoffroy, L., Burov, E.B., and Werner, P., 2015, Volcanic passive margins: another way to break up continents: Nature, Scientific Reports, 5, 14828, DOI: 10.1038/srep14828.

Gladczenko, T.P., Hinz, K., Eldholm, O., Meyer, H., Neben, S., and Skogseid, J., 1997, South Atlantic volcanic margins: Journal Geological Society, 154, 465-470.

Goscombe, B., Hand, M., and Gray, D.R., 2003, Structure of the Kaoko Belt, Namibia: Progressive Evolution of a Classic Transpressional Orogen: Journal of Structural Geology, 25, 1049-1081.

Heilbron, M., Valeriano, C., Tassinari, C. G., Almeida, J. C. H., Tupinamba, M., Siga, O. Jr. and Trouw, R. A. J., 2008, Correlation of Neoproterozoic terranes between the Ribeira Belt, SE Brazil and its African counterpart: comparative tectonic evolution and open questions. In: Pankhurst, R. J., Trouw, R. A. J., Brito-Neves, B. B., and de Wit, M. J. (eds) West Gondwana: Pre-Cenozoic Correlations across the South Atlantic Region: Geological Society, London, Special Publications, 294, 211–237.

Hoffman, P.F., Swart, R., Eckhardt, E.F., and Guowei, H., 1994, Damara orogen of northwest Namibia: Geological Excursion Guide of the Geological Survey of Namibia, p. 55.

Heilbron, M., Valeriano, C., Tassinari, C. G., Almeida, J. C. H., Tupinamba, M., Siga, O. Jr., and Trouw, R. A. J., 2008, Correlation of Neoproterozoic terranes between the Ribeira Belt, SE Brazil and its African counterpart: comparative tectonic evolution and open questions. In: Pankhurst, R. J., Trouw, R. A. J., Brito-Neves, B. B. & de Wit, M. J. (eds) West Gondwana: Pre-Cenozoic Correlations across the South Atlantic Region: Geological Society, London, Special Publications, 294, 211–237, doi.org/10.1144/SP294.12 0305-8719/08.

Hoffman, P.F., Hawkins, D.P., Isachsen, C.E., and Bowring, S.A., 1996, Precise U-Pb zircon ages for early Damaran magmatism in the Summas Mountains and Welwitschia Inlier, northern Damara Belt, Namibia: Communications of the Geological Survey of Namibia, 11, 47-52.

Jensen, L., and Teasdale, J., 2010, Integrated Gravity and Magnetic Workflows in Regional Basin Analysis, a South and Equatorial Atlantic Exploration

Perspective: Conference Abstract: EGM 2010 International Workshop Adding new value to Electromagnetic, Gravity and Magnetic Methods for Exploration Capri, Italy, April 11-14, 2010.

Karner, G. D., Driscoll, N. W., McGinnis, J. P., Brumbaugh, W. D., and Cameron, N. R., 1997, Tectonic significance of syn-rift sediment packages across the Gabon-Cabinda continental margin: Marine and Petroleum Geology, 14, 973–1000.

Koopmann, H., Franke, D., Schreckenberger, B., Schulz, H., Hartwig, A., Stollhofen, H., and di Primio, R., 2014, Segmentation and Volcano-Tectonic Characteristics along the SW African Continental Margin, South Atlantic, as Derived from Multichannel Seismic and Potential Field Data: Marine and Petroleum Geology, 50, 22—39.

Kröner, A., and Cordani, U., 2003, African, southern India and South American cratons were not part of Rodinia supercontinent: evidence from filed relationships and geochronology: Tectonophysics, 375, 325–352.

Kusznir. N. J., and Park, R., G., 1987, The extensional strength of the continental lithosphere: its dependence on geothermal gradient, and crustal composition and thickness N.J. From: Dewey, J.F., and Hancock, P.L. (eds), Continental Extensional Tectonics: Geological Society Special Publication, 28, 35-52.

Le Roy, P., Pique, A., Gall, B.L., Brahim, L.A., Morabet, A.M., and Demnati, A., 1997, Les bassins cotierstriasico-liasiques du Maroc occidental et la diachronie du rifting intra-continental de l'Atlantique central: Bulletin of Society Geological France, 168, 637–648.

Luheshi, M., Roberts, D. G., Nunn, K., Makris, J., Colletta, B., Wilson, H., Monnier, F., Rabary, G. and Dubille, M. 2012, The impact of conjugate margins analysis on play fairway evaluation - an analysis of the hydrocarbon potential of Nova Scotia: First Break, 30, 61- 72, doi:10.3997/1365-2397.2011037.

Mascle, G., Lohmann, P., and Clift, P., 1997, Development of a Passive Transform Margin: Cote d'Ivoire–Ghana Transform Margin—ODP Leg 159 preliminary results: Geology-Marine Letters, 17, 4–11.

Mazur, S., Campbell, S., Green, C., and Bouatmani, R., 2015, Extension across the Laptev Sea continental rifts constrained by gravity modelling: Tectonics, 34, 435–448, doi:10.1002/2014TC003590

Michon, L., and Sokoutis, D., 2005, Interaction between structural inheritance and extension direction during graben and depocentre formation: An experimental approach: Tectonophysics, Elsevier, 409, 125-146.

McKenzie, D., 1978, Some Remarks on the Development of Sedimentary Basins: Earth and Planetary Science Letters, 40, 25-32.

Moulin, M., Aslanian, D., and Unternehr, P., 2010, A new starting point for the South and Equatorial Atlantic Ocean: Earth Science Review, 98, 1-37.

Mohriak, W.U. and Rosendahl, B.R., 2003, Transform Zones in the South Atlantic Rifted Continental Margins. In: Holdsworth, R.E. and Salvini, F. (eds) Intraplate Strike-Slip Deformation Belts: Geological Society, London, Special Publications, 210, 211–228.

Morley, C.K., Karanja, F.M., Wescott, W.A., Stone, D.M., Harper, R.M., Wigger, S.T., and Day, R.A. 1999, Geology and Geophysics of the Western Turkana Basins, Kenya, in C.K. Morley, ed., Geoscience of rift systems-evolution of East Africa: AAPG Studies in Geology, 44, 19-54.

Müller, R. D., Roest, W. R., and Royer, J., 1998, Asymmetric sea-floor spreading caused by ridge-plume interactions: Nature, 396, 455–459.

Muniz, M., and Bosence, D., 2016, Tectono-Stratigraphy Evolution Of The Continental Rift Pre-Salt Carbonates In Southern Campos Basin, Brazil: Conference Abstract: Rio Oil & Gas Expo and Conference October 23, 2016.

Nürnberg, D., and Müller, R. D., 1991, The tectonic evolution of the South Atlantic from Late Jurassic to Present: Tectonophysics, 191, 27–53.

O'Connor, J.M., and Duncan, R.A., 1990, Evolution of the Walvis Ridge-Rio Grande Rise Hot Spot System: Implications for African and South American Plate Motions Over Plumes: Journal of Geophysical Research, 95, 17475–17502.

O'Sullivan, J.M., Jones, S.M., and Hardy, R.J., 2010, Comparative analysis of the Porcupine Median Volcanic Ridge with modern day Pacific Ocean seamounts – further evidence of an amagmatic Mesozoic basin history for the South Porcupine Basin, offshore Ireland: Conjugate Margins Conference 2010, 5, 216–219.

Passarelli, C., Basei, M., Wemmer, K., Siga, O., and Oyhantçabal, P., 2010, Major shear zones of southern Brazil and Uruguay: escape tectonics in the eastern border of Rio de La plata and Paranapanema cratons during the Western Gondwana amalgamation: International Journal of Earth Sciences, 100-2, 391-414.

Pindell, J.L., 1985, Alleghenian reconstruction and subsequent evolution of the Gulf of Mexico, Bahamas, and proto-Caribbean: Tectonics, 4, 1–39.

Planert, L., Behrmann, J., Jokat, W., Fromm, T., Ryberg, T., Weber, M., and Haberland, C., 2016, The wide-angle seismic image of a complex rifted margin, offshore North Namibia: Implications for the tectonics of continental breakup: Tectonophysics, (article in press).

Rabinowitz, P. D., and LaBrecque, J. L., 1979, The Mesozoic South Atlantic Ocean and evolution of its continental margins: Journal of Geophysical Research, 84, 5973–6002.

Reston, T.J., 2009, The structure, evolution and symmetry of the magma poor rifted margins of the North and Central Atlantic: a synthesis: Tectonophysics, 468, 6–27.

Sandwell, D. T., and Smith, W. H. F., 2009, Global marine gravity from retracked Geosat and ERS-1 altimetry: Ridge segmentation versus spreading rate: Journal of Geophysical Research, 114, B01411, doi:10.1029/2008JB006008.

Seton, M., Müller, R.D., Zahirovic, S., Gaina, C., Torsvik, T.H., Shephard, G., Talsma, A., Gurnis, M., Turner, M., Maus, S., and Chandler, M., 2012, Global continental and ocean basin reconstructions since 200 Ma: Earth-Science Reviews, 113, 212-270.

Steckler, M.S., and Watts. A.B., 1978, Subsidence of the Atlantic type continental margin off New York, Earth Planetery Science Letters, 41, 1-13.

Stratford, W., and Thybo, H., 2011, Crustal structure and composition of the Oslo Graben, Norway: Earth Planetary Science Letters, 304, 431–442, doi.org/10.1016/j.epsl.2011.02.021.

Teixeira, B.A., Pimentel, N., and Pena dos Reis, R., 2012, Regional variations in Source Rock maturation in the Lusitanian Basin (Portugal) – the role of rift events, subsidence, sedimentation rate, uplift and erosion: Abstracts III Atlantic Conjugate Margins Conference, 91-92.

Thybo, H., and Nielsen, C., A., 2008, Magma-compensated crustal thinning in continental rift zones: Nature, 457, 873-876.

Tommasi, A. and Vauchez, A., 2001, Continental rifting parallel to ancient collisional belts: An effect of the mechanical anisotropy of the lithospheric mantle: Earth and Planetary Science Letters, 185 (1/2), 199-210.

Trey, H., Cooper, A.K., Pellis, G., della Vedova, B., Cochrane, G., Brancolini, G., and Makris, J., 1999, Transect across the West Antarctic rift system in the Ross Sea, Antarctica: Tectonophysics 301, 61 – 74.

Vink, G., Organa, J., and Zhao, W.L., 1984, Preferential Rifting of Continents: a Source of Displaced Terranes: Journal of Geophysical Research, 89, 10072-10076.

Welford, K., Shannon, P.M., O'Reilly, B.M., and Hall, J. 2012, Comparison of lithospheric density and Moho structure variations across the Orphan Basin/Flemish Cap and Irish Atlantic conjugate continental margins from constrained 3-D gravity inversions: Journal of the Geological Society, London, 169, 405-420.

Whitmarsh, R. B., White, R. S., Horsefield, S. J., Sibuet, J. C., Recq, M., and Louvel, V., 1996, The ocean-continent boundary off the western continental margin of Iberia: Crustal structure west of Galicia Bank: Journal of Geophysical Research, 101, 28291–28314.

Wilson, T., 1965, A new class of faults and their bearing on continental drift: Nature, 207, 343–347.

Wyer, P. and Watts, A.B., 2006, Gravity anomalies and segmentation at the East Coast, USA continental margin: Geophysical Journal International, 166(3), 1015 – 1038, DOI: 10.1111/j.1365-246X.2006.03066.x